Hawaii Ocean Time-series
Data Report 9: 1997

September 1998

Luis Tupas
Fernando Santiago-Mandujano
Dale Hebel
Craig Nosse
Lance Fujieki
Roger Lukas
David Karl

with contribution by
Christopher Winn
Robert Bidigare
Michael Landry
Eric Firing

University of Hawaii
School of Ocean and Earth Science and Technology
1000 Pope Road
Honolulu, Hawaii 96822
U. S.A.

SOEST 98-09

PREFACE

Scientists working on the Hawaii Ocean Time-series (HOT) program have been making repeated observations of the hydrography, chemistry and biology of the water column at a station north of Oahu, Hawaii since October 1988. The objective of this research is to provide a comprehensive description of the ocean at a site representative of the North Pacific subtropical gyre. Cruises are made approximately once a month to the HOT deep-water station (22° 45'N, 158° 00'W) located about 100 km north of Oahu, Hawaii. Measurements of the thermohaline structure, water column chemistry, currents, primary production and particle sedimentation rates are made on each cruise.

This document reports the data collected in 1997. However, we have included some data from 1988-1996 to place the 1997 measurements within the context of our ongoing time-series observations. The data reported here are a screened subset of the complete data set. Summary plots are given for CTD, biogeochemical, optical, meteorological, thermosalinograph, inverted echo sounder and ADCP observations. The complete data set resides on a Sun workstation at the University of Hawaii. These data are in ASCII format, and can easily be accessed using anonymous file transfer protocol (ftp) via Internet or the World Wide Web (WWW). The entire data set is available at NODC.

ACKNOWLEDGMENTS

Many people participated in the 1997 cruises sponsored by the HOT program. Special thanks are due to Karin Bjorkman, Stephanie Christensen, Stuart Donachie, Pat Driscoll, Lance Fujieki, Dale Hebel, Terrence Houlihan, Mai Lopez, Craig Nosse, Hans Ramm, Daniel Sadler, Fernando Santiago-Mandujano and Jefrey Snyder for participating in most of the 1997 cruises and for the tremendous amount of time and effort they have put into the program. Special thanks are given to Lisa Lum for her excellent administrative support of the program, to Sharon DeCarlo for programming and data management, Scott Kaneshiro and Tay Peng Chen for CTD processing and to June Firing and Kalpana Kalianpur for ADCP processing. Ursula Magaard performed many of the core chemical analyses. Karin Bjorkman, Ted Walsh, Terrence Houlihan and Angie Thomson-Bulldis performed the nutrient analyses, Matthew Cochran and Don Wright performed the salinity measurements and Man Kit Tsoi provided additional technical support. We gratefully acknowledge the support from Nordeen Larson and Ken Lawson of Sea-Bird for helping us to maintain the quality of the CTD data throughout the HOT program. We also would like to thank the captain and crew members of the R/V *Moana Wave* and the UH Marine Center staff for their efforts. Without the assistance of these and the many technicians, students and ancillary investigators, the data presented in this report could not have been collected, processed, analyzed and reported. Weather buoy data used in this report were obtained by the NOAA National Data Buoy Center (NDBC) and were provided to us by the National Oceanographic Data Center (NODC). We thank Pat Caldwell for his assistance.

This data set was acquired with funding from the National Science Foundation (NSF) and State of Hawaii general funds. The specific grants which have supported this work are NSF grants OCE-9303094 (WOCE; Lukas and Firing) and OCE-9301368 (JGOFS; Karl, Hebel and Tupas) and the JGOFS sub-components of Christopher Winn (OCE-9315392), Michael Landry (OCE-9218152) and Robert Bidigare (OCE-9315311).

1.0. INTRODUCTION

In response to the growing awareness of the ocean's role in climate and global environmental change, and the need for additional and more comprehensive oceanic time-series measurements, the Board on Ocean Science and Policy (BOSP) of the National Research Council (NRC) sponsored a workshop on "Global Observations and Understanding of the General Circulation of the Oceans" in August 1983. The proceedings of this workshop (National Research Council 1984a) served as a prospectus for the development of the U.S. component of the World Ocean Circulation Experiment (WOCE). US-WOCE has the following objectives:

- To understand the general circulation of the global ocean, to model with confidence its present state and predict its evolution in relation to long-term changes in the atmosphere.
- To provide the scientific background for designing an observation system for long-term measurement of the large-scale circulation of the ocean.

In a parallel effort, a separate research program termed Global Ocean Flux Study (GOFS) focused on the ocean's carbon cycle and associated air-sea fluxes of carbon dioxide. In September 1984, NRC-BOSP sponsored a workshop on "Global Ocean Flux Study" which served as an eventual blueprint for the GOFS program (National Research Council 1984b). In 1986, the International Council of Scientific Unions (ICSU) established the International Geosphere-Biosphere Program: A Study of Global Change (IGBP), and the following year JGOFS (Joint GOFS) was designed as a Core Project of IGBP. US-JGOFS research efforts focus on the oceanic carbon cycle, its sensitivity to change and the regulation of the atmosphere-ocean CO_2 balance (Brewer et al. 1986). The broad objectives of US-JGOFS are:

- To determine and understand on a global scale the time-varying fluxes of carbon and associated biogenic elements in the ocean.
- To evaluate the related exchanges of these elements with the atmosphere, the sea floor and the continental boundaries (SCOR 1990, JGOFS Rep. #5).

In order to achieve these goals, four separate program elements were defined: Process studies to capture key regular events; Long-term time-series observations at strategic sites; A global survey of relevant oceanic properties (e.g., CO_2) and; A vigorous data interpretation and modeling effort to disseminate knowledge and to generate testable hypotheses.

In 1987, two separate proposals were submitted to the US-WOCE and US-JGOFS program committees respectively by scientists at the University of Hawaii at Manoa to establish a multi-disciplinary, deep water hydrostation in Hawaiian waters. In July 1988, these proposals were funded by the National Science Foundation and Station ALOHA was officially on the map (Karl and Lukas 1996). A sister station in the western North Atlantic Ocean, near the historical Panulirus Station, was likewise funded by the US-JGOFS program and is operated by scientists at the Bermuda Biological Station for Research, Inc. (Michaels and Knap 1996).

The primary research objectives of these ocean measurement programs are to establish and maintain deep-water hydrostations for observing and interpreting physical and biogeochemical variability. The initial design called for repeat measurements of a suite of core parameters at approximately monthly intervals, compilation of the data and rapid distribution to the scientific community.

1.1. Hawaii Ocean Time-series Program

The Hawaii Ocean Time-series (HOT) Program consists of several research components lead by scientists at the University of Hawaii at Manoa (Table 1.1). The hydrographic (WOCE) and biogeochemical (JGOFS) components are fully integrated operationally and are both involved in all aspects of planning and execution of HOT Program objectives.

Table 1.1: HOT Research Components in 1997

Principal Investigators	Project Title
Roger B. Lukas	WOCE Core Component
Eric Firing	ADCP Component
David M. Karl, Dale V. Hebel, Luis M. Tupas	JGOFS Core Component
Robert R. Bidigare	Phytoplankton community structure
Michael R. Landry	Zooplankton community structure
Christopher D. Winn	Inorganic Carbon System

1.2. Scientific objectives for HOT

The primary objective of HOT is to obtain a long time-series of physical and biogeochemical observations in the North Pacific subtropical gyre that will address the goals of the US Global Change Research Program. The objectives specific to the WOCE program are to:

- Document and understand seasonal and interannual variability of water masses.
- Relate water mass variations to gyre fluctuations.
- Determine the need and methods for monitoring currents at Station ALOHA.
- Develop a climatology of short-term physical variability.

In addition to these general primary objectives, the physical oceanographic component of HOT provides CTD/rosette sampling support for the JGOFS time-series sampling program, and supports development of new instrumentation for hydrographic observations.

The objectives of HOT specific to the JGOFS program are to:

- Document and understand seasonal and interannual variability in the rates of primary production, new production and particle export from the surface ocean.
- Determine the mechanisms and rates of nutrient input and recycling, especially for N and P in the upper 200 m of the water column.
- Measure the time-varying concentrations of DIC in the upper water column and estimate the annual air-to-sea CO_2 flux.

In addition to these general primary objectives, the HOT Program provides logistical support for numerous complementary research programs (Table 1.2). A complete listing of these projects can be obtained from the HOT-JGOFS web page (http://hahana.soest.hawaii.edu/hot/hot.html).

Table 1.2: Ancillary Projects Supported by HOT in 1997

Principal Investigator(s)	Institution	Agency	Project Title
Mark Abbott Ricardo Letelier	Oregon State University	NASA	HALE ALOHA: biooptics
Edward Boyle	MIT	NSF	HALE ALOHA: Trace metals
Lisa Campbell, Giacomo DiTullio	Univ. of Texas College of Charleston	NSF	Effects of Light and Nitrogen source on *Prochlorococcus* Growth
Steven Emerson	Univ. of Washington	NSF	HALE ALOHA: dissolved gases
Mark Huntley	UCSD Scripps Inst. of Oceanography	ONR	Particle Size Distribution at Stn. ALOHA Measured with an Optical Plankton Counter
Hans Jannasch	MBARI	MBARI	HALE ALOHA: automated nutrients
David Karl	Univ. of Hawaii	NSF	LTER Cross-site Comparison Microbial Loop Dynamics
Charles Keeling	UCSD Scripps Inst. Oceanography	NSF	$^{13}C/^{12}C$ Ratio of Atmosphere Carbon Dioxide and Oceanic Carbon in Relation to the Global Carbon Cycle
Edward Law Brian Popp	Univ. of Hawaii	NSF	Isotopic composition of phytoplankton
Paul Quay	Univ. of Washington	NOAA	$^{13}C/^{12}C$ of Dissolved Inorganic Carbon in the Ocean
Francis Sansone	Univ. of Hawaii	ONR	Upper Ocean Methane Dynamics
Ken Smith	UCSD Scripps Inst. of Oceanography	NSF	Organic carbon utilization by deep-sea sediment communities
Jonathan Zehr	Rensselaer Polytech	NSF	Nitrogen Fixation Genes

1.3. HOT Study Site

There are both scientific and logistical considerations involved with the establishment of any long-term, time-series measurement program. Foremost among these is site selection, choice of variables and general sampling design, including sampling frequency. Equally important design considerations are those dealing with the choice of analytical methods for a given candidate variable, especially an assessment of the desired accuracy and precision, and availability of suitable reference materials, the hierarchy of sampling replication and, for data collected at a fixed geographical location, mesoscale horizontal variability.

We evaluated several major criteria prior to selection of the site for the HOT oligotrophic ocean benchmark hydrostation. First, the station must be located in deep water (>4000 m), upwind (north-northeast) of the main Hawaiian islands and of sufficient distance from land to be free from coastal ocean dynamics and biogeochemical influences. On the other hand, the station should be close enough to the port of Honolulu to make relatively short duration (<5 d) monthly cruises logistically and financially feasible. A desirable, but less stringent criterion would locate

the station at, or near, previously studied regions of the central North Pacific Ocean, in particular Station GOLLUM. Documentation of oceanic time-series measurements in the North Pacific Ocean can be found in Karl and Winn (1991), Karl et al. (1996b), Karl and Lukas (1996) and in the HOT-JGOFS web page (http://hahana.soest.hawaii.edu)

After consideration of these criteria, we established our primary sampling site at 22° 45' N, 158° W at a location approximately 60 nautical miles north of the island of Oahu (Figure 1.1), and generally restrict our monthly sampling activities to a circle with a 6 nautical mile radius around this nominal site. Station ALOHA is in deep water (4750 m) and is more than one Rossby radius (50 km) away from steep topography associated with the Hawaiian Ridge. We also established a coastal station W-SW of the island of Oahu, approximately 10 km off Kahe Point (21° 20.6' N, 158° 16.4' W) in 1500 m of water. Station Kahe serves as a coastal analogue to our deep-water site and the data collected there provide a near-shore time-series for comparison to our primary open ocean site. Station Kahe is also used to test our equipment each month before departing for Station ALOHA, and to train new personnel at the beginning of each cruise. In January 1997, a physical-biogeochemical mooring was deployed to obtain continuous measurements of various atmospheric and oceanographic parameters. The mooring is located at 22° 28' N, 158° 8' W and was designated as Station HALE-ALOHA. Locations and dates of occupancy of HOT water column and bottom recording stations is available at the HOT-JGOFS web page (http://hahana.soest.hawaii.edu).

1.4. Field Sampling Strategy

HOT program cruises are conducted at approximately monthly intervals; the exact timing dictated by the availability of research vessels. From HOT-1 (October 1988) to HOT-65 (August 1995), with the exception of HOT-42 and HOT-43 (November and December 1992), each cruise was 5 days in duration (port to port). Beginning with HOT-66 (September 1995) the standard HOT cruise was reduced by 20 % to 4 days (port to port) in order to accommodate the additional mooring-based HOT field programs within a fixed per annum allocation of ship days.

From HOT-1 (October 1988) to HOT-32 (December 1991), underway expendable bathythermograph (XBT; Sippican T-7 probes) surveys were conducted at 7 nautical mile spacing on the outbound transect from Station Kahe to Station ALOHA. These surveys were later discontinued because the space-time correlation of the energetic, internal semi-diurnal tides made it difficult to interpret these data. From February 1995 until December 1997 we added an instrumented, 1.5 m Endeco towfish package (Sea-Bird CTD, optical plankton counter, fluorometer) to our sampling program (Tupas et al. 1997). Upper water column currents are measured both underway and on station using a hull-mounted Acoustic Doppler Current Profiler (ADCP), when available (Firing 1996). The majority of our sampling effort, approximately 60-72 hours per standard HOT cruise, is spent at Station ALOHA. Underway near-surface measurement of a variety of physical, chemical and biological properties is made possible by sampling seawater through a pumped intake system positioned in the hull of the R/V *Moana Wave*. In May 1995, a thermosalinograph was installed in line to the ships seawater intake system. In July 1996, the existing system was replaced with a non-contaminating PVC/ stainless steel system. Several new sensors such as an underway surface pCO2 measuring system and a flow through fluorometer were installed in 1996.

High vertical resolution environmental data are collected with a Sea-Bird CTD having external temperature (T), conductivity (C), dissolved oxygen (DO) and fluorescence sensors and an internal pressure (P) sensor. A Sea-Bird 24-place carousel and an aluminum rosette that is capable of supporting 24 12-l PVC bottles are used to obtain water samples from desired depths.

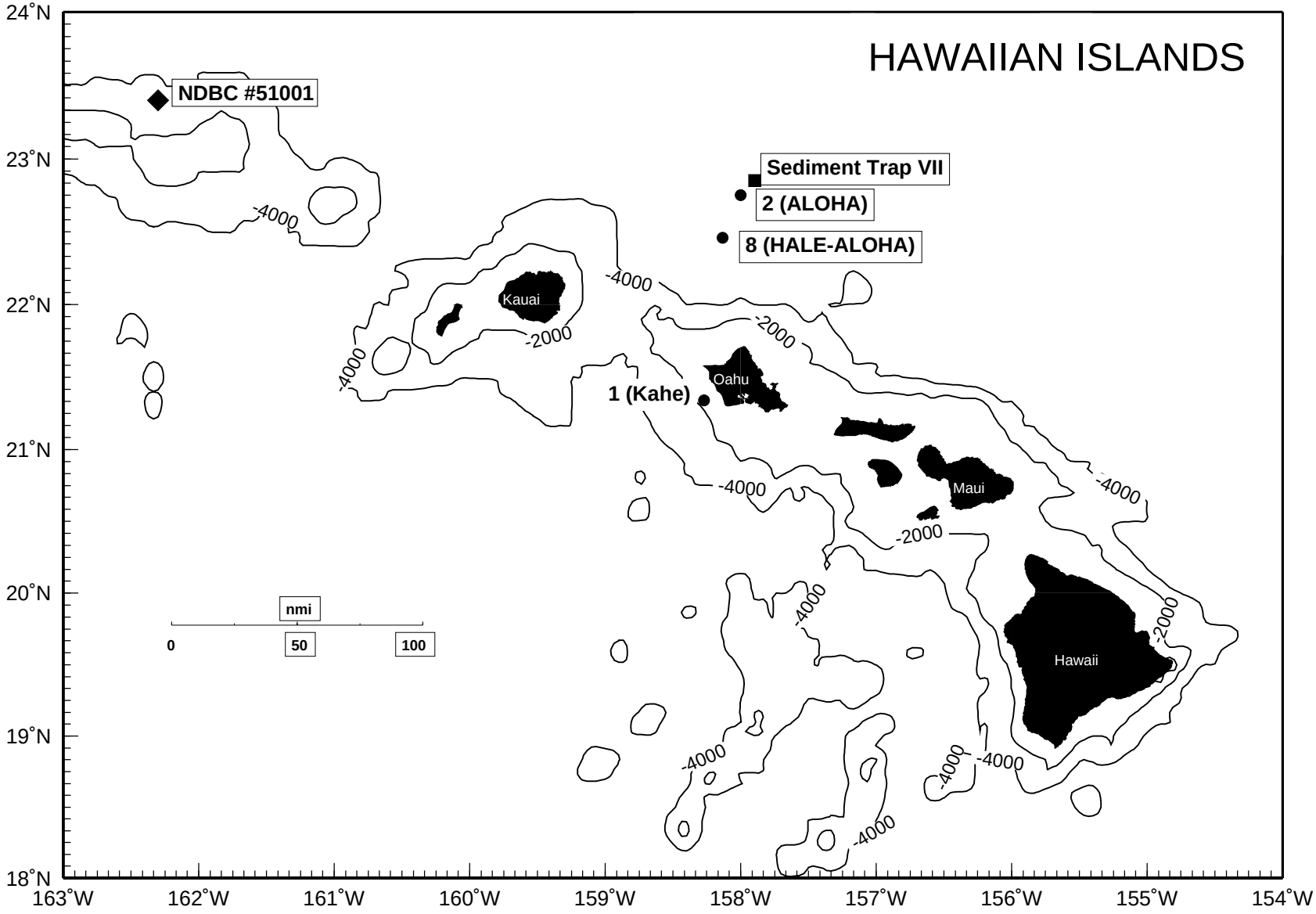

Figure 1.1: Map of the Hawaiian islands showing the locations of the HOT stations and the NOAA-NDBC weather buoy #51001.

The CTD and rosette are deployed on a 3-conductor cable allowing for real-time display of data and for tripping the bottles at specific depths of interest. The CTD system takes 24 samples sec^{-1} and the raw data are stored both on the computer and, for redundancy, on VHS-format video tapes. We also routinely collect "clean" water samples for biological rate measurements using General Oceanics Go-Flo bottles, Kevlar cable, metal-free sheave, Teflon messengers and a stainless steel bottom weight. A free-drifting sediment trap array, identical in design to the VERTEX particle interceptor trap (PIT) mooring (Knauer et al. 1979), is deployed at Station ALOHA for an approximately 2.5 day period to collect sinking particles for chemical and microbiological analyses.

Sampling at Station ALOHA typically begins with sediment trap deployment followed by a deep (> 4700 m) CTD cast and a "burst series" of at least 13 consecutive casts, on 3-hr intervals, to 1000 m to span the local inertial period (~ 31 hr) and three semidiurnal tidal cycles. The repeated CTD casts enable us to calculate an average density profile from which variability on tidal and near-inertial time scales has been removed. These average density profiles are useful for the comparison of dynamic height and for the comparison of the depth distribution of chemical parameters from different casts and at monthly intervals. This sampling strategy is designed to assess variability on time scales of a few hours to a few years. Very high frequency variability (< 6 hr) and variability on time scales of between 3-60 days are not adequately sampled at the present time.

Water samples for a variety of chemical and biological measurements are routinely collected from the surface to within 5 m of the seafloor. To the extent possible, we collect samples for complementary biogeochemical measurements from the same or from contiguous casts to minimize aliasing caused by time-dependent changes in the density field. This is especially important for samples collected in the upper 300 m of the water column. Furthermore, we attempt to sample from common depths and specific density horizons each month to facilitate comparisons between cruises. Water samples for salinity determinations are collected from every water bottle to identify sampling errors. Approximately 20% of the water samples are collected and analyzed in duplicate or triplicate to assess and track our analytical precision in sample analysis.

The HOT program was initially conceived as being a deep-ocean, ship- and mooring-based observation experiment that would have an approximately 20-year lifetime. Consequently, we selected a core suite of environmental variables that might be expected to display detectable change on time scales of several days to one decade. Except for the availability of existing satellite and ocean buoy sea surface data, the initial phase of the HOT program (Oct 1988 - Feb 1991) was entirely supported by research vessels. In February 1991, an array of five inverted echo sounders (IES) was deployed in an approximately 150 km^2 network around Station ALOHA (Chiswell 1996) and in June 1992, a sequencing sediment trap mooring was deployed a few km north of Station ALOHA (Karl et al. 1996a). In 1993, the IES network was replaced with two strategically-positioned instruments: one at Station ALOHA and the other at Station Kaena. The IES at Station Kaena was retired in October 1995. Beginning in 1994, a single IES has been positioned and annually replaced at Station ALOHA. In January 1997, the Hawaii Air-sea Logging Experiment (HALE) was initiated with the deployment of a physical-biogeochemical mooring designated as HALE ALOHA. Details of this mooring can be obtained from the HOT-JGOFS web site (http://hahana.soest.hawaii.edu).

1.5. Core Measurements, Experiments and Protocols

The suite of core measurements provides a data base to validate existing biogeochemical models and to develop improved ones. Our list of core measurements has evolved since the inception of the HOT program in 1988, and now includes both continuous and discrete physical, biological and chemical ship-based measurements, *in situ* biological rate experiments, and observations and sample collections from bottom-moored instruments and buoys (Table 1.3). Continuity in the measurement parameters and their quality, rather than continuity in the methods employed, is of greatest interest. Detailed analytical methods are expected to change over time through technical improvements. In addition to the core data, specialized measurements and process-oriented experiments have also been conducted at Station ALOHA (Table 1.3).

Table 1.3: Parameters Measured at Station ALOHA

Parameter	Depth Range (m)	Analytical Procedure
I. Continuous Measurements		
Pressure (Depth)	0-4800	Pressure transducer on Sea-Bird CTD package
Temperature	0-4800	Thermistor on Sea-Bird CTD package
Conductivity (Salinity)	0-4800	Conductivity sensor on Sea-Bird CTD package, standardization with Guildline AutoSal using Wormley seawater standard
Oxygen	0-4800	YSI sensor on Sea-Bird CTD package with Winkler standardization
Fluorescence	0-1000	Sea-Tech flash fluorometer
II. Water Column Chemical Measurements		
Oxygen	0-4750	Winkler titration
Dissolved Inorganic Carbon	0-4750	Coulometry
Titration Alkalinity	0-4750	Automated Gran titration
pH	0-4750	Spectrophotometric
Nitrate Plus Nitrite	0-4750	Autoanalyzer
Soluble Reactive Phosphorus (SRP)	0-4750	Autoanalyzer
Silicate	0-4750	Autoanalyzer
Low Level Nitrate Plus Nitrite	0-200	Chemiluminescence
Low Level SRP	0-200	Magnesium-induced coprecipitation
Dissolved Organic Carbon	0-1000	High temperature catalytic oxidation
Dissolved Organic Nitrogen	0-1000	UV oxidation of total nitrogen
Dissolved Organic Phosphorus	0-1000	UV oxidation of total phosphorus
Particulate Carbon	0-1000	High temperature combustion
Particulate Nitrogen	0-1000	High temperature combustion
Particulate Phosphorus	0-1000	High temperature combustion
III. Biomass Measurements		
Chlorophyll *a* and Phaeopigments	0-200	Fluorometric analysis
Pigments	0-200	HPLC
Adenosine 5'-Triphosphate	0-1000	Firefly bioluminescence
Bacteria and Cyanobacteria	0-200	Flow cytometry
Meso and Microzooplankton	0-200	Net tows, elemental analysis
IV. Carbon Assimilation and Particle Flux		
Primary Production	0-200	"Clean" ^{14}C incubations
Carbon, Nitrogen, Phosphorus	150	Free-floating particle traps
V. Currents		
Acoustic Doppler Current Profiler	10-300	Hull mounted, RDI #VM-150
Acoustic Doppler Current Profiler	10-4750	Lowered ADCP

Table 1.3: continued

VI. Instrumented Towfish		
Pressure (Depth)	25	Sensor on Sea-Bird package
Temperature	25	Thermistor on Sea-Bird package
Conductivity (Salinity)	25	Sensor on Sea-Bird package
Zooplankton	25	Optical Plankton Counter
Fluorescence	25	WetLabs SeaStar
VII. Bow Intake System		
Temperature	3	Sea-Bird remote temperature sensor
Conductivity (Salinity)	3	Sea-Bird temperature and conductivity sensors inside the thermosalinograph package
pCO2	3	Gas equilibration, infrared detection
Fluorometry	3	Turner Designs 10-AU
VIII. Optical Measurements		
Incident Irradiance	Surface	LI-COR and Biospherical collector
Upwelling and downwelling irradiance	0-175	Biospherical Profiling Reflectance Refractometer PRR-600
IX. Moored Instruments		
Inverted Echo Sounder	4750	Acoustic telemetry, CTD calibration
Sequencing Sediment Traps	4000	Parflux MK7-21
Physical-Biogeochemical Mooring	Surface-800	See HALE ALOHA web site

Table 1.4: Chronology of 1997 HOT Cruises

Cruise	Ship	Depart	Return
79	R/V *Moana Wave*	6 January 1997	10 January 1997
HA-1A	R/V *Moana Wave*	11 January 1997	14 January 1997
80	R/V *Moana Wave*	16 February 1997	20 February 1997
81	R/V *Moana Wave*	10 March 1997	14 March 1997
82	R/V *Moana Wave*	7 April 1997	11 April 1997
83	R/V *Moana Wave*	5 May 1997	9 May 1997
HA-1B	R/V *Moana Wave*	12 May 1997	14 May 1997
HA-2A	R/V *Moana Wave*	19 May 1997	21 May 1997
84	R/V *Moana Wave*	2 June 1997	6 June 1997
AC-2	R/V *Moana Wave*	26 June 1997	2 July 1997
85	R/V *Moana Wave*	3 July 1997	7 July 1997
86	R/V *Moana Wave*	31 July 1997	4 August 1997
87	R/V *Roger Revelle*	24 September 1997	26 September 1997
HA-2B	R/V *Moana Wave*	1 December 1997	2 December 1997
88	R/V *Moana Wave*	3 December 1997	7 December 1997
HA-3A	R/V *Moana Wave*	19 December 1997	22 December 1997

This report presents selected core data collected during the ninth year of the HOT Program (January-December 1997). During this period, 9 regular HOT cruises were conducted using the University of Hawaii research vessel R/V *Moana Wave* and one on the R/V *Roger Revelle* from the Scripps Institution of Oceanography (Table 1.4). In addition, a 7-day cruise was once again made to the historic Climax station to assess spatial variability and was called ALOHA-Climax 2 (AC-2). On January 11, 1997, the HALE ALOHA mooring was deployed for

the first time and several 3-day cruises were conducted to service the mooring. The moored sediment trap was also serviced during these cruises in December 1997. University of Hawaii shipboard technical assistance personnel assisted a total field scientific crew of 71 HOT staff, students and visiting scientists (Table 1.5) in our 1997 field work.

These selected measurements are part of a much larger HOT program data set on physical and biogeochemical variability at Station ALOHA that has been collected since October 1988. The complete data set is available to the community by several methods that are described in a subsequent section of this report.

Table 1.5: 1997 Cruise Personnel (shaded area = cruise participant)

Cruise Participants	79	HA-1A	80	81	82	83	HA-1B	HA-2A	84	AC-2	85	86	87	HA-2B	88	HA-3A
Aicher, Jennifer					■											
Baldwin, Roberta															■	
Bazua-Duran, Maria Carmen													■			
Bjorkman, Karin	■		■	■	■	■			■	■		■	■			
Calbet, Albert						■			■	■	■	■				
Carrillo, Christopher								■			■	■	■	■	■	
Chen, Shui Ming	■															
Christensen, Stephanie	■		■	■	■	■			■	■	■		■		■	
Clark, Bill																■
Clay, Peter		■														
Cochran, Matt		■	■	■		■			■							
Dail, Holly	■															
Dawson, Bess											■					
Donachie, Stuart				■	■	■			■	■	■	■	■		■	
Driscoll, Patrick	■		■		■	■			■		■	■	■		■	
Emerson, Steven								■								
Falter, James					■	■										
Frese, Jennifer										■						
Fujieki, Lance	■		■		■				■	■	■	■	■	■	■	■
Glatts, Robert															■	
Gravatt, Lily														■		■
Guidry, Michael	■															
Hamann, Ilse				■												
Hebel, Dale	■	■	■	■		■			■	■	■	■	■	■	■	■
Hochberg, Eric													■			
Holmes, Beth	■										■					
Houlihan, Terrence		■	■	■		■		■		■		■	■	■	■	■
Jannasch, Hans		■														
Karl, Dave		■						■					■			■
Karl, Tom								■								
Karner, Markus													■		■	

Table 1.5: continued

	79	HA-1A	80	81	82	83	HA-1B	HA-2A	84	AC-2	85	86	87	HA-2B	88	HA-3A
Kayser, Rick								■						■		
Kelly, Kevin													■			
Landry, Michael													■			
Letelier, Ricardo		■												■		
Liebeler, Jennifer													■			
Lopez, Mai	■		■	■	■	■			■		■					
Magaard, Ursula	■			■									■			
Measures, Christopher													■			
Motell, Craig														■		
Nolla, Hector													■			
Nosse, Craig	■		■	■	■	■		■	■		■	■	■		■	
Opie, Jonathan																■
Pickerill, Mark		■														
Porter, John														■		
Ramm, Hans		■						■	■	■		■	■	■	■	■
Robinson, Donna													■			
Sadler, Dan	■		■	■	■				■	■	■	■	■	■		■
Sakamoto, Carol								■								■
Santiago-Mandujano, Fernando			■		■						■	■	■		■	
Sawyer, Michael		■						■								■
Scheinberg, Rebecca										■	■	■	■			
Shackelford, Rachel										■			■			
Smith, Ken															■	
Snyder, Jefrey	■	■	■	■	■	■		■	■		■					
Stump, Charles		■		■								■	■	■		■
Thomson-Buldis, Angie										■						
Troy, Paul										■						
Tupas, Luis					■	■			■				■		■	
Uhlman, Alfred															■	
Vink, Sue													■			
Westley, Marian												■				
Winn, Christopher				■												
Gravatt, Dave	■	■		■	■		■	■	■	■			■	■	■	■
Hervig, Will	■															
Poulos, Steve		■	■			■	■	■	■		■	■	■	■	■	■
Pozzi, Pierluigi			■			■					■	■				
Stahl, Sharon				■	■					■						
Wright, Don	■		■	■	■	■			■	■	■	■	■	■	■	■
Young, Derrick		■														■

2.0. SAMPLING PROCEDURES AND ANALYTICAL METHODS

A comprehensive summary of all sampling and analytical methods currently used in the HOT program along with information on measurement accuracy and precision can be found in the "Hawaii Ocean Time-series Program Field and Laboratory Protocols" manual. This document is available on the World Wide Web (http://hahana.soest.hawaii.edu) or can be obtained in hard copy by contacting David M. Karl [phone: (808) 956-8964; facsimile: (808) 956-5059; electronic mail: dkarl@soest.hawaii.edu]. Brief summaries of methods as well as calibration specifications and quality control / quality assurance information for 1997 are presented in this report. Hydrographic sampling methods are included in "WOCE Hydrographic Sampling Procedure. A primer for ship-board operations at the Hawaii Ocean Time-series Station," and is also available on the web (http://www.soest.hawaii.edu/HOT_WOCE).

2.1. CTD Profiling

Continuous measurements of temperature, salinity, oxygen and fluorescence are made with a Sea-Bird SBE-9/11plus CTD package with dual temperature, salinity and oxygen sensors and fluorometer described in Tupas et al. (1997). CTD casts are made at Stations Kahe, ALOHA and HALE ALOHA during each cruise. A CTD cast to 1000 m is made at Station Kahe. At Station ALOHA a burst of consecutive CTD casts to 1000 m is made over 36 hours to span the local inertial period and three semi-diurnal tidal cycles. One WOCE standard cast within 10 m of the bottom is made during each cruise. During HOT-83 a second deep cast was obtained at station ALOHA. One CTD cast to 1000 m is made less than 1 nautical mile from the HALE ALOHA mooring for calibration of the Seacats and other moored instruments. During cruises HOT-80, 81 and 82, one or two additional shallower casts (less than 300 m deep) were also obtained at this station.

2.1.1. Data Acquisition and Processing

CTD data were acquired at a rate of 24 samples per second. Digital data were stored on an IBM-compatible PC and, for redundancy, the analog signal was recorded on VHS video tapes. Backups of CTD data were made onto Zip disks and later onto DAT tapes. The raw CTD data were quality controlled and screened for spikes as described in Winn et al. (1993). Data alignment, averaging, correction and reporting were done as described in Tupas et al. (1993). Salinity spike rejection parameters were modified for some cruises in 1997 because of rough conditions. Spikes occur when the CTD samples the disturbed water of its wake. Therefore, samples from the downcast are rejected when the CTD is moving upward or when its acceleration exceeds 0.5 m s^{-2} in magnitude. Cruises 79, 80, 81, 85 and 88 were conducted under rough sea conditions, with heavy ship rolling during some of the casts, causing large vertical velocity fluctuation of the CTD package. The acceleration cutoff value had to be increased to between 0.55 and 0.60 m s^{-2} to have points available to average in each 2-dbar bin. The data were additionally screened by comparing the primary and secondary sensor pairs. These differences permitted identification of problems in the sensors. Only the data from one pair of T-C sensors and one oxygen sensor, whichever was deemed most reliable, are reported here.

Temperature is reported in the ITS-90 scale. Salinity and all derived units were calculated using the UNESCO (1981) routines; salinity is reported in the practical salinity scale (PSS-78). Oxygen is reported in μmol kg^{-1}.

2.1.2 Sensor Corrections and Calibrations

2.1.2.1. Pressure

The pressure calibration strategy employed a high-quality quartz pressure transducer as a transfer standard. Periodic recalibrations of this lab standard were performed with a primary pressure standard. The transfer standard was used to check the CTD pressure transducers in January and June 1997, and September 1998. The results of the 1997 tests showed a bias of 1.4 dbar in the 0 to 4500 dbar range between the CTD and transfer standard pressures. A correction for this bias was applied to the CTD pressures during data collection. The other correction applied to the CTD pressures was a constant offset determined at the time that the CTD first enters the water on each cast.

2.1.2.1.1. Transfer Standard Calibration

The transfer standard was a Paroscientific Model 760 pressure gauge equipped with a 10,000 PSI transducer. This instrument was purchased in March 1988, and was originally calibrated against a primary standard. Subsequent recalibrations were performed in May 1991, September 1994, and March 1996 (Karl et al. 1996b).

2.1.2.1.2. CTD Pressure Transducer Bench Tests

CTD pressure transducer bench tests were done using a dead-weight pressure tester and a manifold to apply pressure simultaneously to the CTD pressure transducer and to the transfer standard. All these tests had points at 6 pressure levels between 0 and 4500 dbar, increasing and decreasing pressures.

Our CTD pressure transducers are the same type as the transfer standard. Pressure transducer #26448 was used during all cruises in 1997. Bench tests against the transfer standard from January, June 1997, and September 1998 are given in Table 2.1. A constant value of -5.72 dbar was used to correct the offset at 0 dbar for all the cruises in 1997 (Note that this offset was only used for real-time data acquisition, as more accurate offset was later determined for the time that the CTD first enters the water on each cast). A slope correction of 1.4 dbar between 0 and 4500 dbar was applied to all the cruises in 1997. The hysteresis has remained constant and small. No correction has been applied for hysteresis.

Our backup pressure transducer #51412 was also calibrated against the pressure standard and the results are shown in Table 2.1. The results in Table 2.1 indicate a variation of more than 1 dbar in the 0 dbar offset for sensor #26448 between January and June 1997. However, this variation is not reflected by the surface pressures recorded during cruises. CTD pressures before and after every cast are regularly recorded by the CTD operator when the CTD is on deck, and Figure 2.1 shows the median of these observations for every cruise. The variability shown by this record between January and June 1997 is only about ± 0.1 dbar, and does not correspond to the 1 dbar variability observed in the bench tests. The cause of the variability in the bench tests has been identified as an error in the tests. During these tests, the pressure reading from the transfer standard is manually reset to zero at the initial pressure of the test. This initial pressure is atmospheric pressure only, without any pressure added to the CTD or standard. The pressure offset on the third column of Table 2.1 is the CTD-standard difference at this pressure, and is expected to have only slight variations between tests due to atmospheric pressure. The problem was that during the tests conducted prior to 1998 a residual pressure due to fluid remaining in the

pipes and pump of the testing arrangement was inadvertently affecting this initial pressure. We have confirmed that this residual pressure can reach values of at least 0.6 dbar. The pressure tests have been modified to ensure that the initial test pressure is not affected by any residual pressure by disconnecting all pipes from the CTD and standard (e.g. during the September 1998 calibrations in Table 2.1). Values of the 0-dbar CTD offset obtained prior to 1998 reported here (Table 2.1), and in previous data reports are questionable at best, and can not be used to evaluate its variability. However this variability can be evaluated from the on-deck pressures obtained during cruises.

The on-deck pressure remained nearly constant during 1996 and the first half of 1997 (Figure 2.1), with small variability between cruises probably due to atmospheric pressure. A gradual decrease of about 0.2 dbar is observed during the second half of 1997, followed by nearly constant values during the first half of 1998. This small drift appears to be normal for the sensor.

The results of pressure offset between 0 and 4500 dbar, and hysteresis (Table 2.1) were not affected by the problem in the bench tests described above. The 0-4500 dbar offset has remained nearly constant for sensor #26448, with a 0.2 dbar increase between June 1997 and September 1998. The hysteresis is about 0.2 dbar. This value is larger than the difference between before and after cast pressures from Figure 2.1 because the bench tests reach 4500 dbar, while most of the cruise casts only reach 1020 dbar. The 0-4500 dbar offset has been nearly constant for sensor #51412, with a slight increase in June 1997 and September 1998. The hysteresis has remained small and constant.

Table 2.1: CTD Pressure Calibrations (decibars)

Calibration Date	Offset @ 0 dbar	0-4500 dbar offset	Hysteresis
Sea-Bird SBE-911 Plus #91361 / Pressure Transducer #26448			
31 January 1997	-5.4	1.35	0.2
12 June 1997	-6.7	1.4	0.2
11 September 1998	-6.2	1.6	0.2
Sea-Bird SBE-911 Plus #92859 / Pressure Transducer #51412			
31 January 1997	0.0	1.25	0.2
12 June 1997	-0.7	1.5	0.2
14 September 1998	0.1	1.6	0.2

2.1.2.2. Temperature

Three Sea-Bird SBE-3-02/F temperature transducers, #741, #1416 and #1591, and two new generation transducers (SBE-3-plus) #2202 and #2242, were used in 1997 and were calibrated at Sea-Bird after every cruise (Tupas et al. 1997), with the following exceptions. In May, only sensors #2202 and #2242 were calibrated because the others were taken on the HA-2A cruise; and in December, only sensors #1416, #2202 and #2242 were calibrated because the others were taken on cruise HA-3A. The SBE-3-plus sensors replaced two of our older sensors #886 and #961. The history of the sensors, as well as the procedures followed to obtain the sensor drift from the Sea-Bird calibrations are well-documented in Tupas et al. (1997). Calibration coefficients obtained at Sea-Bird after 1996 and used in the drift estimates are presented Table2.3. These coefficients were used in the following formula that gives the temperature (in °C) as a function of the frequency signal (f):

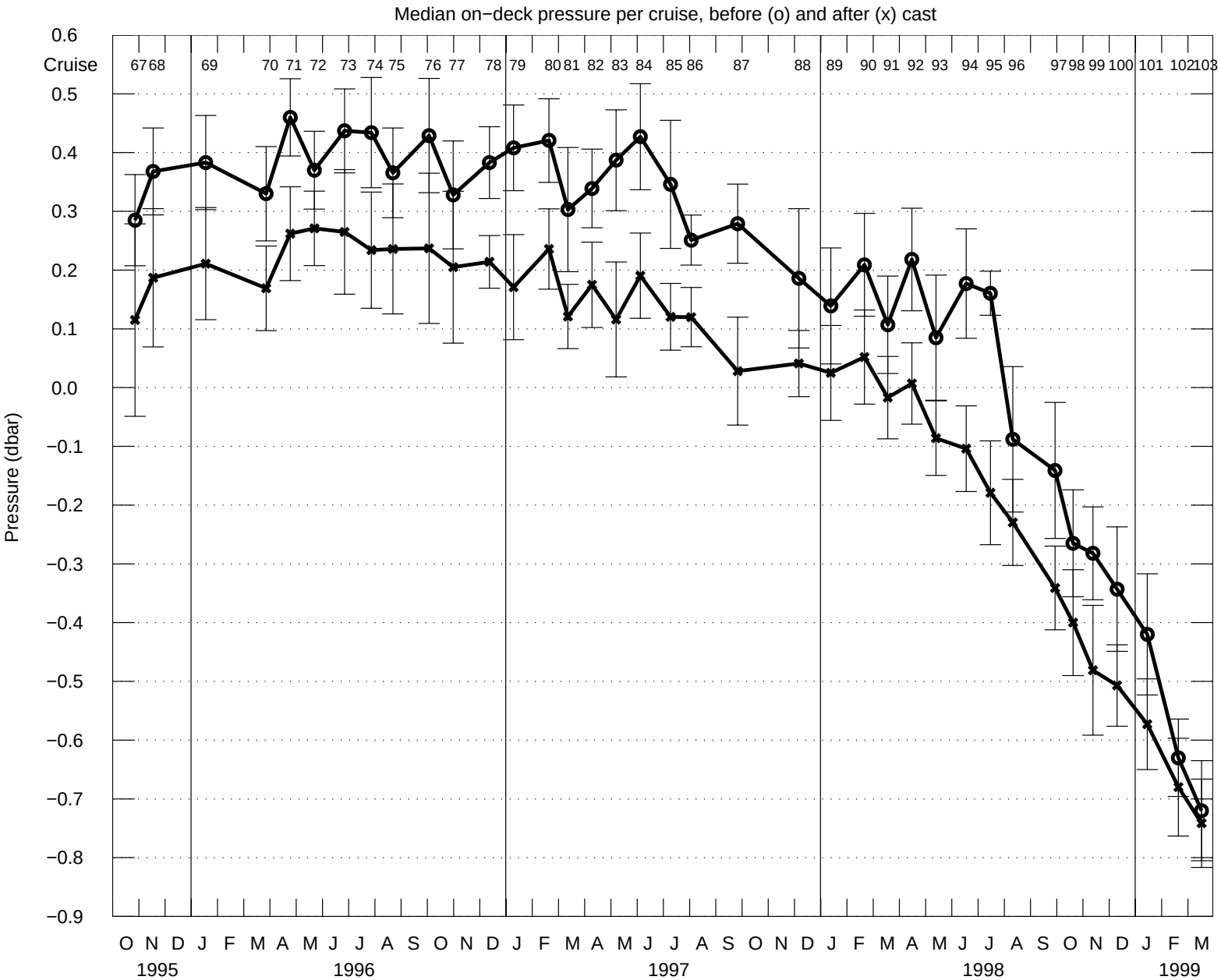

Figure 2.1: Median value of pressure on the ship's deck measured by the CTD pressure sensor before (circles) and after (crosses) each cast for HOT cruises 67-86. Error bars are 1 standard deviation from the mean. Cruise numbers are shown below the upper x-axis.

$$\text{temperature} = 1/\{a+b[\ln(f_0/f)]+c[\ln^2(f_0/f)]+d[\ln^3(f_0/f)]\}-273.15$$

For each sensor, the final calibration consists of two parts: first, a single "baseline" calibration is chosen from among the ensemble of calibrations during the year; second, for each cruise a temperature-independent offset is applied to remove the temporal trend due to sensor drift (Table 2.2). The offset, a linear function of time, is calculated by least squares fit to the 0-30 °C average of each calibration during the year. The maximum drift correction in 1997 was less than 1.6 x 10^{-3} °C. The baseline calibration is selected as the one for which the trend-corrected average from 0-5 °C is nearest to the ensemble mean of these averages.

A small residual pressure effect on the temperature sensors documented in Tupas et al. (1997) has been removed for measurements obtained with sensors #741, #1416 and #1591. Correction factors (k) for the new SBE-3-plus sensors were obtained from Sea-Bird and the temperatures were corrected for this effect. The corrected temperature (Tc) was calculated from the sensor temperature (T) and the pressure (P) as: Tc = T - kP. For sensor #2202, the pressure coefficient (k) was 0.83 x 10^{-3} °C / 5000 dbar and for sensor #2242, 0.33 x 10^{-3} °C / 5000 dbar

Another correction to our temperature measurements is for the viscous heating of the sensor tip due to the water flow. This correction is thoroughly documented in Tupas et al. (1997). Dual sensors were used during each of the 1997 cruises. The temperature differences between sensor pairs were calculated for each cast to evaluate the quality of the data, and to identify possible problems with the sensors. Means and standard deviations of the differences in 2-dbar bins were calculated from the ensemble of all casts at Station ALOHA for each cruise. Both sensors performed correctly during the 1997 cruises, showing temperature differences within expected values. The mean temperature difference as a function of pressure was typically less than 1 x 10^{-3} °C, with a standard deviation of less than 0.5 x 10^{-3} °C below 500 dbar. The largest variability was observed in the thermocline, with standard deviation values of up to 5 x 10^{-3} °C.

2.1.2.2.1. Sensor #741

This sensor was used as part of the dual-sensor configuration during cruises HOT-83 and 84, and during cruises HA-2A and 3A. The calibrations between September 1995 and February 1998 were used to calculate the sensor drift and the drift corrections. A linear fit to the 0-30 °C average offset from each calibration (Table 2.3) relative to 9 September 1995 gave an intercept of -1.07 x 10^{-4} °C with a slope of 1.265 x 10^{-6} °C day^{-1}. The RMS deviation of the offsets from this fit was 1.71 x 10^{-4} °C. The 23 January 1997 calibration was used as a baseline for the cruises. When corrected for linear drift to 15 May 1997 (the midpoint of the cruise dates), this calibration gave the smallest deviation in the 0-5 °C temperature range from the set of all calibrations used to determine the drift (also corrected for linear drift to 15 May 1997). The mean deviation of this calibration was -2.1 x 10^{-5} °C with a range of variation of less than 2 x 10^{-5} °C. The set of all calibrations had deviations in the range ± 5 x10^{-4} °C. The resulting drift corrections for each cruise were very small and inconsequential (Table 2.2).

2.1.2.2.2. Sensor #1416

This sensor was used during cruises HOT-79, 81, 82, and 88. The calibrations after November 1994 revealed a decay in the sensor's drift after March 1996, therefore the calibrations from April 1996 through February 1998 were used to calculate a sensor drift of 2.89 x 10^{-6} °C day^{-1} with a 2.29 x 10^{-5} °C intercept and 1.4 x 10^{-4} °C RMS residual. The 27 March 1997

calibration was used as baseline for the cruises. This calibration yielded the smallest 0-5 °C mean deviation from the others, all drift-corrected to 1 July 1997 (midpoint date between the cruises). The deviation was -2.34 x 10^{-5} °C with less than 2 x 10^{-4} °C range of variation. The set of all calibrations had deviations in the range ± 6 x 10^{-4} °C.

2.1.2.2.3. Sensor #1591

This sensor was used during cruises HOT-80, and HA-2A and 3A. This sensor suffered a calibration shift of about 1 x 10^{-3} °C due to shock damage occurring when the CTD accidentally hit the bottom during the deep cast of HOT-80 (February 1997). The sensor was serviced at Sea-Bird after this cruise. The calibrations from February 1997 throughout February 1998 were used to calculate a sensor drift of 5.72 x 10^{-6} °C day^{-1} with a 1.2 x 10^{-4} °C intercept and 1.3 x 10^{-4} °C RMS residual. The 27 March 1997 calibration was used as baseline for the cruises. This calibration yielded the smallest 0-5 °C mean deviation from the others, all drift-corrected to 17 February 1997 (midpoint date between the cruises). The deviation was -7.9 x 10^{-6} °C with less than 1 x 10^{-4} °C range of variation. The set of all calibrations had deviations in the range ± 4 x 10^{-4} °C.

2.1.2.2.4. Sensor #2202

This is a new SBE-3-plus sensor acquired on 23 January 1997. The calibrations from December 1996 through October 1997 revealed a jump of 1 x 10^{-3} °C in the October calibration level. A Sea-Bird evaluation determined that the cause of the jump was in the sensor's oscillator and decided to replace the sensor by a new one (#2472). It was not determined what caused the problem in the oscillator. The calibrations before October 1997 were used to calculate a sensor drift of 5.6 x 10^{-7} °C day^{-1} with a -9 x 10^{-5} °C intercept and 5.7 x 10^{-5} °C RMS residual. This drift was used to obtain the correction for cruises HOT-80, -83 through -87, and AC-2. The 17 June 1997 calibration was used as baseline for the cruises. This calibration yielded the smallest 0-5 °C mean deviation from the others, all drift-corrected to 1 July 1997 (midpoint date between the cruises). The deviation was 6.7 x 10^{-6} °C with less than 0.5 x 10^{-4} °C range of variation. The set of all calibrations had deviations in the range ± 1 x 10^{-4} °C. This sensor was used together with #1591 when the CTD accidentally hit the bottom during the deep cast of HOT-80, but unlike sensor #1591 this sensor did not show signs of shock damage during the post-cruise Sea-Bird evaluation. Because of the small drift of this sensor, the resulting drift corrections for each cruise were very small and not made (Table 2.2).

2.1.2.2.5. Sensor #2242

This is also a new SBE-3-plus sensor acquired on 23 January 1997, and was used during cruises HOT-79, 81, 82, 85 through 88, HA-1A, and AC-2. The calibrations from December 1996 through February 1998 were used to calculate a sensor drift of -1.45 x 10^{-7} °C day^{-1} with a -1.0 x 10^{-4} °C intercept and 7.7 x 10^{-5} °C RMS residual. The 22 April 1997 calibration was used as baseline for the cruises. This calibration yielded the smallest 0-5 °C mean deviation from the others, all drift-corrected to 1 July 1997 (midpoint date between the cruises). The deviation was 1.6 x 10^{-5} °C with less than 0.5 x 10^{-4} °C range of variation. The set of all calibrations had deviations in the range ± 2 x 10^{-4} °C. Because of the small drift of this sensor, the resulting drift corrections for each cruise were very small and inconsequential (Table 2.2).

Table 2.2: Temperature (T) and Conductivity (C) sensor corrections including the thermal inertia parameter (α). Dual temperature and conductivity sensors were used in all cruises

Cruise	T Sensor #	T Correction (°C)	C Sensor #	α	Data Reported
79	2242	-0.000015	1336	0.020	All casts
	1416	0.000228	679	0.028	
HA-1A	2242	0.000015	1336	0.020	All casts
	1416	-0.000214	619	0.028	
80	2202	0.000068	1336	0.028	All casts
	1591	0.000217	679	0.028	
81	2242	-0.000006	375	0.028	All casts
	1416	0.000043	527	0.028	
82	2242	-0.000002	375	0.028	All casts
	1416	0.000038	527	0.028	
83	2202	0.000024	375	0.028	All casts
	741	-0.000130	527	0.028	
HA-2A	1591	0.000309	375	0.028	All casts
	741	0.000148	527	0.028	
84	2202	0.000008	375	0.028	All casts
	741	-0.000166	527	0.028	
AC-2	2202	-0.000010	1336	0.028	All casts
	2242	-0.000130	679	0.028	
85	2202	-0.000008	1336	0.028	All casts
	2242	0.000010	679	0.028	
86	2202	-0.000026	1336	0.028	All casts
	2242	0.000015	679	0.028	
87	2202	-0.000057	1336	0.028	All casts
	2242	0.000023	679	0.028	
88	1416	-0.000730	1336	0.028	All casts
	2242	0.000033	679	0.028	
HA-3A	741	0.000420	1336	0.028	All casts
	1591	0.001539	679	0.028	

2.1.2.3. Conductivity

Four sensors were used during the 1997 cruises, #1336, #679, #375, and #527. The history of the sensors is well-documented in Tupas et al. (1993, 1994a, 1995, 1997) and Karl et al. (1996b). The dual sensor configurations are shown in Table 2.2. As mentioned earlier, only the data from the most reliable sensor (and its corresponding temperature sensor pair, as shown in Table 2.2) are reported here. Conductivity calibration coefficients are presented in Table 2.4.

Sensors #1336 and #679 were calibrated at Sea-Bird on 19 November 1996, #1336 was calibrated again on 19 March 1997, and #679 on 11 April 1997. Sensors #375 and #527 were calibrated on 20 December 1995, #375 was calibrated again on 8 July 1997, and #527 on 14 August 1997. Sea-Bird advised us not to use the December 1995 calibration as the base set of coefficients after they discovered an error in this calibration performed in artificial seawater. Cruises conducted with sensors #375 and #527 were calibrated using the respective July and August 1997 calibration coefficients.

Table 2.3: Calibration coefficients for Sea-Bird temperature sensors. RMSresiduals from calibration give an indication of quality of the calibration

SN	YYMMDD	f0	a	b	c	d	RMS(m°C)
741	980227	5937.67	3.68155355e-03	6.01994040e-04	1.56127096e-05	2.13185525e-06	0.04
741	980120	5937.88	3.68152817e-03	6.01978087e-04	1.55848283e-05	2.11141726e-06	0.03
741	971011	5937.40	3.68158707e-03	6.02001543e-04	1.56369587e-05	2.15194682e-06	0.03
741	970814	5937.56	3.68157069e-03	6.01992969e-04	1.56065229e-05	2.12451906e-06	0.03
741	970719	5937.58	3.68156604e-03	6.01981643e-04	1.55881395e-05	2.11335449e-06	0.03
741	970618	5937.05	3.68162509e-03	6.02003311e-04	1.56205933e-05	2.13264695e-06	0.04
741	970422	5937.48	3.68157965e-03	6.01978788e-04	1.55824628e-05	2.10869660e-06	0.03
741	970327	5937.01	3.68163293e-03	6.01987582e-04	1.55949123e-05	2.12273364e-06	0.04
741	970225	5937.46	3.68157907e-03	6.01973143e-04	1.55789001e-05	2.10920394e-06	0.04
741	970123	5937.30	3.68159674e-03	6.01976013e-04	1.55601695e-05	2.08726120e-06	0.04
1416	980227	6231.35	3.68155533e-03	6.01819740e-04	1.50117434e-05	2.11346853e-06	0.19
1416	980120	6231.51	3.68152843e-03	6.01783122e-04	1.49889428e-05	2.12875994e-06	0.16
1416	971219	6231.08	3.68157721e-03	6.01762309e-04	1.48775151e-05	2.03100076e-06	0.19
1416	971011	6231.00	3.68158587e-03	6.01772444e-04	1.49377973e-05	2.08917906e-06	0.19
1416	970814	6231.23	3.68157235e-03	6.01853380e-04	1.51359673e-05	2.21983366e-06	0.16
1416	970719	6231.25	3.68156775e-03	6.01841466e-04	1.51167227e-05	2.20814394e-06	0.17
1416	970618	6230.65	3.68162649e-03	6.01835345e-04	1.50897597e-05	2.18854432e-06	0.18
1416	970422	6231.04	3.68158040e-03	6.01796620e-04	1.50123091e-05	2.13406444e-06	0.18
1416	970327	6230.55	3.68163150e-03	6.01765744e-04	1.49244541e-05	2.07898363e-06	0.17
1416	970225	6231.13	3.68157972e-03	6.01817353e-04	1.50793324e-05	2.19439688e-06	0.14
1416	970123	6230.98	3.68159846e-03	6.01858312e-04	1.51837195e-05	2.27180519e-06	0.16
1591	980227	6256.23	3.68155034e-03	6.03679620e-04	1.48418484e-05	1.79773651e-06	0.26
1591	980120	6256.45	3.68152525e-03	6.03654640e-04	1.47921555e-05	1.75952226e-06	0.27
1591	971011	6255.94	3.68158417e-03	6.03709081e-04	1.49386474e-05	1.87766671e-06	0.26
1591	970814	6256.14	3.68156754e-03	6.03680911e-04	1.48545024e-05	1.81037002e-06	0.27
1591	970719	6256.16	3.68156291e-03	6.03661088e-04	1.48254167e-05	1.78995672e-06	0.27
1591	970618	6255.64	3.68162198e-03	6.03703167e-04	1.49054785e-05	1.84097502e-06	0.28
1591	970422	6256.09	3.68157658e-03	6.03656520e-04	1.48263935e-05	1.79425815e-06	0.27
1591	970327	6255.60	3.68162986e-03	6.03686755e-04	1.48793841e-05	1.82713638e-06	0.27
1591	970225	6256.11	3.68157605e-03	6.03656202e-04	1.48601219e-05	1.83218305e-06	0.26
2202	970814	2968.63	3.68019120e-03	6.02995851e-04	1.61962772e-05	2.21877145e-06	0.04
2202	970719	2968.59	3.68019824e-03	6.02994411e-04	1.61961530e-05	2.22144396e-06	0.04
2202	970617	2968.88	3.68014035e-03	6.02993776e-04	1.62033114e-05	2.22796573e-06	0.03
2202	970516	2968.62	3.68019379e-03	6.02993105e-04	1.61911389e-05	2.21784264e-06	0.04
2202	970422	2968.74	3.68016692e-03	6.02989318e-04	1.61805853e-05	2.20315239e-06	0.04
2202	970327	2968.51	3.68021601e-03	6.02995947e-04	1.61898007e-05	2.21149121e-06	0.04
2202	970225	2968.62	3.68019466e-03	6.02994808e-04	1.61858016e-05	2.21016942e-06	0.04
2202	970123	2968.38	3.68024262e-03	6.03001310e-04	1.62034095e-05	2.22387840e-06	0.04
2202	961228	2968.70	3.68017660e-03	6.02999214e-04	1.62045475e-05	2.22619235e-06	0.03
2242	980228	3002.69	3.68017837e-03	6.02889500e-04	1.62591006e-05	2.23335519e-06	0.04
2242	980204	3002.67	3.68018463e-03	6.02881695e-04	1.62314439e-05	2.20937359e-06	0.05
2242	980121	3002.68	3.68018425e-03	6.02885383e-04	1.62412759e-05	2.21882373e-06	0.05
2242	971222	3002.89	3.68014113e-03	6.02897379e-04	1.62838656e-05	2.25600235e-06	0.05
2242	971011	3002.52	3.68021275e-03	6.02884183e-04	1.62401228e-05	2.21905232e-06	0.05
2242	970814	3002.63	3.68019064e-03	6.02894703e-04	1.62751779e-05	2.24821286e-06	0.05
2242	970719	3002.59	3.68019779e-03	6.02895515e-04	1.62821406e-05	2.25501601e-06	0.05
2242	970617	3002.88	3.68014000e-03	6.02882288e-04	1.62548552e-05	2.23587965e-06	0.04
2242	970516	3002.61	3.68019349e-03	6.02878947e-04	1.62387417e-05	2.22256897e-06	0.05
2242	970422	3002.75	3.68016652e-03	6.02879872e-04	1.62417832e-05	2.21932817e-06	0.05
2242	970327	3002.51	3.68021569e-03	6.02887921e-04	1.62540902e-05	2.22923913e-06	0.05
2242	970225	3002.62	3.68019471e-03	6.02888847e-04	1.62475646e-05	2.22115871e-06	0.04
2242	970123	3002.37	3.68024236e-03	6.02888917e-04	1.62589053e-05	2.23400807e-06	0.05
2242	961224	3002.59	3.68019613e-03	6.02898623e-04	1.62986473e-05	2.27081770e-06	0.04
1392	970828	2576.16	3.64747596e-03	5.86289957e-04	9.10581188e-06	-2.15221262e-06	0.20
1392	970820	2576.19	3.64745926e-03	5.86425192e-04	9.88233281e-06	-1.36482724e-06	0.35
2045	980728	2447.02	3.64664780e-03	5.89941753e-04	1.00854316e-05	-3.65944937e-07	0.43
1496	980716	5947.26	3.68153908e-03	5.89975419e-04	1.46589621e-05	2.88623586e-06	0.20

A conductivity offset between the down- and the up-cast was observed during the deep cast of HOT-80. This offset was caused by mud ingestion by the conductivity cells after the CTD

accidentally hit the bottom. The offset was about 3 x 10^{-4} Siemens m^{-1} for sensor #1336, and 6 x 10^{-4} Siemens m^{-1} for #679, with lower up-cast conductivities compared to the down-cast. A post-cruise Sea-Bird evaluation of sensor #1336 showed no cracks on the sensor, and the offset towards lower conductivities (typical of mud/sediment ingestion by conductivity cells) indicated that both sensors were healthy (a crack in the cell would have produced an offset to higher conductivities). The up-cast conductivities near the surface seemed to recover to the down-cast values for both sensors, suggesting that the mud was washing out of the cell. This problem did not affect the data reported here for this cast because we only use the data from the down-cast. The up-cast offset was corrected for both sensors in order to have a reliable CTD salinity calibration (which uses up-cast CTD data at each bottle-trip level) versus bottle salinities. Comparison against bottle data in subsequent casts indicated that the offset disappeared after this cast.

A small residual pressure effect on sensor #1336 was corrected following procedures recommended by Sea-Bird and described in Tupas et al. (1997). The nominal calibrations were used for data acquisition. Final calibration was determined empirically from salinities of discrete water samples acquired during each cast. Prior to empirical calibration, conductivity was corrected for thermal inertia (α) of the glass conductivity cell as described in Chiswell et al. (1990). Table 2.2 lists the value of used for each cruise.

Preliminary screening of bottle samples and empirical calibration of the conductivity cell are described in Tupas et al. (1997). For cruises HOT-79 through -88, the standard deviation cutoff values for screening of bottle samples were: 0.0035 (0-150 dbar), 0.0049 (151-500 dbar), 0.0022 (501- 1050 dbar), and 0.0012 (1051-5000 dbar). The conductivity calibration coefficients (b0, b1, b2) resulting from the least squares fit ($\Delta C = b0 + b1C + b2C^2$) to the CTD minus bottle conductivities (ΔC) as a function of conductivity (C) are given in Table 2.4. The quality of the CTD calibration is illustrated in Figure 2.2, which shows the differences between the corrected CTD salinities and the bottle salinities used for calibration as a function of pressure for each cruise. The calibrations are best below 500 dbar because the weaker vertical salinity gradients at depth lead to less error when the bottle and CTD pressures are slightly mismatched.

The final step of conductivity calibration was a cast-dependent bias correction as described in Tupas et al. (1993) to allow for drift during each cruise or for sudden offsets due to fouling (Table 2.5). Note that a change of 1 x 10^{-4} Siemens m^{-1} in conductivity was approximately equivalent to 0.001 in salinity. Table 2.6 gives the mean and standard deviations for the final calibrated CTD minus water sample values.

Conductivity differences between sensor pairs were calculated the same way as the temperature sensors. The range of variability as a function of pressure was about $\pm$ 1 x 10^{-4} Siemens m^{-1}, with a standard deviation of less than 0.5 x 10^{-4} Siemens m^{-1} below 500 dbar, from the ensemble of all the cruise casts. The largest variability was in the halocline, with standard deviations reaching up to 5 x 10^{-4} Siemens m^{-1} between 50 and 300 dbar.

Table 2.4: Conductivity calibration coefficients

Cruise	Sensor #	b_0	b_1	b_2
79	1336	0.009263	-0.004394	0.000479
	679	0.007725	-0.003587	0.000377
HA-1A	1336	0.000319	-0.000248	0.000000
	679	0.000834	-0.000367	0.000000
80	1336	0.000722	-0.000250	0.000000
	679	0.000667	-0.000298	0.000000
81	375	0.001159	-0.000300	0.000000
	527	0.001224	-0.000265	0.000000
82	375	0.003282	-0.001439	0.000147
	527	0.005706	-0.002553	0.000280
83	375	0.002567	-0.001064	0.000095
	527	0.002857	-0.001219	0.000126
HA-2A	375	-0.001260	-0.000022	0.000000
	527	-0.001011	-0.000139	0.000000
84	375	0.003120	-0.001329	0.000117
	527	0.002099	-0.000881	0.000069
AC-2	1336	0.000872	-0.000322	0.000000
	679	0.001247	-0.000375	0.000000
85	1336	0.001085	-0.000419	0.000000
	679	0.001380	-0.000432	0.000000
86	1336	0.000756	-0.000329	0.000000
	679	0.001163	-0.000378	0.000000
87	1336	0.001829	-0.000840	0.000054
	679	0.003960	-0.001766	0.000158
88	1336	0.002747	-0.001450	0.000107
	679	0.003502	-0.001659	0.000129
HA-3A	1336	0.000746	-0.000501	0.000000
	679	0.001300	-0.000735	0.000000

Table 2.5: Individual cast conductivity corrections (units are Siemens m^{-1})

Cruise	Station	Cast	C correction
80	2	1	-0.00010198
80	2	2	-0.00012904
80	2	3	0.00020300
80	2	6	0.00015234
80	2	15	0.00024606
81	2	1	0.00009606
HA-2A	8	1	0.00008095
86	1	1	0.00015888
86	2	7	0.00011704
86	2	13	-0.00005598

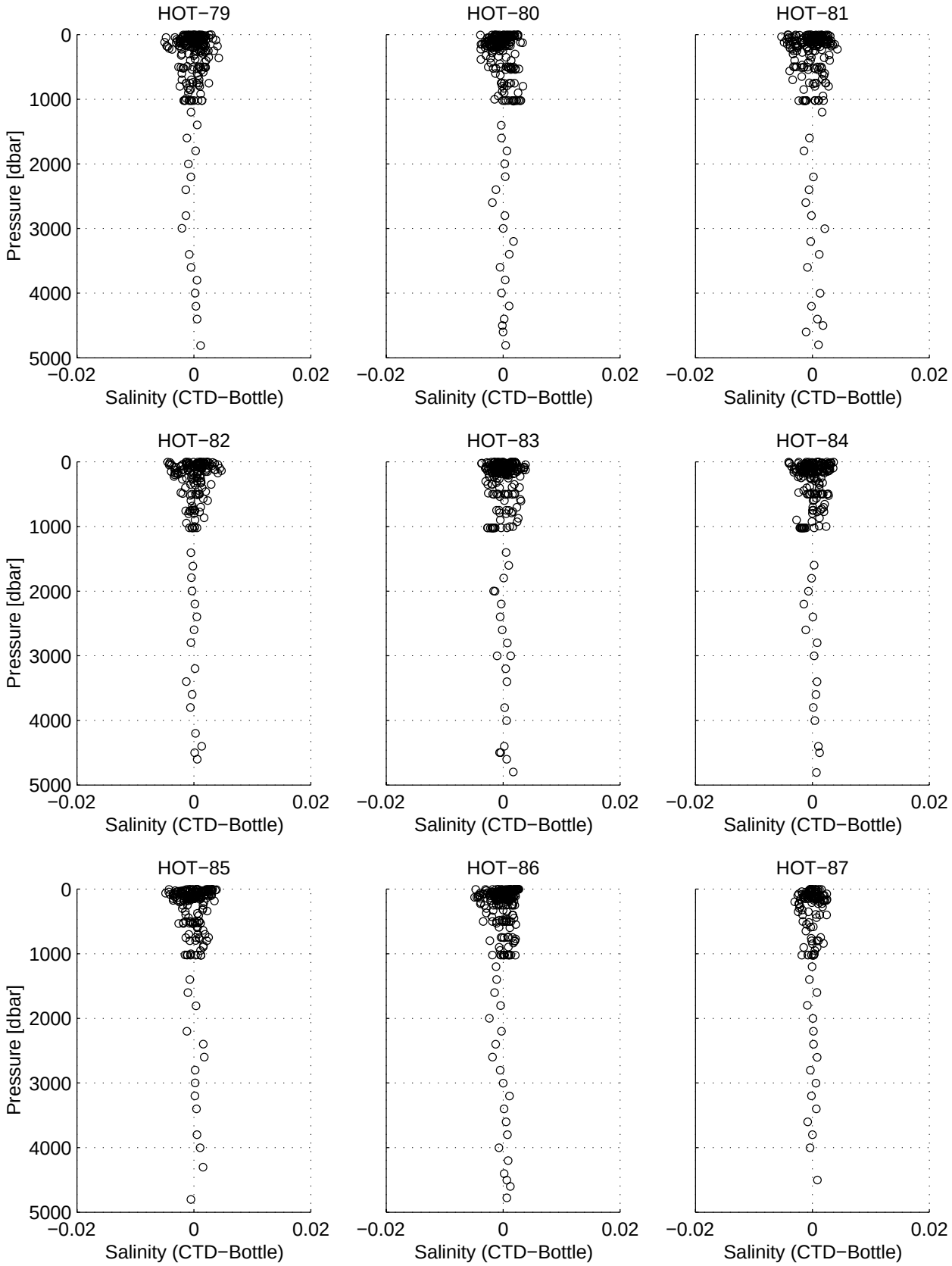

Figure 2.2: Difference between calibrated CTD salinities and bottle salinities for each cruise and all casts at Station ALOHA in 1997.

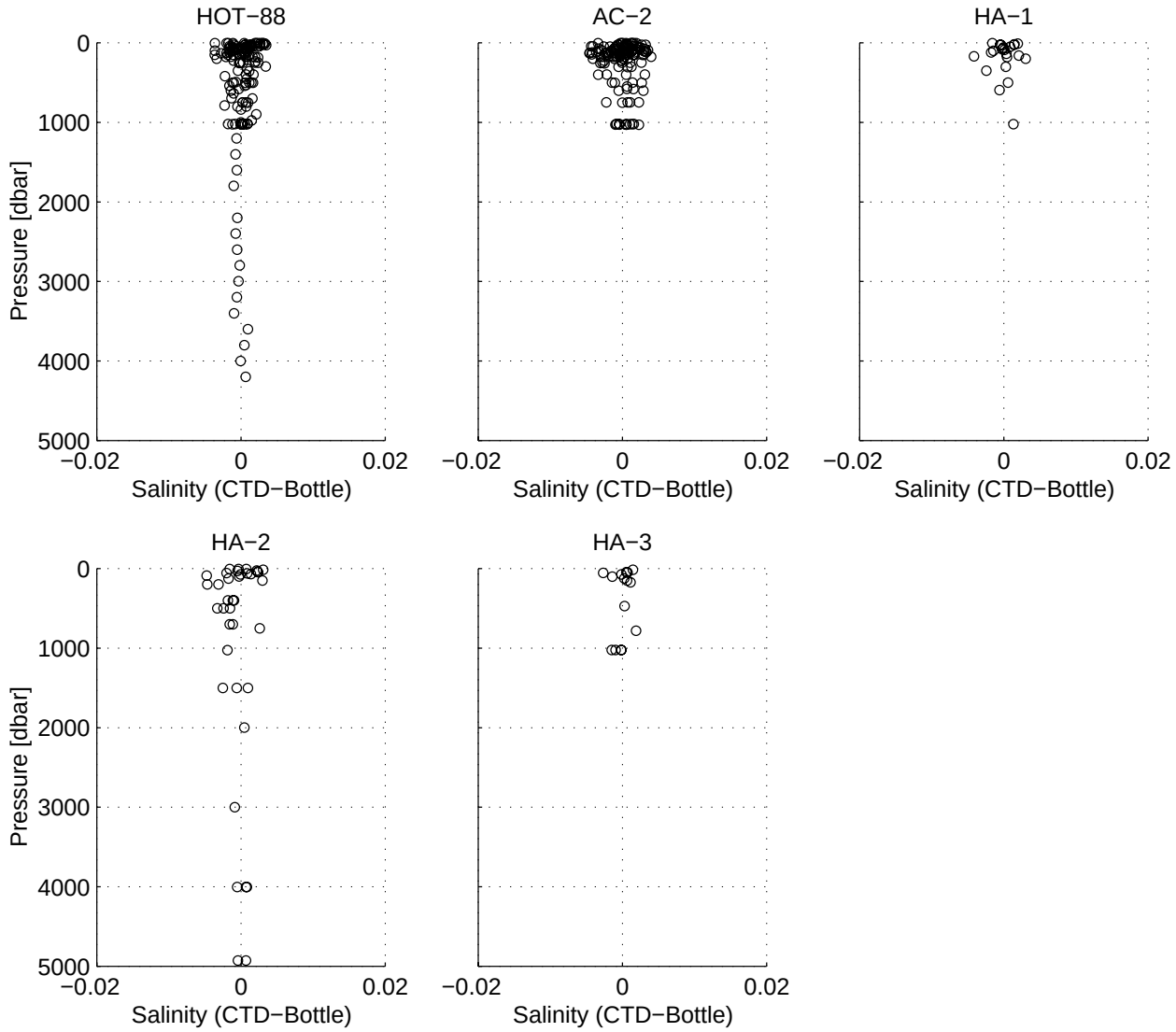

Figure 2.2: continued

Table 2.6: CTD-Bottle salinity comparison for each cruise

Cruise	Sensor #	0 to 4700 dbar		500 to 4700 dbar	
		Mean	SD	Mean	SD
79	1336	-0.0000	0.0016	-0.0001	0.0013
	679	-0.0000	0.0017	-0.0001	0.0016
HA-1A	1336	0.0000	0.0016	0.0004	0.0014
	679	-0.0000	0.0019	-0.0002	0.0024
80	1336	-0.0000	0.0016	0.0007	0.0012
	679	-0.0001	0.0018	0.0005	0.0011
81	375	-0.0001	0.0020	-0.0001	0.0016
	527	-0.0001	0.0022	-0.0000	0.0017
82	375	0.0000	0.0018	0.0000	0.0008
	527	-0.0000	0.0020	-0.0002	0.0012
83	375	0.0000	0.0013	0.0001	0.0009
	527	-0.0000	0.0016	0.0001	0.0014
HA-2A	375	-0.0005	0.0020	-0.0004	0.0014
	527	-0.0002	0.0017	-0.0004	0.0014
84	375	-0.0000	0.0015	0.0000	0.0010
	527	-0.0000	0.0017	-0.0001	0.0013
AC-2	1336	0.0000	0.0019	0.0005	0.0013
	679	0.0000	0.0020	0.0005	0.0013
85	1336	0.0000	0.0016	0.0001	0.0011
	679	0.0000	0.0017	0.0001	0.0011
86	1336	-0.0001	0.0013	0.0002	0.0010
	679	-0.0001	0.0016	0.0001	0.0012
87	1336	0.0000	0.0015	0.0000	0.0010
	679	0.0000	0.0012	0.0000	0.0009
88	1336	-0.0000	0.0015	-0.0001	0.0010
	679	-0.0000	0.0016	-0.0001	0.0010
HA-3A	1336	-0.0000	0.0012	-0.0002	0.0013
	679	-0.0000	0.0013	-0.0003	0.0012

2.1.2.4. Oxygen

Two YSI Inc. dissolved oxygen probes (#13341 and #13251) were used in a dual-sensor configuration during the 1997 cruises. The history of the sensors is documented in in Tupas et al. (1993, 1994a, 1995, 1997) and Karl et al. (1996b). The regular maintenance procedure for these sensors includes inspection of their electrolyte level and membrane before each cruise. Both sensors had electrolyte added prior to HOT-80. Sensor #13251 started showing large values in its temperature channel during HOT-79, this problem was aggravated after the CTD hit the bottom during the deep cast of HOT-80. The sensor was repaired and calibrated at Sea-Bird on 24 April 1997. Sensor #13341 was also calibrated and inspected on 24 March 1997. This sensor was not affected by the CTD hitting the bottom during HOT-80.

Water bottle oxygen data were screened and the sensors were empirically calibrated following procedures described previously (Tupas et al. 1997). Analysis of water bottle samples is described in section 2.6.1. The calibration procedure follows Owens and Millard (1985), and consists of fitting a non-linear equation to the CTD oxygen current and oxygen temperature. The bottle values of dissolved oxygen and the downcast CTD observations at the potential density of each bottle trip were grouped together for each cruise to find the best set of parameters with a

non-linear least squares algorithm. Three sets of parameters were usually obtained per HOT cruise, corresponding to the casts at Stations 1, 2 and 8. Casts from HA-1A and 2A were calibrated with bottle data obtained during these cruises. HA-3A did not have enough bottles for a calibration and was calibrated with coefficients from the following HOT-88 cruise. One set of calibration coefficients was obtained to calibrate the 5 stations of AC-2 cruise. Tables 2.7 and 2.8 gives the means and standard deviations for the final calibrated CTD oxygen minus water sample values from the various CTD stations.

Table 2.7: CTD-Bottle dissolved oxygen per cruise (µmol kg^{-1})

		Station 1, Kahe Point		Station 2, ALOHA			
		0 to 1500 dbar		0 to 4700 dbar		500 to 4700 dbar	
Cruise	Sensor #	Mean	SD	Mean	SD	Mean	SD
79	13251	0.00	1.22	0.07	1.07	0.21	1.07
80	13341	0.00	1.61	0.02	1.64	0.15	1.26
81	13341	0.00	0.00	-0.05	1.51	0.02	1.15
82	13341	0.03	1.62	0.07	1.77	0.18	1.57
83	13341	0.02	1.81	0.00	1.92	0.17	1.67
84	13251	0.00	0.51	0.05	1.29	0.06	0.75
85	13251	0.01	1.42	0.13	1.10	0.28	1.00
86	13251	0.00	1.08	0.11	1.28	0.40	1.14
87	13251	No Data	No Data	0.08	1.32	0.15	1.06
88	13251	0.01	0.88	0.08	0.97	0.08	0.69

Table 2.8: CTD-Bottle dissolved oxygen at HALE ALOHA and AC-2 (µmol kg^{-1})

		0-1500 dbars	
Cruise	Sensor #	Mean	SD
HA-1A	13251	0.01	0.68
80	13341	0.07	1.14
81	13341	0.00	1.03
82	13341	0.07	1.63
83	13341	-0.02	0.55
HA-2A	13251	0.00	0.16
84	13251	0.00	0.56
85	13251	0.00	0.10
86	13251	0.00	0.42
87	13251	0.00	0.02
88	13251	0.00	0.08
AC-2	13251	0.01	1.46

2.1.3. Discrete salinity

Salinity samples were collected, stored and analyzed as described in Tupas et al. (1993). Samples from a large batch of “secondary standard” seawater were measured after every 24 to 36 bottle samples to detect drift in the salinometer for each cruise. Standard deviations of the secondary standard measurements were always less than ± 0.001 (Table 2.9). Secondary standard

seawater batches are made from 60 liters of seawater taken from a depth of 1000 m from Station ALOHA. Secondary standard batch #13 was prepared in October 1996, batch #14 was prepared in March 1997 and batch #15 was prepared in July 1997.

Table 2.9: Precision of salinity measurements using lab standards

Cruise	Mean Salinity ± SD	# Samples*	Substandard Batch #	IAPSO Batch #
79	34.44583 ± 0.00079	23	13	p128
HA-1A	34.44583 ± 0.00079	23	13	p128
80	34.44505 ± 0.00061	22	13	p128, p130
81	34.49307 ± 0.00044	25	14	p130
82	34.49249 ± 0.00029	17	14	p130
83	34.49241 ± 0.00049	23	14	p130
HA-2A	34.49183 ± 0.00034	4	14	p130
84	34.49239 ± 0.00070	20	14	p130
AC-2	34.49181 ± 0.00083	22	15	p130
85	34.49320 ± 0.00070	22	15	p130
86	34.49184 ± 0.00084	22	15	P128
87	34.48876 ± 0.00058	12	15	p128, p130
88	34.48998 ± 0.00070	13	15	p130
HA-3A	34.48900 ± 0.00042	2	15	p132

*Number of secondary standard salinity samples measured during each run.

2.2 Thermosalinograph

2.2.1 Data acquisition

SBE-21 Seacat thermosalinograph systems were used aboard R/V *Moana Wave* for HOT-79 through HOT-86, HOT-88, AC-2, HA-1A, HA-2A, HA-2B and HA-3A cruises. Seacat thermosalinograph sensor #1392 (comprised of one temperature and one conductivity sensor) was used for HOT-79 through HOT-86, AC-2, HA-1A and HA-2A. HOT-88, HA-2B and HA-3A used Seacat thermosalinograph sensor #2045 (also comprised of one temperature and one conductivity sensor). The thermosalinographs were installed in a pumped intake line in the hull of the R/V *Moana Wave* with an intake depth of about 3 m. Near the start of the intake line, a Sea-Bird remote temperature sensor, installed in a sea chest in the bow of the ship, recorded temperature data. This location allows for relatively undisturbed water to enter the thermosalinograph. All cruises aboard R/V *Moana Wave* during 1997 used Sea-Bird remote temperature sensor #1496. The SBE-21 Seacat thermosalinograph is used to calculate salinity using an internal temperature and conductivity sensor. Data were obtained every 10 seconds. In order to calibrate the conductivity sensor, bottle salinity samples were periodically taken from the thermosalinograph intake line. To calculate salinity, a pressure of 20 dbar was assumed to compensate for the pressure caused by the pump for the intake line (30 psi). Approximately 13 hours of data were not recorded during HOT-88 as bad weather caused the shutdown of the thermosalinograph system for about 13 hours. When large seas are encountered, the heaving of

the ship causes bubbles to be introduced into the thermosalinograph system which disrupts its operation and sometimes the system must be shut down to avoid damage.

HOT-87 thermosalinograph data were collected using a Falmouth Scientific Inc. (FSI) thermosalinograph system aboard R/V *Roger Revelle*. This system utilizes two separate sets of temperature and conductivity sensors. The first set (temperature sensor #1381, conductivity sensor #1360) is located near one of the laboratories in order to best obtain salinity samples to calibrate the system. To calculate salinity, a pressure of 7 dbar was assumed to compensate for the pressure caused by the pump for the intake line. The second set of temperature and conductivity sensors (#1382 and #1361, respectively) is located near the bow of the ship collecting water near about 5 m depth in order to obtain a clean, near-surface temperature signal. Data were obtained every 15 seconds.

2.2.2 Data processing and sensor calibration

2.2.2.1 Nominal Calibration

2.2.2.1.1. Temperature

The Sea-Bird internal temperature sensors (#1392 and #2045) and external temperature sensor (#1496) used aboard R/V *Moana Wave* were calibrated at Sea-Bird. The calibration coefficients obtained at Sea-Bird are given in Table 2.3. Since these sensors are the same type as used for the CTD measurements, the same procedure for drift estimation was followed. Temperature drift corrections are presented in Table 2.10.

For the two FSI temperature sensors (#1381 and #1382) used aboard R/V *Roger Revelle* during HOT-87, the ship's scientific support staff supplied equations with correction factors in order to convert the raw temperature into a final data set (Jim Charters, personal communication, 1997).

For sensor #1392, a drift rate of -3.1 x 10-6 °C day^{-1} was determined using the 29 September 1994, 13 October 1995, 20 August 1997 and 28 August 1997 calibrations. The 29 September 1994 calibration was performed after the sensor's electronics had been reworked. This sort of work usually causes a change in the drift of a sensor so the calibrations prior to this date were not used for drift calculation purposes. All the cruises which used internal temperature sensor #1392 (HOT-79 through HOT-86, AC-2, HA-1A and HA-2A) calculated temperatures using the 13 October 1995 baseline calibration.

A temperature drift rate of 9.6 x 10-6 °C day^{-1} was determined using the 2 November 1993, 18 January 1996 and 16 July 1998 calibrations for Sea-Bird remote temperature sensor #1496. Temperatures were calculated with the 18 January 1996 baseline calibration. For internal Sea-Bird temperature sensor #2045, a drift rate of -1.7 x 10^{-8} °C day^{-1} was determined using the 11 October 1995, 30 July 1996 and 28 July 1998 calibrations. Temperatures were calculated with the 30 July 1996 baseline calibration. Drift corrections, however, were not applied to the data as they are very small and inconsequential.

The following equation was given to convert the raw FSI temperature data into final temperature values: $T_{final} = (a * T^3_{raw}) + (b * T^2_{raw}) + (c * T_{raw}) + d$. For FSI sensor #1381, a = 2.26469 x 10^{-7}, b = -6.97975 x 10^{-7}, c = -1.40255 x $10^{-4}$and d = 2.30316 x 10^{-3}. These conversion values were based on a calibration conducted from August 9-10, 1997. The same equation as listed above for FSI sensor #1381 was used to convert the raw FSI temperature data for sensor #1382 into final values. However, for sensor #1382, a = -2.68710 x 10^{-7}, b = 1.2739 x 10^{-5}, c = -2.8031 x 10^{-4} and d = -4.26808 x 10^{-3}. These conversion values were based on a calibration conducted from July 25-31, 1997.

2.2.2.1.2. Conductivity

Sea-Bird conductivity sensor #1392 was used aboard R/V *Moana Wave* to collect thermosalinograph conductivity data for HOT-79 through HOT-86 as well as AC-2, HA-1A and HA-2A. Conductivity sensor #2045 was used to collect thermosalinograph conductivity data for HOT-88, HA-2B and HA-3A. For sensor #1392, all conductivity data were nominally calibrated with coefficients obtained at Sea-Bird on 13 October 1995. For sensor #2045, all conductivity data were nominally calibrated with coefficients which were also obtained at Sea-Bird on 30 July 1996. The raw data from the FSI conductivity sensors (#1360 and #1361) used aboard R/*V Roger Revelle* for HOT-87 were converted with equations and correction factors supplied by the ship's scientific support staff (Jim Charters, personal communication, 1997). However, all the final salinity data reported here (from both the Sea-Bird and FSI sensors) were calibrated against bottle data as explained in Section 2.2.2.3.

Table 2.10: Thermosalinograph temperature drift corrections

Cruise	Sensor #1392	Sensor #1496	Sensor #2045*
79	-1.4×10^{-3}	3.4×10^{-3}	n/a
HA-1A	-1.4×10^{-3}	3.4×10^{-3}	n/a
80	-1.5×10^{-3}	3.8×10^{-3}	n/a
81	-1.6×10^{-3}	4.0×10^{-3}	n/a
82	-1.7×10^{-3}	4.3×10^{-3}	n/a
83	-1.8×10^{-3}	4.5×10^{-3}	n/a
HA-2A	-1.8×10^{-3}	4.7×10^{-3}	n/a
84	-1.9×10^{-3}	4.8×10^{-3}	n/a
AC2	-1.9×10^{-3}	5.0×10^{-3}	n/a
85	-2.0×10^{-3}	5.2×10^{-3}	n/a
86	-2.0×10^{-3}	5.4×10^{-3}	n/a
HA-2B	n/a	6.6×10^{-3}	-8.2×10^{-6}
88	n/a	6.6×10^{-3}	-8.3×10^{-6}
HA-3B	n/a	6.7×10^{-3}	-8.6×10^{-6}

*Sensor #2045 corrections were not used.

2.2.2.2 Processing

The thermosalinograph data were screened for gross errors with upper and lower bounds of 35 °C and 18 °C for temperature and 6 Siemens m^{-1} and 3 Siemens m^{-1} for conductivity. There were no gross errors detected for any of the 1997 cruises. Despite the lack of gross errors, some data have been considered possibly bad. These could be ascribed to such factors as biological fouling of the thermosalinograph, widely varying pump speeds, etc. Hence, a quality control system has been established so that each temperature and salinity point is given a flag to determine whether the data are good, suspect or bad to aid any data user.

A 5-point running median filter was used to detect one or two point temperature and conductivity glitches in the thermosalinograph data. Glitches in temperature and conductivity detected by the 5-point median filter were immediately replaced by the median. Threshold values of 0.3 °C for temperature and 0.1 Siemens m^{-1} for conductivity were used for the median filter. No more than a few points were replaced after running the median filter for each cruise. A 3-

point triangular running mean filter was used to smooth the temperature and conductivity data from all the cruises after they had gone through glitch detection.

2.2.2.3 Empirical Calibration

The thermosalinograph salinity was calibrated empirically by comparing it to bottle salinity samples drawn from the plumbing near the thermosalinograph. Bottle salinity samples were analyzed as described in Section 2.1.3.

For R/V *Moana Wave* the time delay between the water passing through the thermosalinograph and it reaching the bottle sampling area was determined to be about 50 seconds using autocorrelation between bottle and thermosalinograph samples. The thermosalinograph data were extracted within ± 15 seconds around the sample time minus the 50 second delay for the comparison with the bottle data. For R/V *Roger Revelle*, the thermosalinograph used to calculate salinity was located immediately next to the bottle sampling area. Thus, a time delay was not required and thermosalinograph data were simply extracted within ± 15 seconds around the sample time.

As in previously reported cruises (Tupas et al. 1997) a cubic spline was fit to the time-series of the differences between the bottle conductivity and the thermosalinograph conductivity separately for all the 1997 cruises. The correction of the thermosalinograph conductivities was obtained from the cubic spline fit. Salinity was calculated using these corrected conductivities, thermosalinograph temperatures and either a pressure of 20 dbar (for those cruises aboard R/V *Moana Wave*) or 7 dbar (for HOT-87 aboard R/V *Roger Revelle*). The mean values for the salinity bottle minus final calibrated thermosalinograph were less than $\pm 1 \times 10^{-4}$ for each cruise except for HOT-82 and HOT-83. The mean salinity bottle minus final calibrated thermosalinograph values for these two cruises were -6.09×10^{-4} and 2.11×10^{-4} respectively. HOT-82 experienced a large (nearly 0.01) and sudden offset at the end of the cruise between the salinity bottles and the uncalibrated thermosalinograph. This condition continued into HOT-83 until the differences between the salinity bottles and the uncalibrated thermosalinograph suddenly returned to normal values. The thermosalinograph data sampled during the times with the large offset between the salinity bottles and the uncalibrated thermosalinograph for HOT-82 and HOT-83 were corrected by using a mean salinity bottle minus thermosalingraph offset but were flagged as suspect as a cause of the offset could not be determined.

Table 2.11 gives the standard deviations for the salinity bottle minus final calibrated thermosalinograph values for all the cruises. HOT-87 shows a very large standard deviation compared to the other cruises. During the cruise aboard R/V Roger Revelle, the engine room made a change in the way it was using seawater to cool the ship's engine. This cooling water is the seawater which the internal thermosalinograph conductivity sensor uses to measure salinity. Once the engine room changed the engine cooling process, the thermosalinograph salinity data (and therefore the bottle salinity - thermosalinograph comparison) became very noisy and spiked. The change in the engine cooling process must have involved a change in the pumping rate/pressure of the intake water thus affecting the thermosalinograph salinity data. These data had to be flagged as suspect.

2.2.2.4 Comparison with CTD Data

The corrected thermosalinograph salinity data were compared with the downcast CTD salinity at 4 dbar for the purpose of checking the calibration. This procedure was conducted in

the same manner as previously reported HOT cruises (Tupas et al. 1997). The thermosalinograph data were averaged using data sampled one minute after the acquisition time of the CTD sample.

Table 2.11: Bottle-Thermosalinograph salinity comparison

Cruise	Sensor #	Standard Deviation
79	1392	0.0015
HA-1A	1392	0.0005
80	1392	0.0020
81	1392	0.0074
82	1392	0.0073
83	1392	0.0018
HA-2A	1392	0.0023
84	1392	0.0011
AC2	1392	0.0031
85	1392	0.0029
86	1392	0.0016
87	1392	0.0091
HA-3A	2045	0.0031
88	2045	0.0021
HA-3B	2045	0.0034

2.3. Inverted Echo Sounder

The history of the IESs in the HOT site is well documented in Tupas et al. (1997). One IES (#126) was deployed on 28 October 1996 in the center of the ALOHA station, but could not be retrieved as planned on 11 July 1997, during HOT-85. During this cruise, the IES was contacted with the hydrophone and it responded confirming the release signal, but it failed to release from its position at the bottom. Operations were conducted during the following cruise HOT-86 to try to recover the IES. A 100-m wire with weights attached to it was dragged along the bottom for about 10 hours to try to dislodge the instrument from its presumed position. Unfortunately these activities were unsuccessful and IES #126 could not be recovered. Another IES (#127) was deployed 4 nautical miles north from the center of ALOHA during HOT-85 on 11 July 1997.

2.4. Meteorology

Wind speed and direction, atmospheric pressure, wet- and dry-bulb air temperature, sea surface temperature (SST), cloud cover and sea state were recorded at four-hour intervals while on station ALOHA by the science personnel. Meteorological observations were also obtained every 4 hours by the ship's officers on the bridge of the R/V *Moana Wave* throughout each cruise. Additionally, hourly wind speed and direction were obtained from NDBC buoy #51001 (23.4N, 162.3W). This buoy was not operational during HOT-88. The time series of shipboard observations obtained by the science group was plotted and obvious outliers were identified and flagged. The SST-dry air temperature and wet-dry air temperature plots also helped to identify outliers. Bad data points were often replaced with the bridge data. Outliers in the shipboard wind observations were detected by comparison with the buoy winds.

2.5. ADCP Measurements

Upper ocean currents were measured on all ten HOT cruises and the ALOHA-Climax2 cruise, using the ADCP mounted on the R/V *Moana Wave* and the R/V *Roger Revelle* (RD Instruments model VM-150). ADCP velocities were corrected for gyro compass errors as measured by the Ashtec 3DF GPS attitude sensor on the R/V *Moana Wave*.

2.6. Biogeochemical Measurements

At Stations Kahe, ALOHA and HALE-ALOHA, water samples for chemical analyses were collected from discrete depths using 12-liter PVC bottles with teflon coated internal springs as closing mechanisms. Sampling strategies and procedures are well documented in the previous data reports and in the HOT Program Field and Laboratory Protocols manual. This report contains only a subset of the total data base which can be extracted electronically over the Internet (http://hahana.soest.hawaii.edu). To assist in the interpretation of these data and to save users the time to estimate the precision of individual chemical analysis, we have summarized precision estimates from replicate determinations for each constituent on each HOT cruise in 1997.

2.6.1. Dissolved Oxygen

Dissolved oxygen samples were collected and analyzed using a computer-controlled potentiometric end-point titration procedure as described in Tupas et al. (1997). As in previous years we measured, using a calibrated digital thermistor, the temperature of the seawater sample at the time the iodine flask was filled. This was done to evaluate the magnitude of sample temperature error which affects the calculation of oxygen concentrations in units of μmol kg^{-1}. Figure 2.3 (upper panel) shows a plot of the difference between sample temperature and potential temperature computed from the *in situ* temperature measured at the time of bottle trip, versus pressure. The lower panel of the same figure shows a plot of the difference between oxygen concentration using on-deck and potential temperatures versus pressure. The depth dependent variability in Δ oxygen is a result of the absolute magnitude of the oxygen concentration and the standard procedures we employ for sampling the water column.

Precision of the Winkler titration method is presented in Table 2.12. The mean precision of our oxygen analyses in 1997 was 0.11 %. Oxygen concentrations measured over the 9 years of the program are plotted at three constant potential density horizons in the deep ocean along with their mean and 95 % confidence intervals (Figure 2.4). These results indicate that analytical consistency has been maintained over the past 9 years of the HOT program.

Table 2.12: Precision of Winkler titration method

HOT	CV (%)	SD (μmol l^{-1})	N
79	0.15	0.303	11
80	0.18	0.370	12
81	0.10	0.196	16
82	0.17	0.322	13
83	0.12	0.219	14
84	0.08	0.156	16
85	0.09	0.167	16
86	0.08	0.151	18
87	0.09	0.165	15
88	0.08	0.140	16

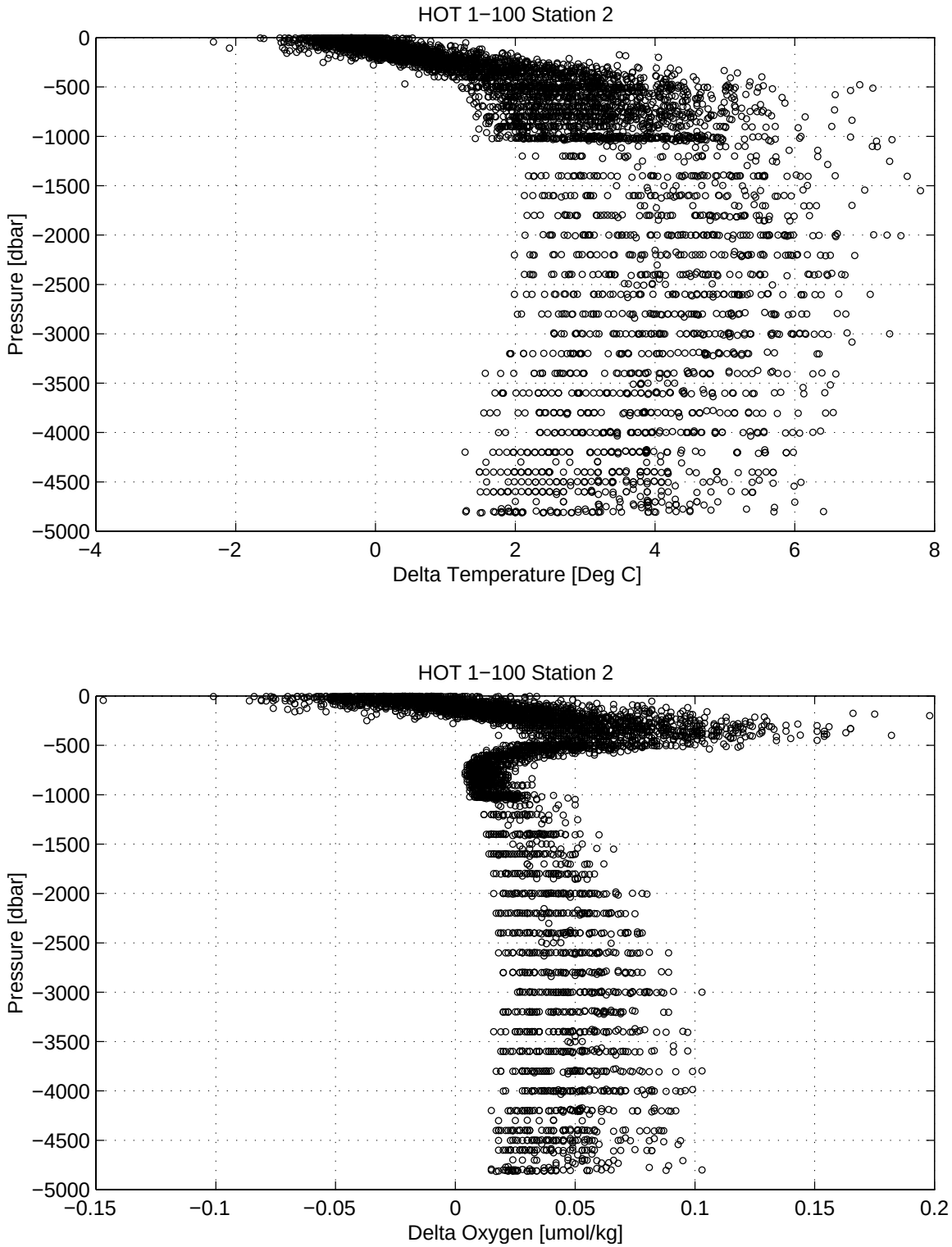

Figure 2.3: [Upper panel] Difference between sample temperature at the time of sample collection and potential temperature calculated from *in situ* temperature at the time of bottle trip. [Lower panel] Difference in oxygen concentration corrected for temperatures measured at the time of sample collection and potential temperature calculated from *in situ* temperature.

2.6.2. Inorganic Carbon Parameters

2.6.2.1. Dissolved Inorganic Carbon and Titration Alkalinity

Samples for dissolved inorganic carbon (DIC) were measured using a Single Operator Multi-parameter Metabolic Analyzer (SOMMA) which was manufactured at the University of Rhode Island and standardized at the Brookhaven National Laboratory. Analyses of primary DIC standards (Tupas et al. 1993) indicated that the precision of replicate samples is approximately 1 µmol kg^{-1}. Titration alkalinity was determined using the Gran titration method as described in Tupas et al. (1997). The precision of the titration procedure was approximately 5 µequiv kg^{-1}. Accuracy was established with certified reference standards obtained from Andrew Dickson at Scripps Institution of Oceanography and compared to analyses by Charles D. Keeling also at Scripps Institution of Oceanography for DIC and Andrew Dickson for alkalinity.

Beginning in 1992, pH was determined spectrophotometrically using the indicator m-cresol purple following the methods described in Tupas et al. (1993). The absorbance of the mixture was measured at wavelengths of 578 and 434 nm on a Perkin Elmer Model 3 dual-beam spectrophotometer and converted to pH on the seawater scale according to Clayton and Byrne (1993). The mean and standard deviation of the difference of sets of duplicate pH measurements was 0.0009 and 0.00077 respectively.

2.6.2.2. pCO_2

In October 1996 (HOT-76) an automated, semi-continuous system for measuring the partial pressure of carbon dioxide in seawater was installed in-line with the ship's clean-seawater intake system to measure underway surface seawater pCO_2. The system is calibrated using three standard gases of known CO_2 concentrations covering the range of 200-400 ppm (Scott Specialty Gases calibrated at SIO). A separate reference gas calibrated at 349.0 ppm is measured for quality assurance. Calibration and standardization are done at system startup and approximately every 2.5 hours. The present system consists of a shower head equilibrator operating at a flow rate of approximately 8 l min^{-1}. Equilibrated gas and bow air are both sampled every 10 minutes. The gases pass through a napthyon tube drier and a magnesium perchlorate scrubber into a LICOR 6250 infrared detector. The reference chamber is purged with reference gas after every 3 cycles of bow/equilibrator measurements. Gas flow rates into the detector are at approximately 0.5 l min^{-1}.

2.6.2.3. pH

The system output gives the CO_2 concentration of the bow-intake air and the surface seawater in ppm. The system begins operating when the ship is in clean open water and is fully operational at Station Kahe. The system is turned off after departing the last station.

2.6.3. Inorganic Nutrients

2.6.3.1. Standard Methods

Samples for the determination of dissolved inorganic nutrient concentrations (soluble reactive phosphorus, [nitrate+nitrite] and silicate) were collected as described in Tupas et al. (1993). Analyses were conducted at room temperature on a four-channel Technicon Autoanalyzer II continuous flow system at the University of Hawaii Analytical Facility. A summary of the precision of analyses for 1997 is shown in Table 2.13. Figures 2.4-2.5 show the mean and 95% confidence limits of nutrient concentrations measured at three potential density horizons for the 9 years of the program. In addition to standard automated nutrient analyses, specialized chemical method are used to determine concentration of nutrients that are normally below the detection limits of autoanalyzer methods.

2.6.3.2. High Sensitivity Methods

The chemiluminescent method of Cox (1980) as modified for seawater by Garside (1982) was used to determine the [nitrate+nitrite] content of near surface (0-200 m interval) water samples (Tupas et al. 1997). The limit of detection for [nitrate+nitrite] was approximately 2 nM with a precision and accuracy of ±1 nM (Dore et al. 1996).

Low level soluble reactive phosphorus (SRP) concentrations in the euphotic zone were determined according to the magnesium induced coprecipitation (MAGIC) method of Karl and Tien (1992). Typical precision estimates for triplicate determinations of SRP are from 1-3 % with a detection limit of 10 nmol l^{-1}. This latter measurement is also corrected for arsenate interference of the molybdenum blue colorimeteric procedure (Johnson 1971), and thus provides a more accurate estimate of SRP.

2.6.4. Dissolved Organic Matter

Dissolved organic carbon (DOC) was determined by the high temperature catalytic oxidation method using an automated DOC analyzer (Qian and Mopper 1996). Dissolved organic nitrogen (DON) was calculated as the difference between total dissolved fixed nitrogen (TDN) and [nitrate+nitrite] concentrations. DON by this definition also includes ammonium, however, ammonium in theses waters are below the detection limit of standard nutrients analysis and are estimated to be less than 100 nmol l^{-1}. Dissolved organic phosphorus (DOP) was calculated as the difference between total dissolved phosphorus (TDP) and SRP concentrations. DOP, by this definition includes inorganic polyphosphates. TDN and TDP were determined by the UV oxidation method as described in Tupas et al. (1997). A summary of the precision of these analyses is given in Table 2.14.

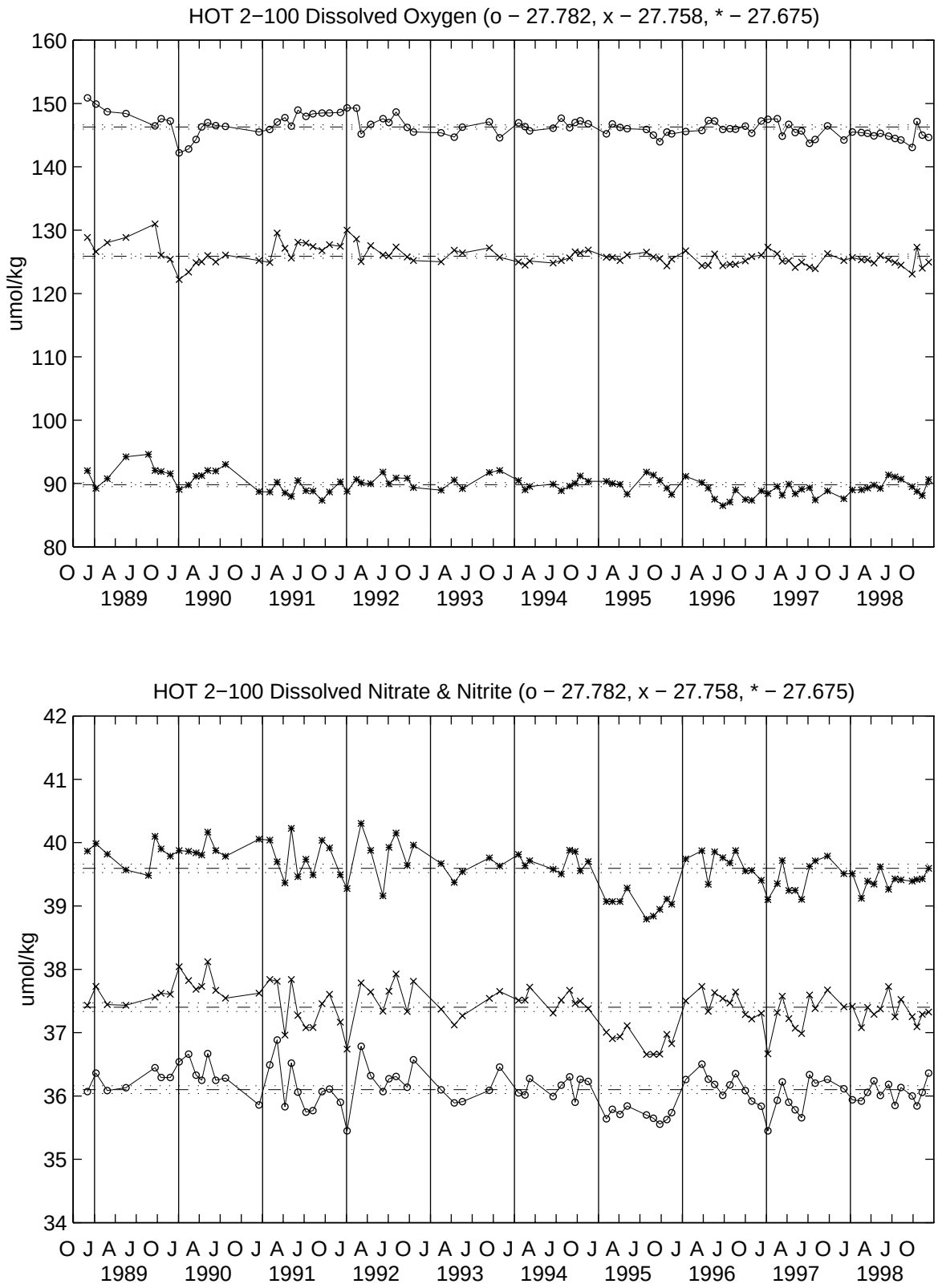

Figure 2.4: Concentrations at potential density horizons of 27.782, 27.758 and 27.675 at Station ALOHA. [Upper panel] Dissolved oxygen. [Lower panel] Nitrate + nitrite.

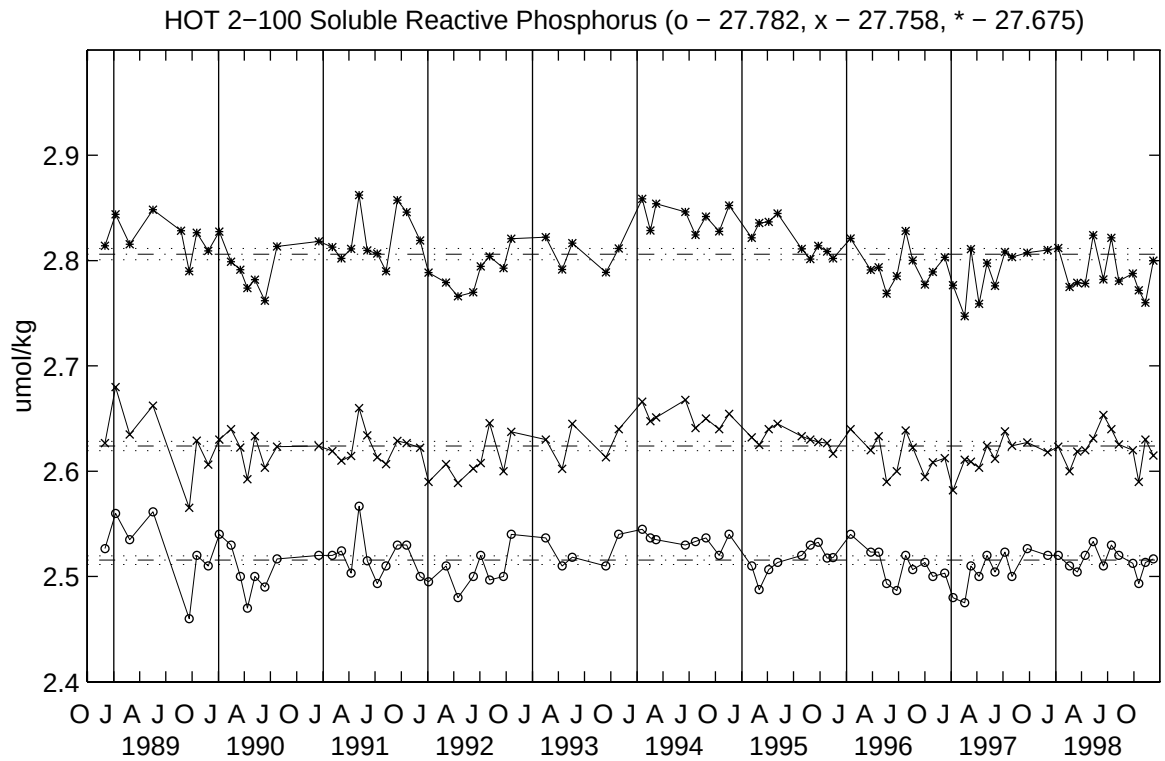

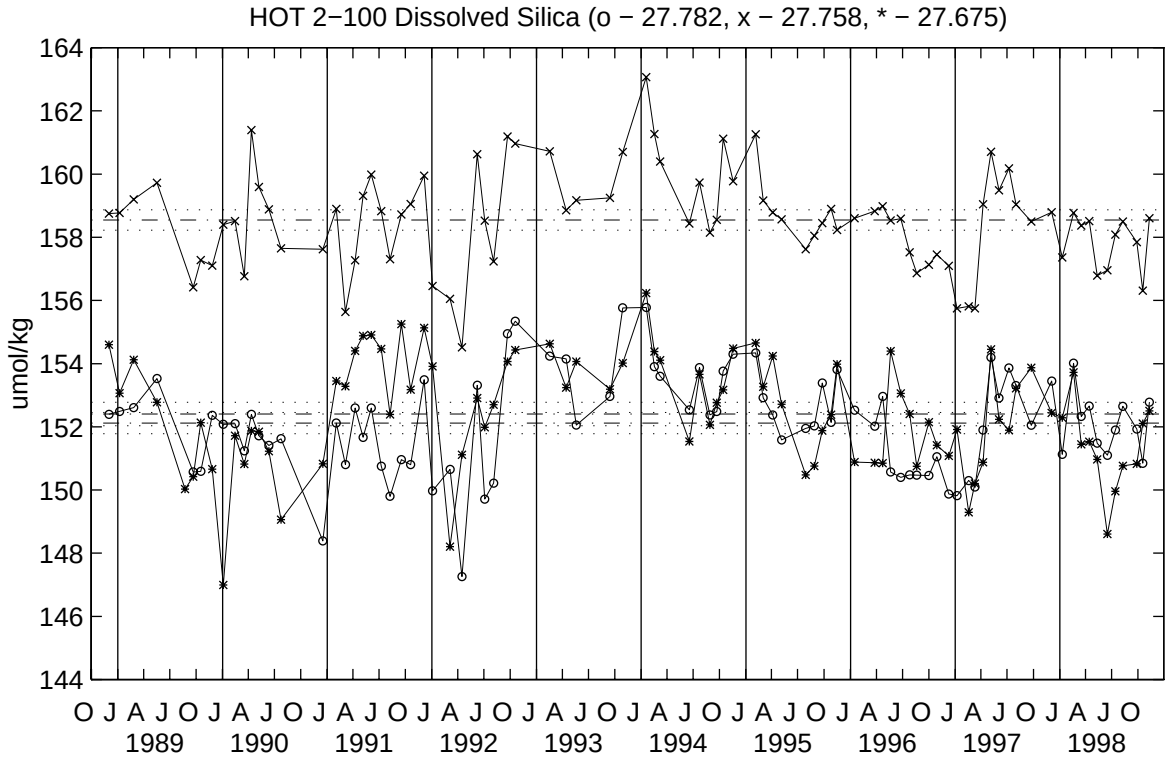

Figure 2.5: Concentrations at potential density horizons of 27.782, 27.758 and 27.675 at Station ALOHA. [Upper panel] Soluble reactive phosphate [Lower panel] Silicate

Table 2.13: Precision of dissolved inorganic nutrient analyses

	Soluble Reactive Phosphorus				[Nitrate+Nitrite]				Silicate			
	Analytical		Field		Analytical		Field		Analytical		Field	
	Mean CV	Mean SD	mean CV	Mean SD	mean CV	mean SD	Mean CV	mean SD	Mean CV	mean SD	mean CV	mean SD
HOT	(%)	(µM)	(%)	(µM)	(%)	(µM)	(%)	(µM)	(%)	(µM)	(%)	(µM)
79	0.2	0.007	0.4	0.008	0.2	0.066	0.5	0.157	0.3	0.280	1.2	0.404
80	0.4	0.011	0.6	0.012	0.2	0.098	0.2	0.034	0.2	0.184	2.3	0.878
81	0.2	0.007	0.3	0.009	0.2	0.083	0.4	0.120	0.1	0.105	3.3	0.340
82	0.3	0.010	0.4	0.006	0.2	0.100	0.3	0.055	0.2	0.174	0.4	0.098
83	0.2	0.005	0.8	0.019	0.4	0.185	0.5	0.049	0.2	0.218	2.3	0.302
84	0.1	0.004	0.4	0.005	0.2	0.099	0.4	0.064	0.2	0.242	3.8	0.573
85	0.2	0.006	0.2	0.004	0.5	0.220	0.3	0.051	0.5	0.515	1.9	0.184
86	0.2	0.006	0.6	0.013	0.1	0.041	0.2	0.047	0.2	0.221	0.7	0.257
87	ND	ND	0.2	0.005	ND	ND	0.1	0.027	ND	ND	4.2	0.340
88	0.9	0.028	0.5	0.011	0.4	0.146	0.3	0.057	0.2	0.199	5.7	0.328
Mean	0.30	0.009	0.44	0.009	0.27	0.115	0.32	0.066	0.23	0.238	2.58	0.370
SD	0.23	0.007	0.19	0.004	0.13	0.057	0.13	0.041	0.11	0.115	1.67	0.219

Table 2.14: Precision of dissolved organic nutrient analyses

	DON		DOP		DOC	
Cruise	Mean CV (%)	mean SD (µmol kg^{-1})	Mean CV (%)	mean SD (µmol kg^{-1})	Mean CV (%)	mean SD (µmol kg^{-1})
79	9.1	0.315	11.1	0.018	2.3	1.450
80	10.2	0.390	23.1	0.028	1.9	1.402
81	7.7	0.331	31.2	0.021	0.2	0.113
82	7.3	0.291	4.1	0.005	1.3	0.806
83	9.4	0.430	35.3	0.035	1.6	0.804
84	14.4	0.409	8.7	0.012	2.3	1.397
85	3.5	0.141	6.9	0.011	3.8	2.036
86	6.6	0.346	11.0	0.010	1.0	0.601
87	10.2	0.444	17.9	0.053	2.5	1.998
88	11.3	0.345	15.9	0.024	1.7	1.237

2.6.5. Particulate Matter

Samples for analysis of particulate matter were prefiltered through 202 µm Nitex mesh to remove large zooplankton and collected onto combusted GF/F glass fiber filters (acid washed for particulate phosphorus). Particulate carbon (PC) and nitrogen (PN) on the filters were analyzed using a Europa automated nitrogen and carbon analyzer. Particulate phosphorus (PP) was analyzed by converting the material to orthophosphate by high temperature ashing followed by acid hydrolysis and determining the orthophosphate content by colorimetry. Precision of particulate matter analysis is presented in Table 2.15.

Table 2.15: Precision of particulate matter analyses

Cruise	Particulate Carbon mean CV (%)	Particulate Carbon mean SD (µmol kg^{-1})	Particulate Nitrogen Mean CV (%)	Particulate Nitrogen mean SD (µmol kg^{-1})	Particulate Phosphorus mean CV (%)	Particulate Phosphorus mean SD (nmol kg^{-1})
79	13.5	2.793	12.2	0.389	17.7	0.067
80	7.6	1.768	10.2	0.389	5.7	0.025
81	6.5	1.320	3.8	0.165	3.1	0.014
82	15.7	3.712	23.4	1.096	6.1	0.018
83	9.5	2.333	6.0	0.247	11.3	0.046
84	5.2	1.379	9.9	0.460	2.3	0.011
85	2.9	0.778	11.5	0.424	5.7	0.025
86	11.1	2.616	4.8	0.212	14.9	0.053
87	1.5	0.354	2.8	0.141	31.1	0.124

2.6.6. Pigments

2.6.6.1. Standard Fluorometric Method

Chlorophyll a (chl *a*) and pheopigments were measured fluorometrically on a Turner Designs Model 10-AU fluorometer using 100% acetone as the extractant and standard techniques (Strickland and Parsons 1972). Analytical precision for this analysis is presented in Table 2.16. Integrated values for pigment concentrations were calculated using the trapezoid rule.

2.6.6.2. High Performance Liquid Chromatography

Chlorophyll *a* and accessory photosynthetic pigments were also measured by high performance liquid chromatography (HPLC) according to Bidigare et al. (1990). A new HPLC method following SCOR recommendation was adopted in 1994. This method is a modification of the method developed by Wright et al. (1991). The new method allows for a better separation of lutein and zeaxanthin as well as monovinyl and divinyl chlorophyll *a* (Table 2.17). Figure 2.6 shows the relationship between chlorophyll *a* measured by fluorometry and chlorophyll *a* measured by HPLC for 1997. A summary of response factors for all HPLC pigment analyses from 1988 to 1997 are shown in Table 2.18.

2.6.6.3. Underway Surface Fluorometry

Beginning with HOT-76 (September 1996), a Turner Designs Model 10-AU fluorometer was installed on the R/V *Moana Wave* to measure continuous *in vivo* chlorophyll (fluorescence) from surface seawater sampled by the ship's seawater intake system. The underway measurements are calibrated by taking discrete samples from the outflow of the fluorometer and extracting the pigments according to standard methods.

Table 2.16: Precision of fluorometric chlorophyll *a* and pheopigment analyses

Cruise	Chlorophyll *a* Mean CV (%)	Chlorophyll *a* SD ($\mu g\ l^{-1}$)	Pheopigment Mean CV (%)	Pheopigment SD ($\mu g\ l^{-1}$)
79	9.1	0.007	8.4	0.010
80	1.7	0.003	5.2	0.012
81	3.4	0.006	4.2	0.012
82	3.7	0.008	8.1	0.016
83	3.5	0.005	5.4	0.012
84	3.8	0.006	4.9	0.013
85	3.1	0.004	5.1	0.015
86	2.7	0.003	5.1	0.010
87	2.5	0.004	4.0	0.005
88	3.6	0.006	5.1	0.012

Table 2.17: 1997 HPLC Pigment Analysis Response Factors

Pigment	RF[a]	RT[b]
Chlorophyll c & Mg 3,8D[c]	0.265	
Peridinin	0.535	0.377
19'-butanoyloxyfucoxanthin	0.420	0.406
Fucoxanthin	0.418	0.445
19'-hexanoyloxyfucoxanthin	0.412	0.482
Prasinoxanthin	0.411	0.547
Violaxanthin	0.411	0.577
Diadinoxanthin	0.273	0.656
Alloxanthin	0.297	0.726
Zeaxanthin	0.320	0.816
MV Chlorophyll b	0.988	0.939
MV Chlorophyll a	0.736	1.000
DV Chlorophyll a	0.530	1.000
α-Carotene	0.310	1.187
β-Carotene	0.320	1.191

[a]RF - Response Factor (ng/L pigment per unit absorbance peak area at 436 nm).
[b]RT - Retention Time (relative to chlorophyll a)
[c]Chlorophyll c = ($c_1 + c_2 + c_3$),
Mg 3,8D = Mg 3,8 divinyl pheoporphyrin a_5 monomethyl ester.

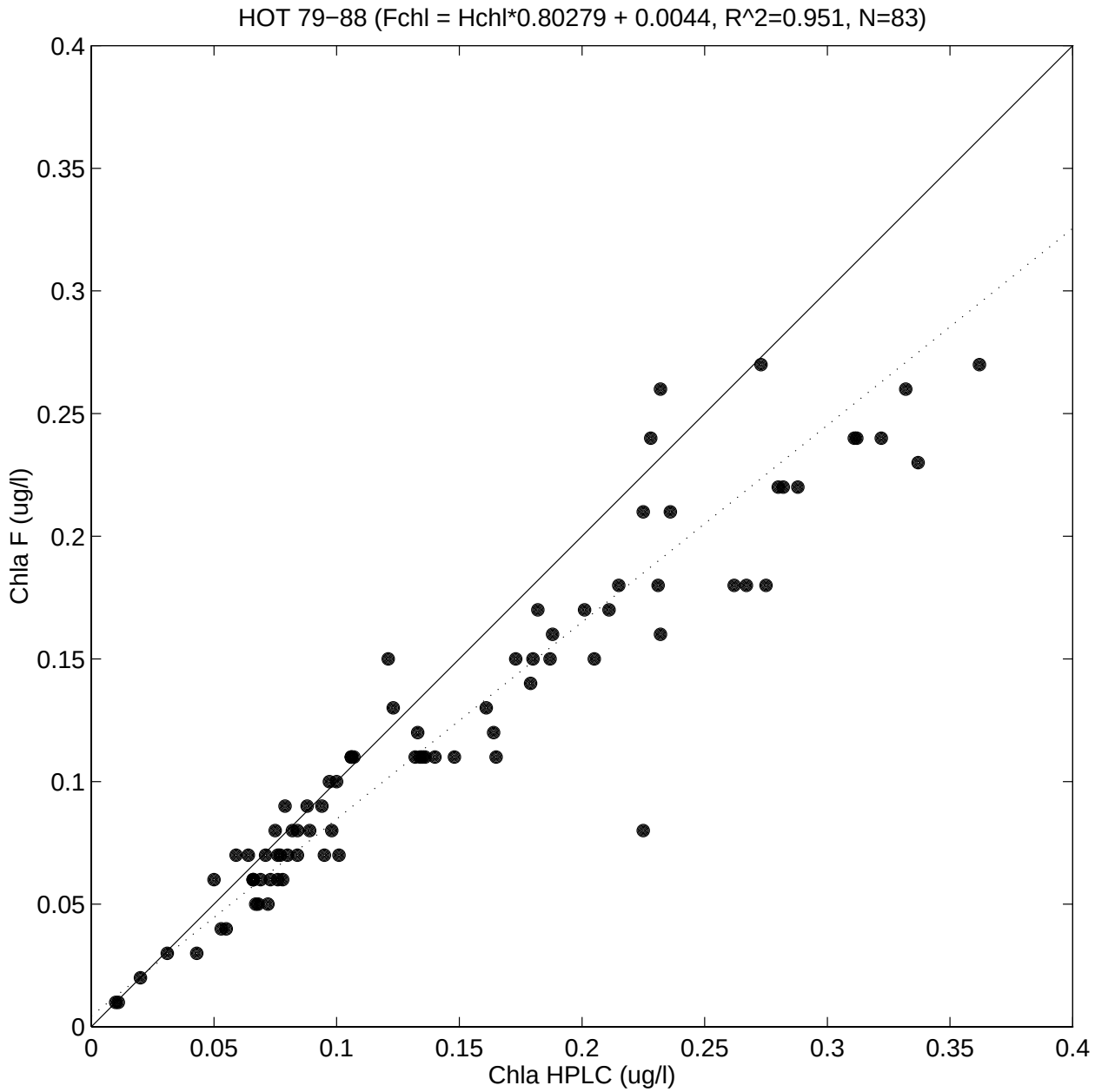

Figure 2.6: Chlorophyll a measured by fluorometry (Chla F) versus chlorophyll a measured by HPLC (Chla HPLC) for all data collected in 1996. The solid line shows the 1:1 x-y relationship while the dashed line is a model II regression analysis of the data set. The regression equation is at the tops of the figure.

Table 2.18: Phytoplankton Pigment Response Factors

HOT Cruise Sample loop volume Method	1-50 500 µL B	51-59 200 µL W	60-69 200 µL W	70-79 200 µL W	80-88 200 µl W
PIGMENT					
Chlorophyll c_3	0.455[a]	0.236[b]	0.241[b]	0.257[b]	0.265[b]
Chlorophyll $c_1 + c_2$	0.455	0.236	0.241	0.257	0.265
Peridinin	0.587	0.498	0.488	0.520	0.535
19'-butanoyloxyfucoxanthin	0.421	0.375	0.383	0.408	0.420
Fucoxanthin	0.454	0.372	0.381	0.406	0.418
19'-hexanoyloxyfucoxanthin	0.401	0.364	0.376	0.401	0.412
Prasinoxanthin	0.434	0.364	0.375	0.400	0.411
Violaxanthin	N/A[c]	N/A[c]	0.375	0.400	0.411
Diadinoxanthin	0.261	0.251	0.249	0.265	0.273
Alloxanthin	N/A[c]	0.268	0.271	.0289	0.297
Lutein	N/A[c]	0.344	0.352	0.376	0.386
Zeaxanthin	0.305	0.273	0.292	0.311	0.320
MV Chlorophyll b	1.423	0.932	0.901	0.960	0.988
Total Chlorophyll a	0.729	N/A[c]	N/A[c]	N/A[c]	N/A[c]
MV Chlorophyll a	N/A[c]	0.697	0.671	0.716	0.736
DV Chlorophyll a	N/A[c]	0.436	0.483	0.515	0.530
Total Carotenes	0.264	N/A[c]	N/A[c]	N/A[c]	N/A
α-Carotene	N/A[c]	0.276	0.282	0.301	0.310
β-Carotene	N/A[c]	0.285	0.292	0.311	0.320

B = Bidigare et. al. (1989), Mar. Ecol. Prog. Ser., 56: 177-188.
W = Wright et. al. (1991), Mar. Ecol. Prog. Ser., 77: 183-196.
[a]units are ng $area^{-1}$ [b]units are ng L^{-1} $area^{-1}$ [c]method not applicable for pigment

2.6.7. Adenosine 5'-Triphosphate

Water column adenosine 5'-triphosphate (ATP) concentrations were determined using the firefly bioluminesence technique as described by Karl and Holm-Hansen (1978). The precision of ATP determinations in 1996 are given in Table 2.19.

Table 2.19: Precision of ATP Analyses

Cruise	Mean CV (%)	Mean SD (µg m^{-3})
79	10.4	1.507
80	14.9	2.416
81	15.2	2.677
82	17.4	4.860
83	12.3	3.085
84	14.6	2.354
85	21.0	2.345
86	14.6	3.268
87	16.4	2.045
88	13.0	1.579

2.7. Biogeochemical Rate Measurements

2.7.1. Primary Production

Photosynthetic production of organic matter was measured by a trace-metal clean, ^{14}C method. Incubations were conducted *in situ* at eight depths for at least 12 hours using a free-drifting array as described by Winn et al. (1991). Integrated carbon assimilation rates were calculated using the trapezoid rule with the shallowest value extended to 0 m and the deepest extrapolated to a value of zero at 200 m.

2.7.2. Particle Flux

Particle flux was measured at a standard reference depth of using sediment traps deployed on a free-floating array for approximately 2.5 days during each cruise. Sediment trap design and collection methods are described in Winn et al. (1991). Samples were analyzed for particulate C, N and P.

2.8. Optical Measurements

2.8.1. Solar Irradiance

Incident irradiance at the sea surface was measured on each HOT cruise with a LI-COR LI-200 data logger and cosine collector. The instrument recorded data from the time the ship departed Snug Harbor until its return.

2.8.2. Downwelling Irradiance and Upwelling Radiance

Vertical profiles of upwelling radiance and downwelling irradiance were made using a Biospherical Profiling Reflectance Refractometer (PRR-600). This instrument measures downwelling irradiance (Ed) and upwelling radiance (Lu) as well as surface irradiance from a deck unit on 7 channels. The radiance channels comply with the SeaWIFS optical parameters. The instrument is lowered by hand and depending on the subsurface currents, is deployed to a depth between 120 and 150 meters.

2.8.3. Flash Fluorescence

Flash fluorescence was measured with a Sea Tech Model ST0250 flash fluorometer and the data collected with the Sea-Bird CTD system. Flash fluorescence traces were collected on as many casts as possible. Because an absolute radiometric standard is not available for flash fluorometers, instrument drift was corrected by checking the relative response of the instrument between cruises using fluorescent plastic sheeting as described in Tupas et al. (1997). A linear relationship of the form, $Vn = b\ Vo + a$, was used to convert all fluorescence data to a common voltage scale, where Vn is the normalized voltage, Vo is the output voltage and a and b are constants derived from the two deep water intervals. The constants used in 1997 were $a = 1.6669$ and $b = 0.6503$.

2.9. Microbial Community Structure

Analysis of bacterial number was made using an EPICS 753 flow cytometer (Coulter Electronics Corporation, Hialeah, FL, USA) which has been upgraded with a Cicero Data Acquisition System (Cytomation Inc., Boulder, Colorado). A consistent delivery of sample volume and sample flow rate (100 µl at 50 µl min^{-1} and 50 µl at 50 µl min^{-1} was regularly achieved using a Microsample Delivery System, Coulter Electronics Corporation, Hialeah, FL, USA). Prior to analysis by flow cytometry, samples were prepared using standard protocols (Campbell et al. 1994). Hoechst 33342 was added to each sample at a final concentration of 1 µg ml^{-1} (Monger & Landry 1993). Samples were also amended with 0.57 and 0.9 µm microspheres (visible excitation, Fluoresbrite Polysciences) as well as 0.46 µm, UV-only excitable beads. Samples were illuminated simultaneously with 1 Watt of the 488 nm line, and 225 mW UV line, originating from a dual platform equipped with 5 Watt Argon lasers (90-5, Coherent Laser Products, Palo Alto CA). Fluorescence was detected using band pass interference filters for orange fluorescence (575 nm), red fluorescence (680 nm) and blue fluorescence (450 nm). Measurements from these parameters, as well as forward angle light scatter (FALS) and 90 degree light scatter (LS), were amplified into a 3-decade logarithmic scale and stored in a list mode file. Analysis of these files, using CYTOPC (Vaulot 1989), permitted the identification and enumeration of the various populations in the microbial community. The enumeration output from this analysis was corrected for volume (cells ml^{-1}). In addition, an enumeration efficiency factor, based on flow cytometer sample counting rates, was derived using 0.98 µm beads.

2.10. Zooplankton Community Structure

2.10.1. Mesozooplankton Collection

Samples for the assessment of mesozooplankton were using a 1 m^2 plankton net with a 202 µm Nitex mesh. The square net frame has a bottom depressor to make it dive steeply and smoothly through the depth range of the tow, and the bridle system does not cross the net mouth thereby minimizing animal avoidance. A Brancker time-depth-temperature recorder is attached to the frame to determine the depth of tow and confirm even collection at each depth. A General Oceanics flow meter is centered at the net mouth to estimate the volume of water filtered. The net is towed obliquely at a speed of 1.0-1.5 knots while deploying and retrieving the tow line at a constant speed (about 20 meters min^{-1}; total line out = 200 meters; 20 minute tow duration; average depth of tow ≈ 175 meters). Three midnight (between 2200-0200 local time) and three mid-day (between 1000-1400 local time) are conducted on each cruise.

2.10.2. Sample Processing

Contents of the net cod ends are immediately anesthetized with carbonated water to prevent gut evacuation. The net samples are then divided using a Folsom splitter with one-half preserved in 4% buffered formaldehyde with 2 mg l^{-1} strontium sulfate to prevent acantharians from dissolving, and approximately one-fourth (depending on sample density) size fractionated through nested screens of 5, 2, 1, 0.5 and 0.2 mm Nitex mesh. The remaining one-fourth sample is prepared for live silhouette photography (Ortner et al. 1979) which provides a permanent record of delicate gelatinous forms. Each size fraction is concentrated on a preweighed Nitex screen, rinsed with isotonic ammonium formate to remove salts, sucked dry under low vacuum

and flash frozen in liquid nitrogen. Frozen samples are defrosted in the dark at room temperature, weighed wet (moist) on an analytical balance before (total weight wet) and after (fraction removed) drying. Random subsamples of the zooplankton mass are set aside for enumeration and pigment analysis. The remaining sample is dried at 60 °C, reweighed [total sample dry weight = measured dry weight/fraction of total wet weight dried] and analyzed for carbon and nitrogen.

2.11. Regional Study

In July of 1996 a transect study was conducted to evaluate regional variability in hydrographic and biogeochemical parameters between Station ALOHA and the historical Climax study area (Tupas et al. 1997). From June 26 to July 2, 1997 a second transect cruise was conducted covering the same track and stations established in 1996 (Table 2.20). As in the previous transect cruise, its primary purpose was to:

- Determine the regional variability and gradients in selected biogeochemical and physical properties of the upper water column from Station ALOHA to the Climax Program study site.
- Assess upper water column characteristics at Climax using modern techniques for comparison to the historical data set.
- Compare depth specific phytoplankton and mesozooplankton communities with near synoptic resolution at ALOHA and Climax.
- Determine regional variability in phosphorus pool inventories and dynamics.
- Determine along-track variability in particle concentration, pCO_2, chlorophyll *a* and hydrographic parameters.

Parameters studied during this cruise are presented in Table 2.21. Protocols were obtained from Climax investigators (e.g. Hayward 1987) to be used in comparison to HOT methods.

Table 2.20: Location and dates of stations for ALOHA-Climax 2 cruise

Station	Location	Date	Comments
1	21° 29.04’ N, 158° 22.44’ W	26 June 1997	
2	22° 45.00’ N, 158° 00.00’ W	26 June & 1 July 1997	Station ALOHA
3	24° 34.20’ N, 157° 00.00’ W	27 June 1997	
4	26° 22.50’ N, 156° 10.02’ W	28 June 1997	
5	28° 00.00’ N, 155° 24.60’ W	29 June 1997	Station Climax

Table 2.21: Parameters measured during ALOHA-Climax 1 cruise

Station	1	2	3	4	5
Water Column					
Hydrography	■	■	■	■	■
Salinity	■	■	■	■	■
Dissolved Oxygen	■	■	■	■	■
Dissolved inorganic carbon		■	■	■	■
pH	■	■	■	■	■
Alkalinity		■	■	■	■
Nitrate + Nitrite	■	■	■	■	■
Soluble Reactive Phosphorus (SRP)	■	■	■	■	■
Silicate	■	■	■	■	■
Dissolved Organic Carbon	■	■	■	■	■
Dissolved Organic Nitrogen	■	■	■	■	■
Dissolved Organic Phosphorus	■	■	■	■	■
Particulate Carbon		■			■
Particulate Nitrogen		■			■
Particulate Phosphorus		■			■
Low-level Nitrogen	■	■	■	■	■
Low-level SRP	■	■	■	■	■
Chlorophyll a	■	■	■	■	■
Pheopigments	■	■	■	■	■
HPLC Pigments		■			■
Heterotrophic Bacteria	■	■	■	■	■
Photosynthetic Bacteria	■	■	■	■	■
Adenosine 5’ Triphosphate		■			■
Bacterial Lipopolysacharride	■	■	■	■	■
Primary Production					
Salinity		■			■
Chlorophyll a		■			■
Pheopigments		■			■
Light incubations		■			■
Dark Incubations		■			■
Heterotrophic Bacteria		■			■
Photosynthetic Bacteria		■			■
Protocol Comparison					
Light incubations		■			■
Dark Incubations		■			■
Chlorophyll a		■			■
Phaeopigments		■			■

3.0. CRUISE SUMMARIES

The cruise summaries presented here give an overview of the activities conducted during the 1997 HOT cruises. The official Chief Scientist's report can be found on the HOT-JGOFS and HOT-WOCE web pages.

3.1. HOT-79: Dale Hebel, Chief Scientist

The R/V *Moana Wave* departed Snug Harbor at 0840 HST on 6 January, 1997 with 17 scientists on-board. All objectives of the JGOFS and WOCE programs were accomplished. Stations Kahe and ALOHA were occupied. All core samples were taken within the 36-hour CTD burst sampling period. All samples for ancillary projects were taken. Floating sediment trap and primary production arrays were successfully deployed and recovered. Zooplankton tows were conducted mid-day and mid-night while at Station ALOHA. The ADCP and thermosalinograph were running throughout the cruise. The ship arrived at Snug Harbor at 0715 on 10 January, 1997.

3.2. HOT-80: Fernando Santiago-Mandujano, Chief Scientist

The R/V *Moana Wave* departed Snug Harbor at 0900 HST on February 16, 1997 with 13 scientists on-board. The transit to ALOHA was rough but once on station, all objectives of the JGOFS and WOCE programs were accomplished. Stations Kahe, ALOHA and HALE ALOHA were occupied. All core samples were taken within the 36-hour CTD burst sampling period. All samples for ancillary projects were taken. Floating sediment trap and primary production arrays were successfully deployed and recovered. Zooplankton tows were conducted mid-day and mid-night while at Station ALOHA. The ADCP and thermosalinograph were running throughout the cruise. The ship arrived at Snug Harbor at 0730 on February 20, 1997.

3.3. HOT-81: Dale Hebel, Chief Scientist

The R/V *Moana Wave* departed Snug Harbor at 0900 HST on March 10, 1997 with 14 scientists on-board. All objectives of the JGOFS and WOCE programs were accomplished. Stations Kahe, ALOHA and HALE ALOHA were occupied, however, the cast at Station Kahe was conducted on the transit back to Honolulu. All core samples were taken within the 36-hour CTD burst sampling period. All samples for ancillary projects were taken. Floating sediment trap and primary production arrays were successfully deployed and recovered. Zooplankton tows were conducted mid-day and mid-night while at Station ALOHA. The ADCP and thermosalinograph were running throughout the cruise. The ship arrived at Snug Harbor at 0800 on March 14, 1997.

3.4. HOT-82: Luis Tupas, Chief Scientist

The R/V *Moana Wave* departed Snug Harbor at 0830 HST on April 7, 1997 with 14 scientists on-board. Rough sea conditions slowed the transit to Station ALOHA but all objectives of the JGOFS and WOCE programs were accomplished with the exception that the flash fluorometer was not operable. Stations Kahe, ALOHA and HALE ALOHA were occupied. All core samples were taken within the 36-hour CTD burst sampling period. All samples for ancillary projects were taken. Floating sediment trap and primary production arrays were successfully deployed and recovered. Zooplankton tows were conducted mid-day and mid-night

while at Station ALOHA. The ADCP and thermosalinograph were running throughout the cruise. The ship arrived at Snug Harbor at 0800 on April, 11 1997.

3.5. HOT-83: Luis Tupas, Chief Scientist

The R/V *Moana Wave* departed Snug Harbor at 0930 HST on May 5, 1997 with 13 scientists on-board. All objectives of the JGOFS and WOCE programs were accomplished. Stations Kahe, ALOHA and HALE ALOHA were occupied. All core samples were taken within the 36-hour CTD burst sampling period. All samples for ancillary projects were taken. Floating sediment trap and primary production arrays were successfully deployed and recovered. Zooplankton tows were conducted mid-day and mid-night while at Station ALOHA. The ADCP and thermosalinograph were running throughout the cruise. The ship arrived at Snug Harbor at 0730 on May 9, 1997.

3.6. HOT-84: Luis Tupas, Chief Scientist

The R/V *Moana Wave* departed Snug Harbor at 0900 HST on June 2, 1997 with 15 scientists on-board. All objectives of the JGOFS and WOCE programs were accomplished. Stations Kahe, ALOHA and HALE ALOHA were occupied. All core samples were taken within the 36-hour CTD burst sampling period. All samples for ancillary projects were taken. Floating sediment trap and primary production arrays were successfully deployed and recovered. Zooplankton tows were conducted mid-day and mid-night while at Station ALOHA. The ADCP and thermosalinograph were running throughout the cruise. The ship arrived at Snug Harbor at 0800 on June 6,1997.

3.7. HOT-85: Fernando Santiago-Mandujano, Chief Scientist

The R/V *Moana Wave* departed Snug Harbor at 0900 HST on July 7 , 1997 with 15 scientists on-board. Weather conditions were rough during the cruise with 15-22 knot easterlies and 5-6 ft waves. Despite of the bad weather there was no major damage to the equipment. All objectives of the JGOFS and WOCE programs were accomplished. Stations Kahe, ALOHA and HALE ALOHA were occupied. All core samples were taken within the 36-hour CTD burst sampling period. All samples for ancillary projects were taken. Floating sediment trap and primary production arrays were successfully deployed and recovered. Zooplankton tows were conducted mid-day and mid-night while at Station ALOHA. The ADCP and thermosalinograph were running throughout the cruise. An attempt to recover the Inverted Echo Sounder was unsuccessful. The ship arrived at Snug Harbor at 0800 on July 11, 1997.

3.8. HOT-86: Dale Hebel, Chief Scientist

The R/V *Moana Wave* departed Snug Harbor at 0800 HST on July 31, 1997 with 16 scientists on-board. All objectives of the JGOFS and WOCE programs were accomplished. Stations Kahe, ALOHA and HALE ALOHA were occupied. All core samples were taken within the 36-hour CTD burst sampling period. All samples for ancillary projects were taken. Floating sediment trap and primary production arrays were successfully deployed and recovered. Zooplankton tows were conducted mid-day and mid-night while at Station ALOHA. Two net tows were not completed due to problems with the captsan. The ADCP and thermosalinograph

were running throughout the cruise. A dragging operation to recover the IES was unsuccessful. The ship arrived at Snug Harbor at 0710 on August 4, 1997.

3.9. HOT-87: Luis Tupas, Chief Scientist

The R/V *Roger Revelle* departed Snug Harbor at 0001 HST on September 24, 1997 with 35 scientists on-board. All objectives for this abbreviated cruise were accomplished. Only Stations ALOHA and HALE ALOHA were occupied and all core samples were taken. All samples for ancillary projects were taken. Sediment trap experiment was not conducted because of the short cruise period. Primary production array was deployed with some difficulty but was recovered successfully. ADCP measurements were made throughout the cruise. The pCO2 systems of Chris Winn (Pat Driscoll operating) and Dave Karl (Chris Carrillo operating) were installed and worked using the ship's uncontaminated seawater intake system. The *Revelle's* thermosalinograph was also used. The large berthing capacity of the Revelle allowed graduate students from the Marine Microplankton Ecology course to conduct at-sea experiments under the instruction of Professor's Karl and Landry. The ship arrived at Snug Harbor at 0800 on September 26, 1997.

3.10. HOT-88: Dale Hebel, Chief Scientist

The R/V *Moana Wave* departed Snug Harbor at 0900 HST on December 3, 1997 with 17 scientists on-board. Due to the rough sea conditions the floating sediment trap and OPC operations were cancelled. In addition to the regular HOT scientific contingency, we had four scientists from SIO to deploy 2 benthic respirometers (FVGR & ROVER). Four stations were occupied during HOT 88, Kahe Pt. (sta. 1), Station ALOHA (sta. 2), FVGR/ROVER deployment site, and HALE ALOHA mooring location (sta. 8). CTD operations were conducted at stations 1, 2 & 8. Nine casts were conducted at Station ALOHA and one each at stations 1 & 8. During the cruise all underway measurement systems (thermosalinograph, ADCP, meteorological, pCO2 and fluorometer) were operable and functioned normally except for a period when the feed water was turned off due to air in the lines from the rough seas on the outward transit. The seas were rough, throughout the cruise, with sustained winds 20-30 knots and gusts over 40 knots, swells 5-15 feet and mostly cloudy skies. The ship arrived at Snug Harbor at 0700 on December 7, 1997.

4.0. RESULTS

4.1 Hydrography

The 1997 hydrographic data described in detail below reveal an increase in temperature and salinity in the upper 500 dbar at Station ALOHA that started in the late months of 1996 and continued throughout February 1997. This was followed by a temperature and salinity decrease from March through May 1997, returning to normal afterwards. Associated with these variations was a decrease in potential density in early 1997 followed by an increase that reached maximum values during March. In the salinity maximum region (50-150 dbar), the salinity remained below 35.1 throughout 1997; values this small have only been seen for short periods of time in previous years. The intermediate waters recovered from anomalously low soluble reactive phosphorus (SRP), a decreasing trend established in early 1994 ended in February 1997, and values increased during 1997. In the bottom water, the cold anomaly that reached record low temperatures in late 1996 (Tupas et al. 1997), recovered to normal temperatures during 1997 (Lukas et al. submitted).

4.1.1 1997 CTD Profiling Data

Profiles of temperature, salinity, oxygen and potential density (σ_θ) were collected at both Station Kahe and Station ALOHA. The profiles from Station ALOHA during 1997 are presented in Figure 6.1.1. The results of bottle determinations of oxygen, salinity and inorganic nutrients are also shown. In addition, stack plots of CTD temperature and salinity profiles for all 1000 m casts conducted at Station ALOHA are presented (Figure 6.1.2). The data collected for Station Kahe during 1997, and at Station HALE-ALOHA beginning on HOT-80 are presented in Figure 6.1.3. Note that there were no bottle data taken at station Kahe during HOT-87. The temperature, salinity and oxygen profiles obtained from the deep casts at Station ALOHA during 1997 are presented in Figures 6.1.4-6. The cold water anomaly that developed near the bottom at the end of 1996 (Tupas et al. 1997), returned to normal temperatures by the end of 1997 as indicated by the potential temperature profiles (Figure 6.1.4). The profiles with the lowest temperatures are from cruises conducted early in the year.

4.1.2 Time-series Hydrography, 1988-1997

The hydrographic data collected during the first nine years of HOT are presented in a series of contour plots (Figures 6.1.7-14). These figures show the data collected in 1997 within the context of the longer time-series database. The CTD data used in these plots are obtained by averaging the data collected during the 36-hour period of burst sampling. Therefore, much of the variability which would otherwise be introduced by internal tides in the upper ocean has been removed. Figures 6.1.7a and b show the contoured time-series record for potential temperature and density in the upper 1000 dbar for all HOT cruises through 1997. Seasonal variation in temperature for the upper ocean is apparent in the maximum of near-surface temperature of about 26 °C and the minimum of approximately 23 °C. Oscillations in the depth of the 5 °C isotherm below 500 dbar appear to be relatively large with displacements up to 100 dbar. The main pycnocline is observed between 100 and 600 dbar, with a seasonal pycnocline developing between June and December in the 50-100 dbar range (Figure 6.1.7b). The cruise-to-cruise changes between February and July 1989, and between January and June 1997 in the upper pycnocline illustrate that variability in density is not always well resolved by our quasi-monthly sampling.

Figures 6.1.8-9 show the contoured time-series record for salinity in the upper 1000 dbar for all HOT cruises through 1997. The plots show both the CTD and bottle results plotted against pressure and potential density. Most of the differences between the contoured sections of bottle salinity and CTD salinity are due to the coarse distribution of bottle data in the vertical as compared to the CTD observations. Some of the bottles in Figure 6.1.9b are plotted at density values lower than the indicated sea surface density. This is due to surface density changing from cast to cast within each cruise, and even between the downcast and the upcast during a single cast.

Surface salinity is variable from cruise-to-cruise, with no obvious seasonal cycle and some substantial interannual variability. The surface salinity is low in late 1989, increases to a maximum in late 1990, decreases again during 1991 and 1992, rises to an extreme high in late 1993 and decreases again in 1994. For about five months in early 1995 it reaches extreme low values only comparable to those in 1989. It increases in late 1995 and decreases again to extreme values for about five months in mid 1996. Very small variability is seen during 1997.

The salinity maximum is generally found between 50 and 150 dbar, and within the potential density range 24-25 kg m^{-3}. A salinity maximum region extends to the sea surface in the later part of 1990 and 1993, as indicated by the 35.2 contour reaching the surface. This contour nearly reaches the surface late in 1988 and 1989. The maximum shows salinities lower than normal in early 1995 and 1996, and throughout these two years the values are below 35.2 During 1997 the salinities decrease even further, with values below 35.1 throughout the year. The maximum value of salinity in this feature is subject to short-term variations of about 0.1 which is probably due to the proximity of Station ALOHA to the region where this water is formed at the sea surface (Tsuchiya 1968). The variability of this feature is itself variable. Throughout 1989 there were extreme variations of a couple of months duration with 0.2 amplitude. The variability was much smaller and of a lower frequency thereafter, except for a few months of rapid variation in earlier 1992.

The salinity minimum is found between 400 and 600 dbar (26.35-26.85 kg m^{-3}). There is no obvious seasonal variation in this feature, but there are distinct periods of higher than normal minimum salinity in early 1989, in the fall of 1990, in early 1992 and in the summer of 1996. These variations are related to the episodic appearance at Station ALOHA of energetic fine structure and submesoscale water mass anomalies (Lukas and Chiswell 1991; Kennan and Lukas 1995).

Figure 6.1.10 shows contoured time-series data for oxygen in the upper 1000 dbar at Station ALOHA. The oxygen data show a strong oxycline between 400 and 625 dbar (26.25-27.0 kg m^{-3}), and an oxygen minimum centered near 800 dbar (27.2 kg m^{-3}). During 1989, there was a persistent oxygen maximum near 300 dbar (25.75 kg m^{-3}), which appeared again during 1991, shortly in early 1993, mid 1994, and more persistent in late 1995 and 1996. At the same level, an oxygen minimum developed in early 1990 and late 1991, mid 1992, late 1994, and early 1996. This minimum was accompanied by an increase in the concentration of nutrients (see below), and a decrease in salinity. The oxygen minimum exhibited some interannual variability as well, with values less than 30 µmol kg^{-1} appearing in the last half of 1989 and the first half of 1990, reappearing, less intensely, in 1991 and 1992, again strongly in 1993 and 1994, weakening in 1995, reappearing strongly in 1996 and 1997, and less intense by the end of 1997.

A time series of mean oxygen obtained from bottle data in a layer spanning the oxygen minimum (27-27.8 kg m^{-3}) also shows this variability. Superimposed on this variability is a general trend towards lower values of dissolved oxygen in the intermediate waters. The surface layer shows a seasonality in oxygen concentrations, with highest values in the winter. This roughly corresponds to the minimum in surface layer temperature (Figure 6.1.7a). An oxygen

maximum at about 100 m appears in the latter half of 1991 and persists through 1992, reappears again in 1993 and persists through 1994, it reappears again in the latter half of 1995, 1996 and 1997 with less intensity.

Figures 6.1.11-14 show [nitrate+nitrite], SRP, and silica at Station ALOHA plotted against both pressure and potential density. The nitricline is located between about 200 and 600 dbar (25.75-27 kg m^{-3}). Most of the variations seen in these data is associated with vertical displacements of the density structure, and when [nitrate+nitrite] is plotted versus potential density, most of the contours are level. An increase in [nitrate+nitrite] can be seen in early 1996 between 25-26.25 kg m^{-3}. This increase appears similar to events seen in March-April 1990, January 1992, February 1993 and February-March 1995. These events can likely be attributed to mesoscale features such as eddies. It is possible for eddies to transport water with different biogeochemical characteristics from distant sources into the region of Station ALOHA. As in the previous events, the increase of [nitrate+nitrite] in March 1996 is accompanied by a decrease in the oxygen concentration apparent between 25-26.25 kg m^{-3}. The SRP record is similar to the [nitrate+nitrite] in the upper water column .

During 1996, the intermediate waters between 27.0-27.8 kg m^{-3} recovered from anomalously low [nitrate+nitrite] which was observed during 1995 (Fig. 6.1.12a). This anomaly is apparent in a time series of mean [nitrate+nitrite] obtained from bottle data between 27.0-27.8 kg m^{-3} (Fig. 6.1.15b). A decrease in [nitrate+nitrite] between 27.0-27.8 kg m^{-3} began in late 1994, with a comparable increase from mid-1995 through early 1996. The maximum decrease appears to be about 1 μmol kg^{-1} below 27.5 kg m^{-3} where nitrate concentrations are about 40 μmol kg^{-1}. This decrease appears to be real as it does have coherence over time. A precision estimate of 0.3% has been made for [nitrate+nitrite] measurements involving the high concentration samples associated with intermediate water (Dore et al. 1995). This translates to a precision of roughly 0.12 μmol kg^{-1} for samples with a concentration of 40 μmol kg^{-1}. Hence, the 1 μmol kg^{-1} decrease seen during 1995 is well within the precision level for the concentrations observed. However, the amount of the decrease could be approaching the accuracy limits of [nitrate+nitrite] measurements. The absolute value of these limits are currently being researched. Further research is in progress to determine the validity of the 1995 low [nitrate+nitrite] episode. This work includes analysis of the standards used when measuring [nitrate+nitrite], consistency checks with other variables, as well as comparisons with independent data sources. The low [nitrate+nitrite] episode observed in 1995 (Fig. 6.1.15b) is accompanied by an increase in oxygen concentration (Fig. 6.1.15a) in the intermediate waters between 27.0-27.8 kg m^{-3}.

Intermediate water SRP (between 27.0-27.8 kg m^{-3}) starts increasing in early 1997, after a decreasing trend established in early 1994 (Fig. 6.1.12b). A time series of mean SRP in this layer shows this trend clearly (Figure 6.1.15c). Decreases in phosphate in the deeper waters could persist for long periods of time as the oceanic ecosystem associated with Station ALOHA has been hypothesized to be phosphorus limited in recent years (Karl et al. 1995; Karl and Tien 1997). Oxygen concentrations between 27.0-27.8 kg m^{-3} vary during the decrease of phosphate from early 1994 through 1997 without any apparent correlation.

4.2. Thermosalinograph data

Underway measurements of near surface temperature (NST) and near surface salinity (NSS) measured by the thermosalinograph as well as navigation and ship speed during HOT-79 through HOT-88 are presented in Figure 6.1.16.

4.2.1 HOT-79

Time-series of NST and NSS measured by the thermosalinograph during this cruise are shown in Figure 6.1.16a. Temperatures for HOT-79 ranged from 23.4 to 24.6 ºC and salinities ranged from 34.7 to almost 35.

4.2.2 HOT-80

Figure 6.1.16b shows the time-series of NST and NSS during HOT-80. Temperatures for HOT-80 ranged from 23.7 to 25 ºC and salinities ranged from 34.7 to values greater than 34.9 including some values above 35 which occurred on the transit back to Honolulu. Some instances of small-scale variability in both temperature and salinity can be seen at times near and after local noon from February 17-20 possibly due to solar heating.

4.2.3 HOT-81

Figure 6.1.16c shows the time-series of NST and NSS during HOT-81. Temperatures for HOT-81 ranged from 23 to 25.5 ºC and salinities ranged from 34.3 to 35.1 Some instances of small-scale variability in both temperature and salinity can be seen at times near and after local noon, possibly due to solar heating on March 12 and 13. Large salinity variation can also be observed later in the day on March 13.

4.2.4 HOT-82

Figure 6.1.16d shows the time-series of NST and NSS during HOT-82. A large and sudden offset between the thermosalinograph and salinity bottle samples developed near the end of the cruise (April 11). A cause for this offset was not discovered. Thermosalinograph salinity readings for this time period were corrected using the bottle samples however, these readings are considered suspect and are plotted with a dotted line. Some instances of small-scale variability in both temperature and salinity can be seen at times near and after local noon, possibly due to solar heating on April 9 and 10.

4.2.5 HOT-83

The large offset between the thermosalinograph salinities and bottle salinity samples observed in HOT-82 persisted until HOT-83. However, on the second day of HOT-83 (on May 6) the difference between the thermosalinograph salinities and the bottle salinity samples returned to normal levels. Figure 6.1.16e shows the time-series of NST and NSS during HOT-83. The NSS points plotted with a dotted line indicate the time period when the thermosalinograph salinities and the salinity bottle samples had a large offset. These thermosalinograph data were corrected using the salinity bottle samples but are considered suspect. Rainy weather encountered during this cruise could be responsible for the sharp drops seen in salinity from May 7-9.

4.2.6 HOT-84

Figure 6.1.16f shows the time-series of NST and NSS during HOT-84. Temperatures for HOT-84 ranged from 24.8 to 27 °C and salinities ranged from 34.7 to 35.

4.2.7 HOT-85

Figure 6.1.16g shows the time-series of NST and NSS during HOT-85. Temperatures for HOT-85 ranged from 23.5 to 27 °C and salinities ranged from 34.7 to 35.1.

4.2.8 HOT-86

Figure 6.1.16h shows the time-series of NST and NSS during HOT-86. Temperatures for HOT-86 ranged from 25.7 to 27.6 °C and salinities ranged from 34.7 to 35.1.

4.2.9 HOT-87

HOT-87 was conducted aboard R/V *Roger Revelle*. As mentioned in Section 2.2.2.3 the near-surface water which was measured for salinity by the thermosalinograph aboard R/V *Roger Revelle* was also used to cool the ship's engines. At times, this caused a very noisy salinity signal which also had a large amount of spikes. These data were flagged suspect and are plotted as a dotted in Figure 6.1.16i which shows the time-series of NST and NSS during HOT-87.

4.2.10 HOT-88

As mentioned in Section 2.2.1, the thermosalinograph aboard R/V *Moana Wave* had to be shutdown for about 13 hours due to bad weather and large seas. Time-series of NST and NSS measured by the thermosalinograph during HOT-88 are shown in Figure 6.1.16j. The shutdown of the thermosalinograph is apparent in the time-series plot as there is a large gap in Figure 6.1.16j for both temperature and salinity. Temperatures for HOT-88 ranged from 24.4 to 26.6 ºC and salinities ranged from 34.6 to almost 35.2. Rainy weather encountered during this could be responsible for some of the sharp drops seen in salinity throughout the cruise. Also, bubbles were introduced in to the thermosalinograph intake system due to the bow heaving through the large seas which could have also caused drops in salinity.

4.3. Meteorology

The meteorological data collected by HOT program scientists include atmospheric pressure, sea-surface temperature and wet and dry bulb air temperature. These data are presented in Figures 6.1.17 to 6.1.19. As described by Winn et al. (1991), parameters show evidence of annual cycles, although the daily and weekly ranges are nearly as high as the annual range for some variables. Wind speed and direction are also collected on HOT cruises. These data are presented in Figure 6.1.20.

One National Data Buoy Center (NDBC) meteorological buoy is located in the vicinity of the ALOHA Station (Fig. 1.1). Buoy #51001 is 400 km west of ALOHA at 23.4 °N, 162.3 °W. This buoy collects hourly observations of air temperature, sea surface temperature, atmospheric pressure, wind speed and direction and significant wave height. The coherence of the data from Buoy #51001 with the data collected on HOT cruises was examined and reported in Tupas et al. (1993). We concluded from these analyses, that the data from this buoy can be used to get useful estimates of air temperature, sea-surface temperature and atmospheric pressure at Station ALOHA when the station is not occupied. The wind vectors from buoy #51001 are plotted

together with the ship observations in Figure 6.1.20. As explained earlier (Section 2.4), data from this buoy were not available during cruise HOT-88.

4.4. Biogeochemistry

4.4.1. Dissolved oxygen

A contour plot of dissolved oxygen in the upper 200 m of the water column from 1988-1997 analyzed from water samples collected at discrete depths is shown in Figure 6.2.1. Dissolved oxygen shows a maximum between 20 and 120 m depth and is fairly mixed in that layer. Gradients begin to form below 100 meters. The development of this maximum appears to occur during the spring and summer months and becomes mixed down in the winter.

4.4.2. Inorganic carbon

Time-series of titration alkalinity and DIC in the mixed layer are presented in Figure 6.2.2. Titration alkalinity normalized to 35 ppt salinity averages approximately 2305 µequiv kg^{-1} and, within the precision of the analysis, appears to remain relatively constant at Station ALOHA. This observation is consistent with the results of Weiss et al. (1982) who concluded that titration alkalinity normalized to salinity remains constant in both the North and South Pacific subtropical gyres. In contrast to titration alkalinity, the concentration of DIC varies annually. DIC in the mixed layer is highest in March and April and lowest in September and October. This oscillation is consistent with an exchange of carbon dioxide across the air-sea interface driven by temperature dependent changes in mixed layer pCO_2.

4.4.3. Inorganic nutrients

Euphotic zone nutrient concentrations at Station ALOHA are at or well below the detection limits of the autoanalyzer methods. Other analytical techniques and instrumentation are used to measure the nanomolar levels of [nitrate + nitrite] and SRP in the upper water column. Figure 6.2.3 show the profiles obtained from our low level nitrate analyses at Station ALOHA and HALE ALOHA respectively. The upper 100 m is generally depleted in [nitrate + nitrite] with a few intrusions during the winter periods. At depths shallower than 100 dbar, SRP is typically less than 150 nmol kg^{-1} and on occasion, as low as 15 nmol kg^{-1} (Figure 6.2.4). SRP concentrations appear to vary by at least 3-fold in this region. Concentrations of [nitrate + nitrite] at depths less than 100 m are always less than 10 nmol kg^{-1} and are often less the 5 nmol kg^{-1}.

4.4.4. Organic nutrients

Contour plots of dissolved organic carbon (DOC), nitrogen (DON) and phosphorus (DOP) are presented in Figures 6.2.5-7. DOC concentrations are about 100 µmol kg^{-1} at the surface and decrease rapidly to about 60 µmol kg^{-1} at about 300 m. DON is about 6 µmol kg^{-1} at the surface and gradually decreases to about 2 µmol kg^{-1} about 800 meters. DOP is about 0.3 µmol kg^{-1} at the surface and gradually decrease to about 0.1 µmol kg^{-1} at about 300 m.

4.4.5. Particulate matter

Particulate carbon (PC), nitrogen (PN) and phosphorus (PP) concentrations in the surface ocean over the nine years of the program are shown in Figure 6.2.8. PC varies between 1.3-3.3 µmol kg^{-1}, PN between 0.08-0.65 µmol kg^{-1} and PP between 8-35 nmol kg^{-1} in the upper 100 m of the water column. PC and PN appear to have an annual cycle with the greatest particulate concentrations in summer/fall and lowest in winter. A significantly larger PN concentration was observed in the late fall of 1993 with only a slight increase in PC and a decrease in PP. The temporal distributions and magnitude of PC, PN, and PP in 1996 were similar to previous years.

4.4.6. Pigments

A contour plot of chlorophyll *a* concentrations measured using standard fluorometric techniques from 0 to 200 dbar over the eight years of the program is shown in Figure 6.2.9. As expected a chlorophyll maximum with concentrations up to 300 µg m^{-3} is observed at approximately 100 dbar. The chlorophyll *a* concentrations at depths shallower than 50 m display a clear annual cycle increasing in the fall and winter and decreasing through spring and summer which is approximately 4-6 months out of phase with the annual oscillation at the base of the euphotic zone (Winn et al. 1995).

4.4.7. Adenosine 5' Triphosphate

The concentration of particulate ATP closely resembles that of particulate matter with a maximum concentration at the surface and decreasing with depth (Figure 6.2.10). An annual cycle is evident at about 100 meters where the chlorophyll maximum also occurs. There appears to be coherence in the dynamics of chlorophyll and ATP at this depth (Winn et al. 1995).

4.5. Biogeochemical Rates

4.5.1. Primary Productivity

The results of the ^{14}C incubations and pigment determinations for samples collected from Go-Flo casts in 1997 are presented in Tables 4.1 and 4.2. Table 4.1 presents the primary production and fluorometric pigment measurements made at individual depths on all 1997 cruises. Table 4.2 presents integrated values for irradiance, pigment concentration and primary production rates. The pigment concentrations and ^{14}C incorporation rates reported are the average of triplicate determinations.

Integrated primary production rates measured over all 9 years of the program are shown in Figure 6.2.11 in order to place the 1997 results within the context of the time-series data set. Rates of primary production, integrated over the euphotic zone during the nine years of the time-series program, show a seasonal cycle. Measured rates ranged from less than 200 to greater than 800 mg C m^{-2} d^{-1} with the highest rate being observed in May 1995. This variability, with a range of a factor of 4, is surprisingly large. However, the majority of the primary production estimates were between 250 and 600 mg C m^{-2} d^{-1}, and the average rate of primary production was approximately 477 mg C m^{-2} d^{-1}. Although this value is higher than historical measurements for the central ocean basins (Ryther 1969), it is consistent with more recent measurements using modern methodology (Martin et al. 1987; Laws et al. 1989; Knauer et al. 1990).

Table 4.1: Primary production and Pigment summary

Cruise	Depth	Chl a	Chl a	Phaeo	Phaeo	L12	L12	L12	D12	D12	D12
	(m)	mg/m3	mg/m3	mg/m3	mg/m3	mgC/m3	mgC/m3	mgC/m3	mgC/m3	mgC/m3	mgC/m3
			STD		STD	rep #1	rep #2	rep #3	rep #1	rep #2	rep #3
79	5	0.088	0.005	0.075	0.008	5.27	7.12	6.76	0.14	0.22	0.16
79	25	0.075	0.000	0.093	0.016	4.25	4.53	4.36	0.18	0.19	0.18
79	45	0.094	0.014	0.118	0.023	0.78	0.42	0.64	0.12	0.25	0.25
79	75	0.221	0.002	0.473	0.009	2.98	2.53	3.52	0.16	0.13	0.13
79	100	0.140	0.010	0.438	0.067	0.68	0.79	0.91	0.12	0.15	0.14
79	125	0.094	0.003	0.332	0.021	0.24	0.24	0.25	0.09	0.08	0.07
79	150	0.054	0.003	0.171	0.004	0.11	0.13	0.11	0.10	0.16	0.11
79	175	0.022	0.001	0.086	0.004	0.04	0.04	0.05	0.05	0.04	0.04
80	5	0.097	0.000	0.071	0.007	6.80	6.11	5.97	0.15	0.16	0.13
80	25	0.096	0.002	0.075	0.002	5.35	4.49	bad value	0.21	0.19	0.17
80	45	0.094	0.001	0.071	0.003	2.28	2.80	2.52	0.19	0.25	0.17
80	75	0.125	0.009	0.107	0.013	3.58	3.38	3.60	0.24	0.37	0.26
80	100	0.198	0.004	0.198	0.021	2.28	2.31	2.18	0.17	0.21	0.18
80	125	0.222	0.015	0.362	0.043	0.65	0.76	0.76	0.17	0.13	0.14
80	150	0.146	0.001	0.224	0.011	0.25	0.27	0.24	0.23	0.26	0.20
80	175	0.072	0.006	0.177	0.009	0.10	0.10	0.12	0.06	0.07	0.06
81	5	0.091	0.002	0.069	0.003	6.72	7.22	7.01	0.13	0.12	0.11
81	25	0.084	0.004	0.069	0.003	1.65	1.44	1.55	0.14	0.17	0.15
81	45	0.098	0.002	0.087	0.006	4.58	4.80	5.18	0.19	0.16	0.20
81	75	0.173	0.001	0.210	0.009	3.13	2.65	2.85	0.11	0.08	0.10
81	100	0.273	0.034	0.456	0.000	2.35	2.76	2.79	0.09	0.09	0.08
81	125	0.127	0.005	0.322	0.011	0.52	0.57	0.56	0.08	0.10	0.08
81	150	0.054	0.000	0.130	0.006	0.12	0.12	0.12	0.05	0.06	0.06
81	175	0.055	0.003	0.139	0.048	0.06	0.08	0.07	0.05	0.05	0.05
82	5	0.064	0.004	0.061	0.022	2.90	11.56	2.91	0.12	0.10	no sample
82	25	0.076	0.014	0.058	0.004	1.54	1.32	1.84	0.17	0.27	0.27
82	45	0.086	0.000	0.087	0.013	1.54	0.79	2.21	0.21	0.24	0.17
82	75	0.266	0.001	0.457	0.004	2.78	2.90	2.94	0.09	0.07	0.08
82	100	0.119	0.002	0.311	0.007	1.11	1.08	1.24	0.06	0.11	0.08
82	125	0.031	0.000	0.071	0.011	0.08	0.09	0.10	0.04	0.04	0.04
82	150	0.010	n=1	0.029	n=1	0.04	0.03	0.04	0.07	0.13	0.05
82	175	0.022	0.002	0.047	0.005	0.03	0.03	0.03	0.07	0.05	0.06
83	5	0.075	0.000	0.063	0.002	4.13	4.86	5.68	0.08	0.10	0.09
83	25	0.087	0.022	0.079	0.002	4.93	5.25	5.58	0.10	0.21	0.10
83	45	0.125	0.008	0.110	0.009	6.86	7.36	9.35	0.24	0.15	no sample
83	75	0.175	0.003	0.173	0.012	3.18	1.99	5.09	0.08	0.07	0.08
83	100	0.256	0.001	0.448	0.052	4.95	4.62	no sample	0.14	0.12	no sample
83	125	0.131	0.005	0.384	0.012	1.18	1.31	no sample	no sample	0.09	no sample
83	150	0.042	n=1	0.137	0.137	0.21	0.22	no sample	bad value	bad value	no sample
83	175	0.016	0.001	0.047	0.006	0.04	0.04	no sample	bad value	bad value	no sample

Table 4.1: continued

Cruise	Depth	Chl a	Chl a	Phaeo	Phaeo	L12	L12	L12	D12	D12	D12
	(m)	mg/m3	mg/m3	mg/m3	mg/m3	mgC/m3	mgC/m3	mgC/m3	mgC/m3	mgC/m3	mgC/m3
			STD		STD	rep #1	rep #2	rep #3	rep #1	rep #2	rep #3
84	5	0.058	0.001	0.047	0.003	10.46	10.06	6.07	0.20	0.21	0.14
84	25	0.055	0.003	0.047	0.005	9.20	8.78	6.35	0.20	0.22	0.23
84	45	0.084	0.003	0.076	0.002	5.53	6.13	4.31	0.23	0.26	0.19
84	75	0.095	0.001	0.086	0.009	2.70	2.32	2.13	0.22	0.18	0.17
84	100	0.157	0.008	0.182	0.001	2.21	2.31	1.63	0.11	0.11	0.09
84	125	0.255	0.003	0.575	0.007	1.18	1.08	1.09	0.08	0.09	0.09
84	150	0.076	0.005	0.230	0.008	0.19	0.21	0.21	0.09	0.07	0.09
84	175	0.010	0.000	0.039	0.010	0.04	0.04	0.03	0.04	0.03	0.03
85	5	0.077	0.007	0.061	0.002	5.19	2.54	no sample	0.23	no sample	no sample
85	25	0.084	0.002	0.068	0.005	7.43	6.26	no sample	0.19	no sample	no sample
85	45	0.070	0.004	0.065	0.011	4.14	4.07	no sample	0.15	no sample	no sample
85	75	0.113	0.003	0.142	0.056	2.17	2.36	no sample	0.15	no sample	no sample
85	100	0.207	0.006	0.282	0.022	1.60	1.52	no sample	0.06	no sample	no sample
85	125	0.182	0.001	0.510	0.043	0.43	0.62	no sample	0.08	no sample	no sample
85	150	0.056	0.001	0.178	0.003	0.12	0.11	no sample	0.03	no sample	no sample
85	175	0.086	0.003	0.170	0.007	0.12	0.10	no sample	0.09	no sample	no sample
86	5	0.054	0.003	0.055	0.003	3.53	3.59	3.60	0.18	0.20	0.19
86	25	0.059	0.002	0.053	0.014	6.41	6.70	7.75	0.19	0.22	0.17
86	45	0.069	0.001	0.061	0.000	6.07	5.91	6.16	0.21	0.25	0.22
86	75	0.121	0.016	0.117	0.026	2.20	2.35	2.49	0.23	0.22	0.22
86	100	0.225	0.005	0.313	0.002	1.81	1.77	1.95	0.12	0.12	0.13
86	125	0.124	0.002	0.423	0.026	0.53	0.68	0.62	0.04	0.06	0.06
86	150	0.055	0.002	0.214	0.006	0.15	0.13	0.15	0.03	0.04	0.04
86	175	0.048	0.003	0.122	0.002	0.10	0.10	0.14	0.05	0.08	no sample
87	5	0.055	0.004	0.057	0.01	6.04	5.43	6.04	0.29	0.26	0.24
87	25	0.058	0.001	0.051	0.01	6.92	6.03	6.31	0.29	0.24	0.23
87	45	0.055	0.001	0.053	0.01	4.57	4.23	4.26	0.33	0.35	0.32
87	75	0.104	n=1	0.097	n=1	2.73	2.44	2.66	0.23	0.23	no sample
87	100	0.188	0.023	0.215	0.02	1.22	1.19	1.20	0.23	0.25	0.24
87	125	0.184	0.001	0.509	0.00	0.65	0.68	0.70	0.06	0.07	0.08
87	150	0.080	0.004	0.283	0.00	0.18	0.16	0.17	0.06	0.06	0.12
87	175	0.072	0.003	0.159	0.01	0.16	0.15	0.16	0.20	0.24	0.22

Table 4.2: Primary production and pigment summary integrated values (0-200 m)

Cruise	Incident Irradiance ($E\ m^{-2}\ d^{-1}$)	Pigments ($mg\ m^{-2}$) Chl a	Phaeo	Incubation Duration (hrs)	Assimilation Rates ($mg\ C\ m^{-2}\ d^{-1}$) Light	Dark
79	36.0	19.0	44.6	11.8	314	25
80	43.1	25.1	31.3	14.0	436	35
81	47.5	23.0	36.5	12.2	420	19
82	58.6	16.5	28.3	14.0	233	20
83	57.6	21.9	35.4	14.2	603	15
84	42.7	19.3	32.1	14.0	579	26
85	42.1	22.1	38.4	14.0	418	22
86	57.5	19.0	35.0	14.5	476	24
87	47.0	20.2	37.1	13.0	452	39

4.5.2. Particle Flux

Particulate carbon (PC), nitrogen (PN) and phosphorus (PP) fluxes at 150 m are presented in Table 4.3 and Figures 6.2.12 for the nine years of the program. PC flux displays an annual cycle with peaks in both the early spring and in the late summer months. The magnitude of particle flux varies by a factor of approximately three. With the exception of anomalous PP fluxes measured on the first two HOT cruises, temporal variability in PN and PP show similar trends and also vary between cruises by about a factor of three. Elemental ratios of carbon-to-nitrogen (atom:atom) at 150 m are typically between 6-10 and show no obvious temporal pattern. These particle flux measurements and elemental ratios are consistent with those measured in the central North Pacific Ocean during the VERTEX program (Martin et al. 1987; Knauer et al. 1990).

Table 4.3: Station ALOHA sediment trap flux data

Cruise *	PC Flux ($mg\ m^{-2}\ d^{-1}$) mean	SD	n	PN Flux ($mg\ m^{-2}\ d^{-1}$) Mean	SD	n	PP Flux ($mg\ m^{-2}\ d^{-1}$) Mean	SD	n
79	18.2	1.6	3	2.9	0.1	3	0.14	0.11	3
80	35.8	2.5	3	4.8	0.8	3	0.49	0.08	3
81	23.7	4.2	6	3.2	0.6	6	0.26	0.07	3
82	32.3	4.8	6	3.4	0.5	6	0.28	0.06	3
83	46.0	6.4	3	5.4	1.1	3	0.34	0.06	3
84**							0.35	0.12	3
85	32.4	5.6	3	4.3	0.7	3	0.45	0.13	3
86	28.7	5.4	3	4.2	0.6	3	0.25	0.04	3

*Sediment traps were not deployed on cruises HOT-87 and 88
**Analytical problems during PC/PN analysis

4.6. Microbial Community Structure

Depth profiles of counts of heterotrophic and photosynthetic bacteria for each cruise are presented in Figure 6.2.13. At the surface, heterotrophic bacterial number range from 4 to 6 x 10^5 cells ml^{-1}. In some cases bacterial number decrease with depth although there are some profiles where the numbers remain fairly constant with depth. *Prochlorococcus* –like cells about 2 x 10^5 ml^{-1} at the surface and usually decrease with depth but with a subsurface maximum between 50 and 100 m.

4.7. Zooplankton Community Structure

Carbon biomass estimates for the mesozooplankton community at Station ALOHA from 1994-1997 are presented in Figures 6.2.14 and 6.2.15. Mean depth-integrated zooplankton carbon in the euphotic zone varies annually over a large range of 2-4 times with the highest values (300-700 mg C m^{-2}) typically in the late spring or summer month and lowest values (<100-300 mg C m^{-2}) in the winter. No one size category dominates the biomass distribution consistently, but larger animals (>500 μm) appear to contribute disproportionately relative to smaller forms (200-500 μm) in 1996 than in the previous two years (Figure 6.2.14). Standing stocks of zooplankton are generally higher in the euphotic zone in night-time tows due to diel migrations of animals which position themselves at deeper depth during the day (Figure 6.2.15). These day-night differences in standing stocks, which is composed mostly of animals in the larger size fractions (> 500 μm), averages approximately a factor of two. In contrast to the migration pattern of previous years, the magnitude of the day-night difference in mesozooplankton standing stock appeared to be depressed during 1997, a major El Niño year.

4.8. ADCP

Upper ocean currents were measured using the ADCP mounted on the R/V Moana Wave (RD Instruments model VM-150) on nine of the HOT cruises, on all five HALE mooring deployment and/or recovery cruises, and on the ALOHA CLIMAX cruise. For one HOT cruise (HOT87) measurments were made by the ADCP aboard the R/V Roger Revelle. There were no significant data recording gaps. GPS navigation (differential or PCODE) was available throughout all cruises. ADCP velocities were corrected for gyro compass errors as measured by the Ashtech 3DF GPS attitude sensors on the Moana Wave and Revelle. Gaps were very short and infrequent. ALOHA CLIMAX-2 had 2 gaps of ~40 minutes; all other gaps were less than 25 minutes. All gaps were filled by linearly interpolating the gyro error estimates. Rough weather or seas on the northward transit, combined with an acoustic ringing problem in the upper bins of data collected aboard the Revelle (HOT-87), resulted in sections of reduced and complete loss of the returning signal. HOT-80, HOT-83, and HOT-88 also experienced reduced signal returns due to rough weather on northward transits. These conditions resulted in velocity bias in the direction of ship's motion. Biased regions have been edited out, and will therefore appear as gaps in the plots. Gaps in the on-station data of HOT-79, HOT-81, and HOT-85 are due to excursions to retrieve the primary productivity array and floating sediment traps.

5.0 REFERENCES

Bidigare, R.R., J. Marra, T.J. Dickey, R. Iturriaga, K.S. Baker, R.C. Smith and H. Pak. 1990. Evidence for phytoplankton succession and chromatic adaptation in the Sargasso Sea during Spring 1985. *Marine Ecology Progress Series*, 60, 113-122.

Brewer, P.G., K.W. Bruland, R.W. Eppley and J.J. McCarthy. 1986. The Global Ocean Flux Study (GOFS): Status of the US-GOFS program. *EOS, Transactions of the American Geophysical Union*, 67, 827-832.

Campbell, L., H. Nolla and D. Vaulot. 1994. The importance of *Prochlorococcus* to community structure in the central North Pacific Ocean. *Limnology and Oceanography*, 39, 954-961.

Chiswell, S.M. 1996. Intra-annual oscillations at Station ALOHA, north of Oahu, Hawaii. *Deep-Sea Research II*, 43, 305-319.

Chiswell, S.M., E. Firing, D. Karl, R. Lukas, C. Winn. 1990. *Hawaii Ocean Time-series Program Data Report 1, 1988-1989.* School of Ocean and Earth Science and Technology, University of Hawaii, SOEST 90-1, 269 pp.

Clayton, T.D. and R.H. Byrne. 1993. Spectrophotometric seawater pH measurements: total hydrogen ion concentration scale calibration of m-cresol purple and at-sea results. *Deep-Sea Research*, 40, 2115-2129.

Cox, R.D. 1980. Determination of nitrate at the parts per billion level by chemiluminescence. *Analytical Chemistry*, 52, 332-335.

Dore, J.E. and D.M. Karl. 1996. Nitrite distributions and dynamics at Station ALOHA. *Deep-Sea Research*, 43, 385-402.

Dore, J.E., T. Houlihan, D.V. Hebel, G. Tien, L.M. Tupas and D.M. Karl. 1996. Freezing as a method of seawater preservation for the analysis of dissolved inorganic nutrients. *Marine Chemistry*, 53, 173-185.

Garside, C. 1982. A chemiluminescent technique for the determination of nanomolar concentrations of nitrate and nitrite in seawater. *Marine Chemistry*, 11, 159-167.

Hayward, T.L. 1987. The nutrient distribution and primary production in the central North Pacific. *Deep-Sea Research*, 34, 1593-1627.

Johnson, D.L. 1971. Simultaneous determination of arsenate and phosphate in natural waters. *Environmental Science and Technology*, 5, 411-414.

Karl, D.M., J.R. Christian, J.E. Dore, D.V. Hebel, R.M Letelier, L.M. Tupas and C.D. Winn. 1996a. Seasonal and interannual variability in primary production and particle flux at Station ALOHA. *Deep-Sea Research*, 43, 539-568.

Karl, D.M. and O. Holm-Hansen. 1978. Methodology and measurement of adenylate energy charge ratios in environmental samples. *Marine Biology*, 48, 185-197.

Karl, D.M., R. Letelier, D. Hebel, L. Tupas, J. Dore, J. Christian and C. Winn. 1995 Ecosystem changes in the North Pacific subtropical gyre attributed to the 1991-92 El Niño. *Nature*, 373, 230-234.

Karl, D.M., R. Letelier, L. Tupas, J. Dore, J. Christian and D. Hebel. 1997. The role of nitrogen fixation in biogeochemical cycling in the subtropical North Pacific Ocean. *Nature*, 388, 533-538.

Karl, D.M. and R. Lukas. 1996. The Hawaii Ocean Time-series (HOT) program: Background, rationale and field implementation. *Deep-Sea Research*, 43, 129-156.

Karl, D.M. and G. Tien. 1992. MAGIC: A sensitive and precise method for measuring dissolved phosphorus in aquatic environments. *Limnology and Oceanography*, 37, 105-116.

Karl, D.M. and G. Tien. 1997. Temporal variability in dissolved phosphorus concentrations at Station ALOHA (22°45'N, 158°W). *Marine Chemistry*, 56, 77-96.

Karl, D., L. Tupas, F. Santiago-Mandujano, C. Nosse, D. Hebel, E. Firing and R. Lukas, 1996b. *Hawaii Ocean Time-series Program Data Report 7, 1995.* School of Ocean and Earth Science and Technology, University of Hawaii, SOEST 96-09, 228 pp.

Karl, D.M. and C.D. Winn, 1991. A sea of change: Monitoring the oceans carbon cycle. *Environmental Science and Technology*, 25, 1967-1981.

Kennan, S.C. and R. Lukas. 1995. Saline intrusions in the intermediate waters north of Oahu, Hawaii. *Deep-Sea Research*, 43, 215-241.

Knauer, G.A., J.H. Martin and K.W. Bruland. 1979. Fluxes of particulate carbon, nitrogen and phosphorus in the upper water column of the northeast Pacific. *Deep-Sea Research*, 26, 97-108.

Knauer, G.A., D.G. Redalje, W.G. Harrison and D.M. Karl. 1990. New production at the VERTEX time-series site. *Deep-Sea Research*, 37, 1121-1134.

Larson , N. and A.M. Pederson. 1996. Temperature measurements in flowing water: Viscous heating of sensor tips. 1st International Group for Hydraulic Efficiency Measurements (IGHEM) Meeting, Montreal, Canada, June 1996.

Laws, E.A., G.R. DiTullio, P.R. Betzer, D.M. Karl and R.L. Carder. 1989. Autotrophic production and elemental fluxes at 26° N, 155° W in the North Pacific subtropical gyre. *Deep-Sea Research*, 36, 103-120.

Lukas, R. and S. Chiswell. 1991. Submesoscale water mass variations in the salinity minimum of the north Pacific near Hawaii. *WOCE Notes*, 3(1), 6-8.

Lukas, R., F. Santiago-Mandujano, F. Bingham and A. Mantyla. Cold water events observed in the Hawaii Ocean Time-series: Implications for vertical mixing. Submitted to *Deep Sea Research*.

Martin, J.H., G.A. Knauer, D.M. Karl and W.W. Broenkow. 1987. VERTEX: Carbon cycling in the northeast Pacific. *Deep-Sea Research*, 34, 267-285.

Michaels, A. and A. Knap. 1996. Overview of the U.S.-JGOFS Bermuda Atlantic Time-series Study and Hydrostation S program. *Deep-Sea Research*, 43, 157-198.

Monger, B,C, and M.R. Landry. 1993. Flow cytometry analysis of marine Bacteria with Hoechst 3342. *Applied and Environmental Microbiology*, 59, 905-911.

National Research Council. 1984a. *Global Observations and Understanding of the General Circulation of the Oceans: Proceedings of a Workshop*, National Academy Press, Washington, DC, 418 pp.

National Research Council. 1984b. *Global Ocean Flux Study: Proceedings of a Workshop*, National Academy Press, Washington, DC, 360 pp.

Ortner, P.B. E.M. Hulbert and P.H. Wiebe. 1979. Gulf Stream rings, phytohydrography and herbivore habitat contrasts. *Journal of Experimental Marine Biology and Ecology*, 39, 101-124.

Owens, W.B. and R.C. Millard. 1985. A new algorithm for CTD oxygen calibration. *Journal of Physical Oceanography*, 15, 621-631.

Qian, J. and K. Mopper. 1996. Automated high-performance, high-temperature combustion total organic carbon analyzer. *Analytical Chemistry*, 68, 3090-3097.

Quay, P.D., B. Tilbrook and C.S. Wong. 1992. Oceanic uptake of fossil fuel CO_2: Carbon-13 evidence. *Science*, 256, 74-79.

Ryther, J.H. 1969. Photosynthesis and fish production in the sea. The production of organic matter and its conversion to higher forms of life vary throughout the world ocean. *Science*, 166, 72-76.

Scientific Committee on Oceanic Research. 1990. *The Joint Global Ocean Flux Study (JGOFS) Science Plan.* JGOFS Report No. 5. International Council of Scientific Unions, 61 pp.

Strickland, J.D.H. and T.R. Parsons. 1972. *A Practical Handbook of Seawater Analysis*. Fisheries Research Board of Canada, 167 pp.

Tsuchiya, M. 1968. *Upper Waters of the Intertropical Pacific Ocean*. Johns Hopkins Oceanographic Studies, 4, 49 pp.

Tupas, L., F. Santiago-Mandujano, D. Hebel, E. Firing, F. Bingham, R. Lukas and D. Karl. 1994. *Hawaii Ocean Time-series Program Data Report 5, 1993.* School of Ocean and Earth Science and Technology, University of Hawaii, 156 pp.

Tupas, L., F. Santiago-Mandujano, D. Hebel, E. Firing, R. Lukas and D. Karl. 1995. *Hawaii Ocean Time-series Data Report 6: 1994*. School of Ocean and Earth Science and Technology, University of Hawaii, 199 pp.

Tupas, L., F. Santiago-Mandujano, D. Hebel, R. Lukas, D. Karl and E. Firing. 1993. *Hawaii Ocean Time-series Program Data Report 4, 1992*. School of Ocean and Earth Science and Technology, University of Hawaii, 248 pp.

Tupas, L., F. Santiago-Mandujano, D. Hebel, C. Nosse, L. Fujieki, E. Firing, R. Lukas and D. Karl. 1997. *Hawaii Ocean Time-series Program Data Report 8, 1996*. School of Ocean and Earth Science and Technology, University of Hawaii, SOEST 96-4, 296 pp.

UNESCO. 1981. *Tenth Report of the Joint Panel on Oceanographic Tables and Standards*. UNESCO Technical Papers in Marine Science, No. 36., UNESCO, Paris.

Vaulot, D. 1989. CYTOPC: Processing software for flow cytometric data. *Signal and Noise,* 2, 8.

Weiss, R.F., R.A. Jahnke and C.D. Keeling. 1982. Seasonal effects of temperature and salinity on the partial pressure of CO_2 in seawater. *Nature*, 300, 511-513.

Winn, C.D., L. Campbell, J.R. Christian, R.M. Letelier, D.V. Hebel, J.E. Dore, L. Fujieki and D.M. Karl. 1995. Seasonal variability in the phytoplankton community of the North Pacific subtropical gyre. *Global Biogeochemical Cycles*, 9, 605-620.

Winn, C., S.M. Chiswell, E. Firing, D. Karl, R. Lukas. 1991. *Hawaii Ocean Time-series Program Data Report 2, 1990*. School of Ocean and Earth Science and Technology, University of Hawaii, SOEST 92-01, 175 pp.

Winn, C., R. Lukas, D. Karl, E. Firing. 1993. *Hawaii Ocean Time-series Program Data Report 3, 1991*. School of Ocean and Earth Science and Technology, University of Hawaii, SOEST 93-3, 228 pp.

Wright, S.W., S.W. Jeffrey, R.F.C. Mantoura, C.A. Llewellyn, T. Bjornland, D. Repeta and N. Welschmeyer. 1991. Improved HPLC method for the analysis of chlorophylls and carotenoids from marine phytoplankton. *Marine Ecology Progress Series*, 77, 183-196.

6.0. FIGURES

6.1. HYDROGRAPHY

Figure 6.1.1a to j: [Upper left panel] Temperature, salinity, oxygen and potential density (σ_θ) as a function of pressure for the WOCE deep cast at Station ALOHA for each HOT cruise. [Upper right panel] Plot of [nitrate + nitrite], soluble reactive phosphate, silicate, and bottle dissolved oxygen as a function of potential temperature for all water samples. [Lower left panel] CTD temperature and salinity plotted as a function of pressure to 1000 dbar. [Lower right panel] Salinity and oxygen from CTD and water samples plotted as a function of potential temperature. Only the CTD oxygen traces in which bottle oxygen's were sampled are included.

Figure 6.1.2a to e: [1st and 3rd panel] Stack plots of temperature versus pressure to 1000 dbar at Station ALOHA. Offset is 2 °C. [2nd and 4th panel] Stack plots of salinity versus pressure to 1000 dbar at Station ALOHA. Offset is 0.1.

Figure 6.1.3a to j: [Upper left panel] Temperature, salinity, oxygen and potential density (σ_θ) as a function of pressure for the cast at Station Kahe for each HOT cruise. [Upper right panel] Plot of [nitrate + nitrite], soluble reactive phosphate, silicate, and CTD bottle dissolved oxygen and salinity as a function of potential temperature for all water samples. [Lower left panel] Plot of temperature, salinity, oxygen and potential density (σ_θ) as a function of pressure at Station HALE ALOHA. [Lower right panel] Plot of CTD and bottle salinity and oxygen as a function of potential temperature at Station HALE ALOHA. Station HALE ALOHA commenced on HOT-80.

Figure 6.1.4: [Upper panel] Potential temperature versus pressure for all deep casts in 1997. [Lower panel]: Potential temperature versus pressure for all deep casts in 1997 from 2500 dbar.

Figure 6.1.5: [Upper panel] Salinity versus potential temperature for all deep casts in 1997. [Lower panel]: Salinity versus potential temperature for all deep casts in 1997 in the 1-5 °C range.

Figure 6.1.6: [Upper panel] Oxygen concentrations from calibrated oxygen sensor data versus potential temperature for all deep casts in 1997. [Lower panel] Oxygen versus potential temperature for all deep casts in 1997 in the 1-5 °C range.

Figure 6.1.7: [Upper panel] Contour plot of CTD potential temperature versus pressure for HOT cruises 1-88. [Lower panel] Contour plot of potential density (σ_θ), calculated from CTD pressure, temperature and salinity, versus pressure for HOT cruises 1-88.

Figure 6.1.8: [Upper panel] Contour plot of CTD salinity versus pressure for HOT cruises 1-88. [Lower panel] Contour plot of CTD salinity versus potential density (σ_θ) to 27.5 kg m^{-3} for HOT cruises 1-88. The average density of the sea surface is connected by the heavy line.

Figure 6.1.9: [Upper panel] Contour plot of bottle salinity versus pressure for HOT cruises 1-88. Location of samples in the water column are indicated by the solid circles. [Lower panel] Contour plot of bottle salinity versus potential density (σ_θ)to 27.5 kg m^{-3} for HOT cruises 1-88. The average density of the sea surface is connected by the heavy line.

Figure 6.1.10: [Upper panel] Contour plot of bottle oxygen versus pressure for HOT cruises 1-88. Location of samples in the water column are indicated by the solid circles. [Lower panel]

Contour plot of bottle oxygen versus potential density (σ_θ) to 27.5 kg m^{-3} for HOT cruises 1-88. The average density of the sea surface is connected by the heavy line.

Figure 6.1.11: [Upper panel] Contour plot of [nitrate + nitrite] versus pressure for HOT cruises 1-88. Location of samples in the water column are indicated by the solid circles. [Lower panel] Contour plot of [nitrate + nitrite] versus potential density (σ_θ) to 27.5 kg m^{-3} for HOT cruises 1-78. The average density of the sea surface is connected by the heavy line.

Figure 6.1.12: [Upper panel] Contour plot of [nitrate + nitrite] versus potential density (σ_θ) from 27.0 to 27.8 kg m^{-3} for HOT cruises 1-88. [Lower panel] Contour plot of soluble reactive phosphate versus potential density (σ_θ) to 27.5 kg for HOT cruises 1-88.

Figure 6.1.13: [Upper panel] Contour plot of soluble reactive phosphate versus pressure for HOT cruises 1-88. Location of samples in the water column are indicated by the solid circles. [Lower panel] Contour plot of soluble reactive phosphate versus potential density (σ_θ) from 27.0 to 27.8 kg m^{-3} for HOT cruises 1-88. The average density of the sea surface is connected by the heavy line.

Figure 6.1.14: [Upper panel] Contour plot of silicate versus pressure for HOT cruises 1-88. Location of samples in the water column are indicated by the solid circles. [Lower panel] Contour plot of silicate versus potential density (σ_θ) to 27.5 kg m^{-3} for HOT cruises 1-88. The average density of the sea surface is connected by the heavy line.

Figure 6.1.15: Time series of mean bottle dissolved oxygen (upper panel), [nitrate + nitrite] (middle panel) and soluble reactive phosphate (lower panel) between 27.0 and 27.8 kg m^{-3} isopycnals. The smooth line is the spline fit to the data. The asterisks in the middle of each year is the annual mean.

Figure 6.1.16a to j: Thermosalinograph data for each HOT cruise in 1997, [Upper panel per cruise] Continuous surface salinity (upper line) and surface temperature (lower line). [Lower panel per cruise] Navigation (upper line: longitude, lower line: latitude) over time during the cruise. The vertical lines indicate the 36-hour period of burst sampling while on station.

Figure 6.1.17: [Upper panel] Atmospheric pressure while at Station ALOHA for 1997 HOT cruises. Open circles are individual measurements. [Lower panel] Sea surface temperature measured from a bucket sample while at Station ALOHA for 1997 HOT cruises.

Figure 6.1.18: [Upper panel] Dry bulb air temperature while at Station ALOHA for 1997 HOT cruises. [Lower panel] Wet bulb air temperature while at Station ALOHA for 1997 HOT cruises.

Figure 6.1.19: [Upper panel] Sea surface temperature minus dry air temperature while at Station ALOHA for 1997 HOT cruises. [Lower panel] Dry minus wet air temperature while at Station ALOHA for 1997 HOT cruises.

Figure 6.1.20a to c: [Upper panel per cruise] True winds measured at Station ALOHA. [Lower panel per cruise] True winds measured by NDBC buoy #51001. The orientation of the arrows indicate the wind direction; up is northward, right is eastward.

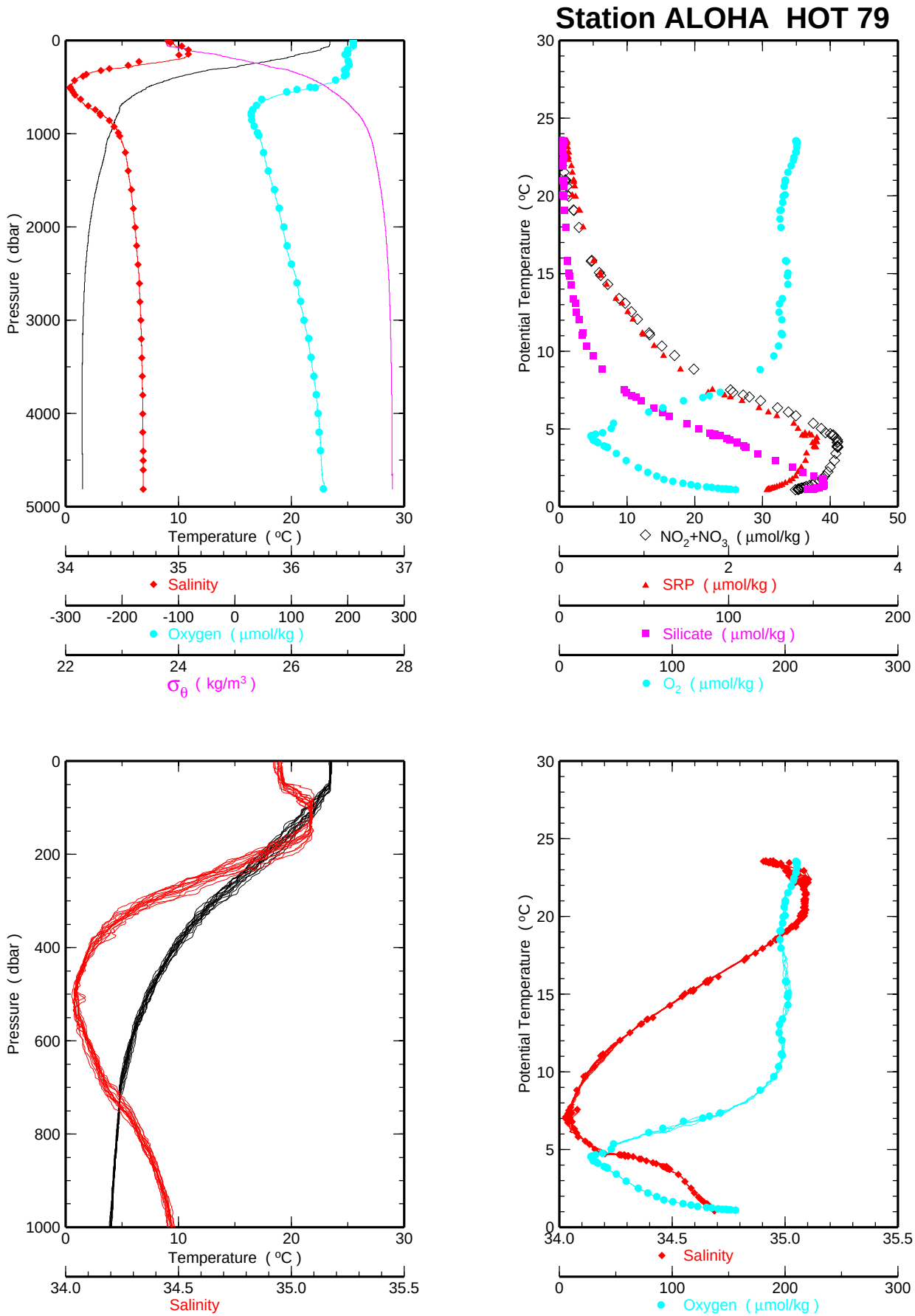
Station ALOHA HOT 79
Pressure (dbar)
Temperature (°C)
Salinity
Oxygen (µmol/kg)
σθ (kg/m³)
Potential Temperature (°C)
NO2+NO3 (µmol/kg)
SRP (µmol/kg)
Silicate (µmol/kg)
O2 (µmol/kg)

Figure 6.1.1a

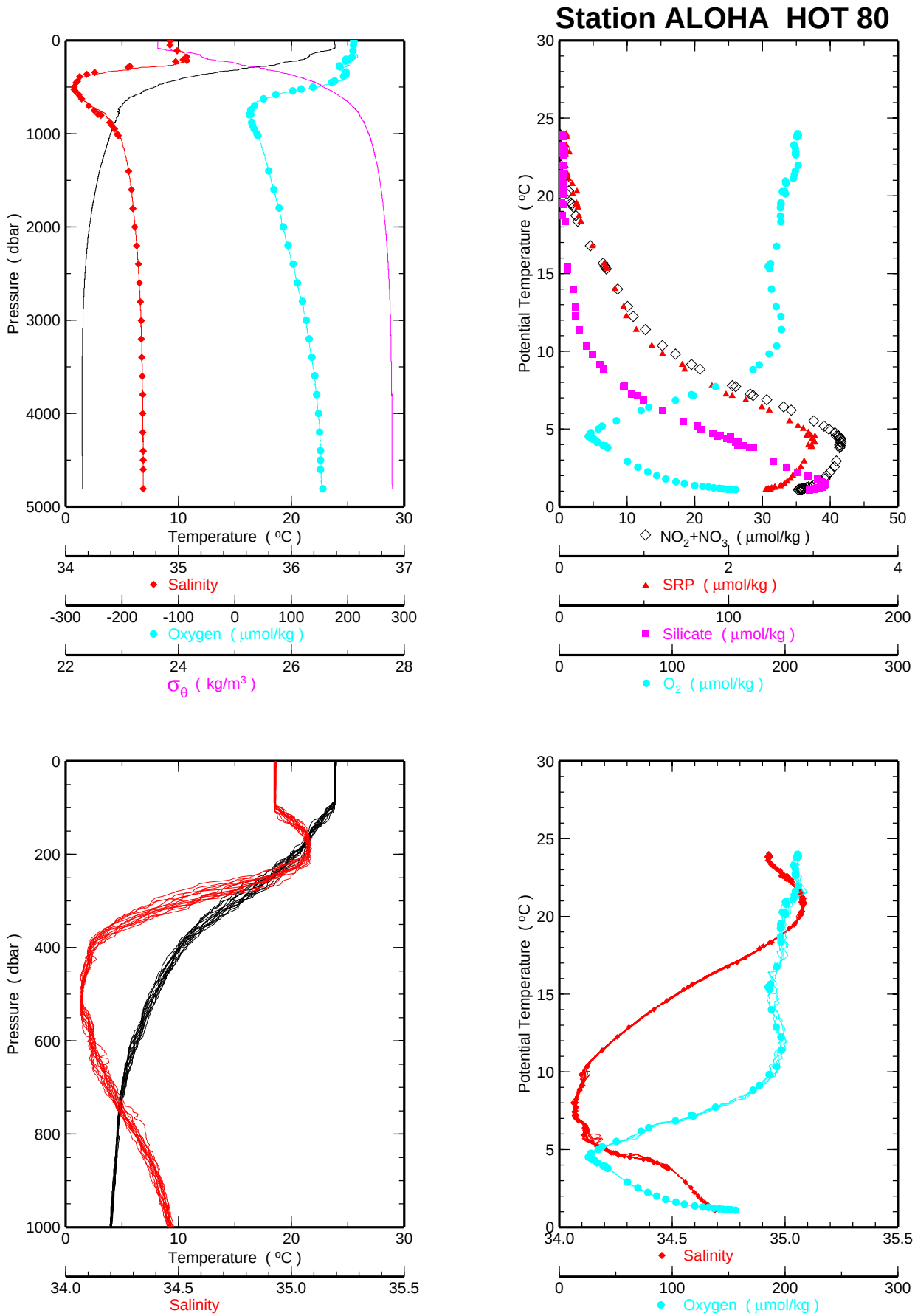
Station ALOHA HOT 80
Pressure (dbar)
Temperature (°C)
Salinity
Oxygen (µmol/kg)
σθ (kg/m³)
Potential Temperature (°C)
NO2+NO3 (µmol/kg)
SRP (µmol/kg)
Silicate (µmol/kg)
O2 (µmol/kg)

Figure 6.1.1b

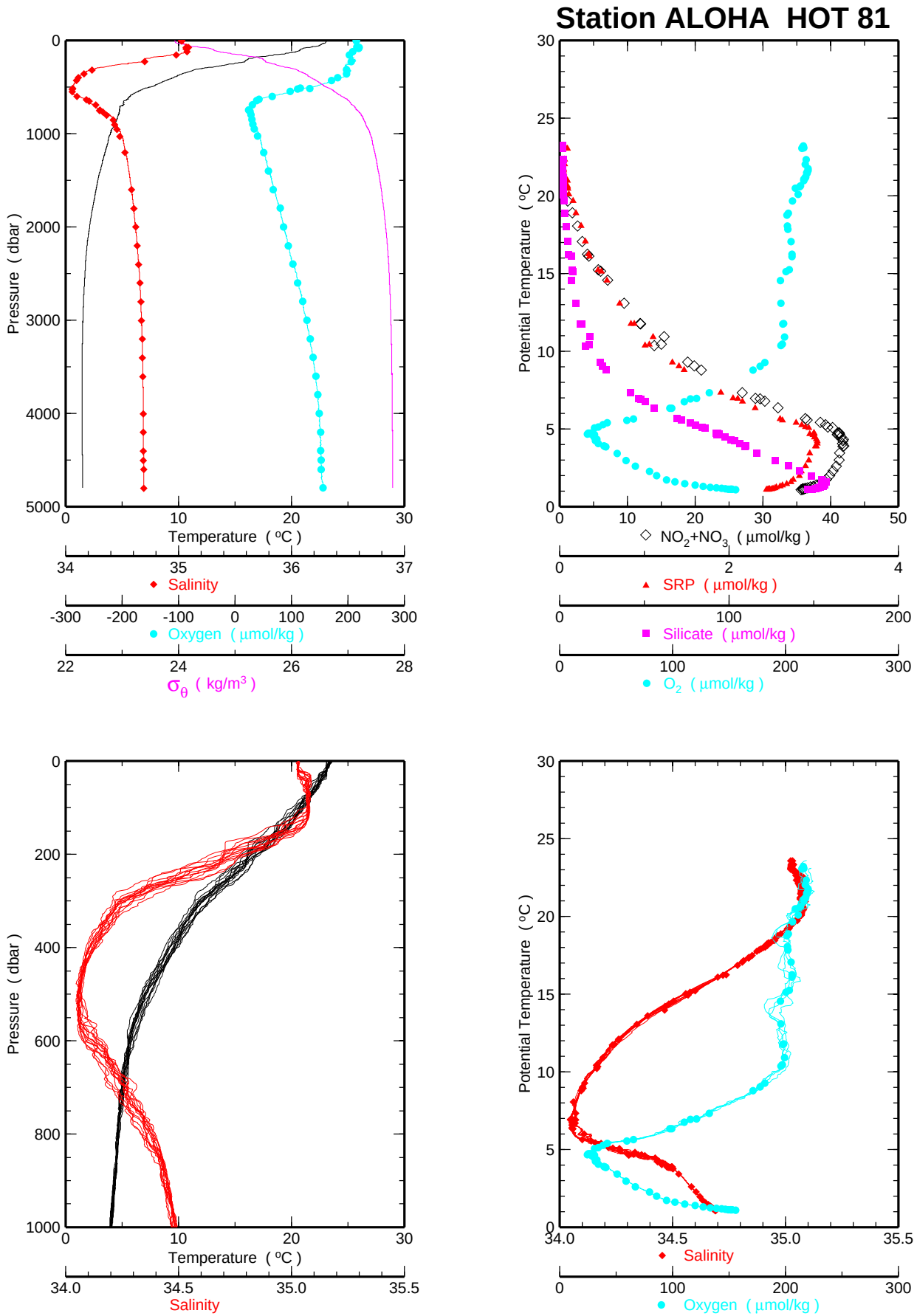
Station ALOHA HOT 81
Pressure (dbar)
Temperature (°C)
Salinity
Oxygen (µmol/kg)
σθ (kg/m³)
Potential Temperature (°C)
NO2+NO3 (µmol/kg)
SRP (µmol/kg)
Silicate (µmol/kg)
O2 (µmol/kg)

Figure 6.1.1c

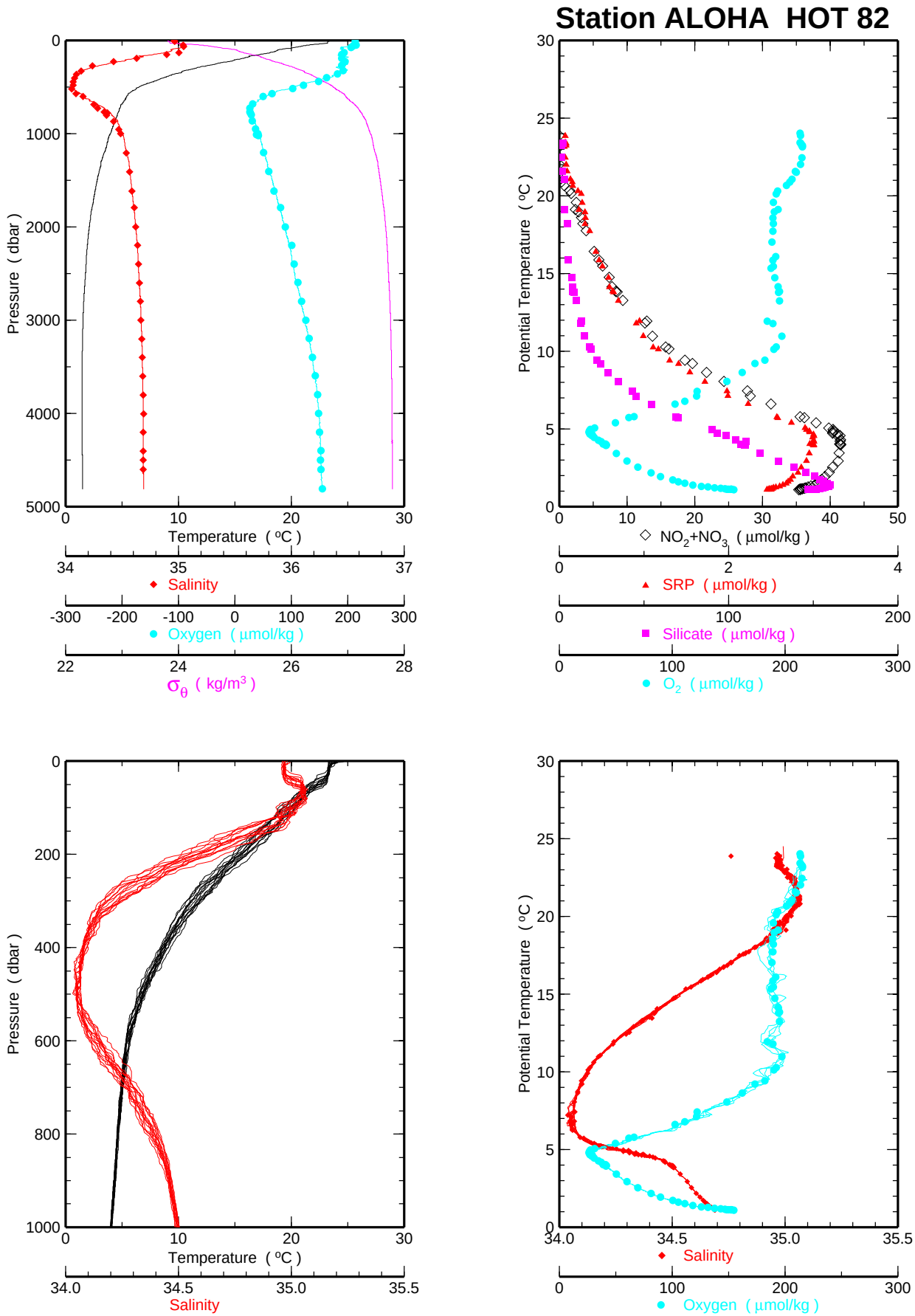
Station ALOHA HOT 82
Pressure (dbar)
Temperature (°C)
Salinity
Oxygen (µmol/kg)
σθ (kg/m³)
Potential Temperature (°C)
NO2+NO3 (µmol/kg)
SRP (µmol/kg)
Silicate (µmol/kg)
O2 (µmol/kg)

Figure 6.1.1d

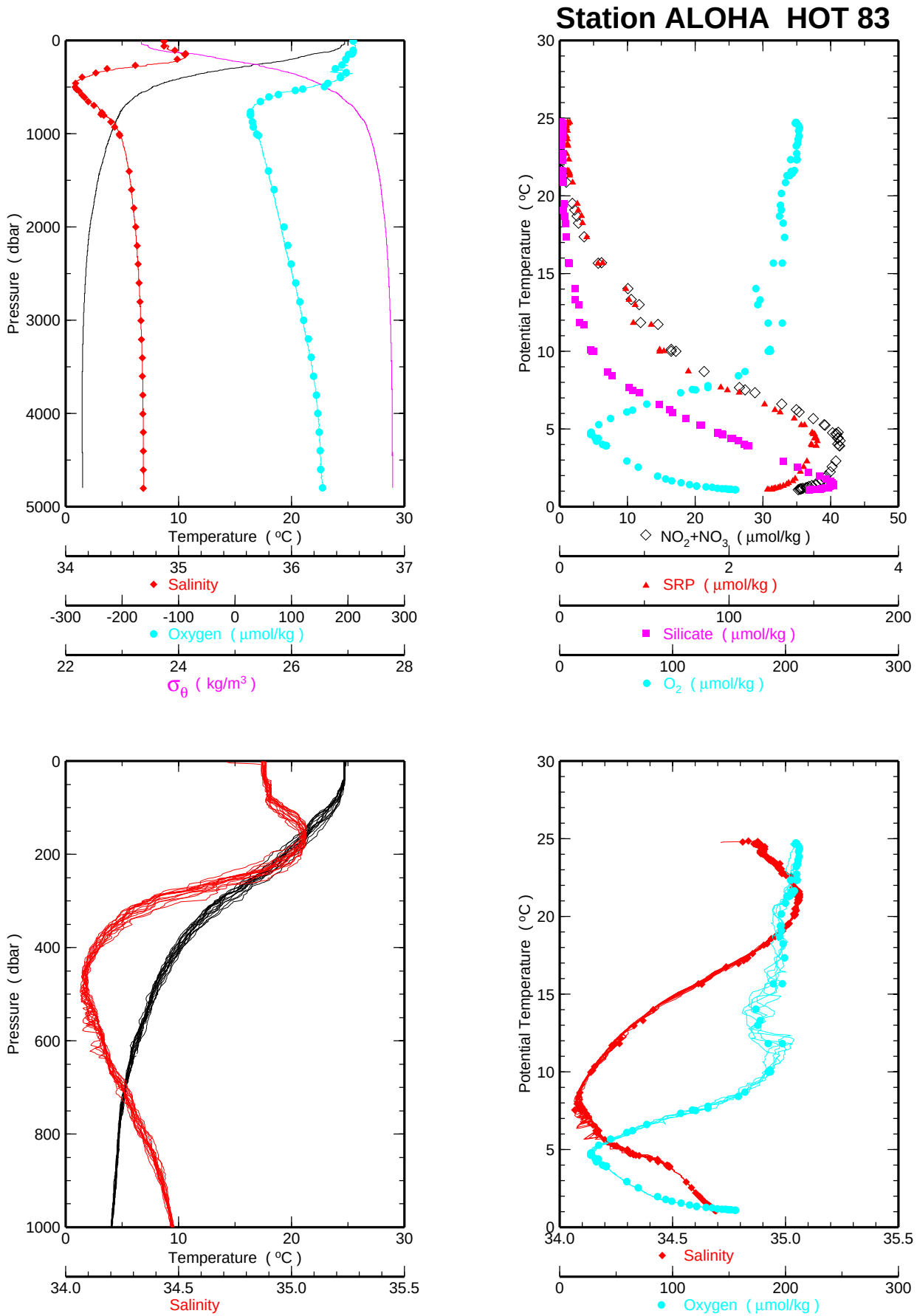
Station ALOHA HOT 83
Pressure (dbar)
Temperature (°C)
Salinity
Oxygen (µmol/kg)
σθ (kg/m³)
Potential Temperature (°C)
NO2+NO3 (µmol/kg)
SRP (µmol/kg)
Silicate (µmol/kg)
O2 (µmol/kg)
Pressure (dbar)
Temperature (°C)
Salinity
Potential Temperature (°C)
Salinity
Oxygen (µmol/kg)

Figure 6.1.1e

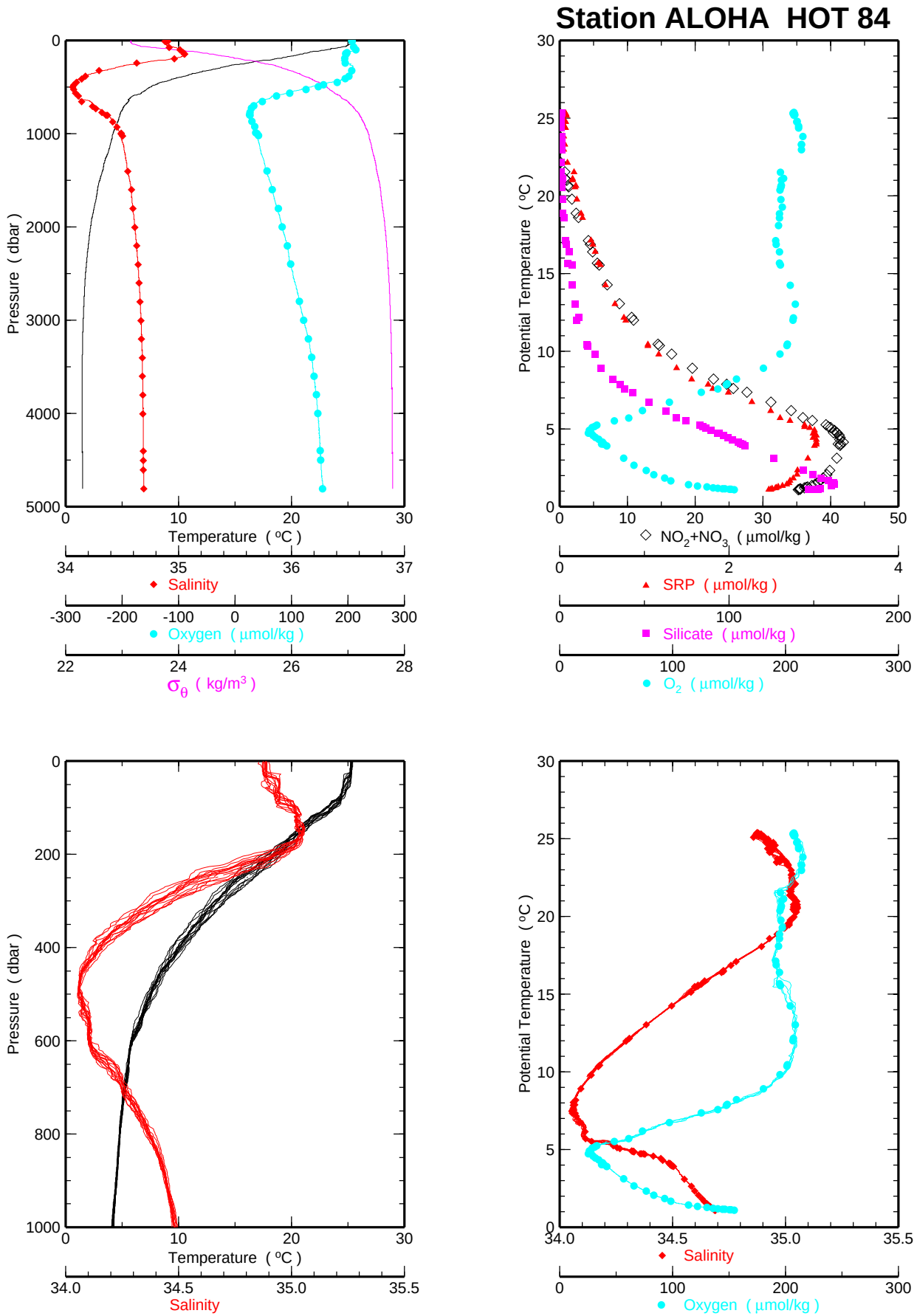
Station ALOHA HOT 84
Pressure (dbar)
Temperature (°C)
Salinity
Oxygen (µmol/kg)
σθ (kg/m³)
Potential Temperature (°C)
NO2+NO3 (µmol/kg)
SRP (µmol/kg)
Silicate (µmol/kg)
O2 (µmol/kg)
Pressure (dbar)
Temperature (°C)
Salinity
Potential Temperature (°C)
Salinity
Oxygen (µmol/kg)

Figure 6.1.1f

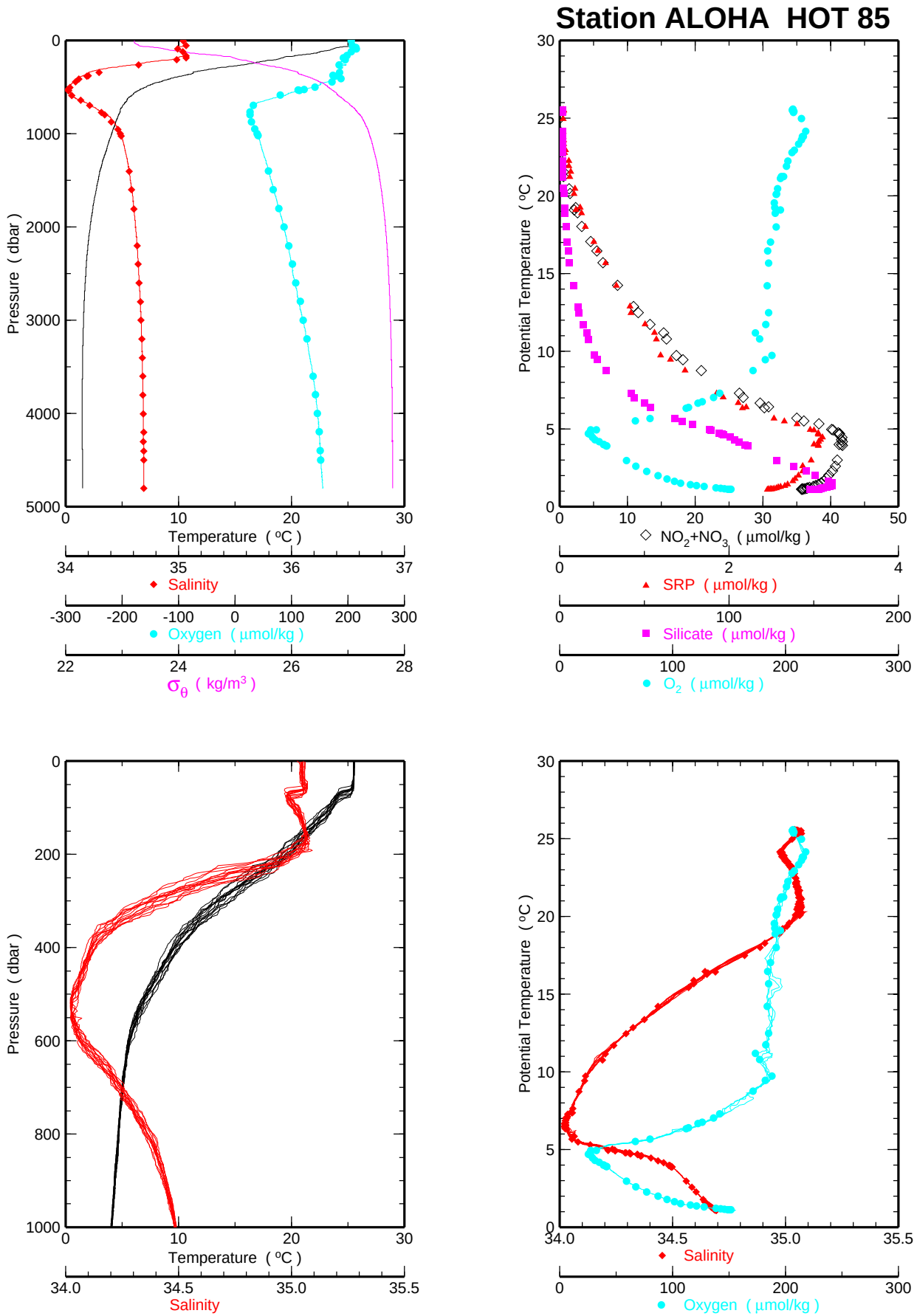
Station ALOHA HOT 85
Pressure (dbar)
Temperature (°C)
Salinity
Oxygen (µmol/kg)
σθ (kg/m³)
Potential Temperature (°C)
NO2+NO3 (µmol/kg)
SRP (µmol/kg)
Silicate (µmol/kg)
O2 (µmol/kg)

Figure 6.1.1g

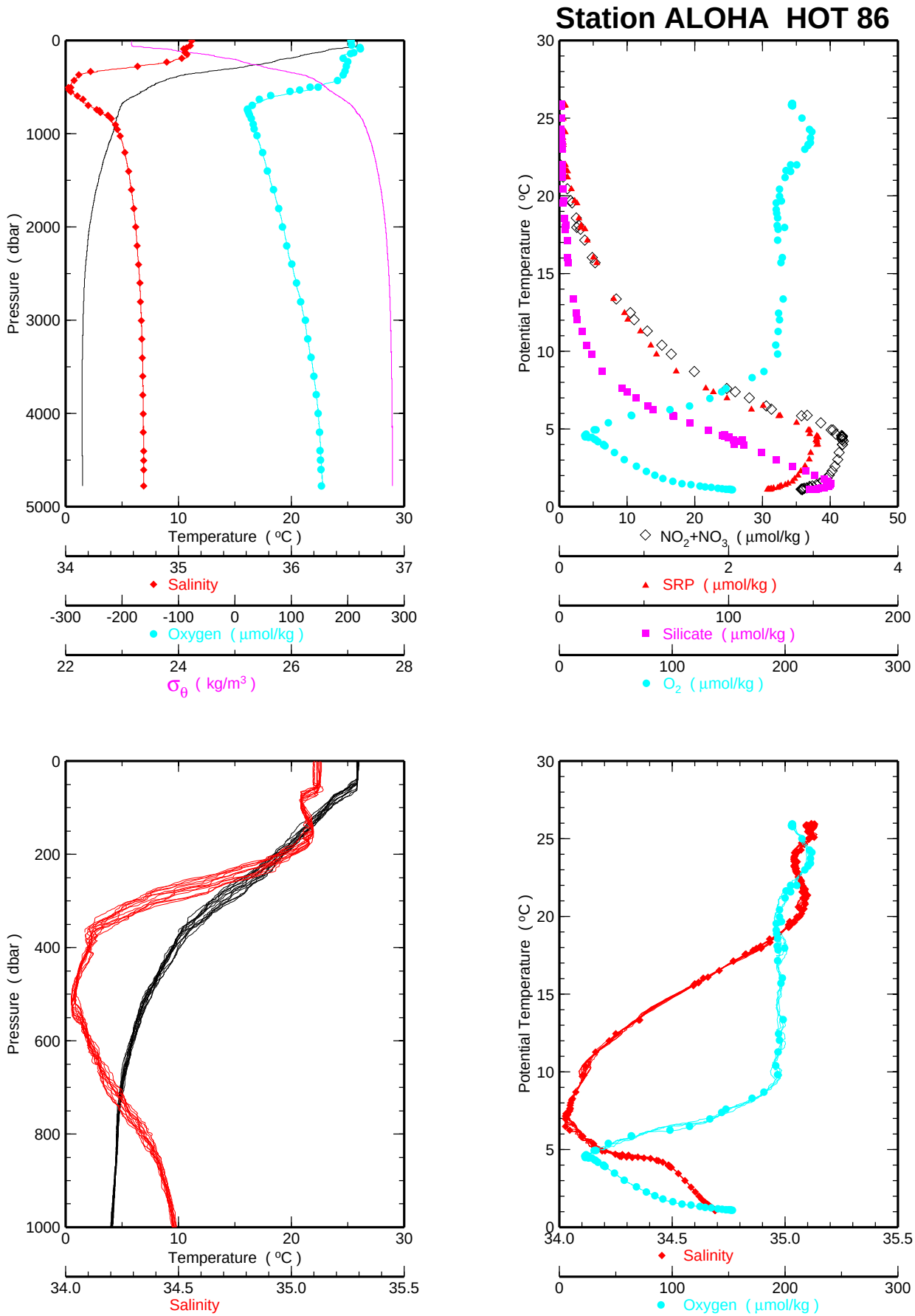
Station ALOHA HOT 86
Pressure (dbar)
Temperature (°C)
Salinity
Oxygen (µmol/kg)
σθ (kg/m³)
Potential Temperature (°C)
NO2+NO3 (µmol/kg)
SRP (µmol/kg)
Silicate (µmol/kg)
O2 (µmol/kg)

Figure 6.1.1h

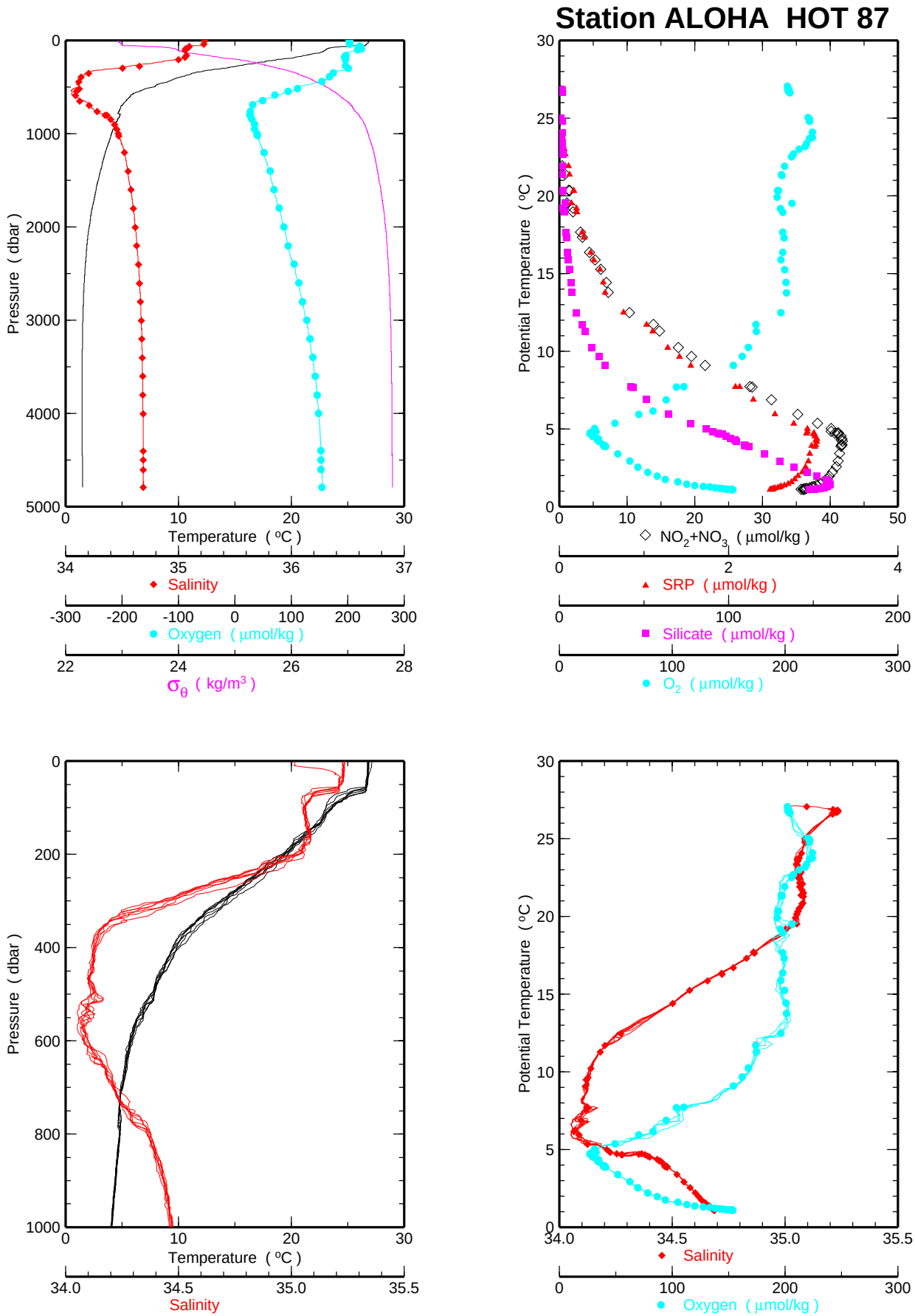
Station ALOHA HOT 87
Pressure (dbar)
Temperature (°C)
Salinity
Oxygen (µmol/kg)
σθ (kg/m³)
Potential Temperature (°C)
NO2+NO3 (µmol/kg)
SRP (µmol/kg)
Silicate (µmol/kg)
O2 (µmol/kg)

Figure 6.1.1i

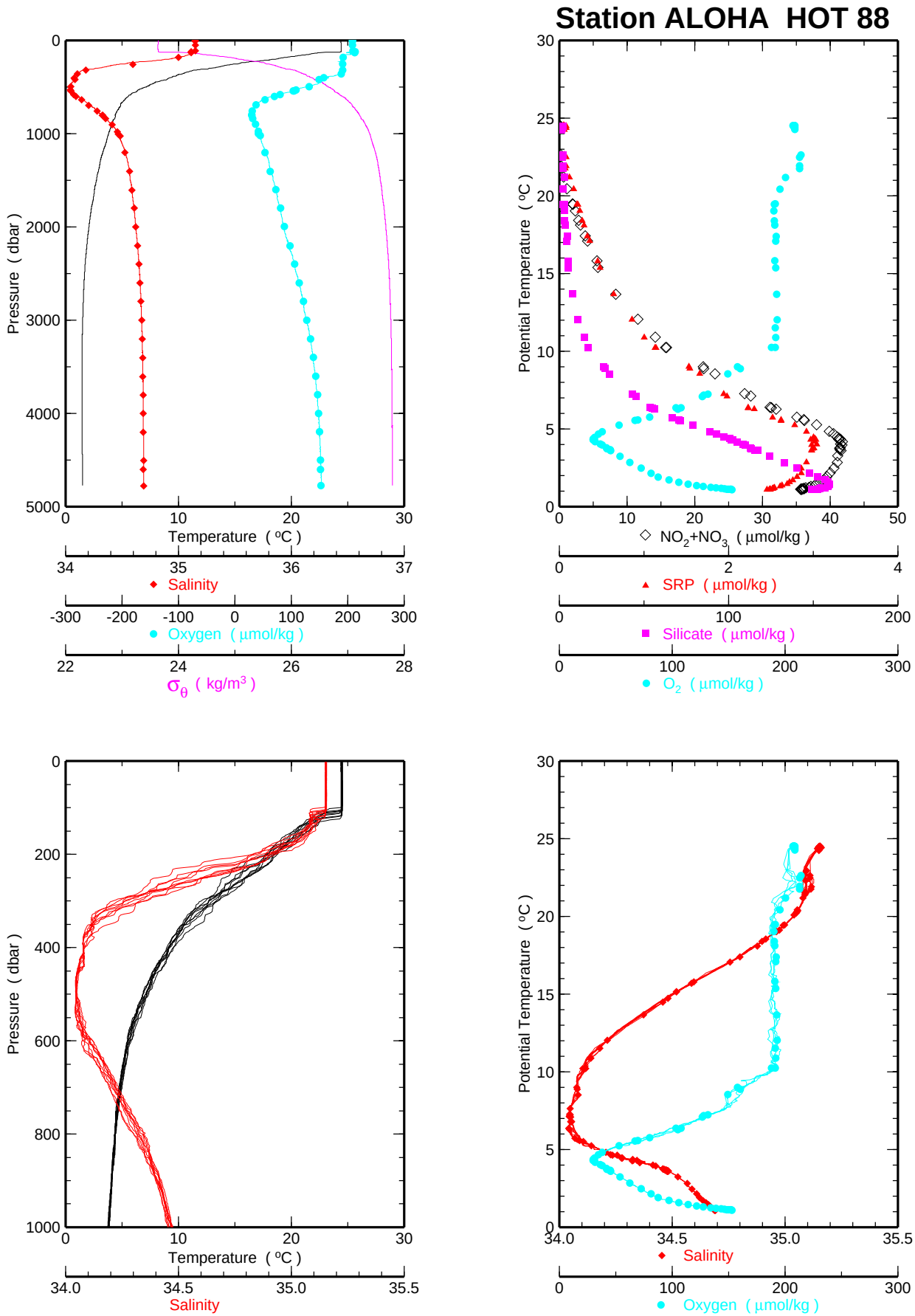
Station ALOHA HOT 88
Pressure (dbar)
Temperature (°C)
Salinity
Oxygen (µmol/kg)
σθ (kg/m³)
Potential Temperature (°C)
NO2+NO3 (µmol/kg)
SRP (µmol/kg)
Silicate (µmol/kg)
O2 (µmol/kg)
Pressure (dbar)
Temperature (°C)
Salinity
Potential Temperature (°C)
Salinity
Oxygen (µmol/kg)

Figure 6.1.1j

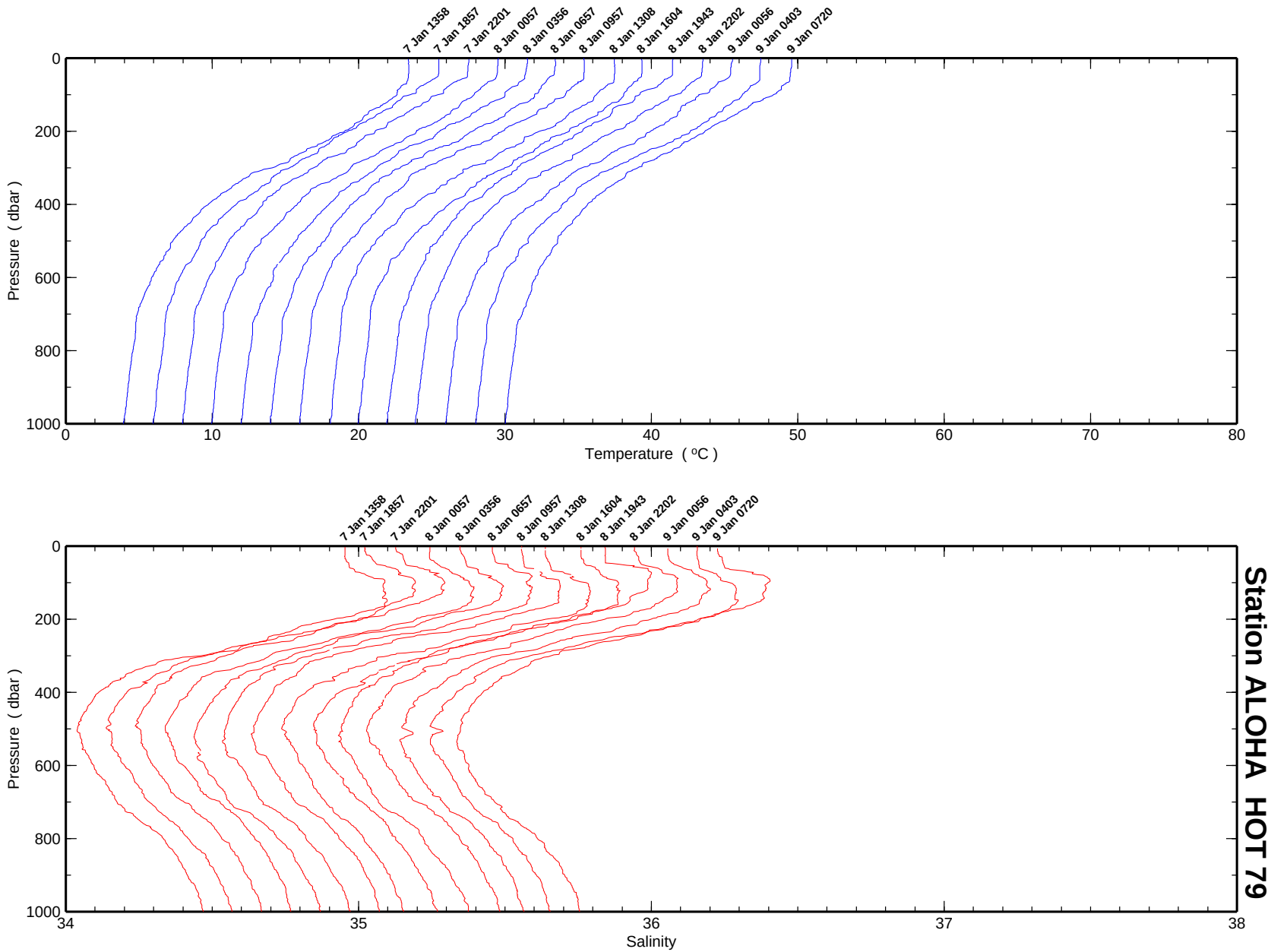
7 Jan 1358
7 Jan 1857
7 Jan 2201
8 Jan 0057
8 Jan 0356
8 Jan 0657
8 Jan 0957
8 Jan 1308
8 Jan 1604
8 Jan 1943
8 Jan 2202
9 Jan 0056
9 Jan 0403
9 Jan 0720
Pressure (dbar)
Temperature (°C)
Salinity
Station ALOHA HOT 79

Figure 6.1.2a

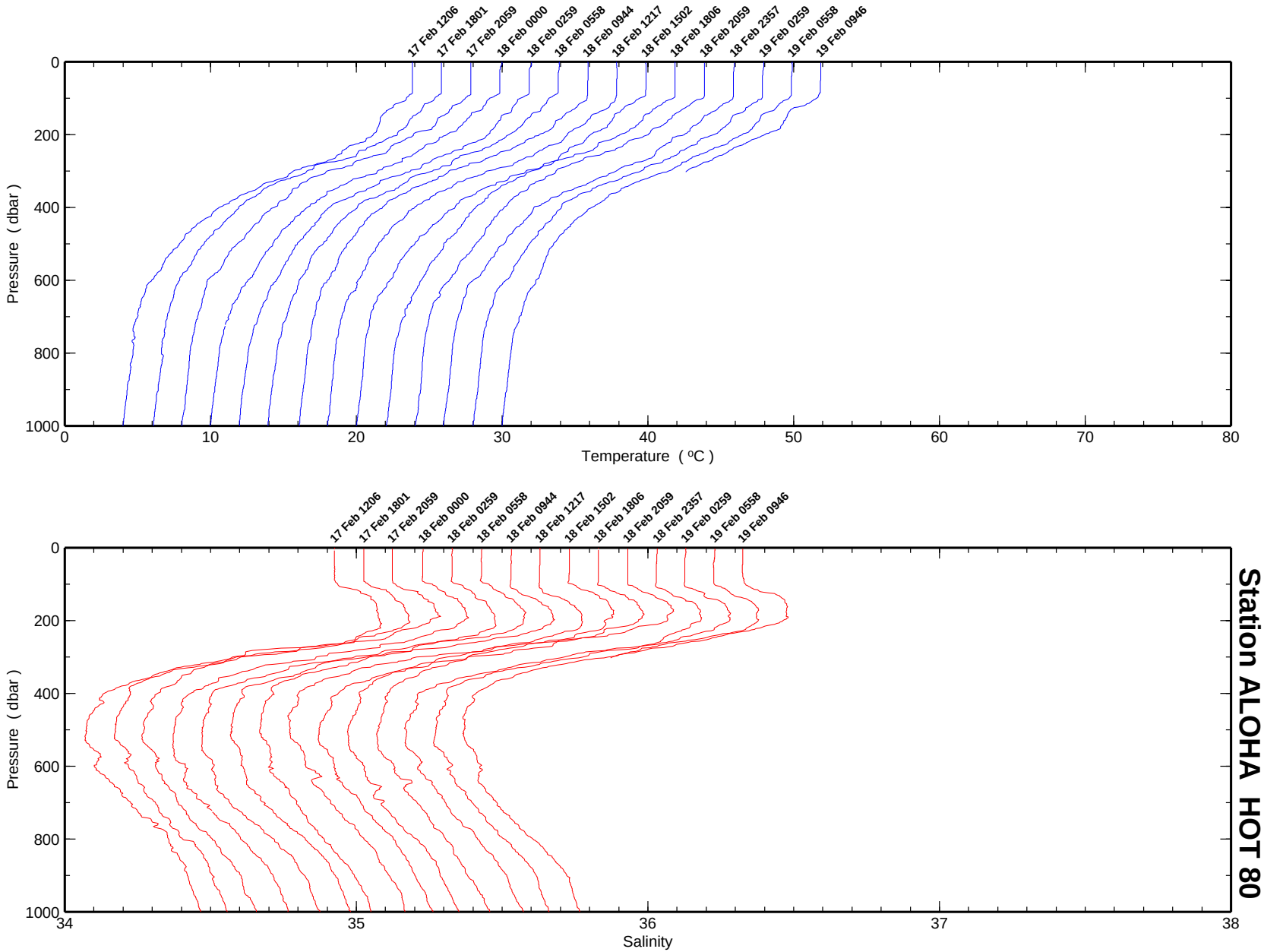
17 Feb 1206
17 Feb 1801
17 Feb 2059
18 Feb 0000
18 Feb 0259
18 Feb 0558
18 Feb 0944
18 Feb 1217
18 Feb 1502
18 Feb 1806
18 Feb 2059
18 Feb 2357
19 Feb 0259
19 Feb 0558
19 Feb 0946
Pressure (dbar)
Temperature (ºC)
Salinity
Station ALOHA HOT 80

Figure 6.1.2b

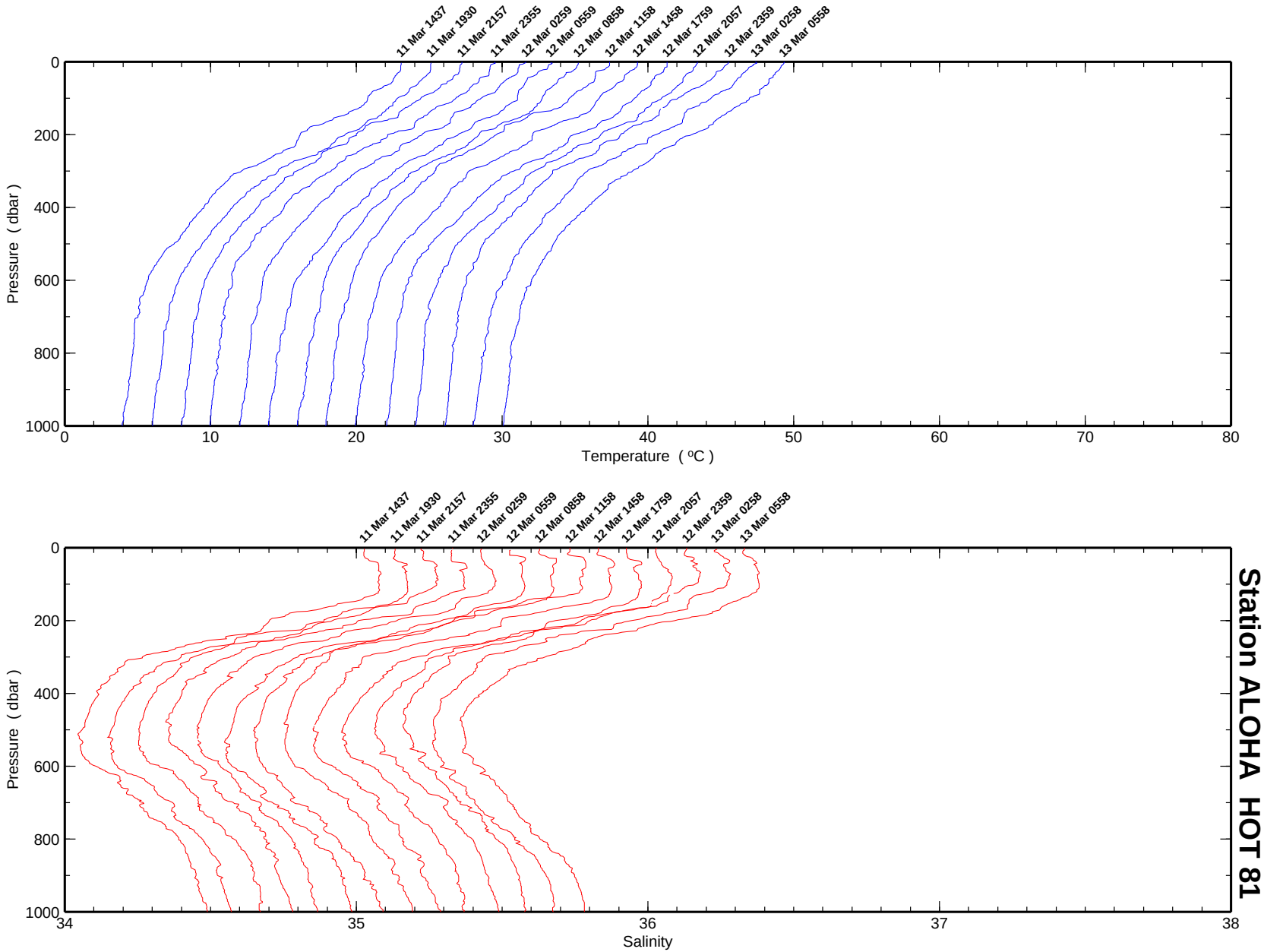
11 Mar 1437
11 Mar 1930
11 Mar 2157
11 Mar 2355
12 Mar 0259
12 Mar 0559
12 Mar 0858
12 Mar 1158
12 Mar 1458
12 Mar 1759
12 Mar 2057
12 Mar 2359
13 Mar 0258
13 Mar 0558
Pressure (dbar)
Temperature (ºC)
Salinity
Station ALOHA HOT 81

Figure 6.1.2c

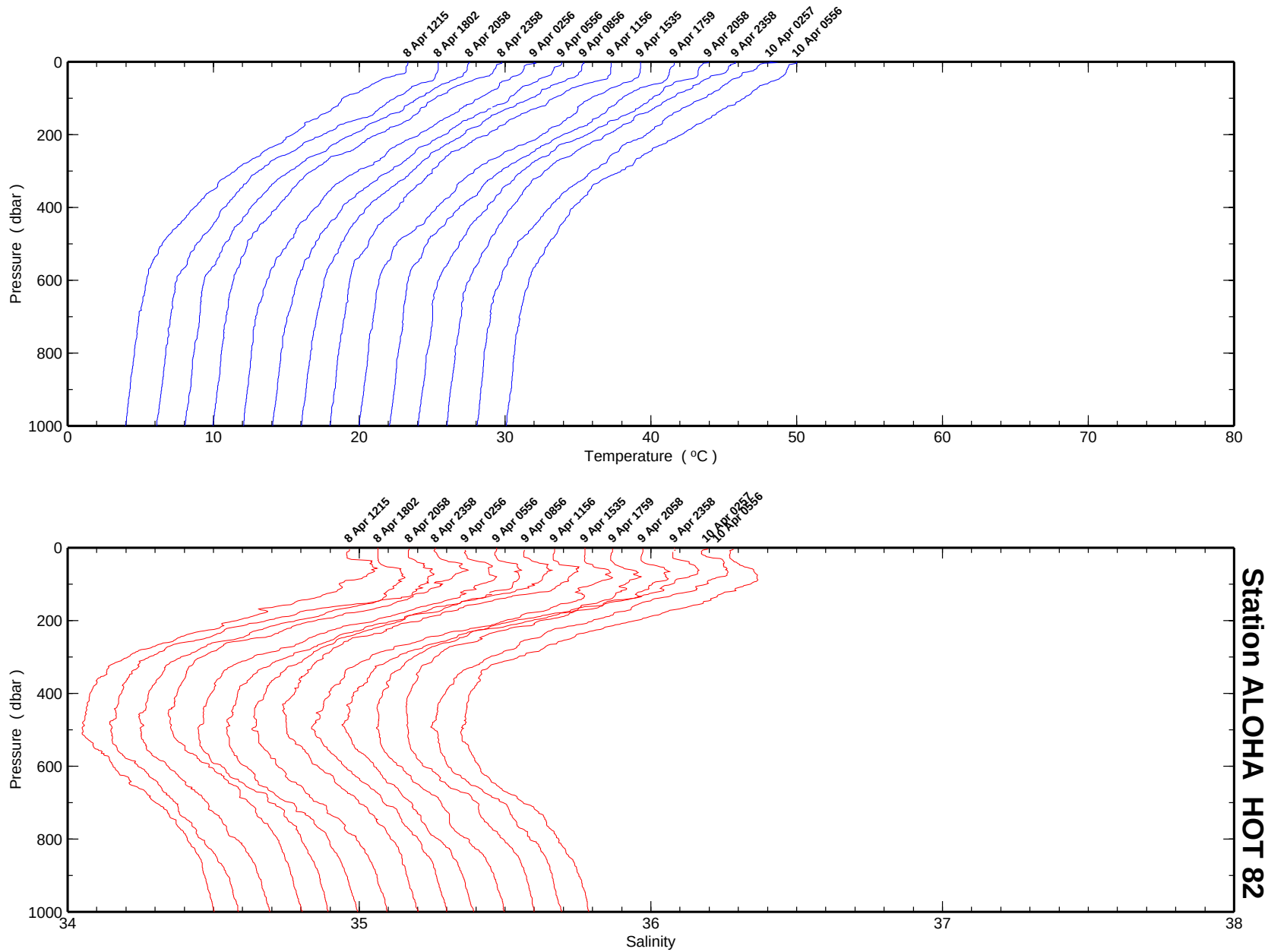
8 Apr 1215
8 Apr 1802
8 Apr 2058
8 Apr 2358
9 Apr 0256
9 Apr 0556
9 Apr 0856
9 Apr 1156
9 Apr 1535
9 Apr 1759
9 Apr 2058
9 Apr 2358
10 Apr 0257
10 Apr 0556
Pressure (dbar)
Temperature (ºC)
Salinity
Station ALOHA HOT 82

Figure 6.1.2d

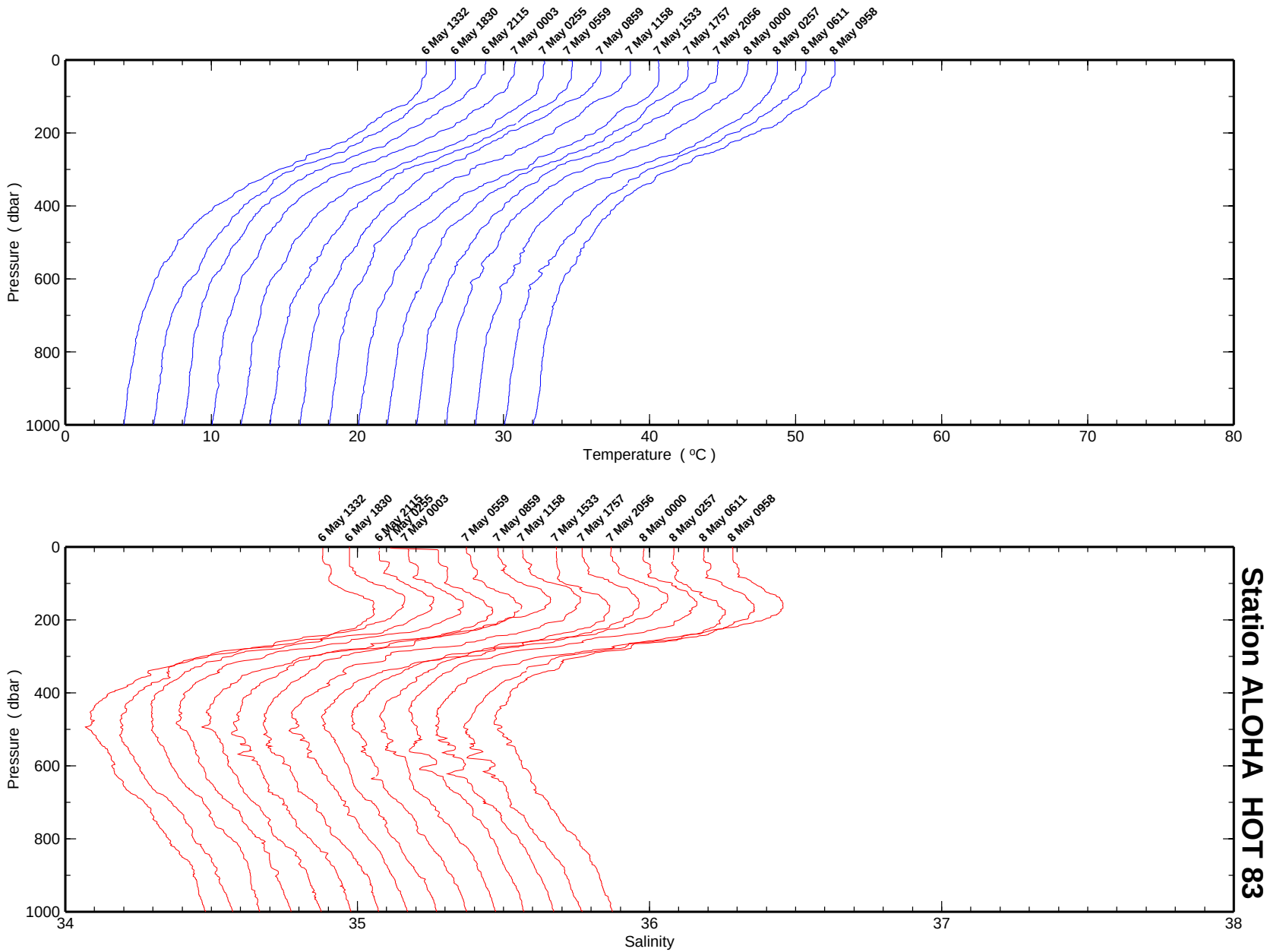
6 May 1332
6 May 1830
6 May 2115
7 May 0003
7 May 0255
7 May 0559
7 May 0859
7 May 1158
7 May 1533
7 May 1757
7 May 2056
8 May 0000
8 May 0257
8 May 0611
8 May 0958
Pressure (dbar)
Temperature (°C)
Salinity
Station ALOHA HOT 83

Figure 6.1.2e

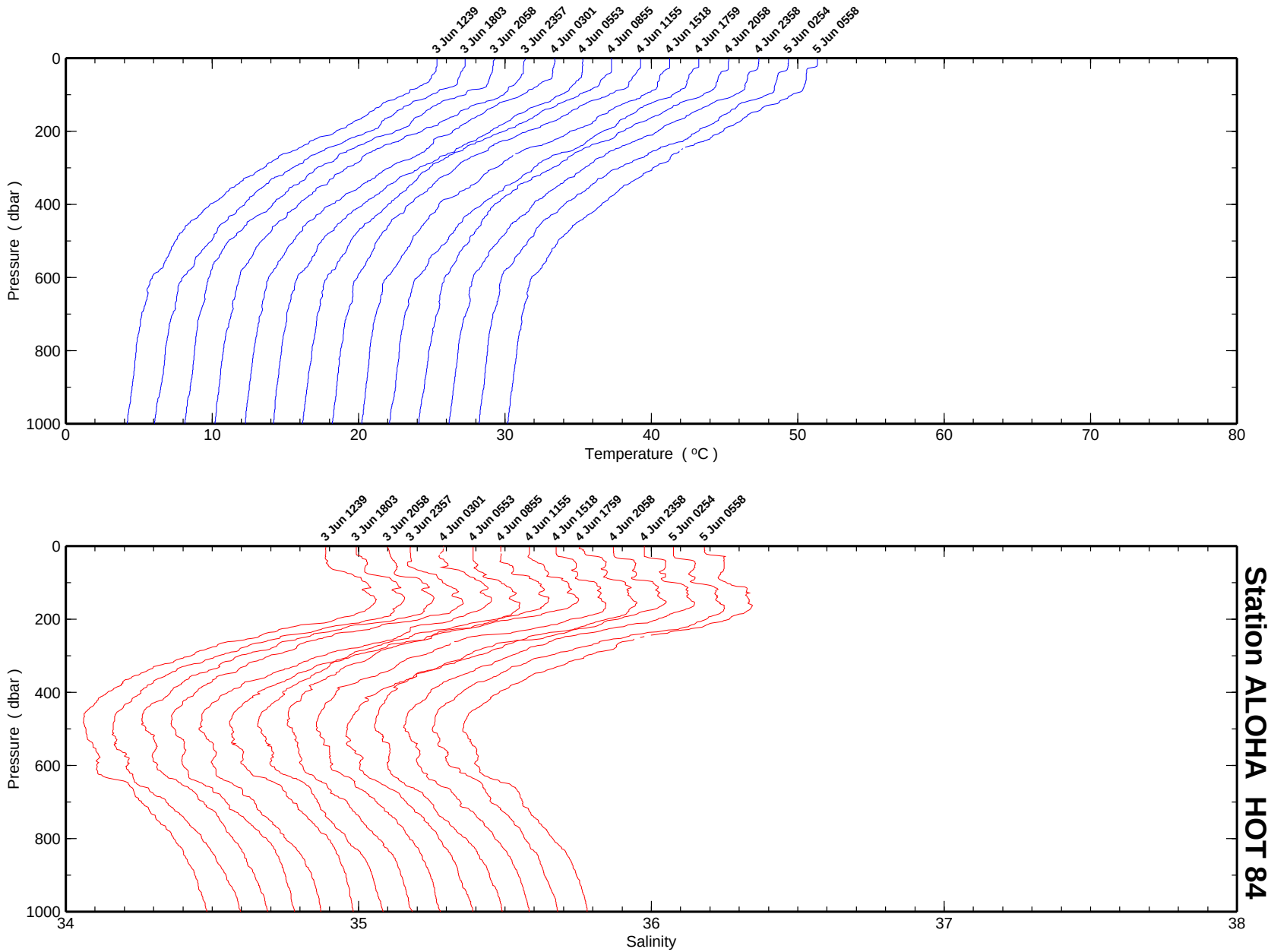
3 Jun 1239
3 Jun 1803
3 Jun 2058
3 Jun 2357
4 Jun 0301
4 Jun 0553
4 Jun 0855
4 Jun 1155
4 Jun 1518
4 Jun 1759
4 Jun 2058
4 Jun 2358
5 Jun 0254
5 Jun 0558
Pressure (dbar)
Temperature (°C)
Salinity
Station ALOHA HOT 84

Figure 6.1.2f

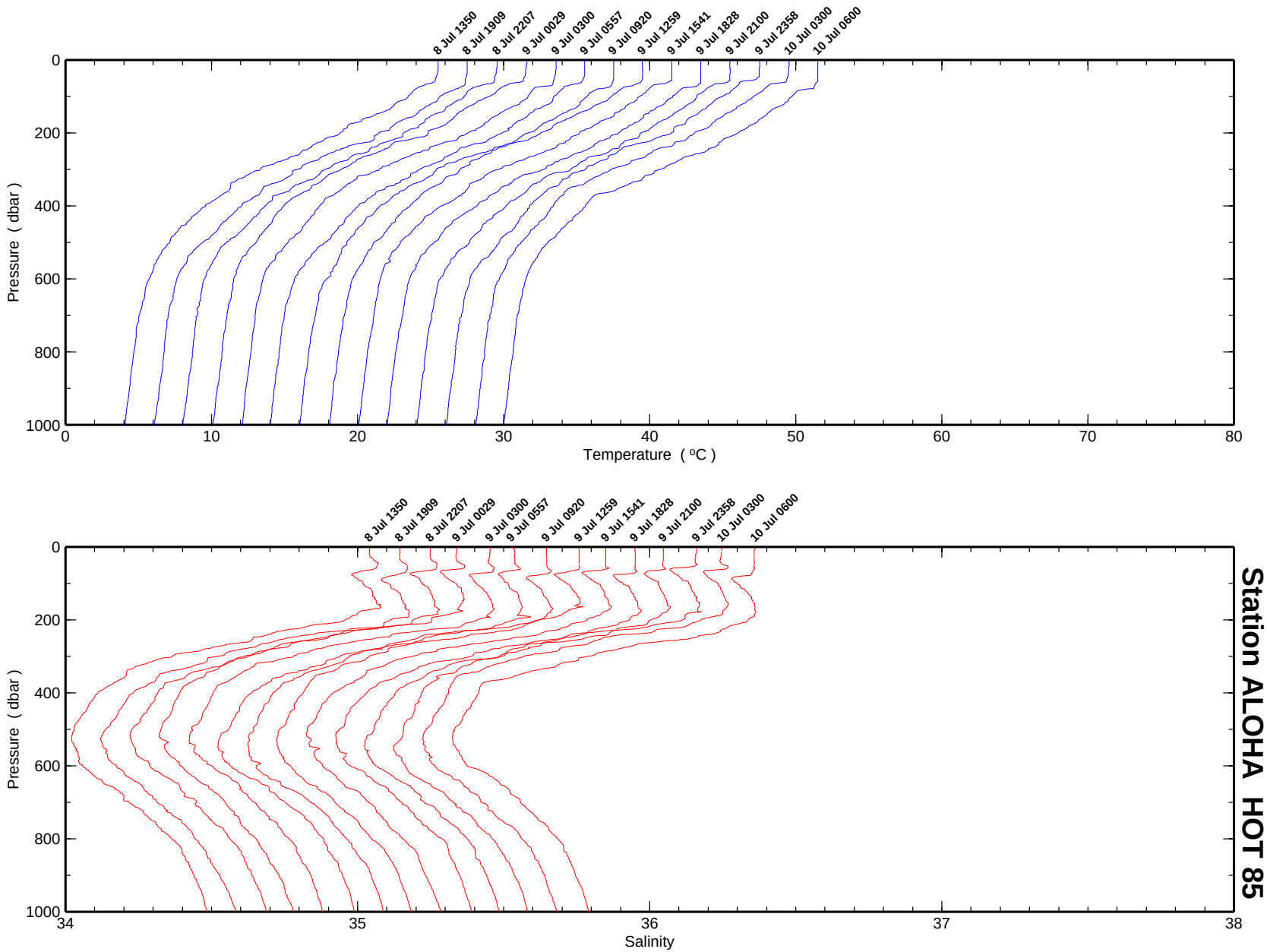
8 Jul 1350
8 Jul 1909
8 Jul 2207
9 Jul 0029
9 Jul 0300
9 Jul 0557
9 Jul 0920
9 Jul 1259
9 Jul 1541
9 Jul 1828
9 Jul 2100
9 Jul 2358
10 Jul 0300
10 Jul 0600
Pressure (dbar)
Temperature (°C)
Salinity
Station ALOHA HOT 85

Figure 6.1.2g

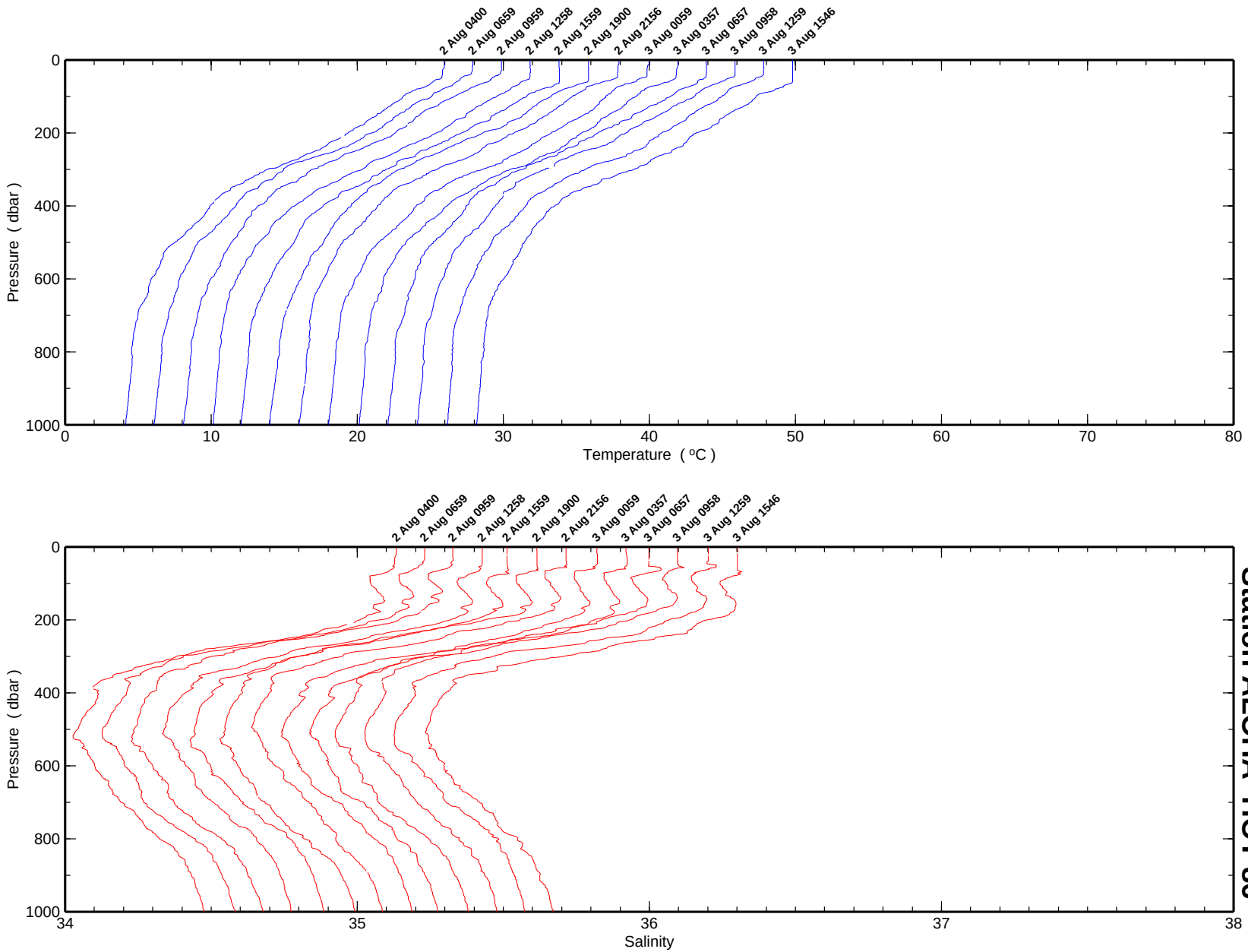

Station ALOHA HOT 86

Figure 6.1.2h

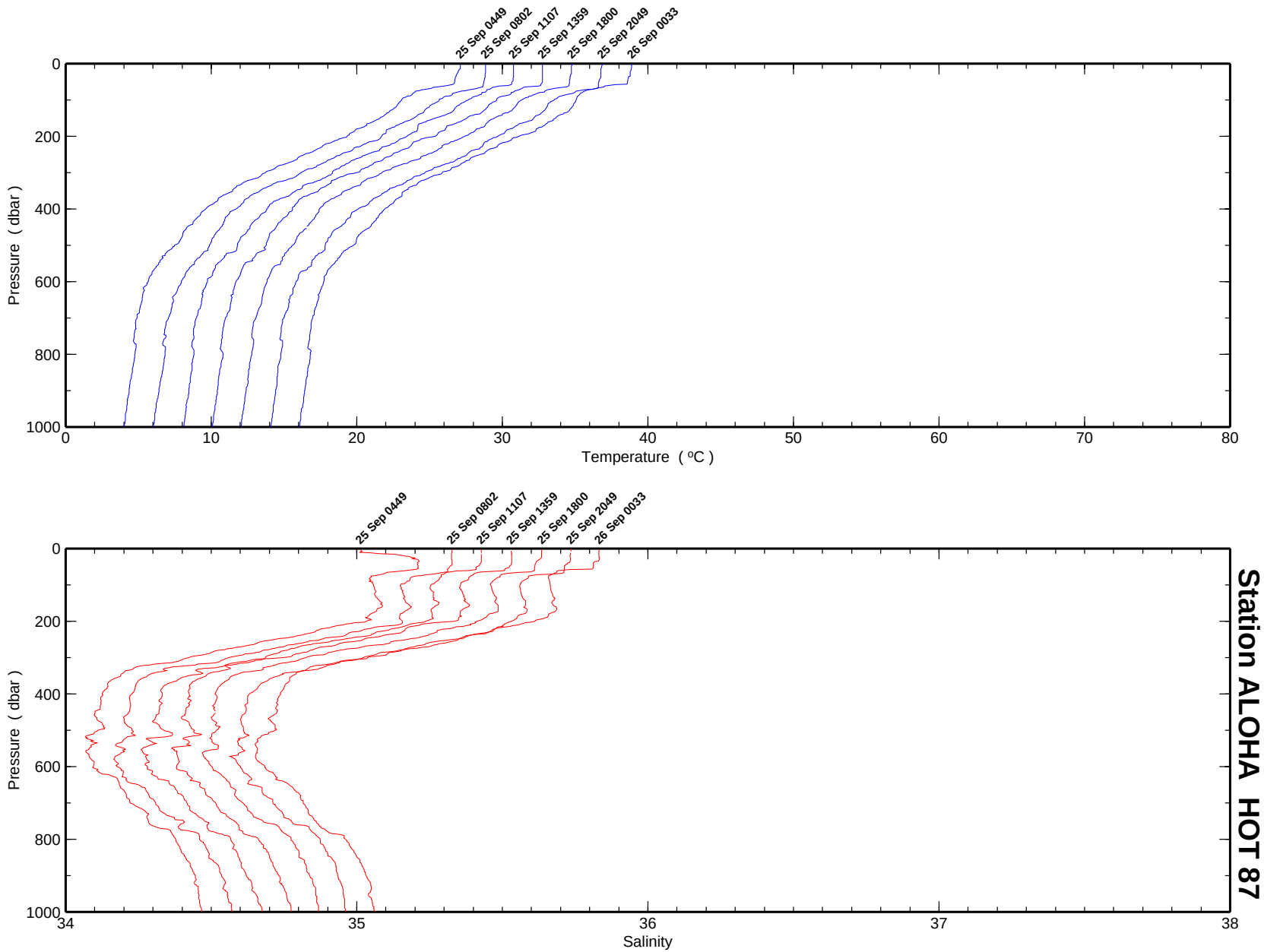
25 Sep 0449
25 Sep 0802
25 Sep 1107
25 Sep 1359
25 Sep 1800
25 Sep 2049
26 Sep 0033
Pressure (dbar)
Temperature (°C)
Salinity
Station ALOHA HOT 87

Figure 6.1.2i

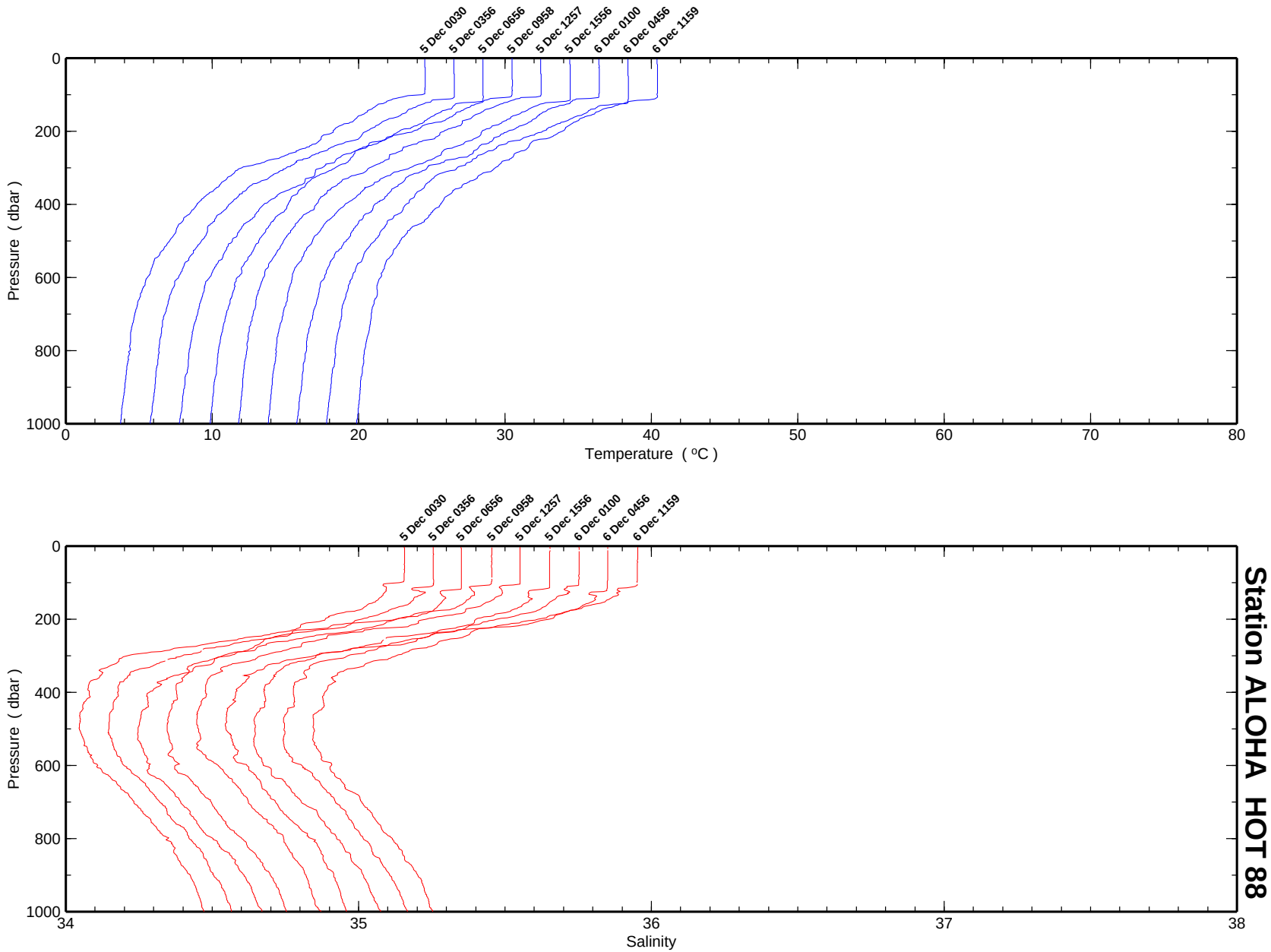
5 Dec 0030
5 Dec 0356
5 Dec 0656
5 Dec 0958
5 Dec 1257
5 Dec 1556
6 Dec 0100
6 Dec 0456
6 Dec 1159
Pressure (dbar)
Temperature (°C)
Salinity
Station ALOHA HOT 88

Figure 6.1.2j

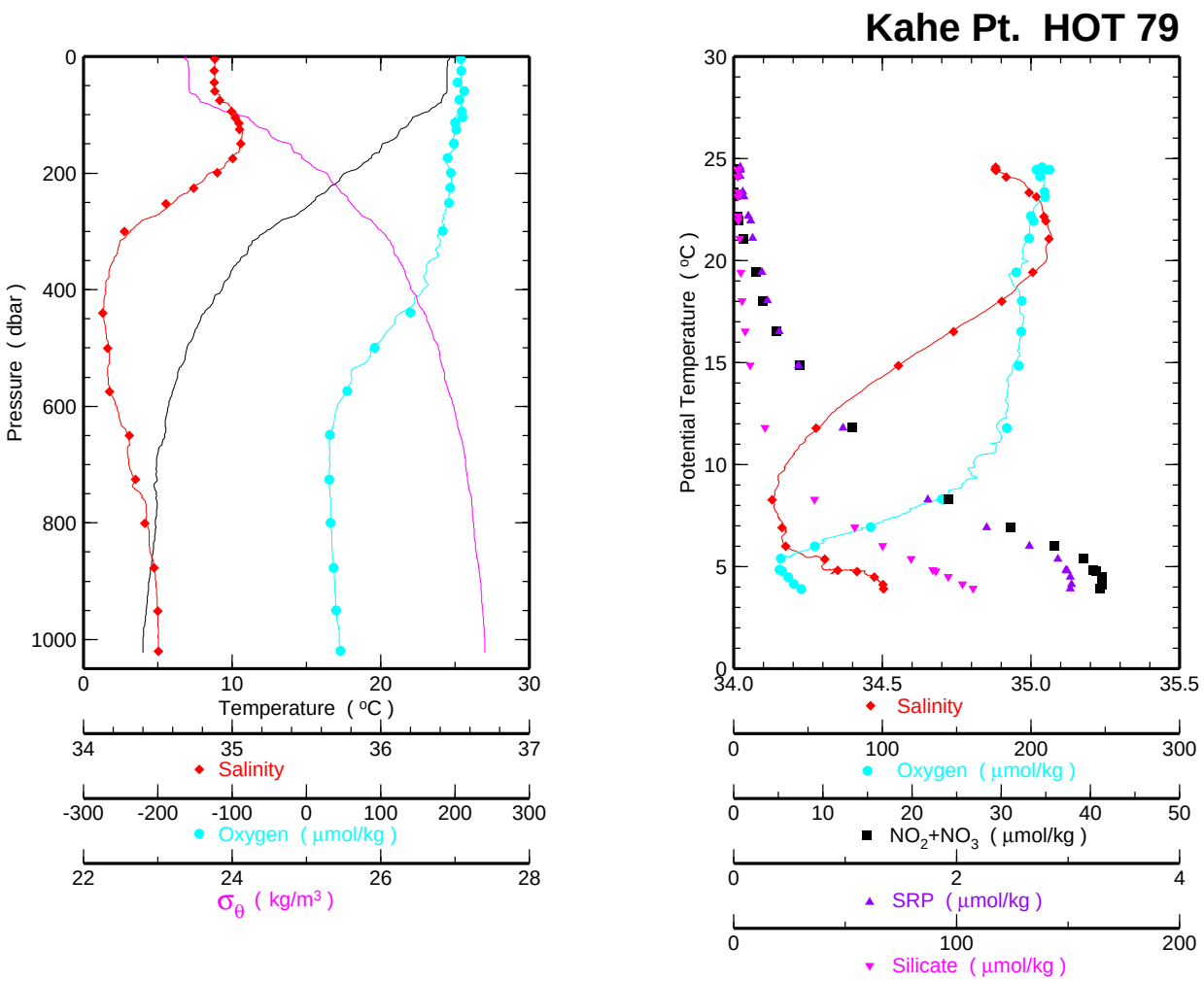
Kahe Pt. HOT 79
Pressure (dbar)
Temperature (ºC)
Salinity
Oxygen (µmol/kg)
σθ (kg/m3)
Potential Temperature (ºC)
Salinity
Oxygen (µmol/kg)
NO2+NO3 (µmol/kg)
SRP (µmol/kg)
Silicate (µmol/kg)

Figure 6.1.3a

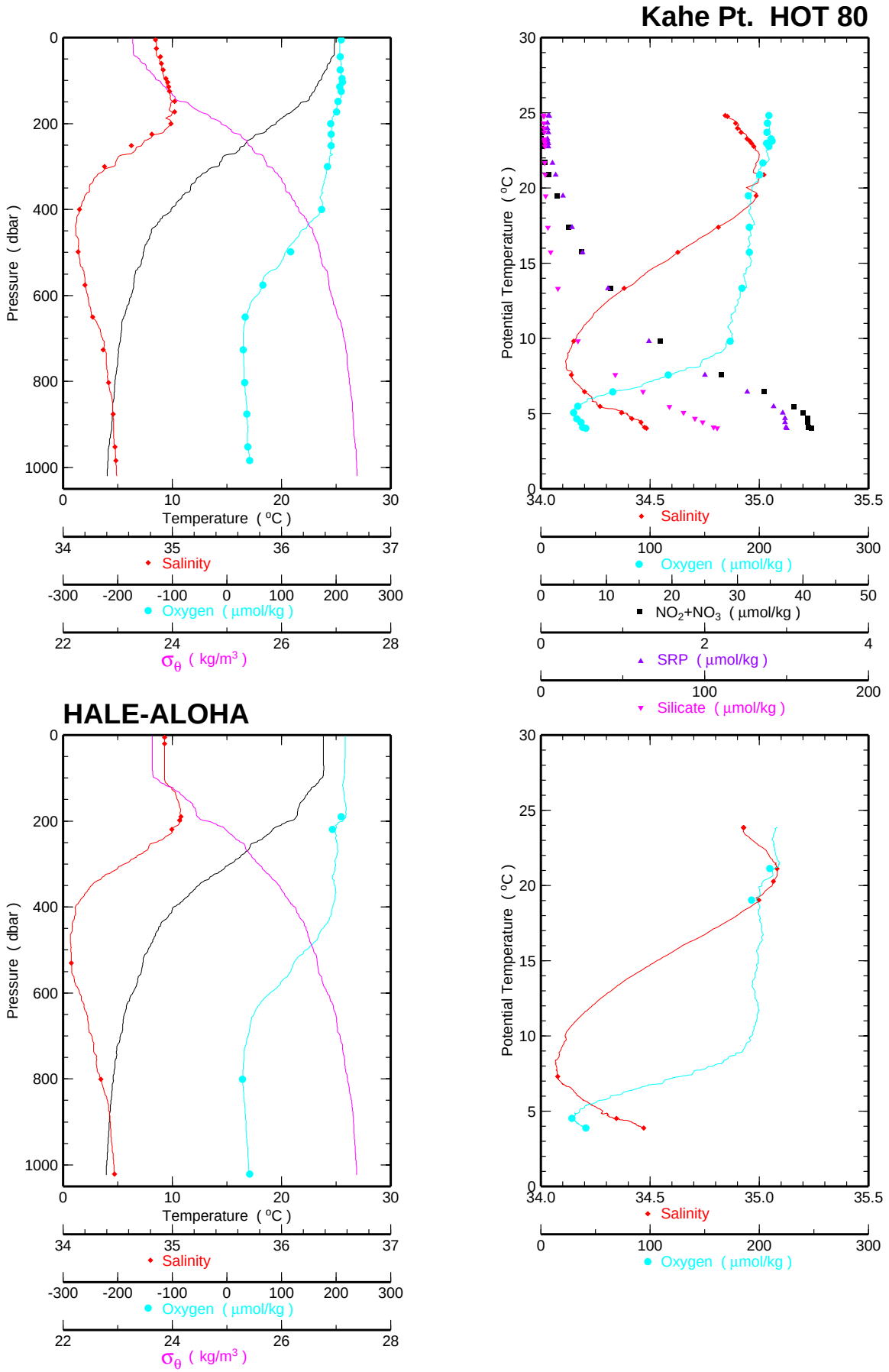
Kahe Pt. HOT 80
Pressure (dbar)
Temperature (ºC)
Salinity
Oxygen (µmol/kg)
σθ (kg/m3)
Potential Temperature (ºC)
NO2+NO3 (µmol/kg)
SRP (µmol/kg)
Silicate (µmol/kg)
HALE-ALOHA

Figure 6.1.3b

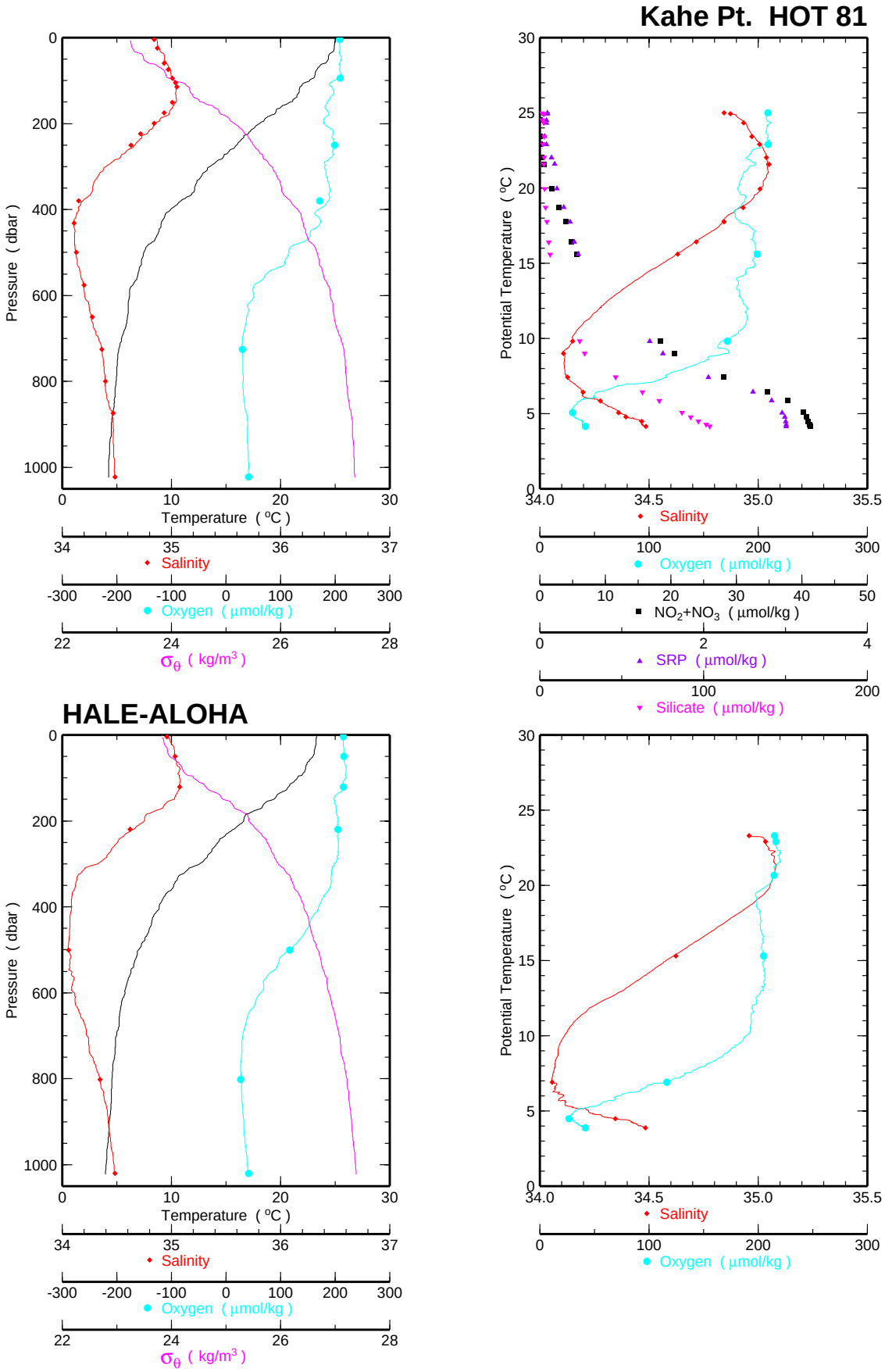
Kahe Pt. HOT 81
Pressure (dbar)
Temperature (°C)
Salinity
Oxygen (µmol/kg)
σθ (kg/m3)
Potential Temperature (°C)
NO2+NO3 (µmol/kg)
SRP (µmol/kg)
Silicate (µmol/kg)
HALE-ALOHA

Figure 6.1.3c

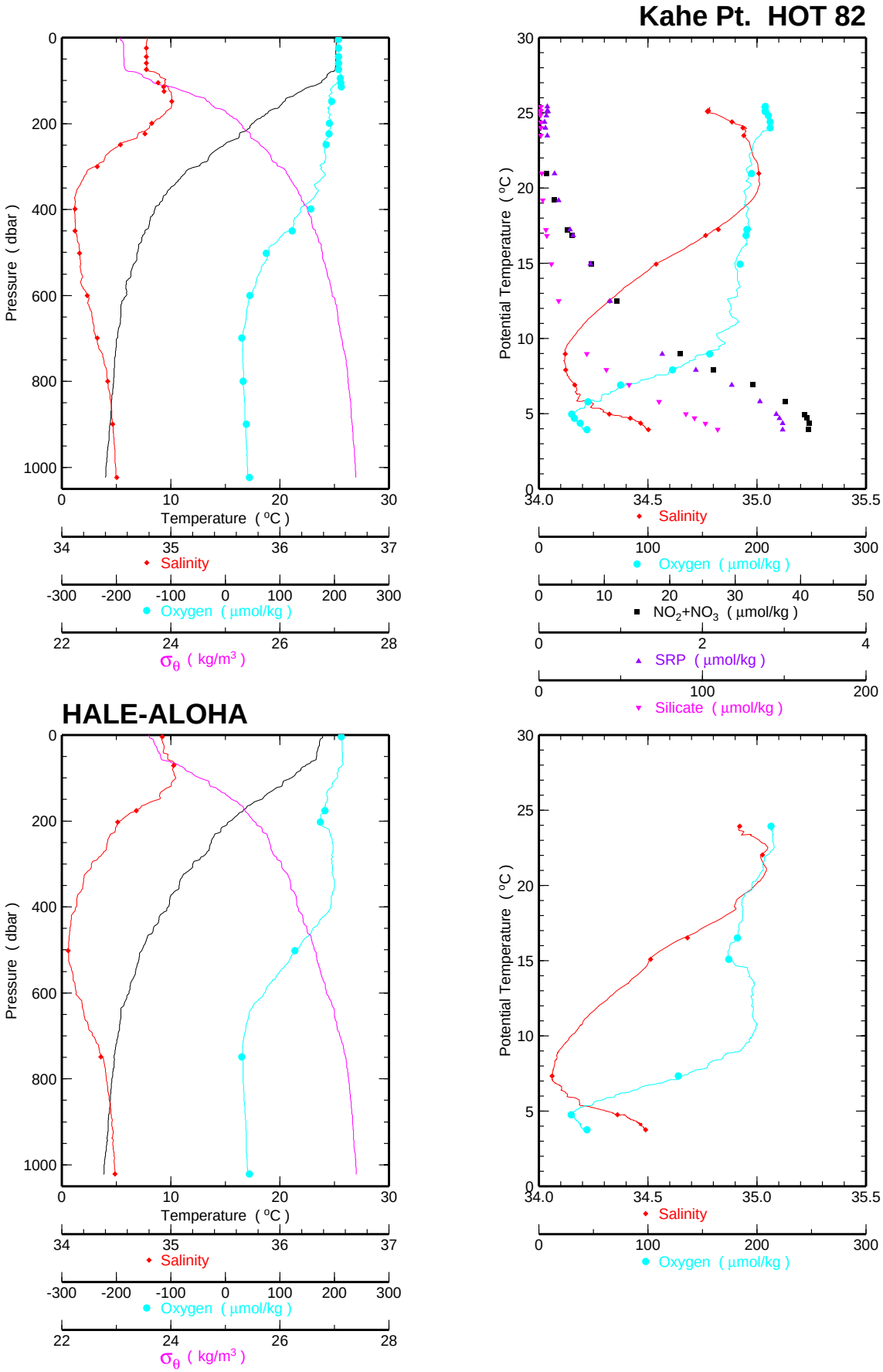
Kahe Pt. HOT 82
Pressure (dbar)
Temperature (°C)
Salinity
Oxygen (µmol/kg)
σθ (kg/m3)
Potential Temperature (°C)
NO2+NO3 (µmol/kg)
SRP (µmol/kg)
Silicate (µmol/kg)
HALE-ALOHA

Figure 6.1.3d

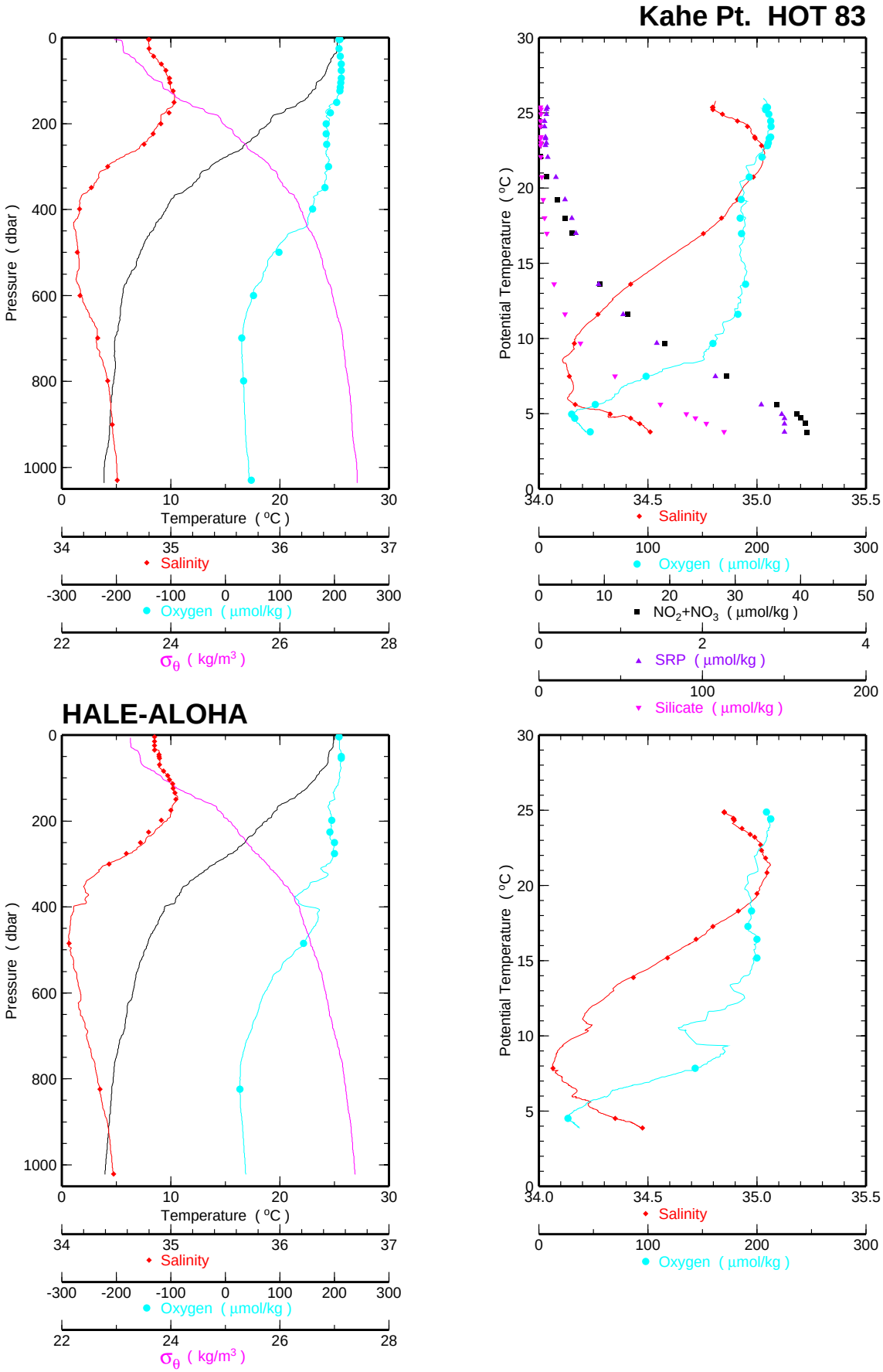
Kahe Pt. HOT 83
Pressure (dbar)
Temperature (°C)
Salinity
Oxygen (µmol/kg)
σθ (kg/m³)
Potential Temperature (°C)
NO2+NO3 (µmol/kg)
SRP (µmol/kg)
Silicate (µmol/kg)
HALE-ALOHA

Figure 6.1.3e

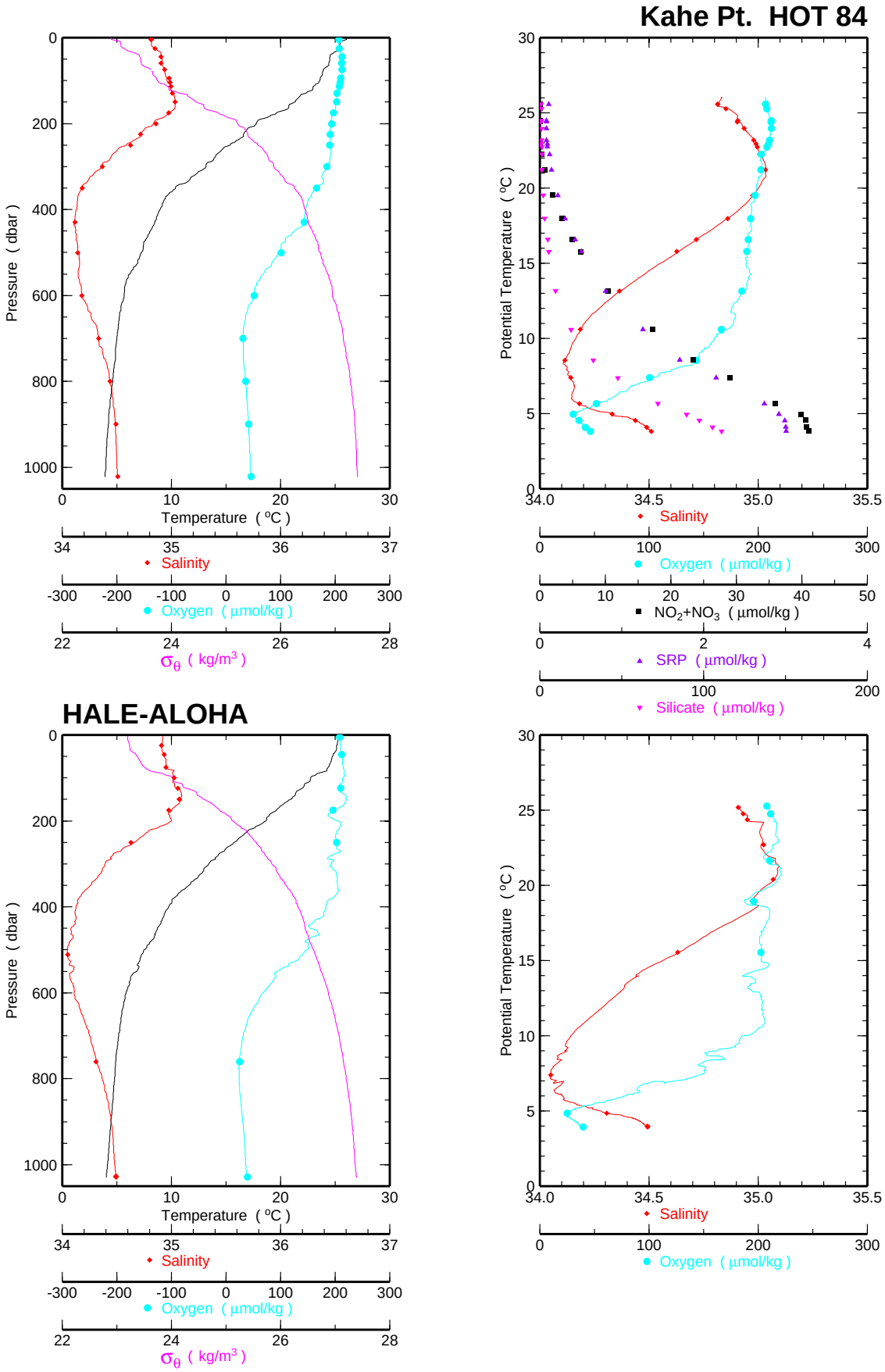
Kahe Pt. HOT 84
Pressure (dbar)
Temperature (°C)
Salinity
Oxygen (µmol/kg)
σθ (kg/m3)
Potential Temperature (°C)
NO2+NO3 (µmol/kg)
SRP (µmol/kg)
Silicate (µmol/kg)
HALE-ALOHA

Figure 6.1.3f

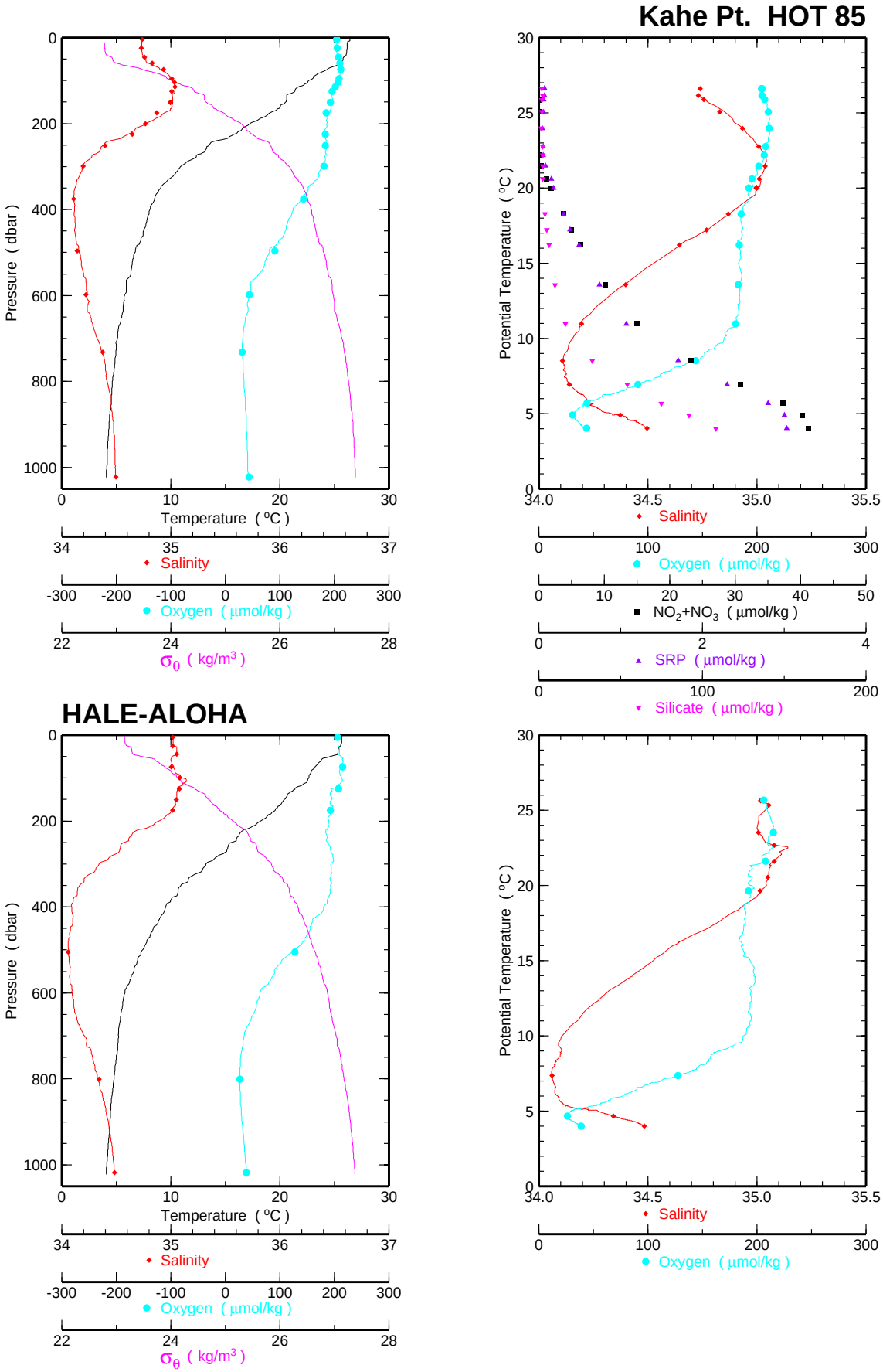
Kahe Pt. HOT 85
Pressure (dbar)
Temperature (°C)
Salinity
Oxygen (µmol/kg)
σθ (kg/m3)
Potential Temperature (°C)
NO2+NO3 (µmol/kg)
SRP (µmol/kg)
Silicate (µmol/kg)
HALE-ALOHA

Figure 6.1.3g

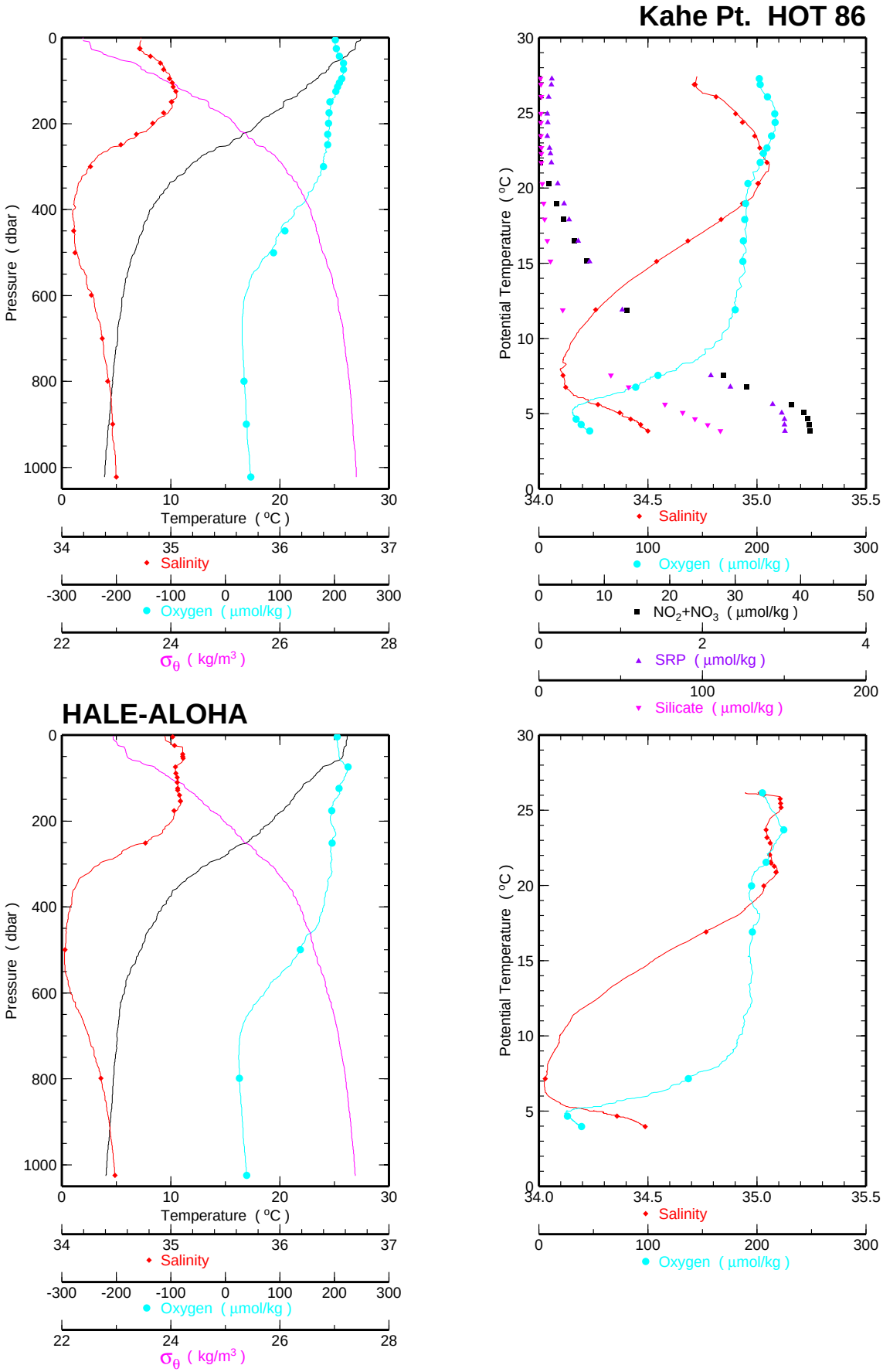
Kahe Pt. HOT 86
Pressure (dbar)
Temperature (°C)
Salinity
Oxygen (µmol/kg)
σθ (kg/m3)
Potential Temperature (°C)
Salinity
Oxygen (µmol/kg)
NO2+NO3 (µmol/kg)
SRP (µmol/kg)
Silicate (µmol/kg)
HALE-ALOHA
Pressure (dbar)
Temperature (°C)
Salinity
Oxygen (µmol/kg)
σθ (kg/m3)
Potential Temperature (°C)
Salinity
Oxygen (µmol/kg)

Figure 6.1.3h

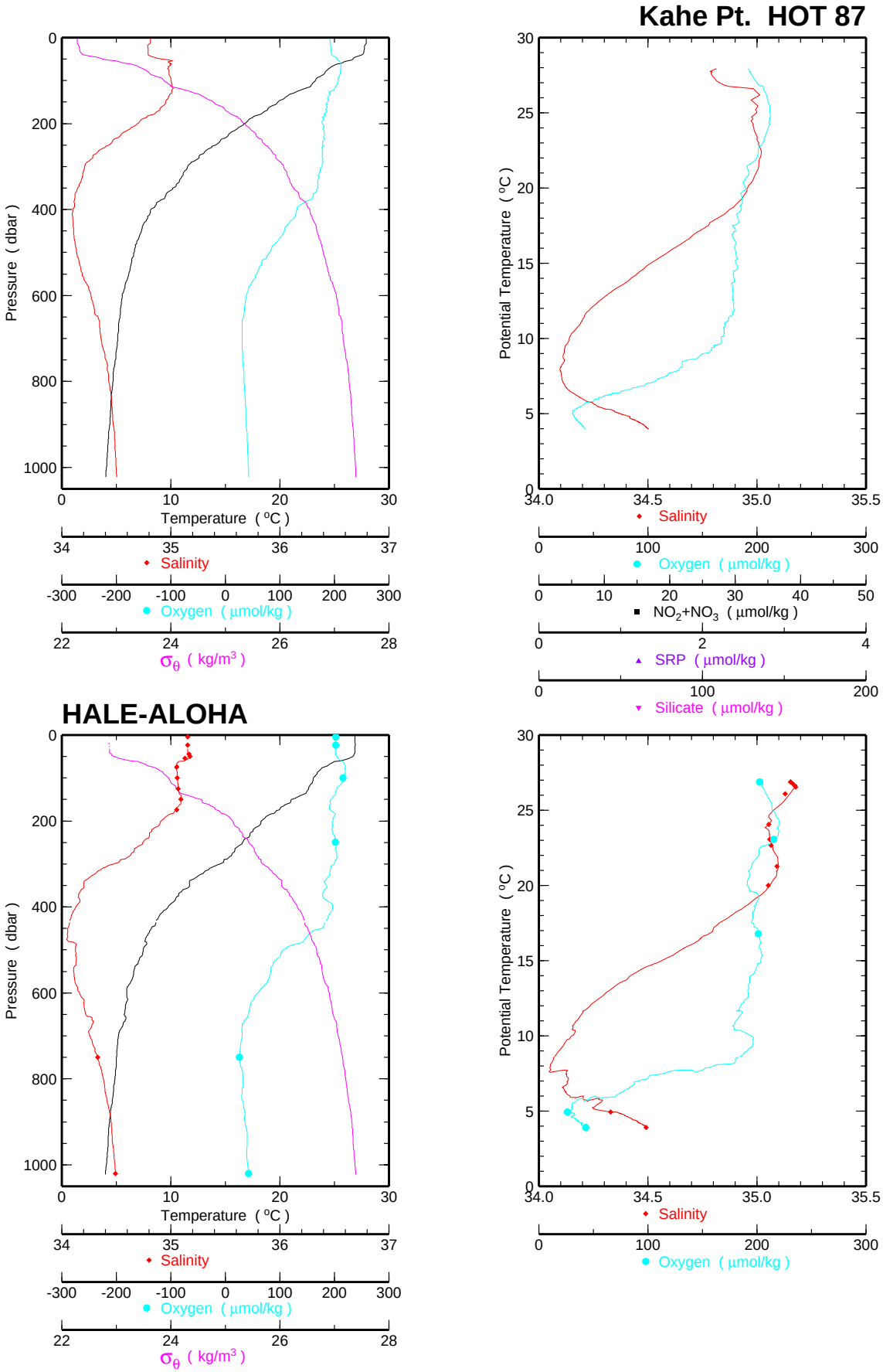
Kahe Pt. HOT 87
Pressure (dbar)
Temperature (°C)
Salinity
Oxygen (µmol/kg)
σθ (kg/m3)
Potential Temperature (°C)
NO2+NO3 (µmol/kg)
SRP (µmol/kg)
Silicate (µmol/kg)
HALE-ALOHA

Figure 6.1.3i

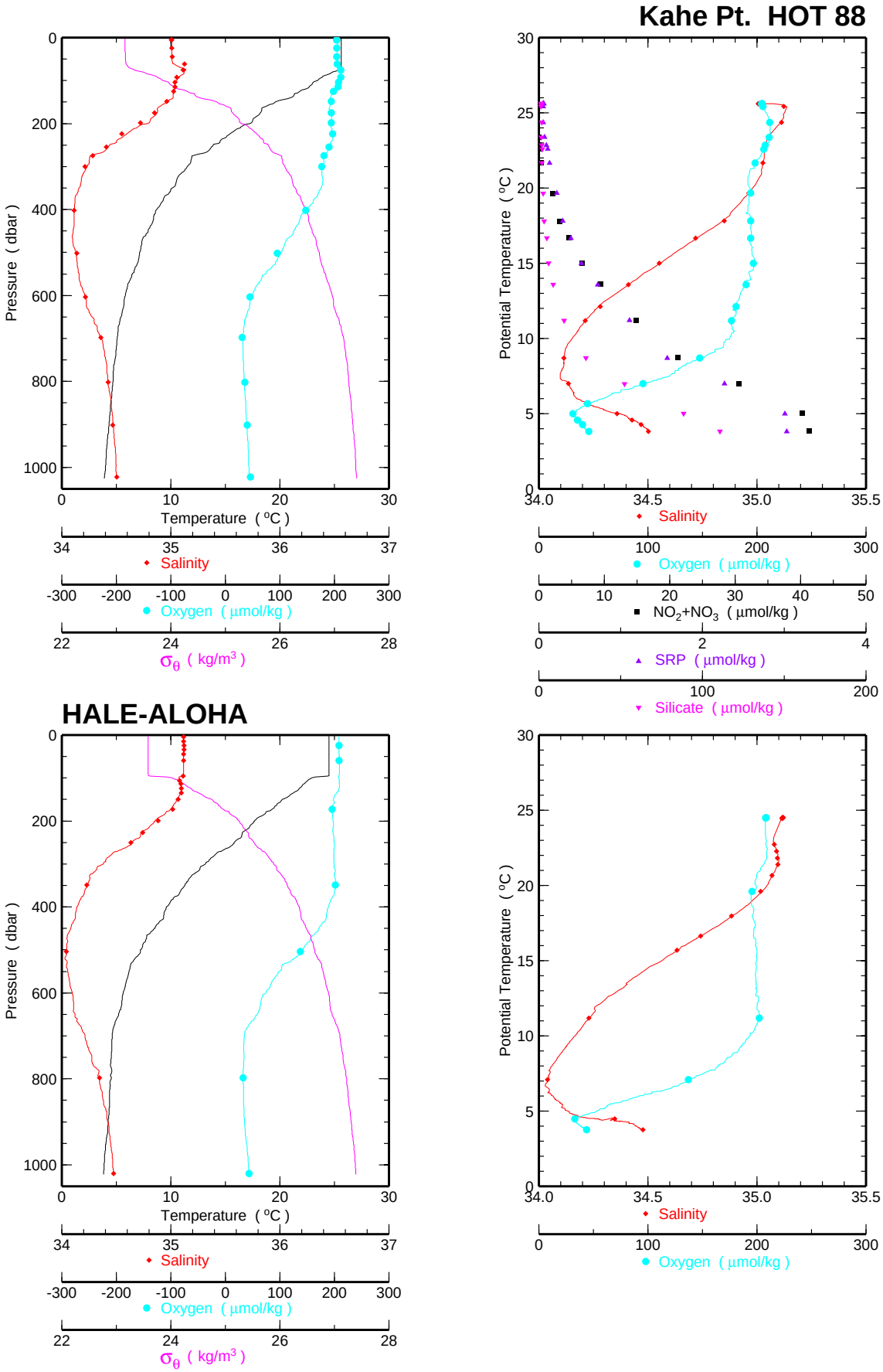
Kahe Pt. HOT 88
Pressure (dbar)
Temperature (°C)
Salinity
Oxygen (µmol/kg)
σθ (kg/m³)
Potential Temperature (°C)
NO2+NO3 (µmol/kg)
SRP (µmol/kg)
Silicate (µmol/kg)
HALE-ALOHA

Figure 6.1.3j

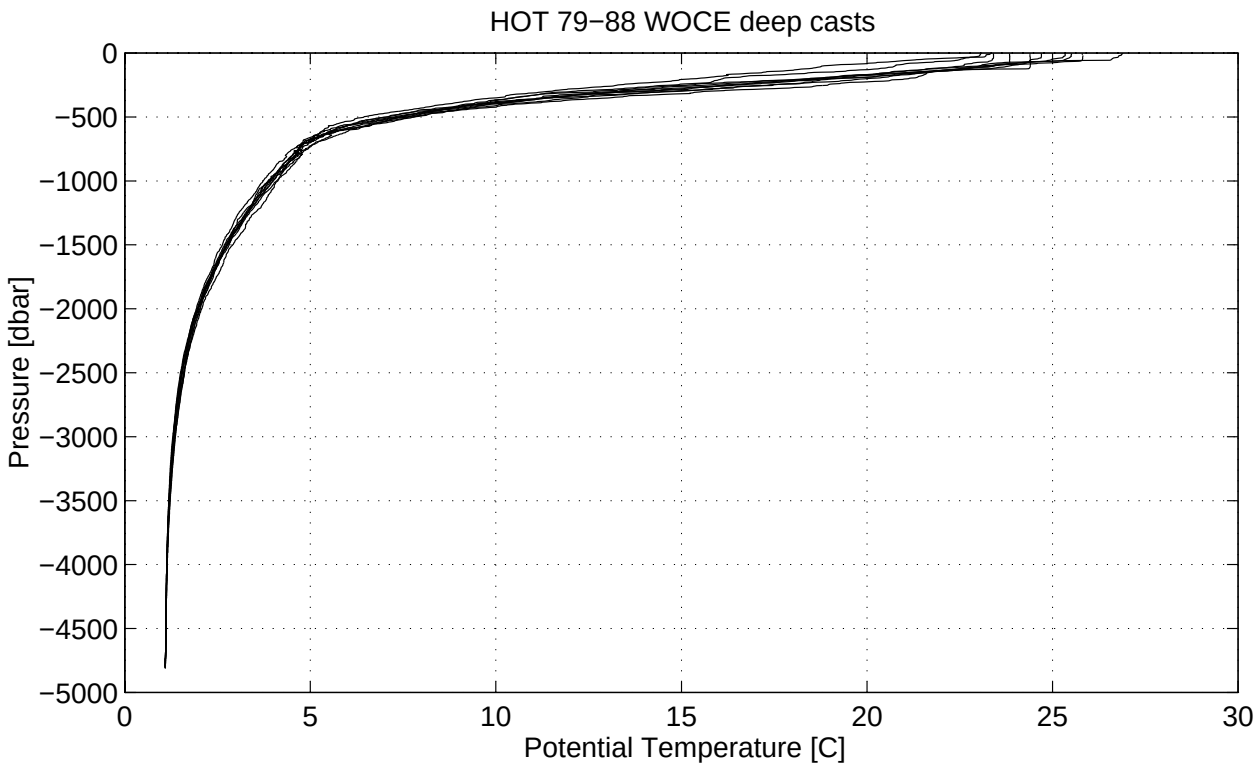
HOT 79−88 WOCE deep casts
Pressure [dbar]
Potential Temperature [C]
0
−500
−1000
−1500
−2000
−2500
−3000
−3500
−4000
−4500
−5000
0
5
10
15
20
25
30

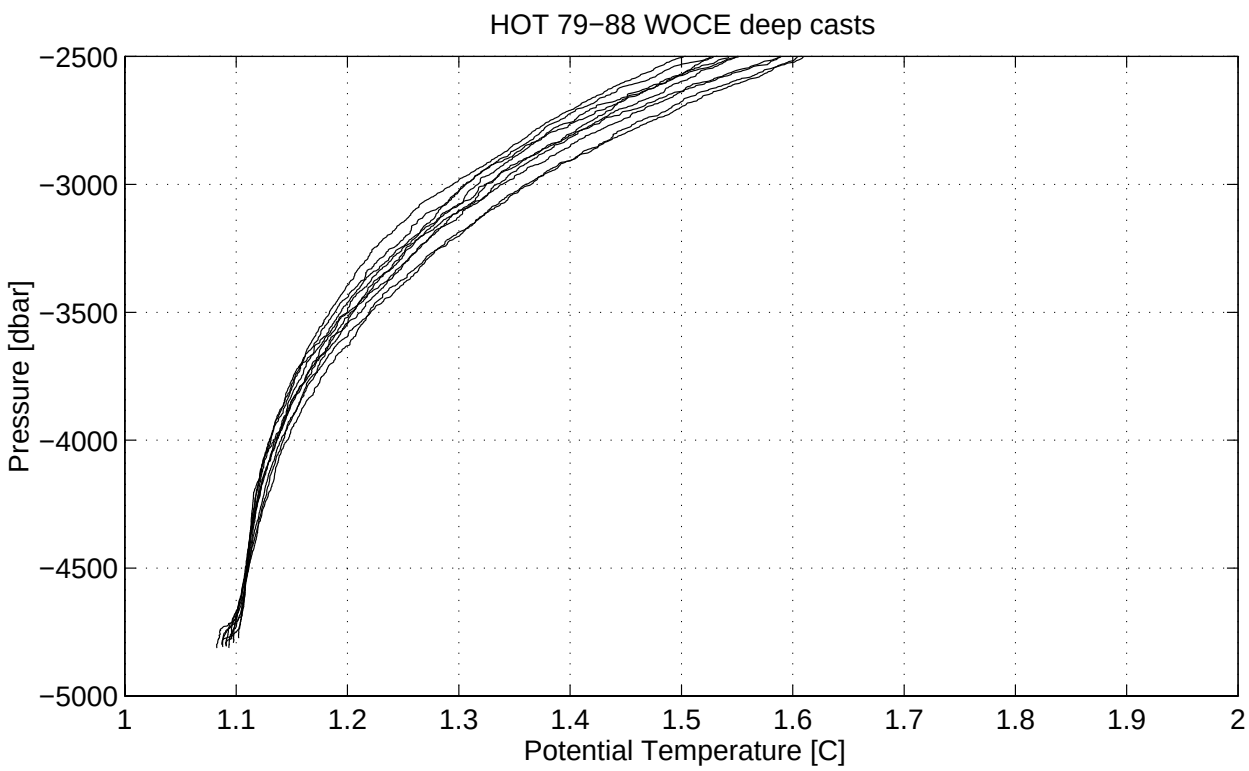
HOT 79−88 WOCE deep casts
Pressure [dbar]
Potential Temperature [C]
−2500
−3000
−3500
−4000
−4500
−5000
1
1.1
1.2
1.3
1.4
1.5
1.6
1.7
1.8
1.9
2

Figure 6.1.4

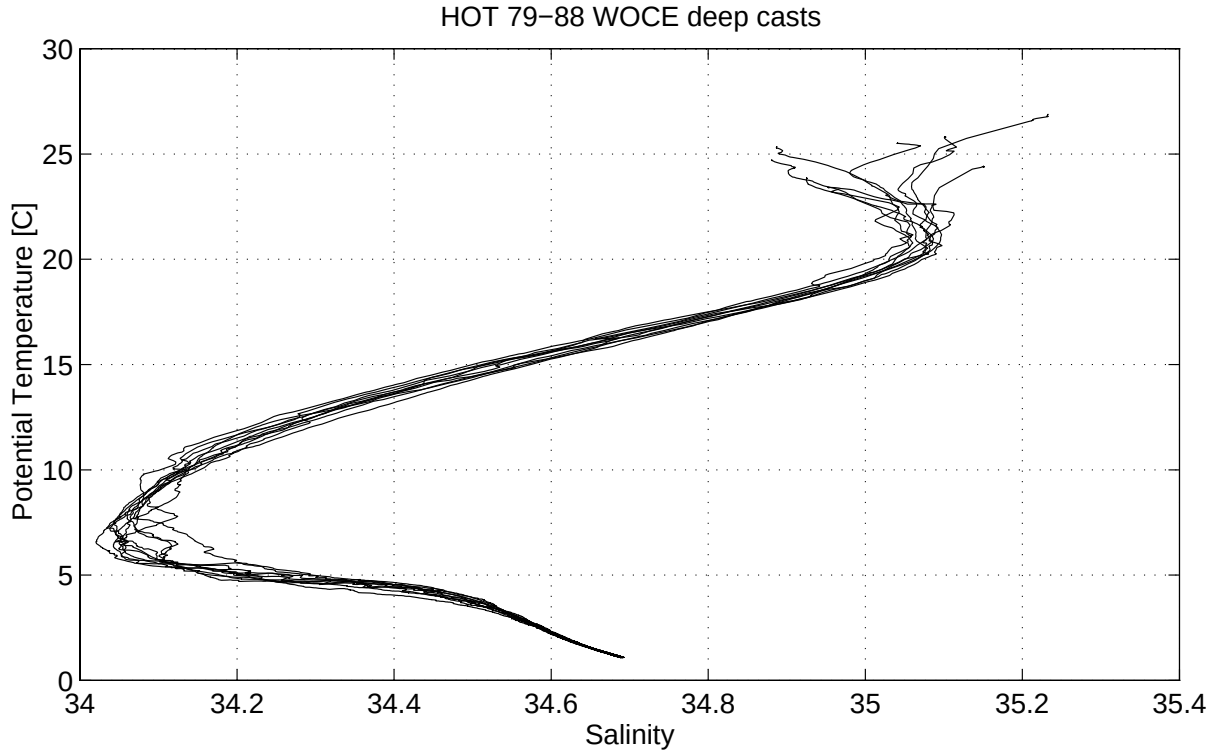
HOT 79−88 WOCE deep casts
Potential Temperature [C]
Salinity
30
25
20
15
10
5
0
34
34.2
34.4
34.6
34.8
35
35.2
35.4

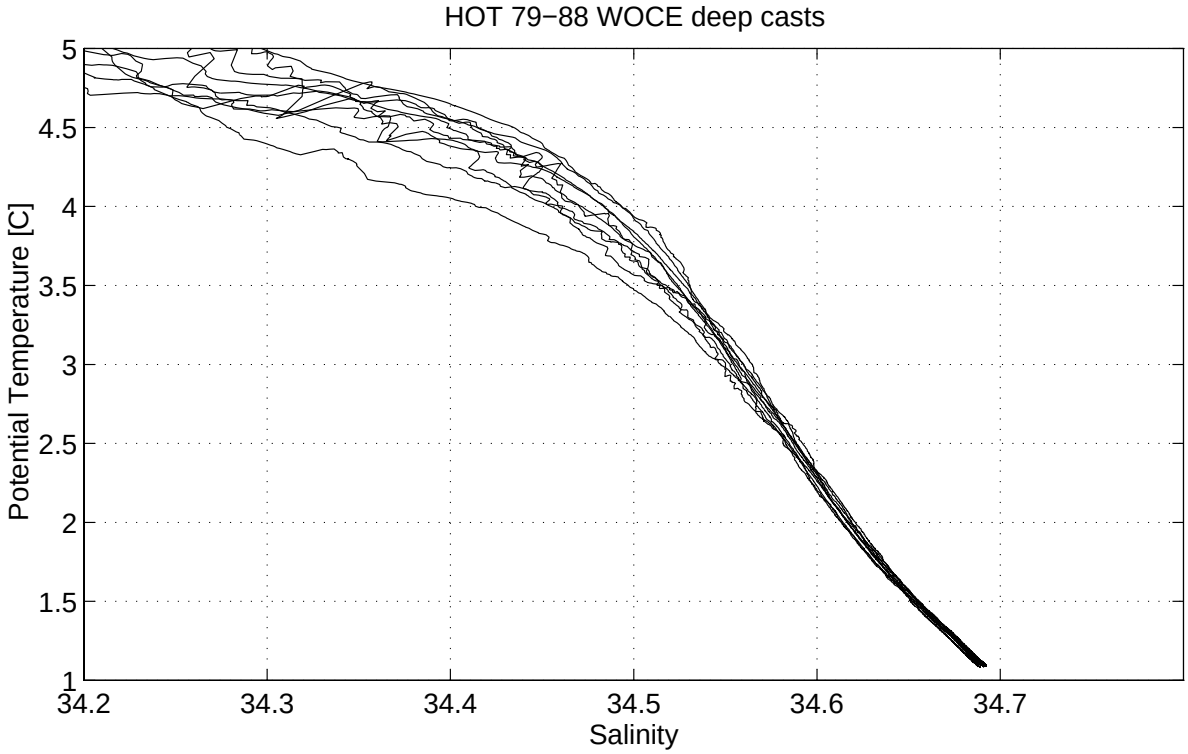
HOT 79−88 WOCE deep casts
Potential Temperature [C]
Salinity
5
4.5
4
3.5
3
2.5
2
1.5
1
34.2
34.3
34.4
34.5
34.6
34.7

Figure 6.1.5

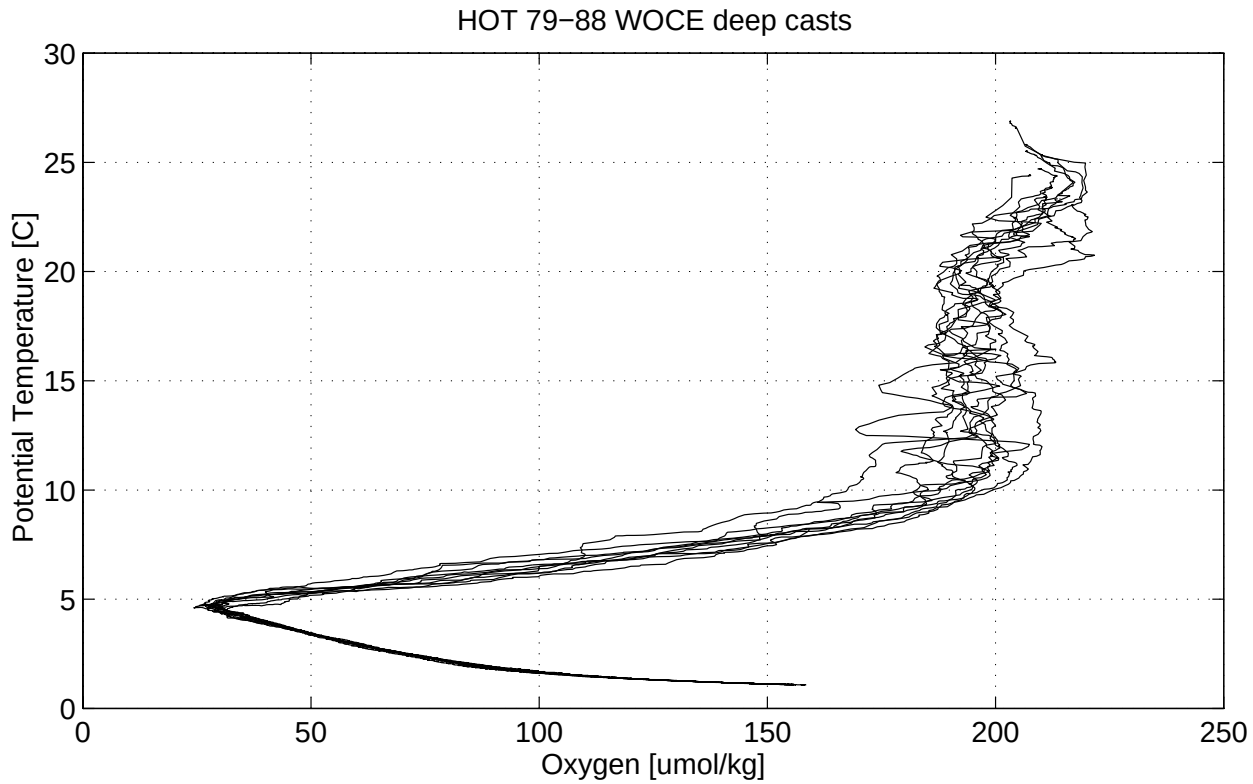
HOT 79−88 WOCE deep casts
Potential Temperature [C]
Oxygen [umol/kg]
0
5
10
15
20
25
30
0
50
100
150
200
250

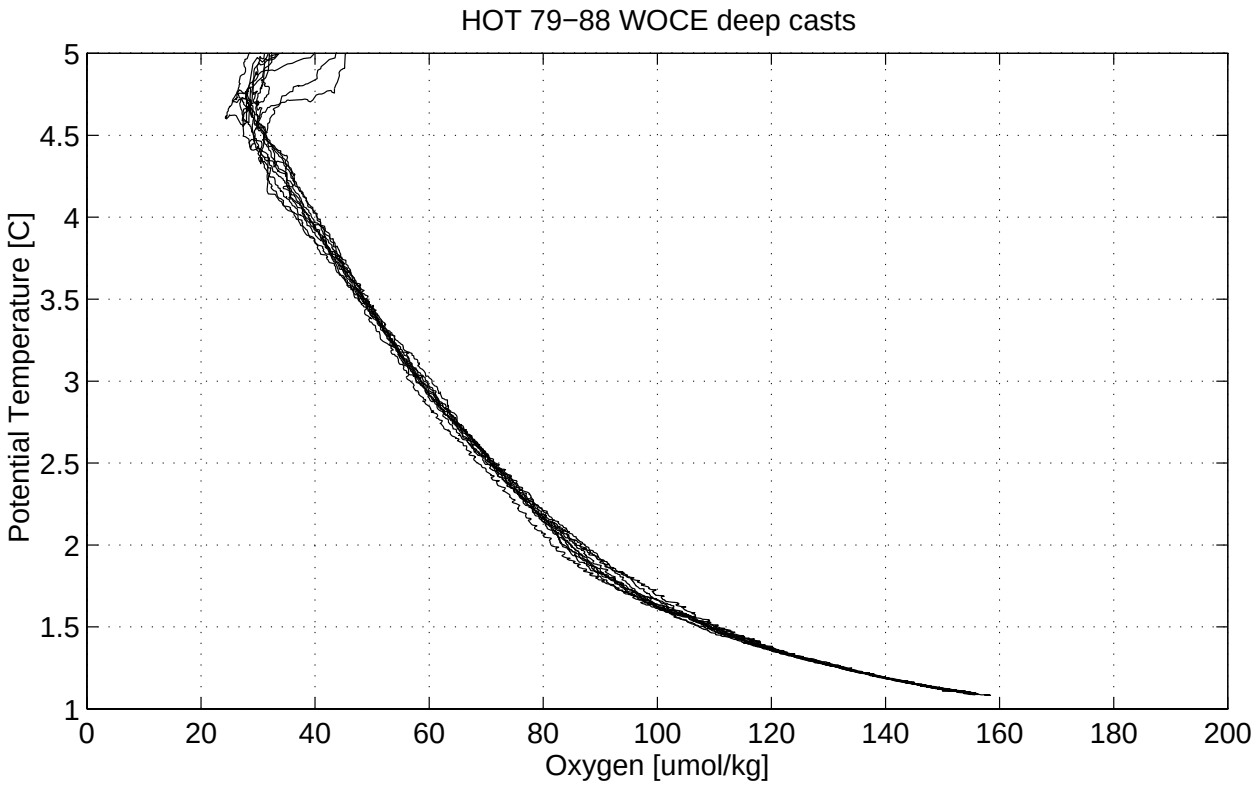
HOT 79−88 WOCE deep casts
Potential Temperature [C]
Oxygen [umol/kg]
1
1.5
2
2.5
3
3.5
4
4.5
5
0
20
40
60
80
100
120
140
160
180
200

Figure 6.1.6

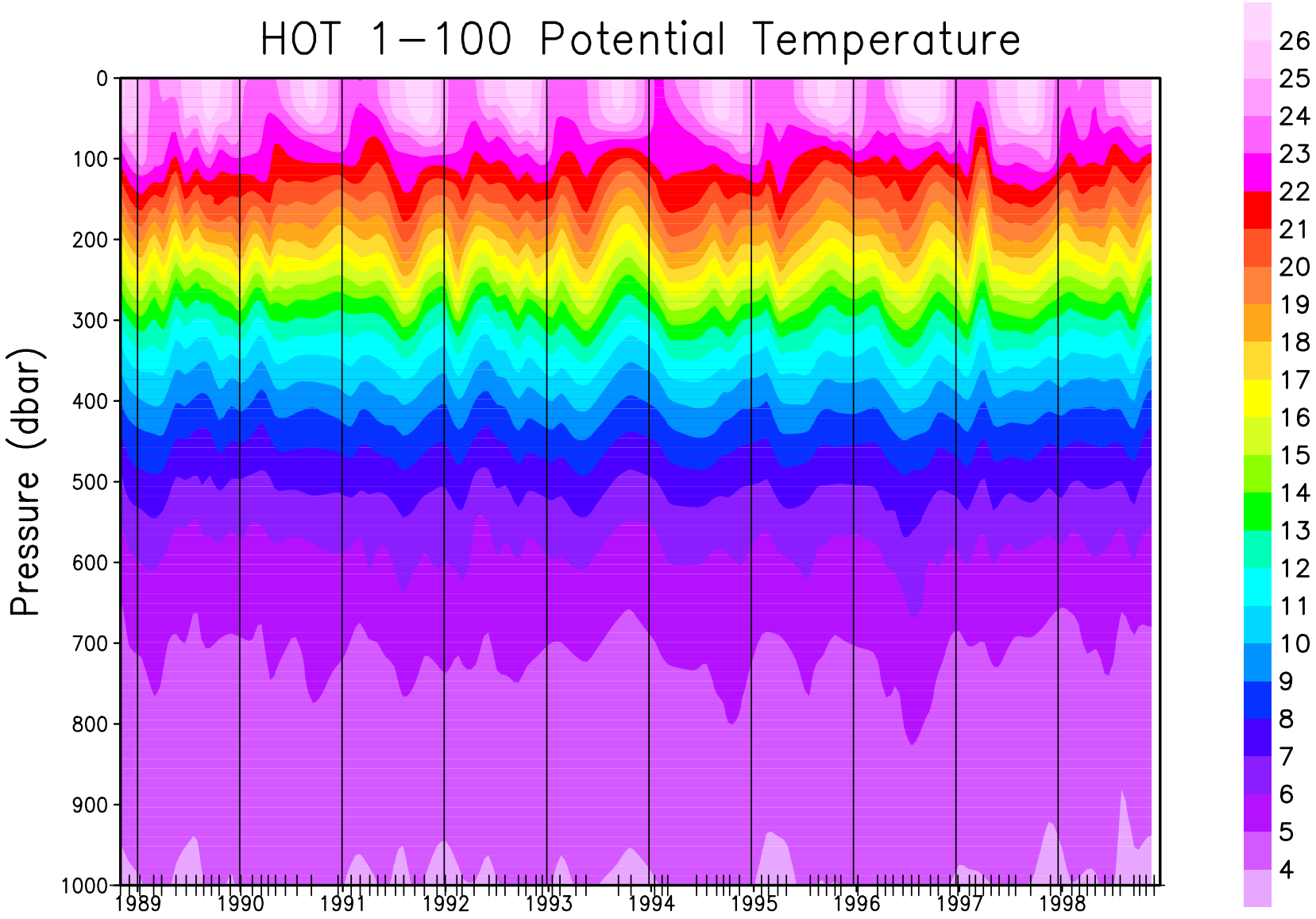
HOT 1–100 Potential Temperature
Pressure (dbar)
0
100
200
300
400
500
600
700
800
900
1000
1989
1990
1991
1992
1993
1994
1995
1996
1997
1998
26
25
24
23
22
21
20
19
18
17
16
15
14
13
12
11
10
9
8
7
6
5
4

Figure 6.1.7a

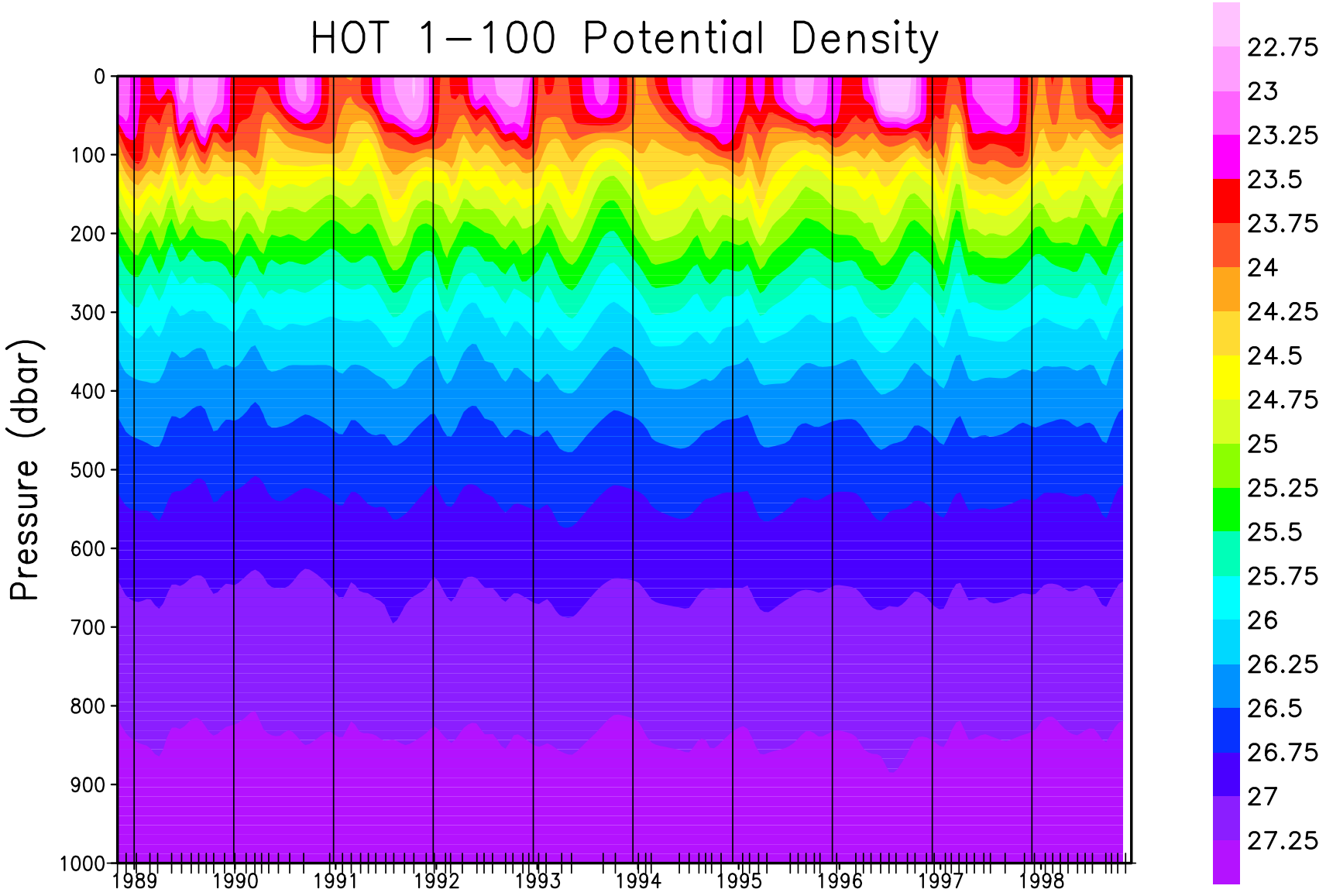
HOT 1–100 Potential Density
Pressure (dbar)
0
100
200
300
400
500
600
700
800
900
1000
1989
1990
1991
1992
1993
1994
1995
1996
1997
1998
22.75
23
23.25
23.5
23.75
24
24.25
24.5
24.75
25
25.25
25.5
25.75
26
26.25
26.5
26.75
27
27.25

Figure 6.1.7b

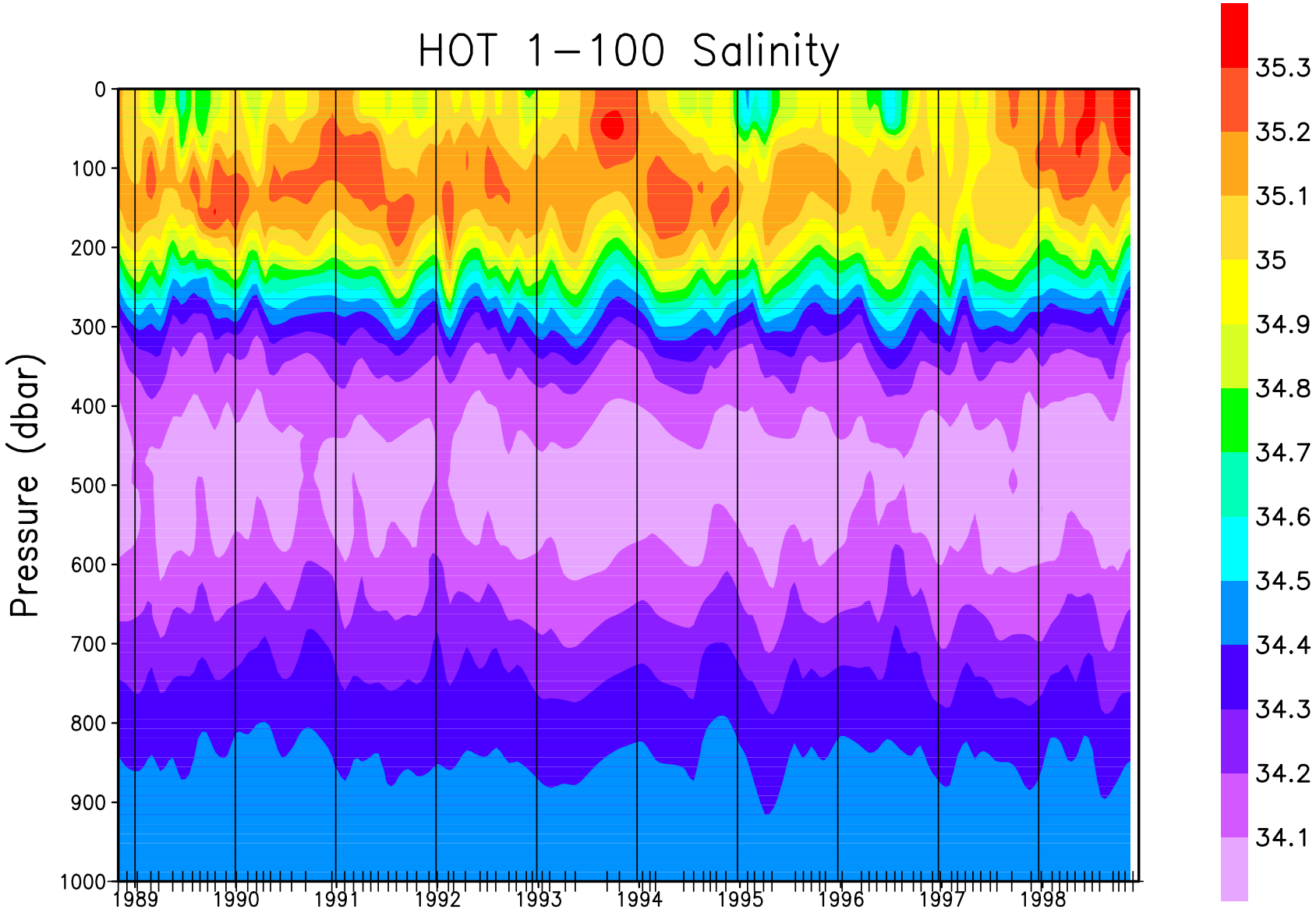
HOT 1–100 Salinity
Pressure (dbar)
0
100
200
300
400
500
600
700
800
900
1000
1989
1990
1991
1992
1993
1994
1995
1996
1997
1998
35.3
35.2
35.1
35
34.9
34.8
34.7
34.6
34.5
34.4
34.3
34.2
34.1

Figure 6.1.8a

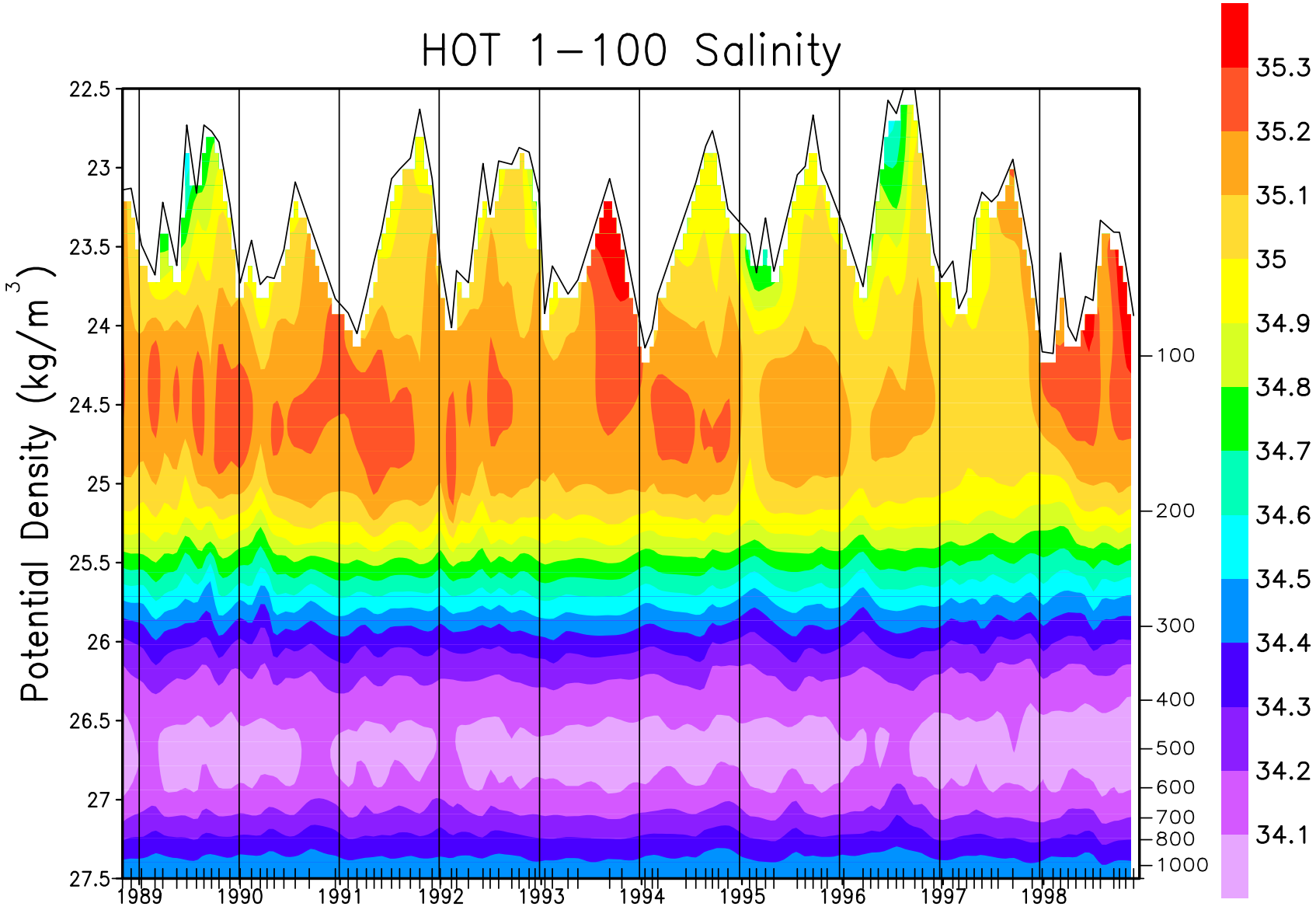
HOT 1–100 Salinity
Potential Density (kg/m3)
22.5
23
23.5
24
24.5
25
25.5
26
26.5
27
27.5
1989
1990
1991
1992
1993
1994
1995
1996
1997
1998
100
200
300
400
500
600
700
800
1000
35.3
35.2
35.1
35
34.9
34.8
34.7
34.6
34.5
34.4
34.3
34.2
34.1

Figure 6.1.8b

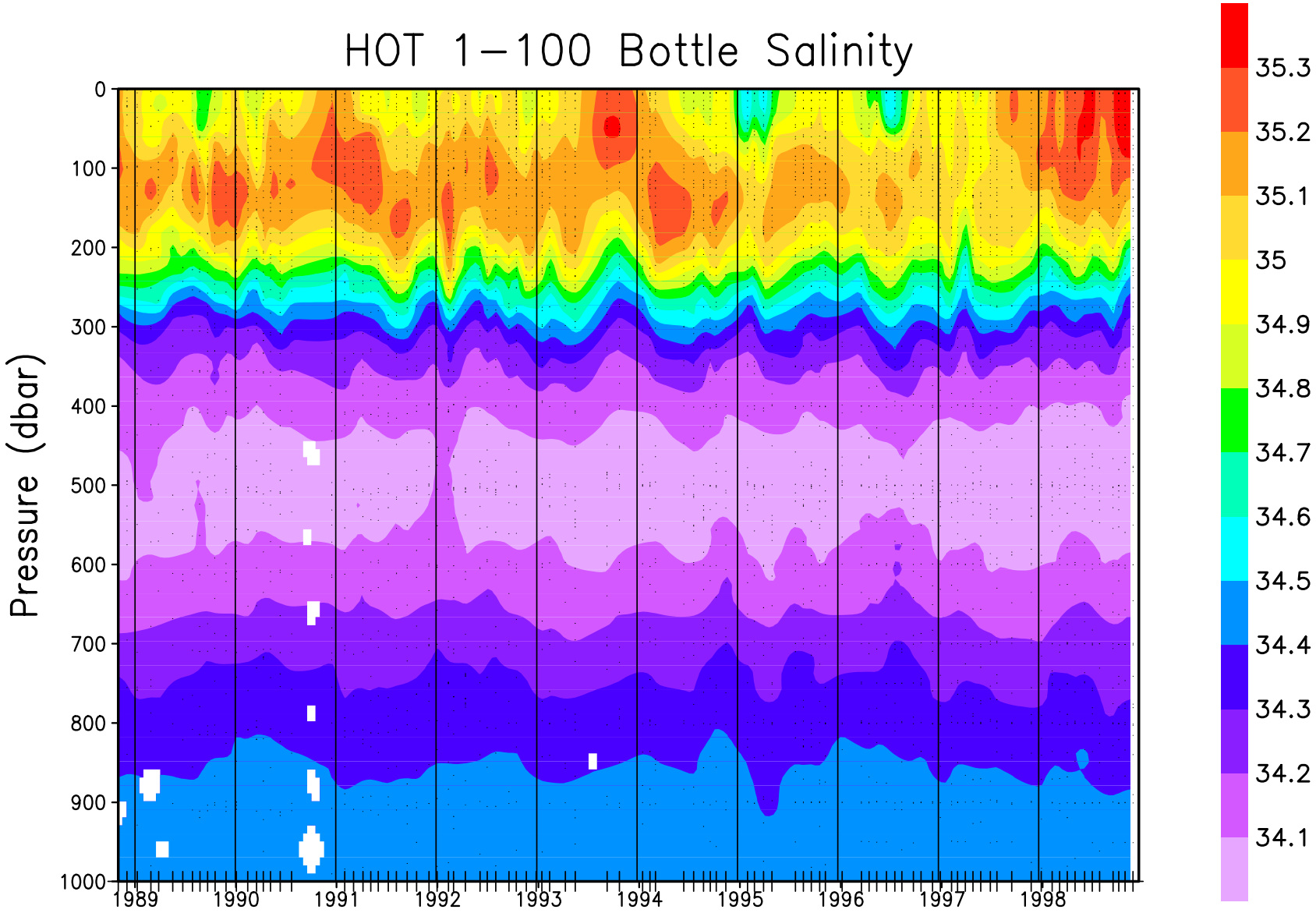
HOT 1–100 Bottle Salinity
Pressure (dbar)
0
100
200
300
400
500
600
700
800
900
1000
1989
1990
1991
1992
1993
1994
1995
1996
1997
1998
35.3
35.2
35.1
35
34.9
34.8
34.7
34.6
34.5
34.4
34.3
34.2
34.1

Figure 6.1.9a

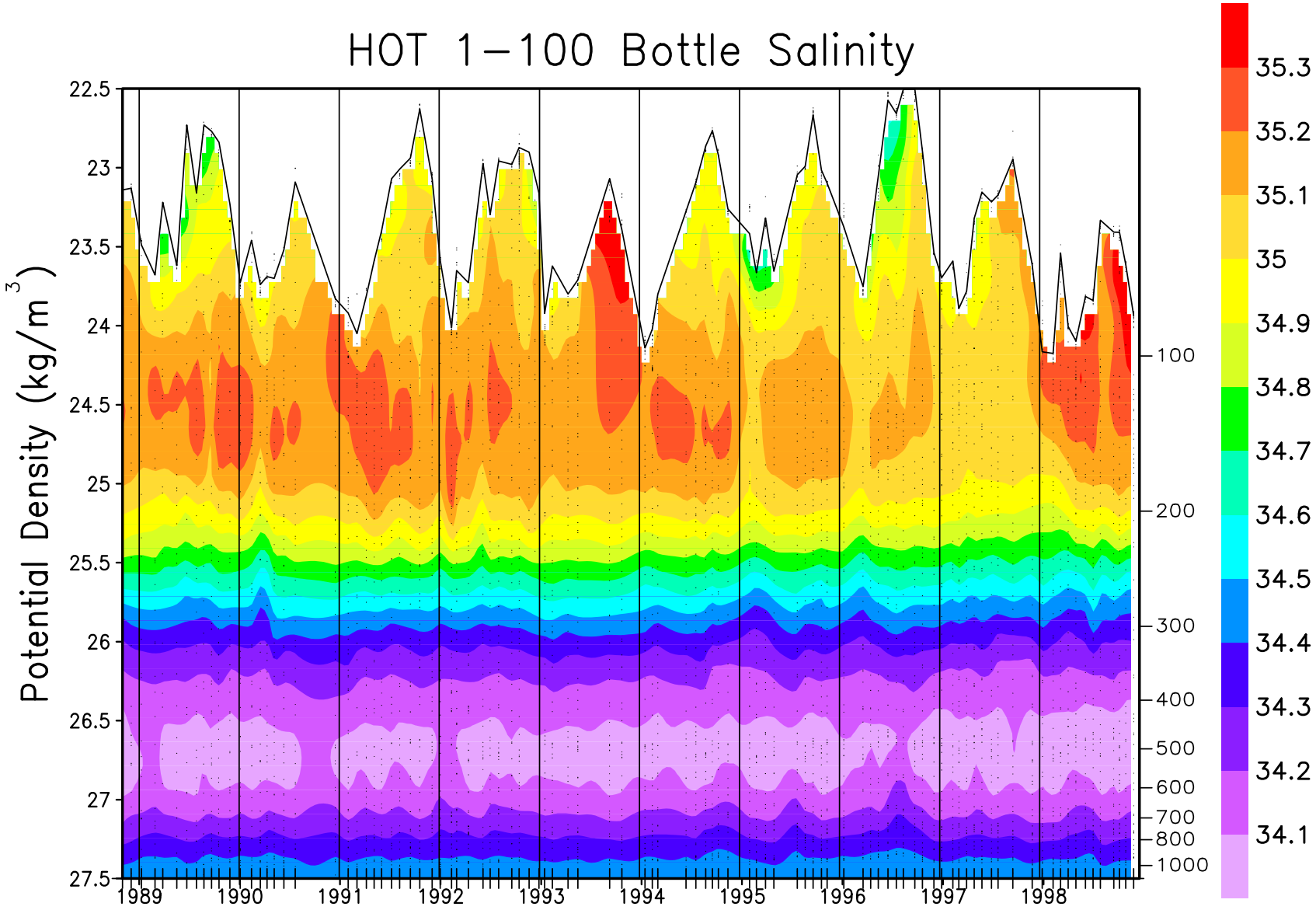
HOT 1–100 Bottle Salinity
Potential Density (kg/m3)
22.5
23
23.5
24
24.5
25
25.5
26
26.5
27
27.5
1989
1990
1991
1992
1993
1994
1995
1996
1997
1998
100
200
300
400
500
600
700
800
1000
35.3
35.2
35.1
35
34.9
34.8
34.7
34.6
34.5
34.4
34.3
34.2
34.1

Figure 6.1.9b

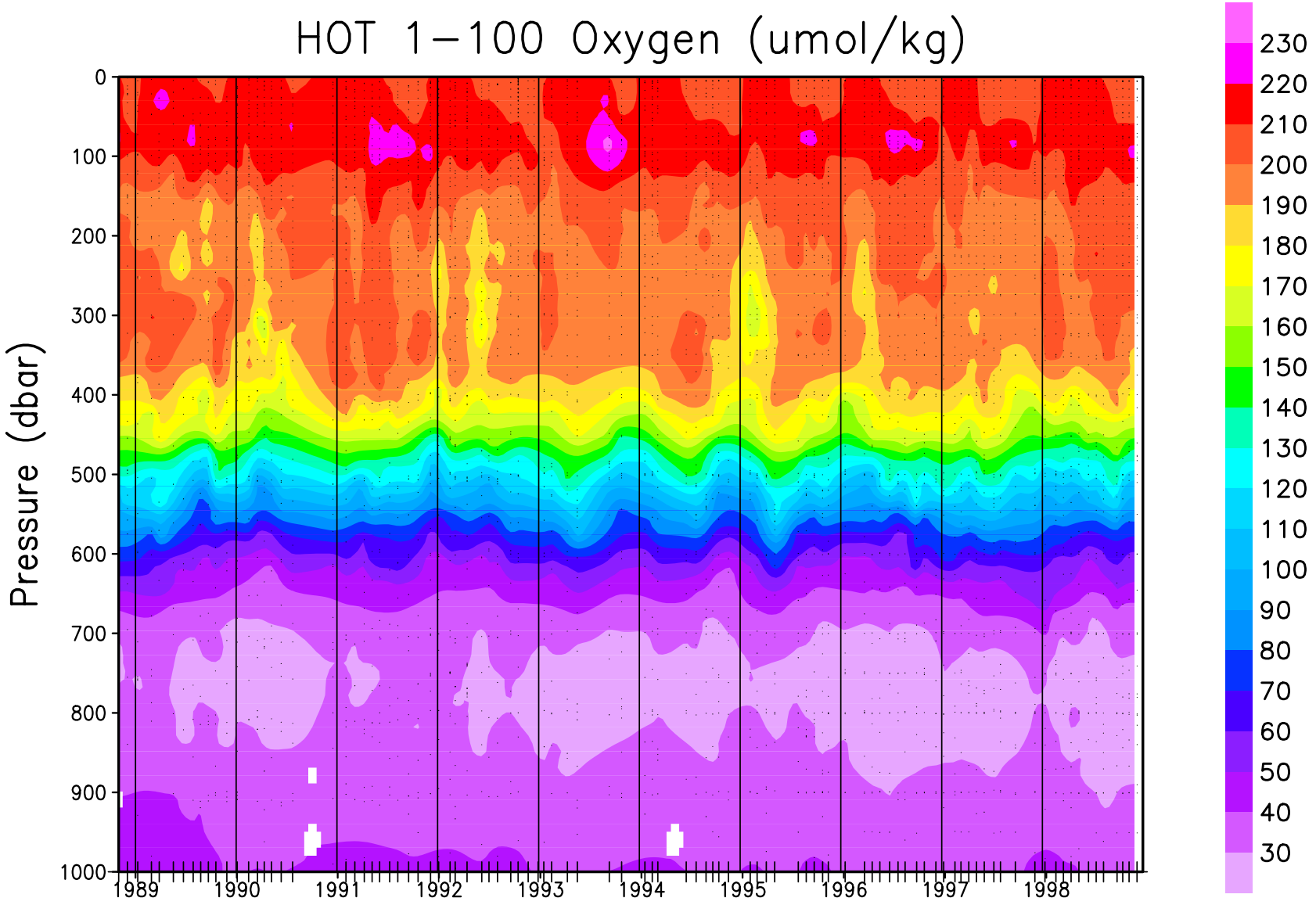

Figure 6.1.10a

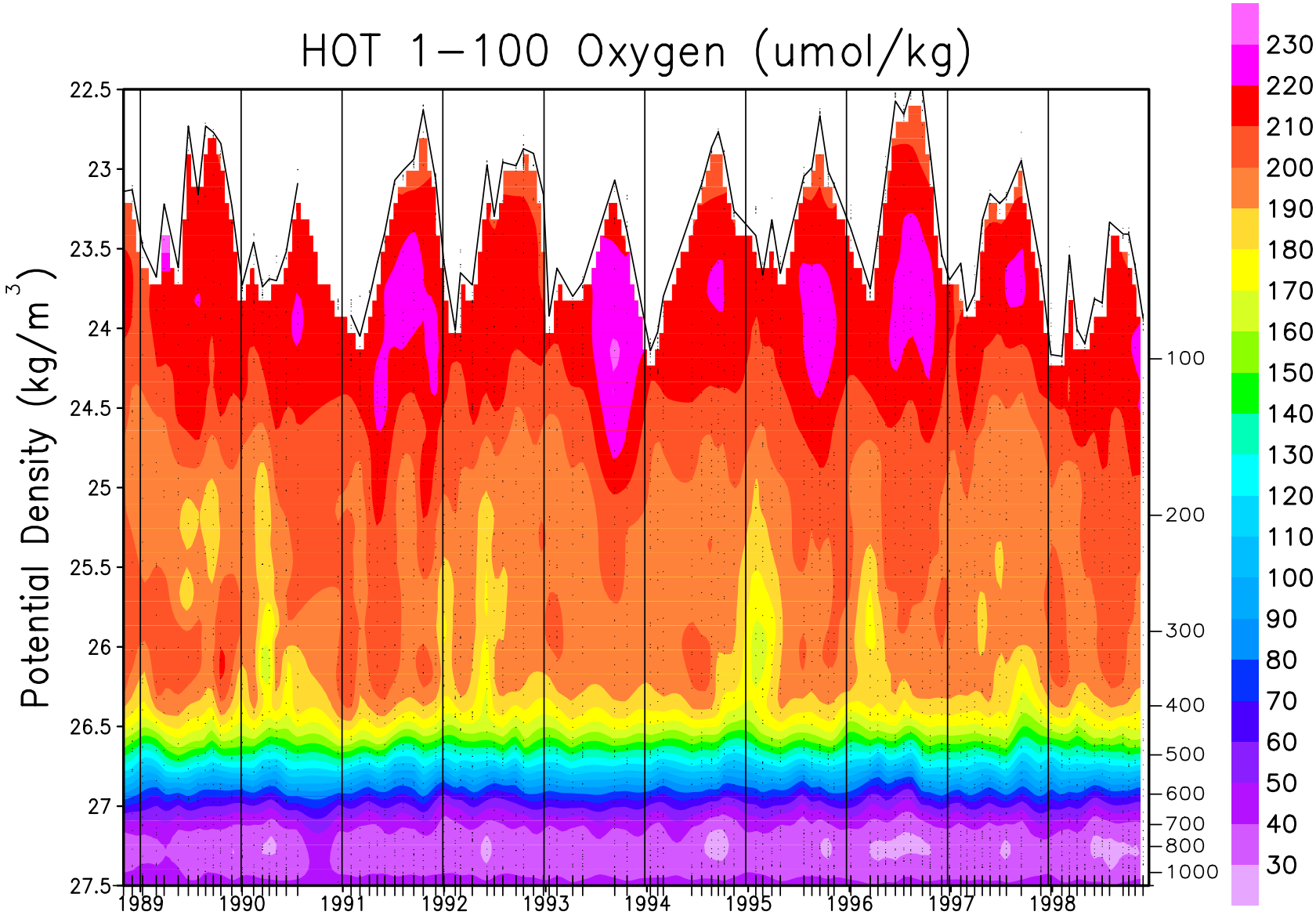

Figure 6.1.10b

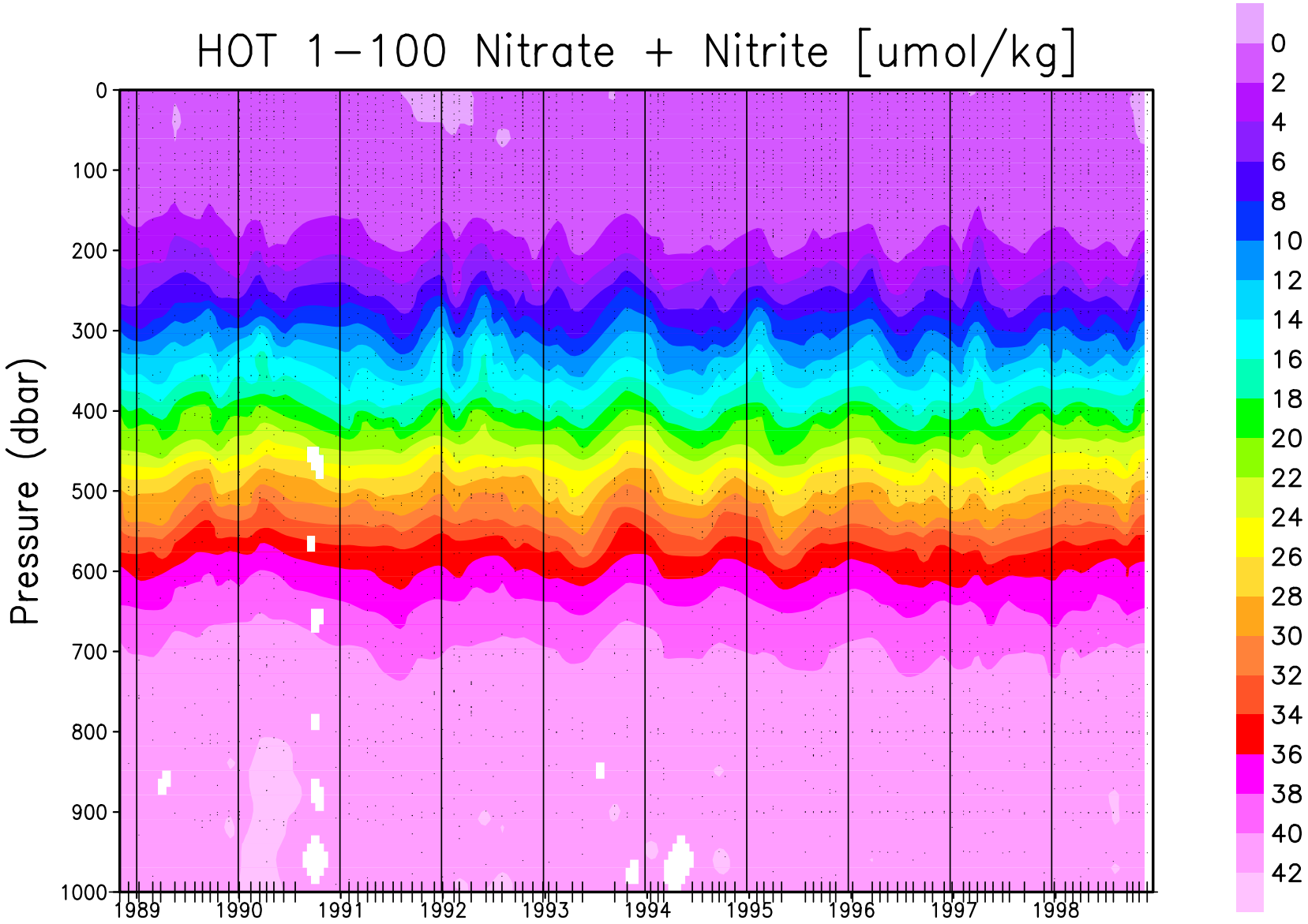

Figure 6.1.11a

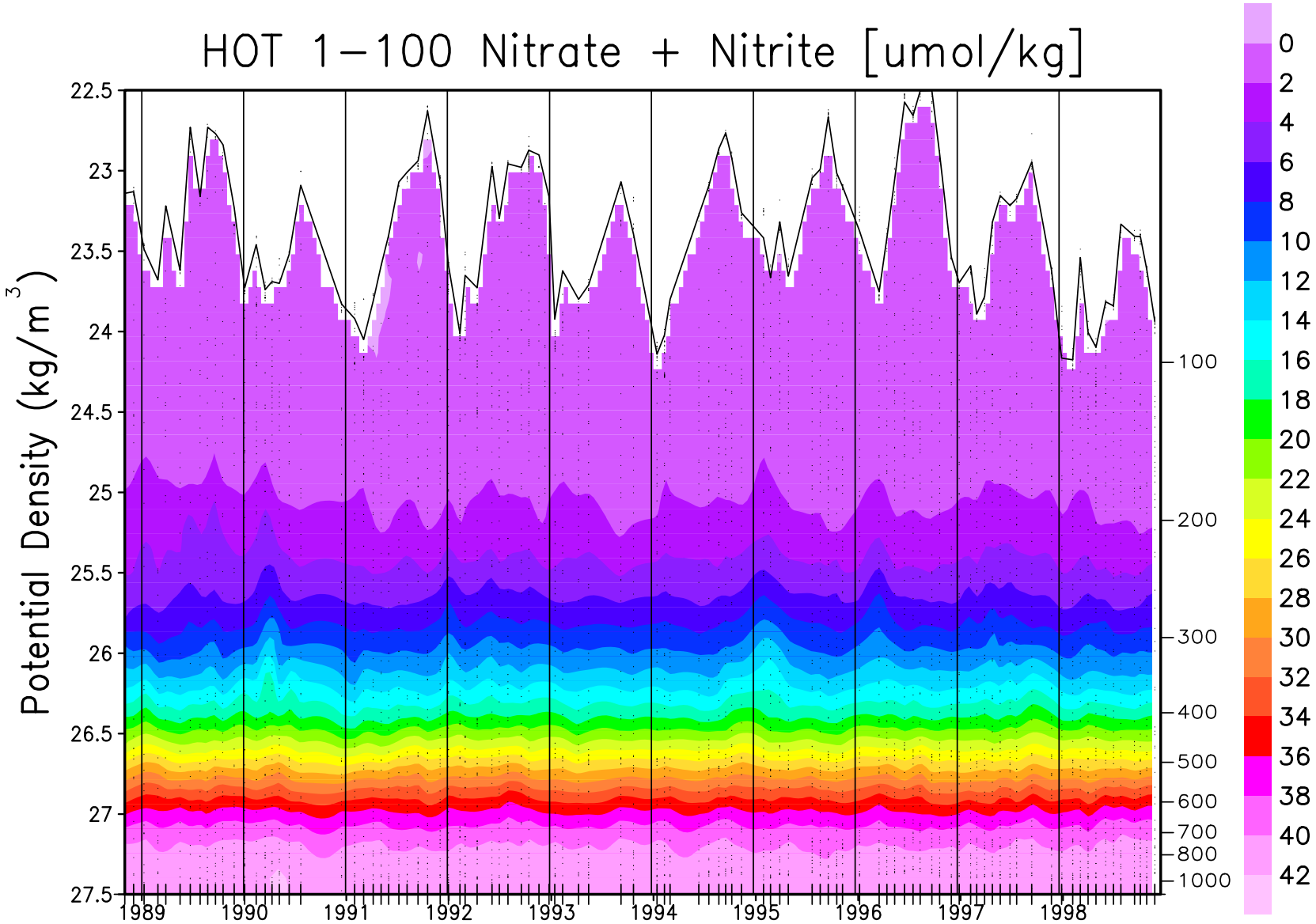

Figure 6.1.11b

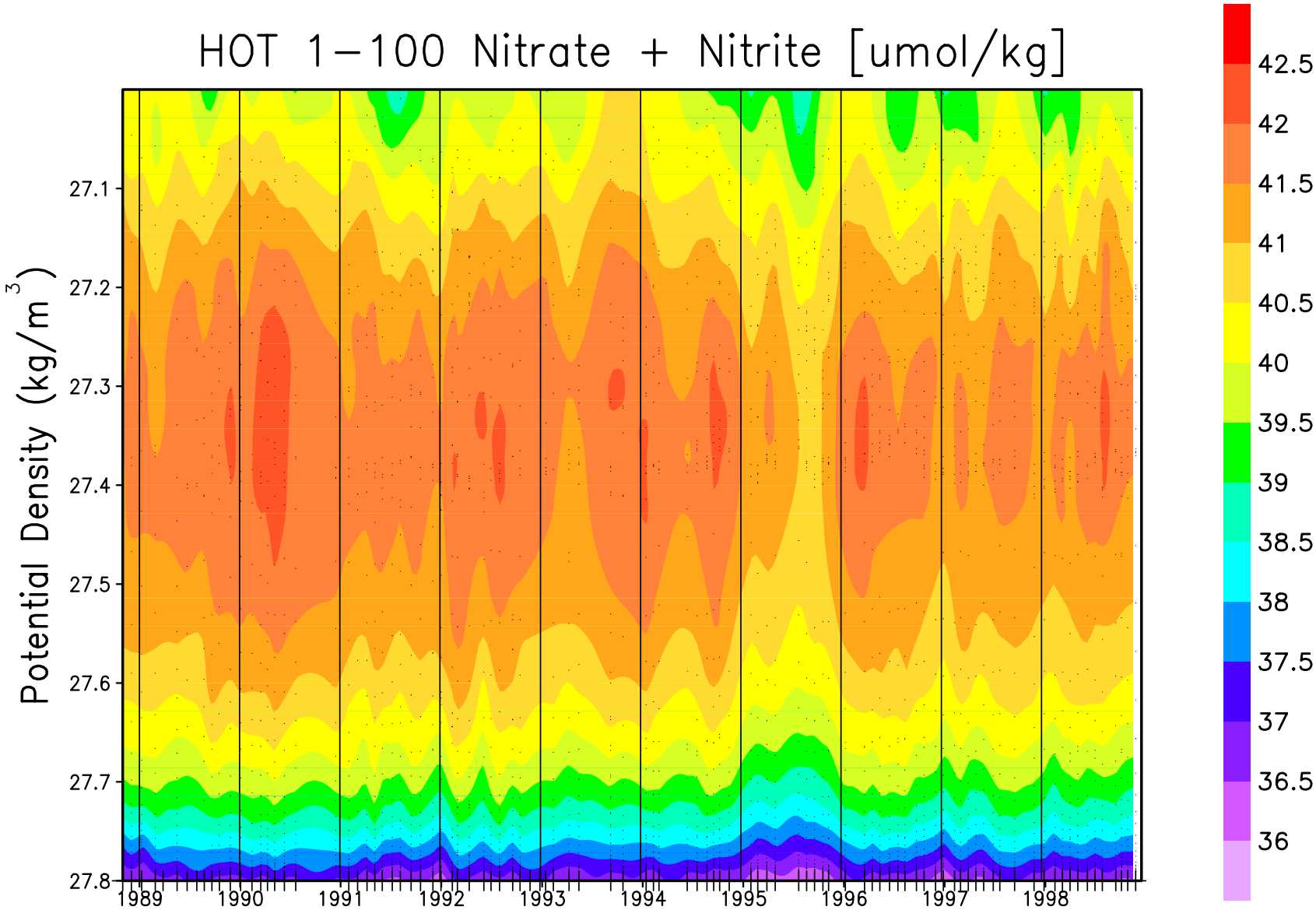

Figure 6.1.12a

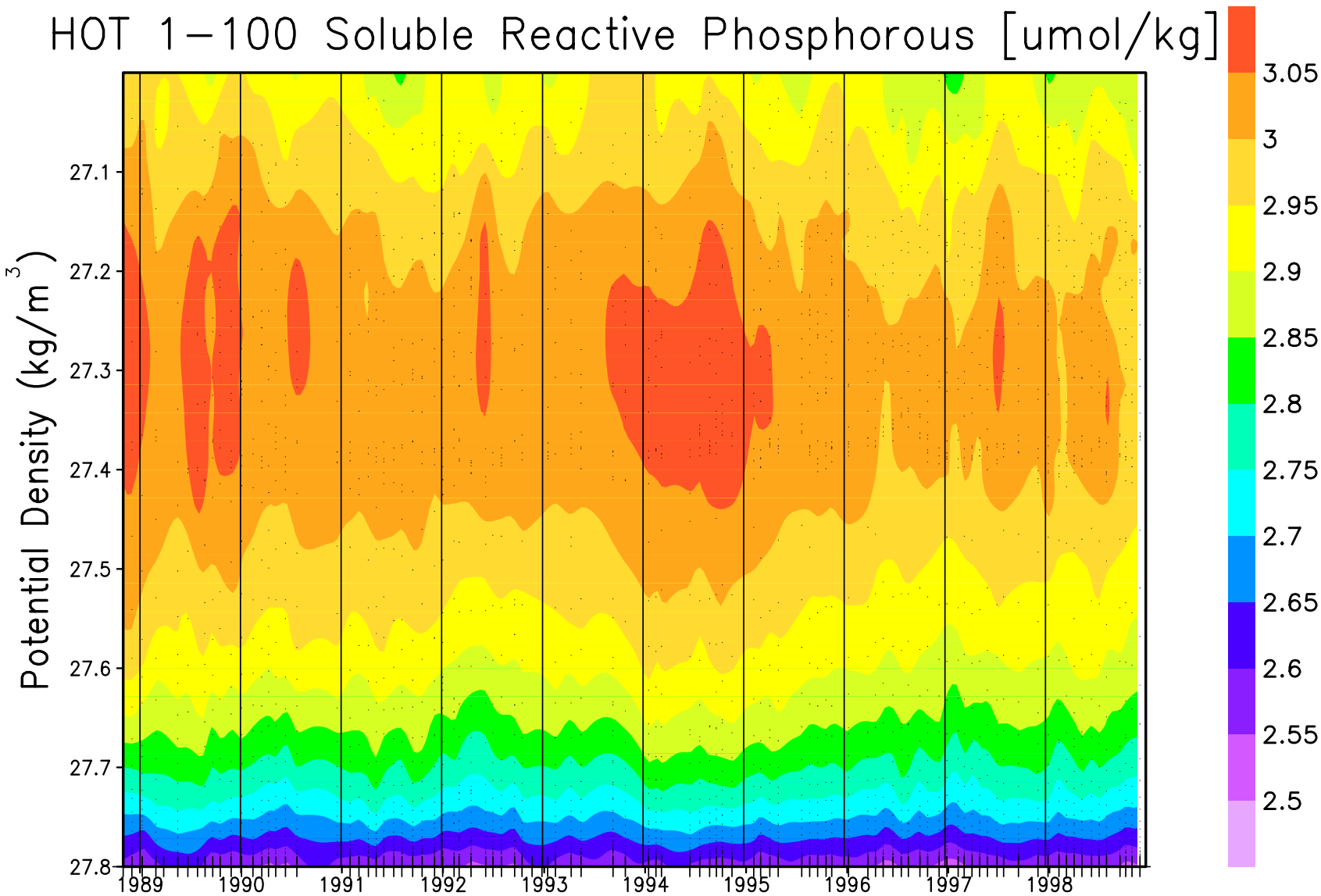

Figure 6.1.12b

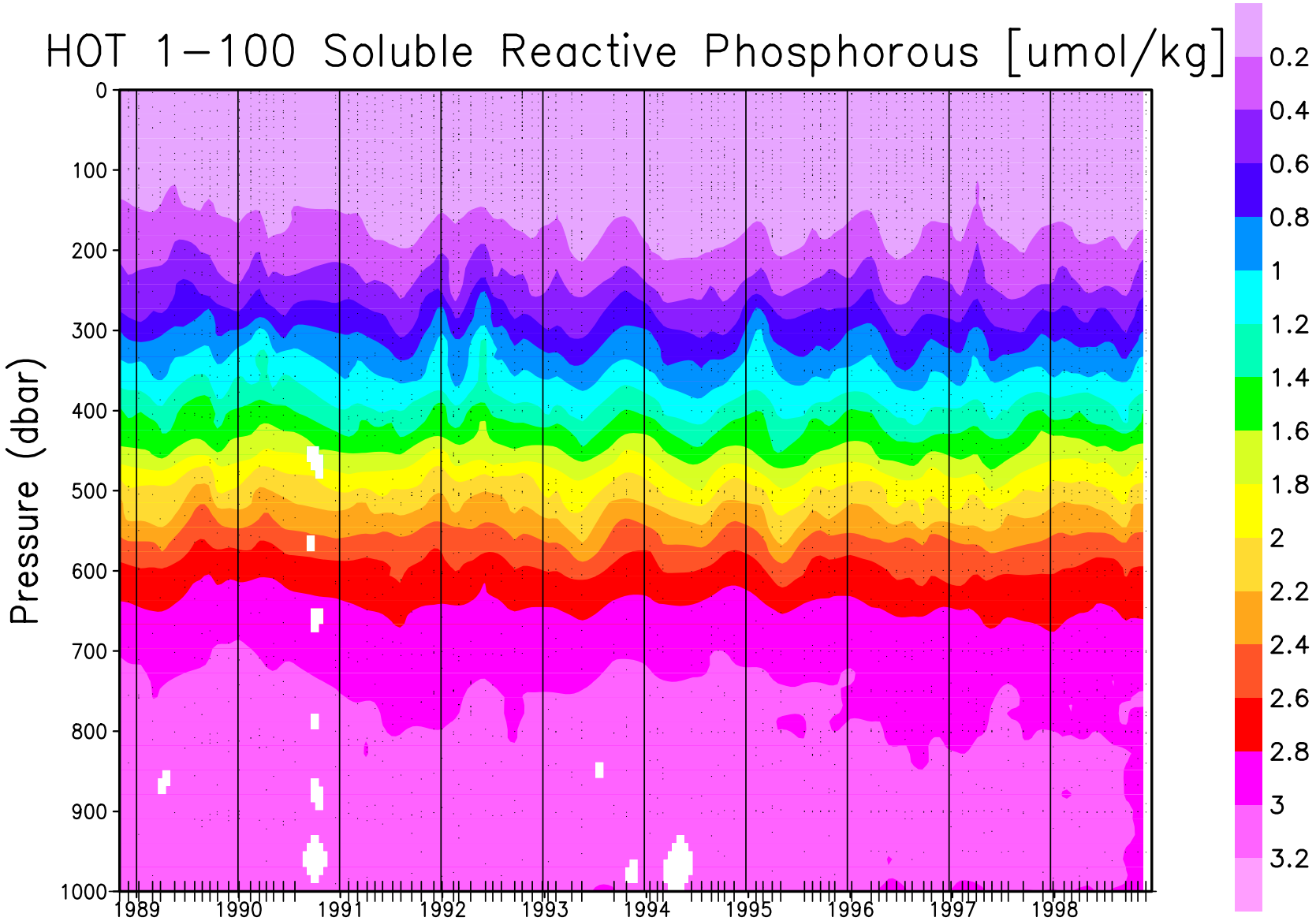

Figure 6.1.13a

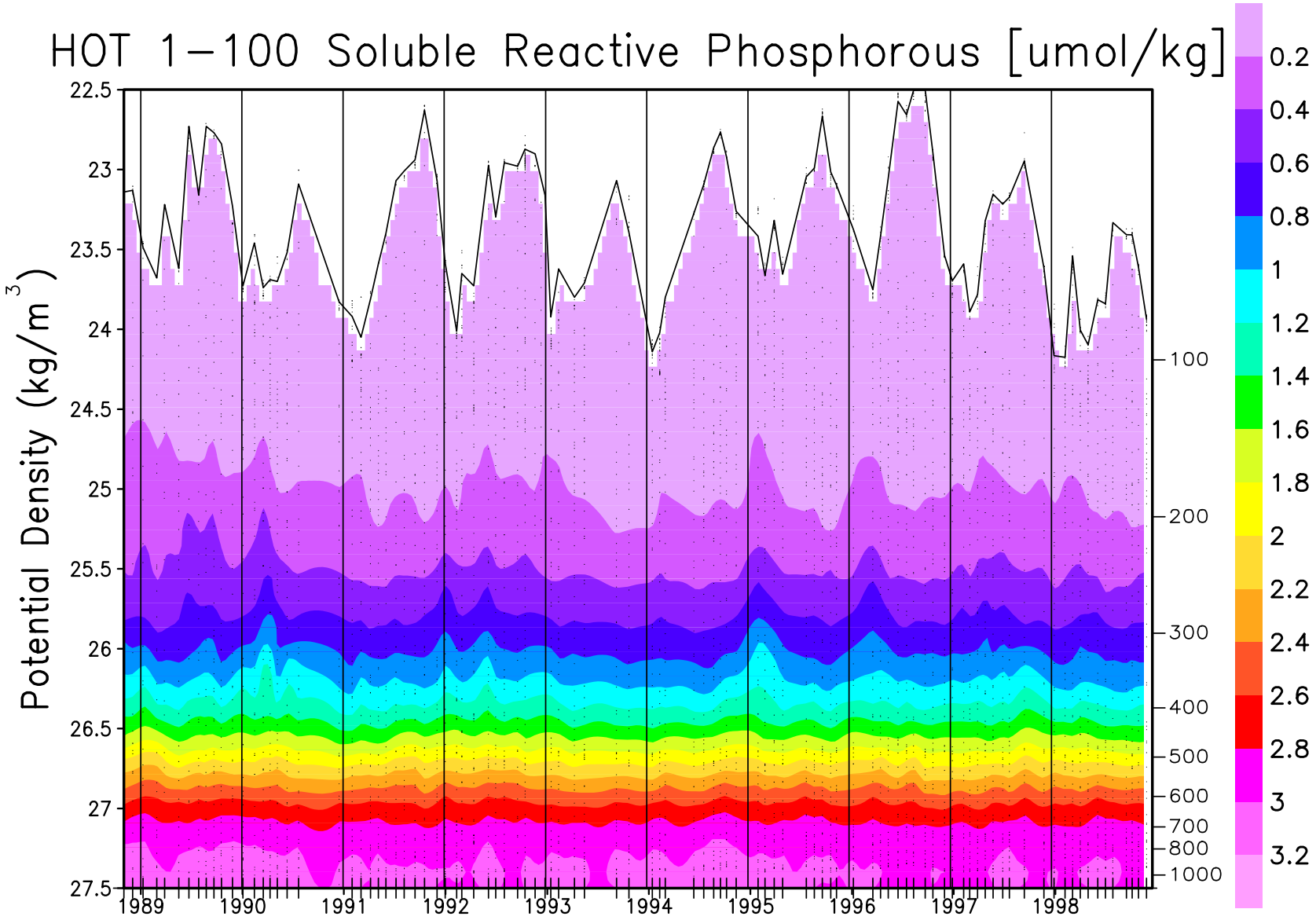

Figure 6.1.13b

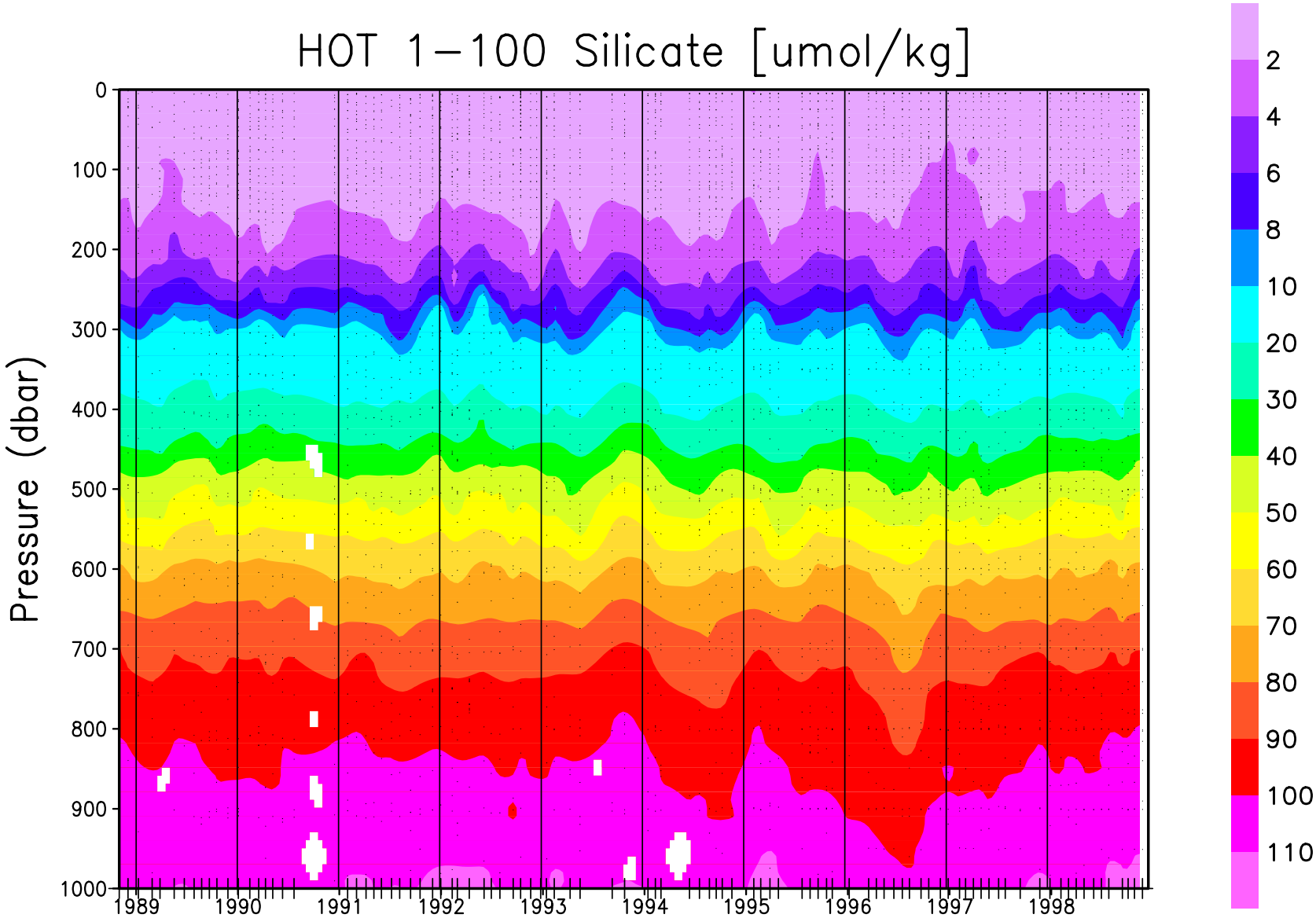

Figure 6.1.14a

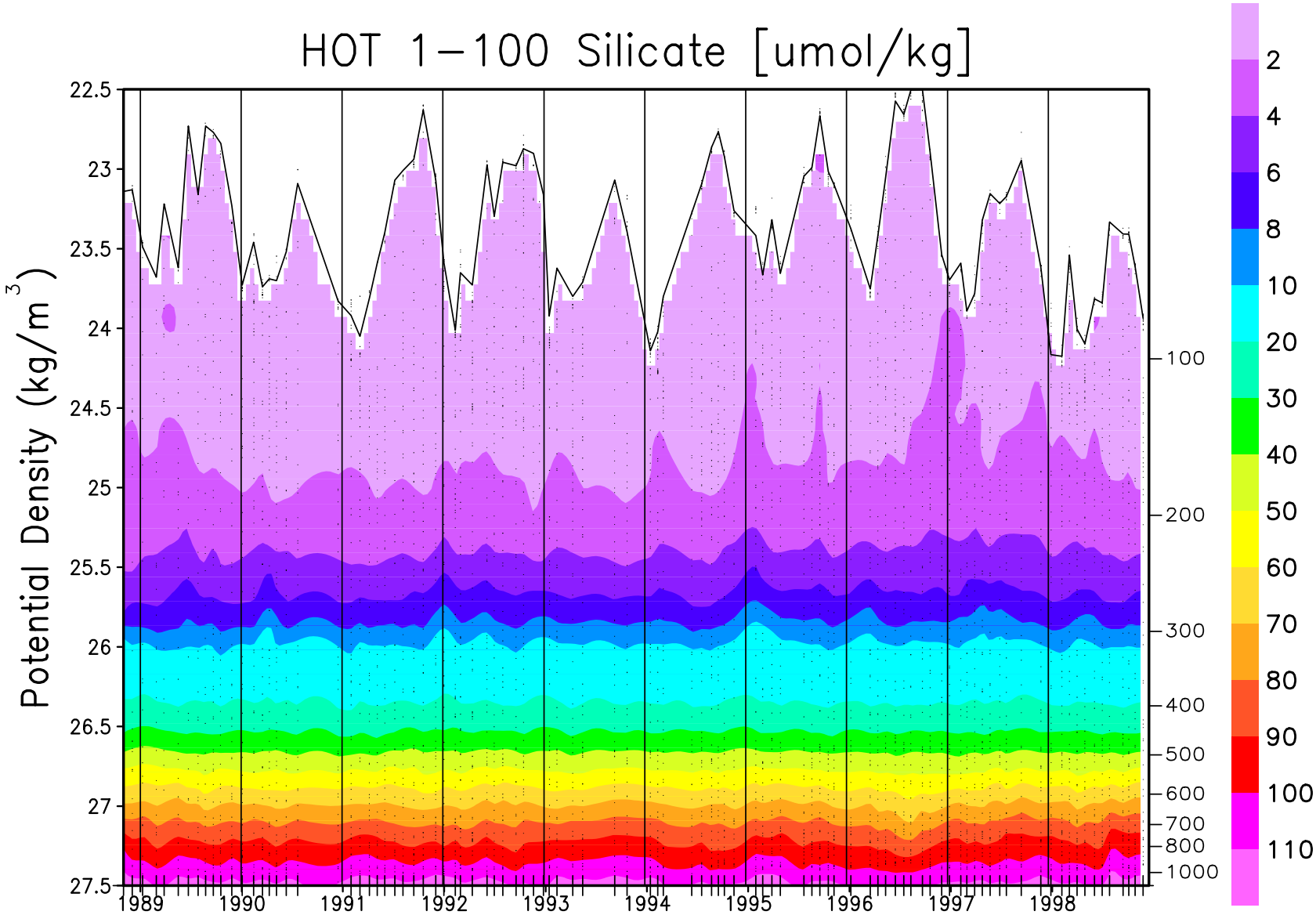

Figure 6.1.14b

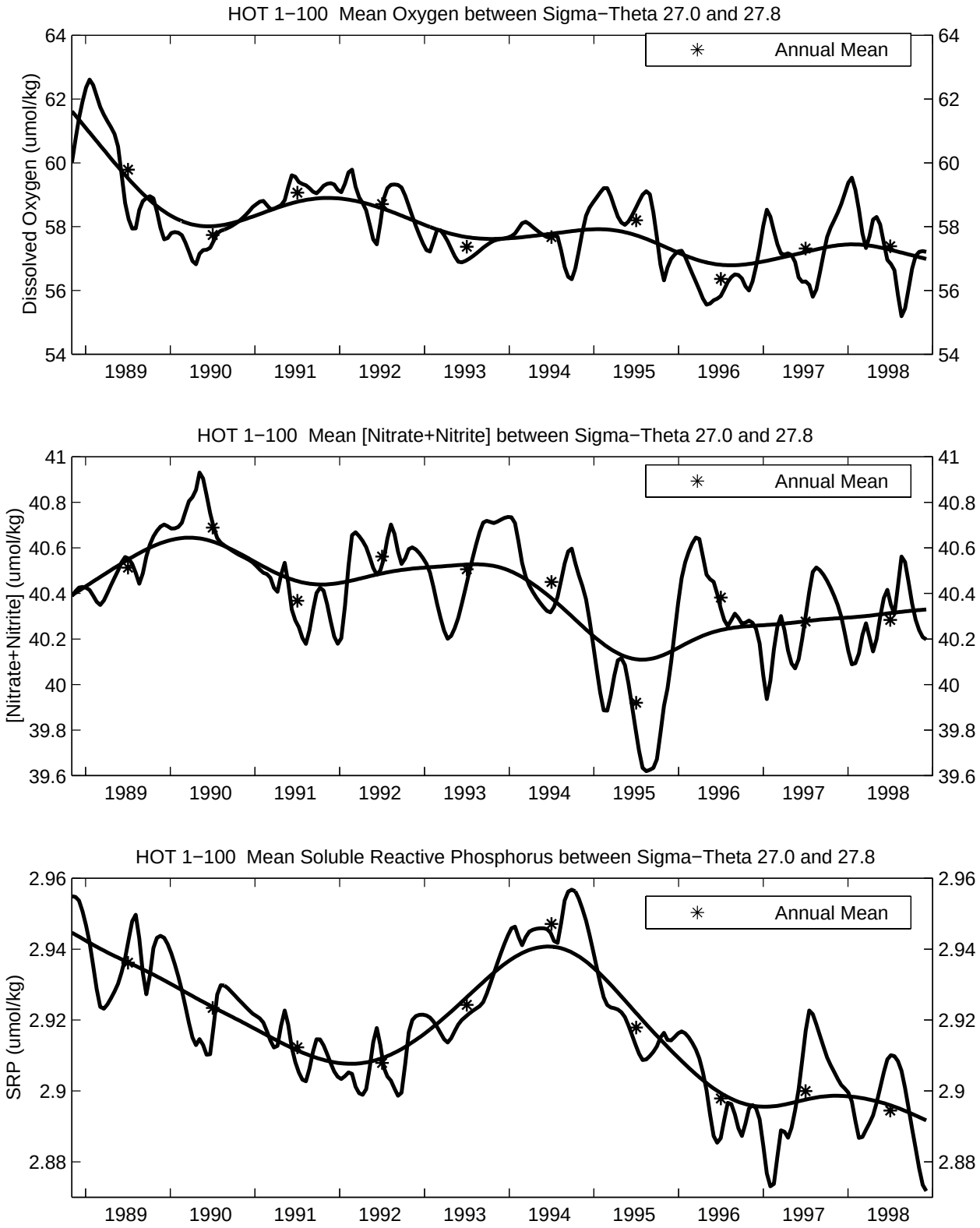
HOT 1−100 Mean Oxygen between Sigma−Theta 27.0 and 27.8
Dissolved Oxygen (umol/kg)
Annual Mean
64
62
60
58
56
54
1989
1990
1991
1992
1993
1994
1995
1996
1997
1998
HOT 1−100 Mean [Nitrate+Nitrite] between Sigma−Theta 27.0 and 27.8
[Nitrate+Nitrite] (umol/kg)
Annual Mean
41
40.8
40.6
40.4
40.2
40
39.8
39.6
HOT 1−100 Mean Soluble Reactive Phosphorus between Sigma−Theta 27.0 and 27.8
SRP (umol/kg)
Annual Mean
2.96
2.94
2.92
2.9
2.88

Figure 6.1.15

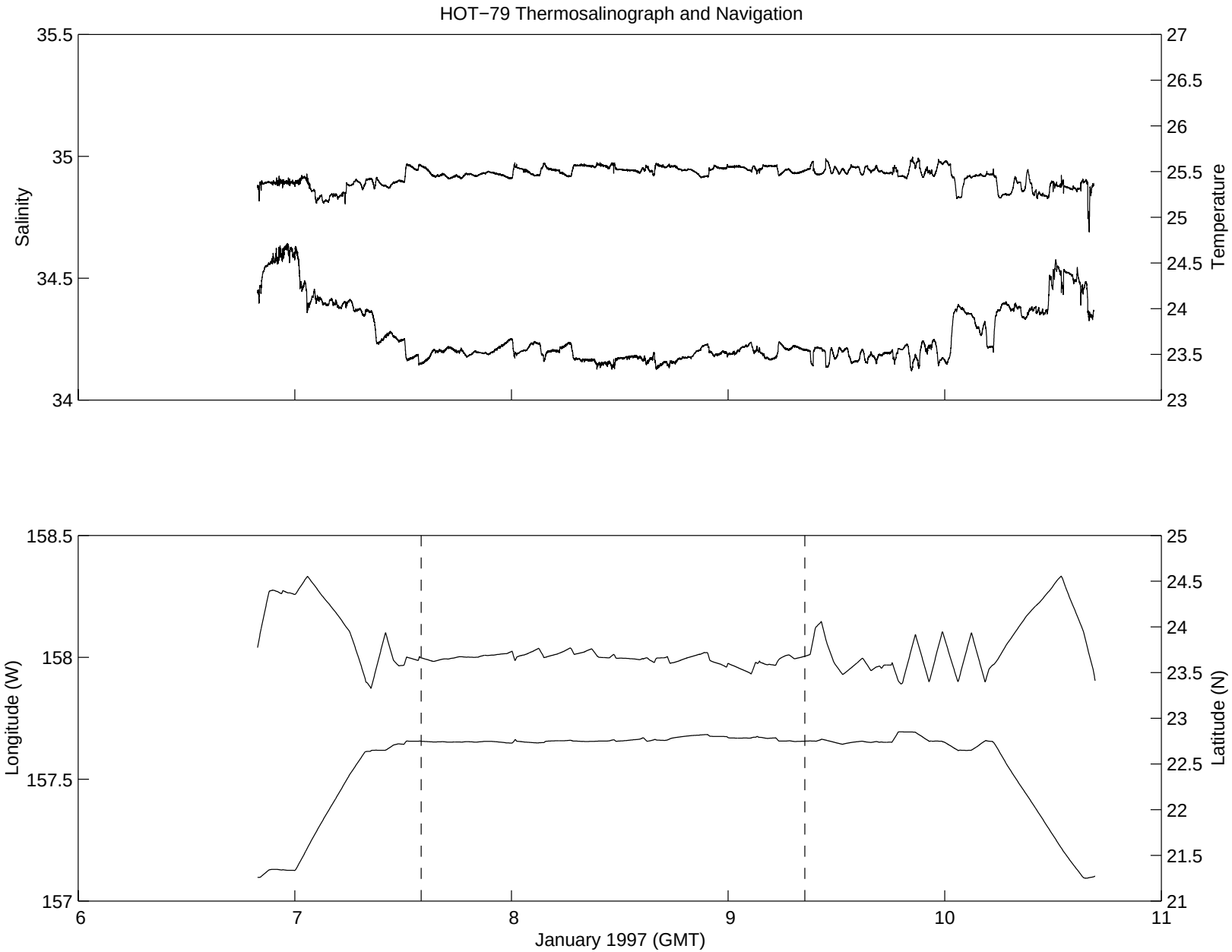

Figure 6.1.16a

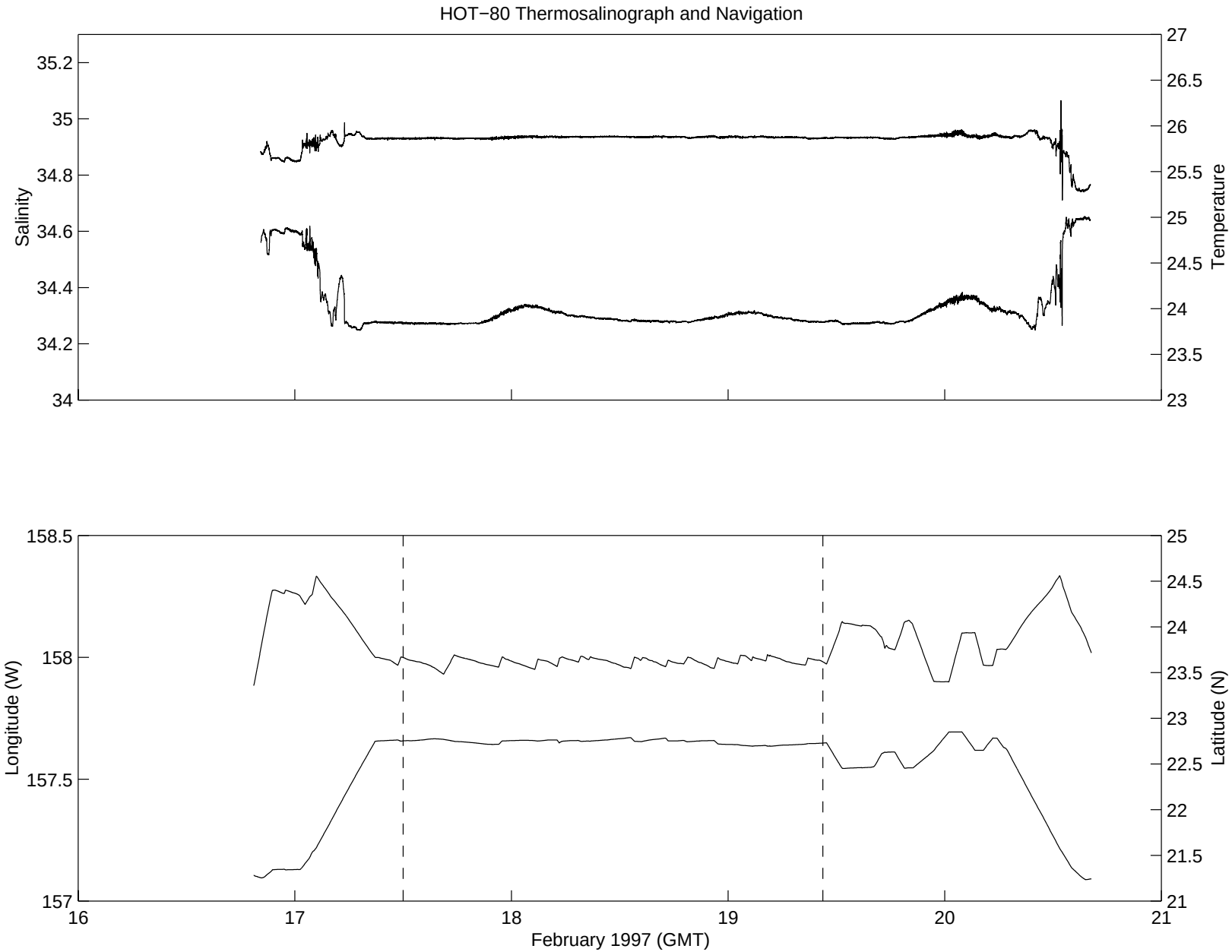

Figure 6.1.16b

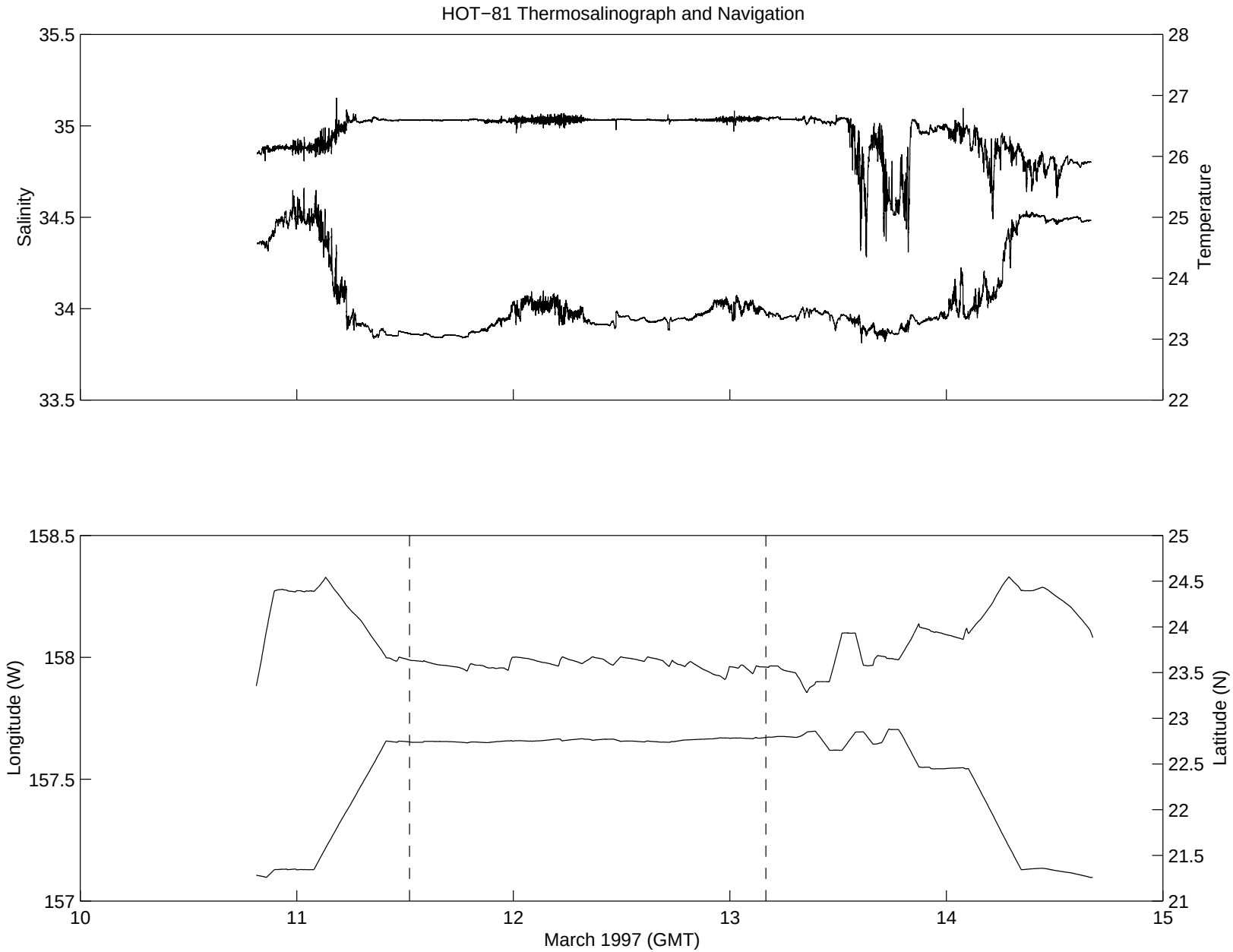

Figure 6.1.16c

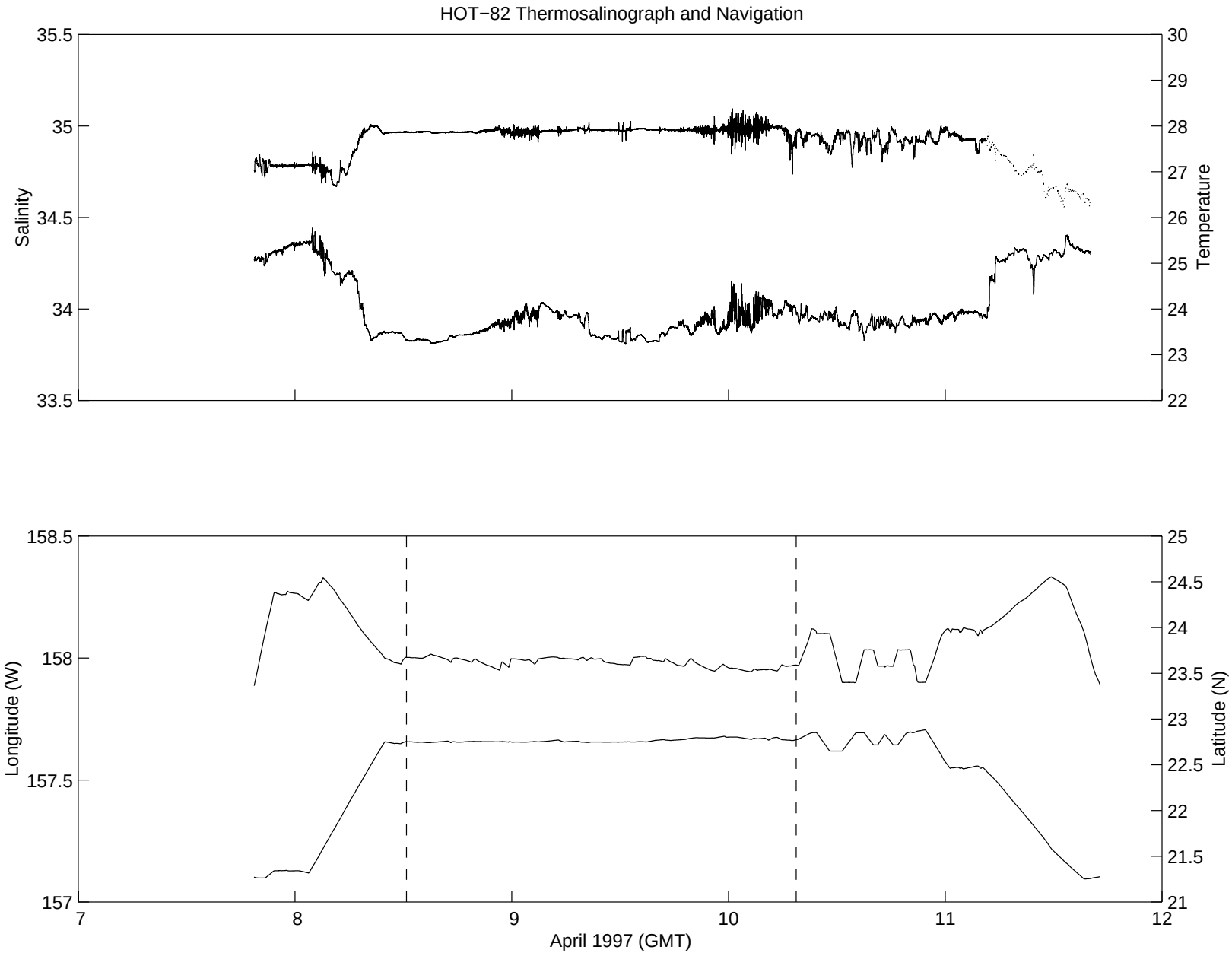

Figure 6.1.16d

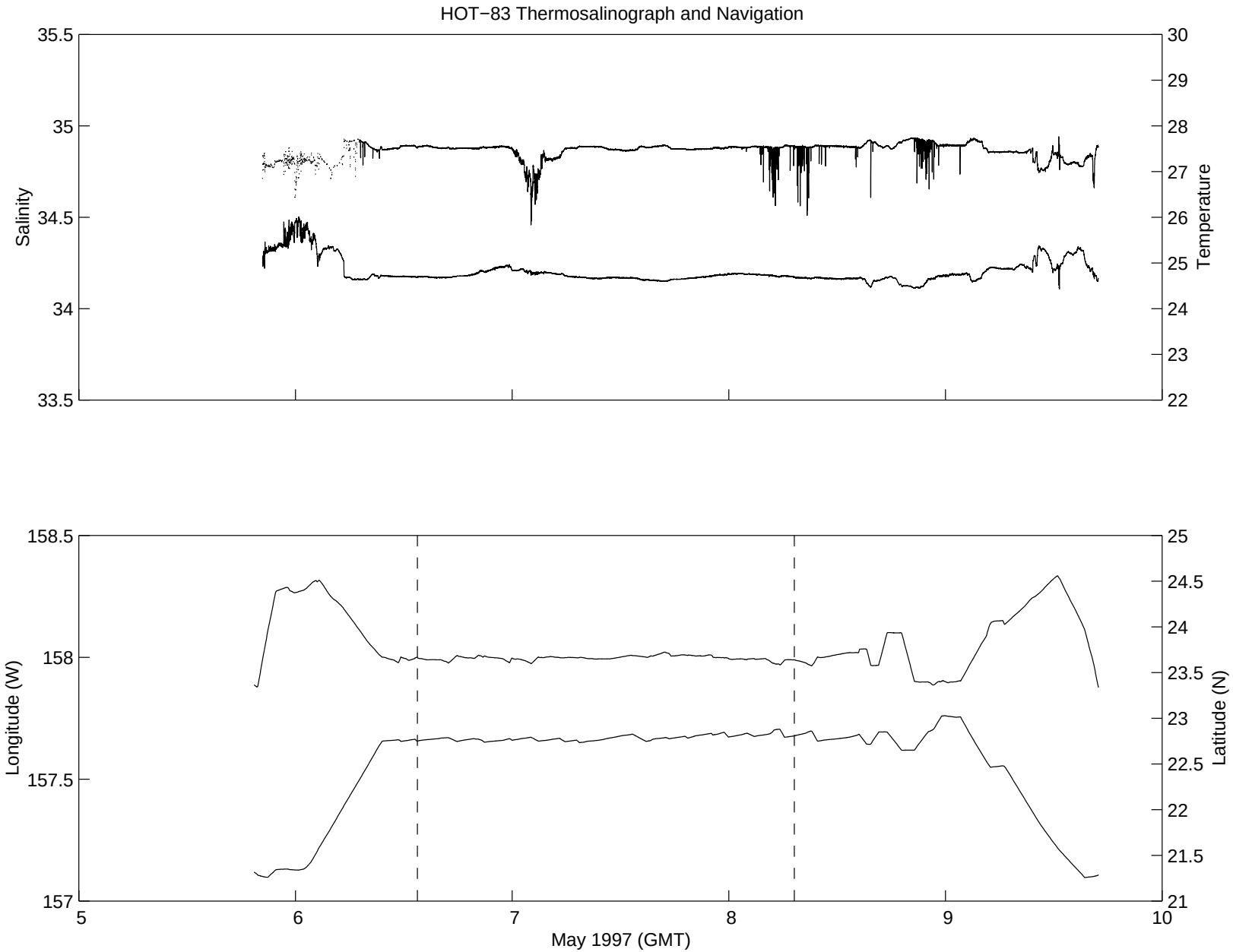

Figure 6.1.16e

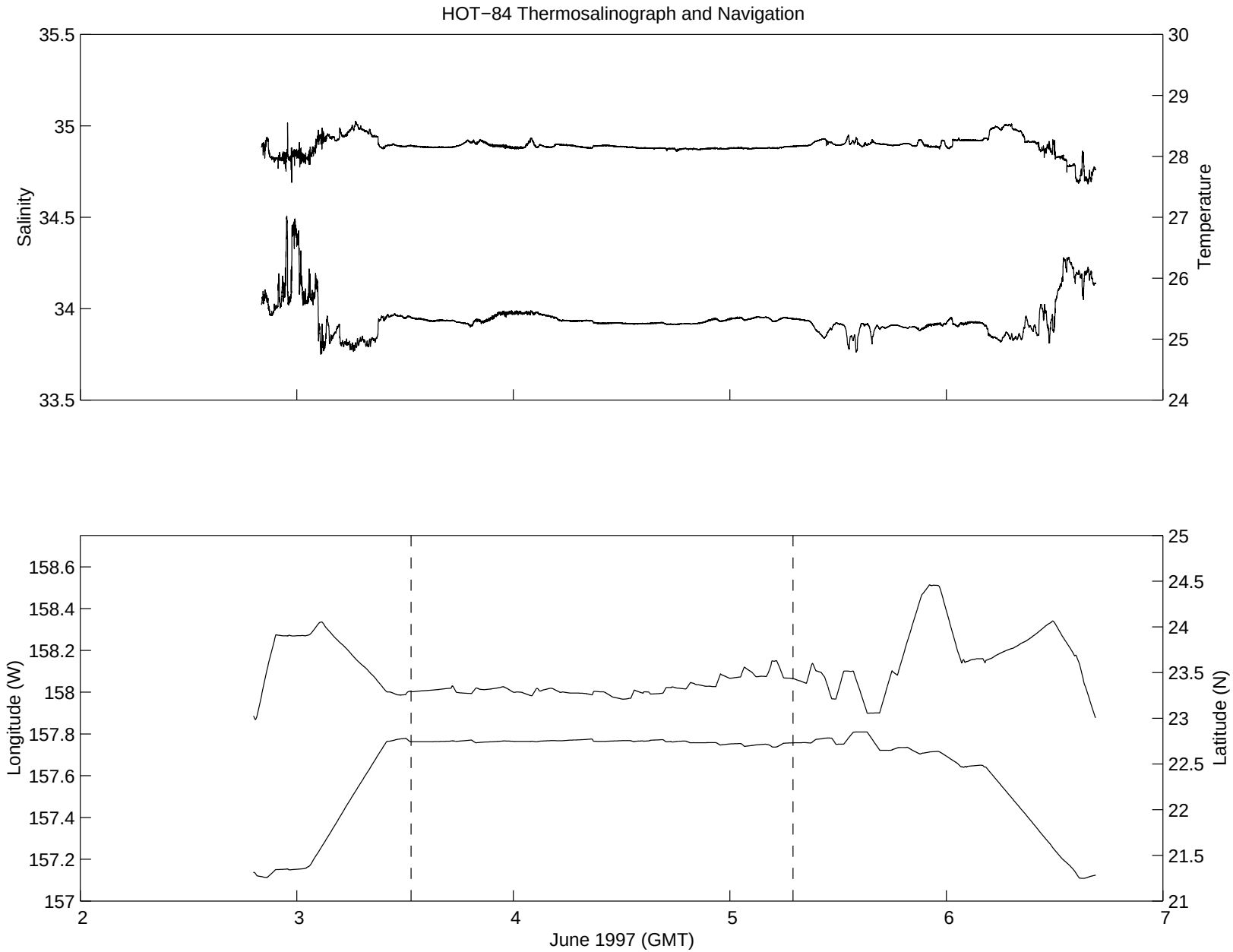

Figure 6.1.16f

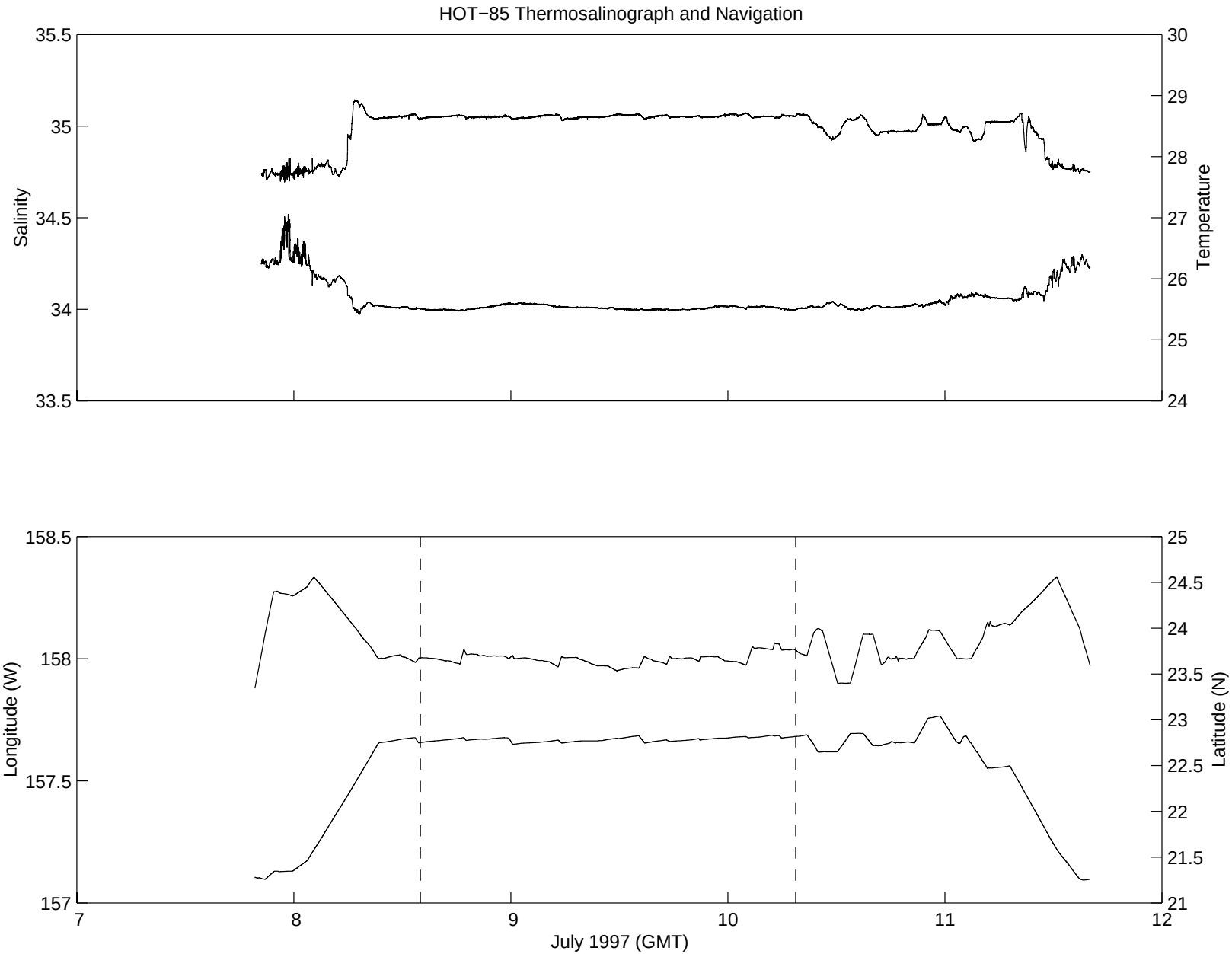

Figure 6.1.16g

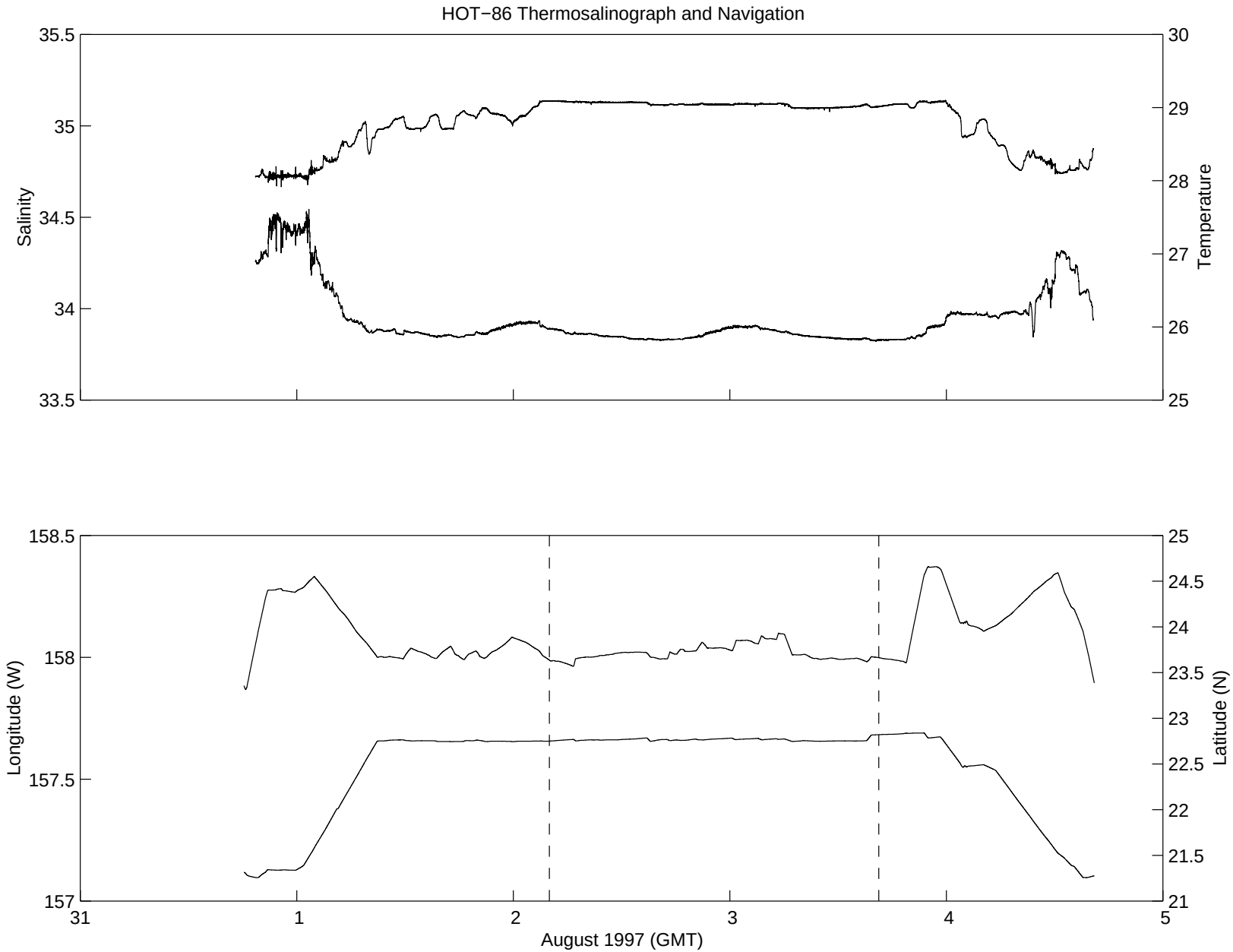

Figure 6.1.16h

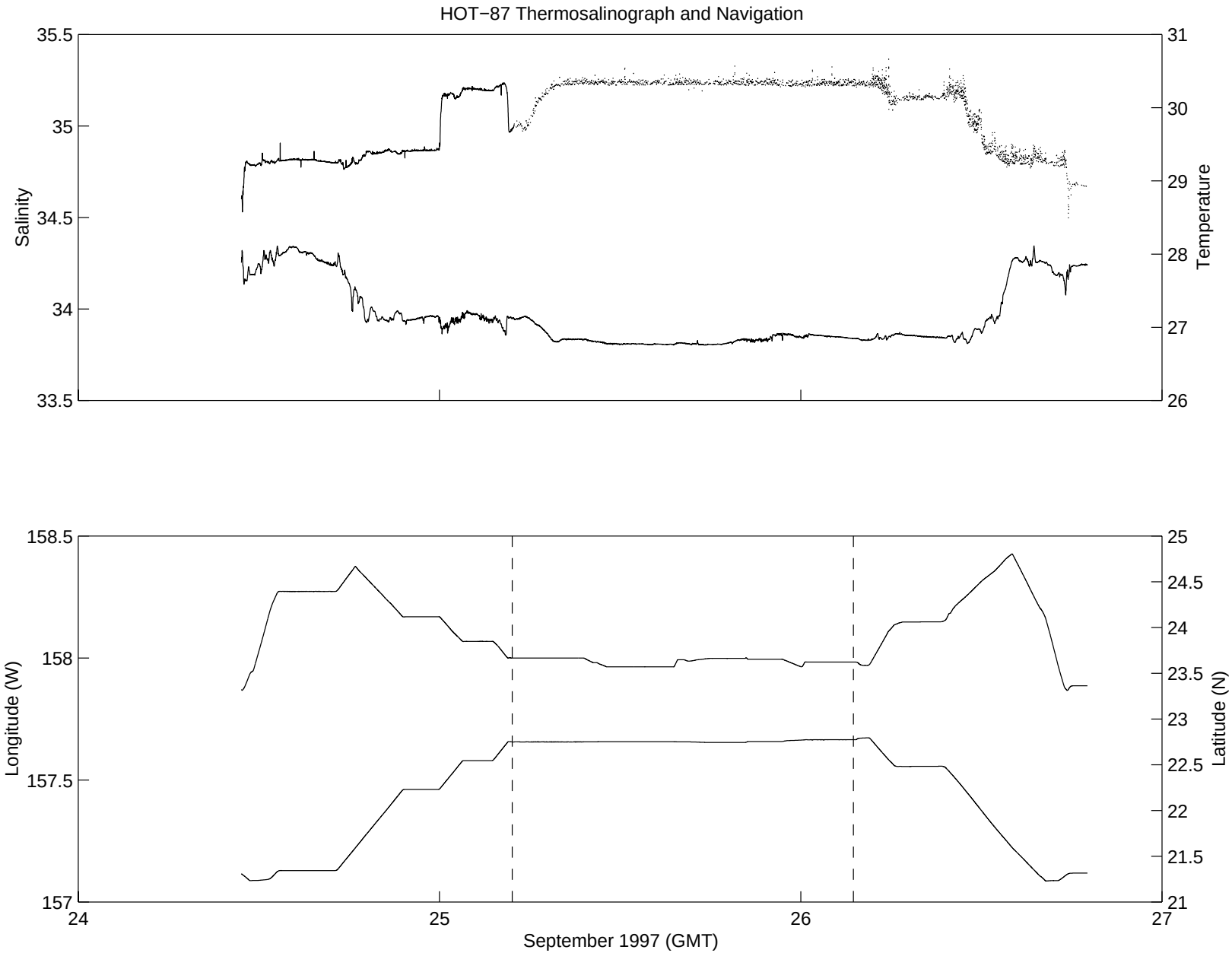

Figure 6.1.16i

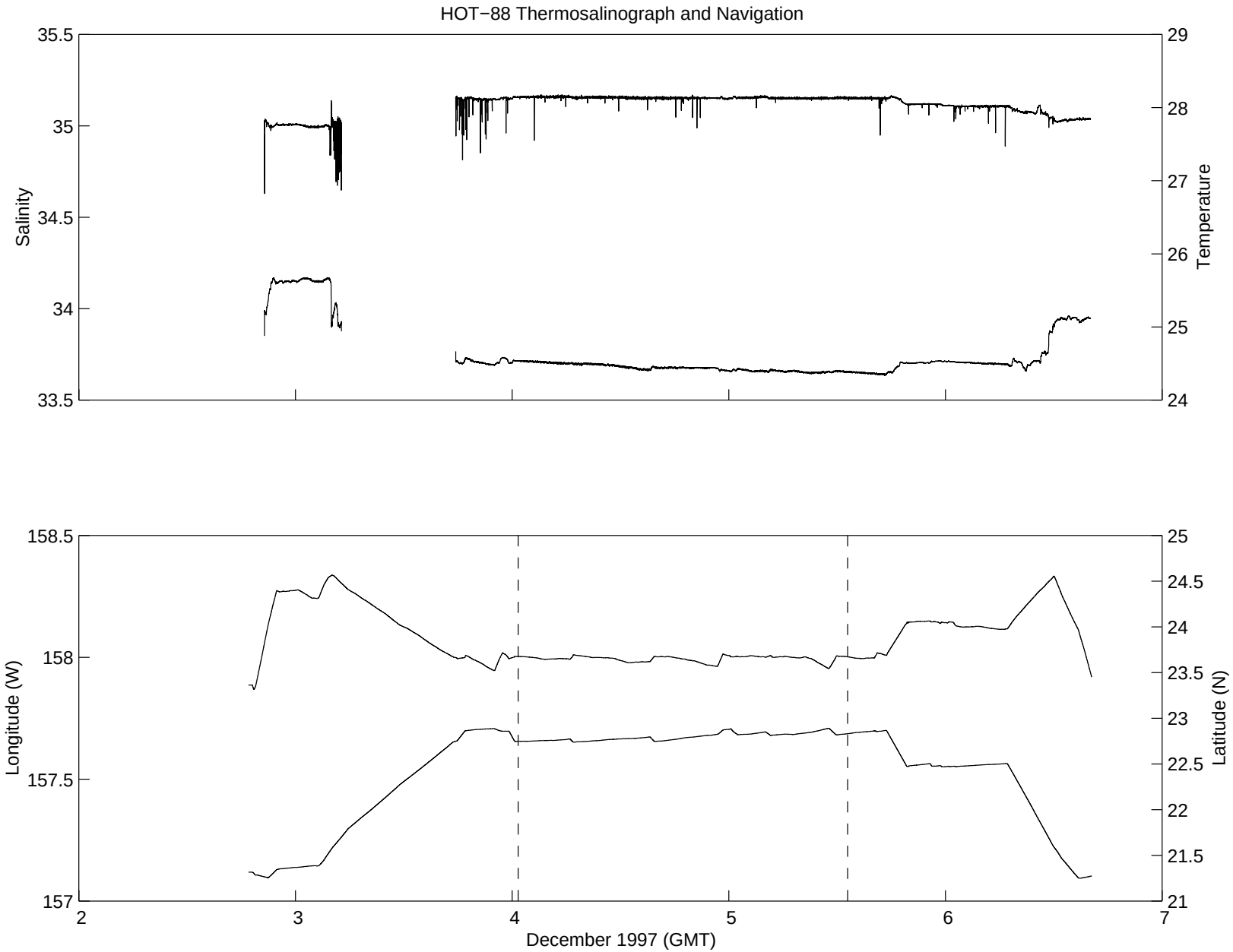

Figure 6.1.16j

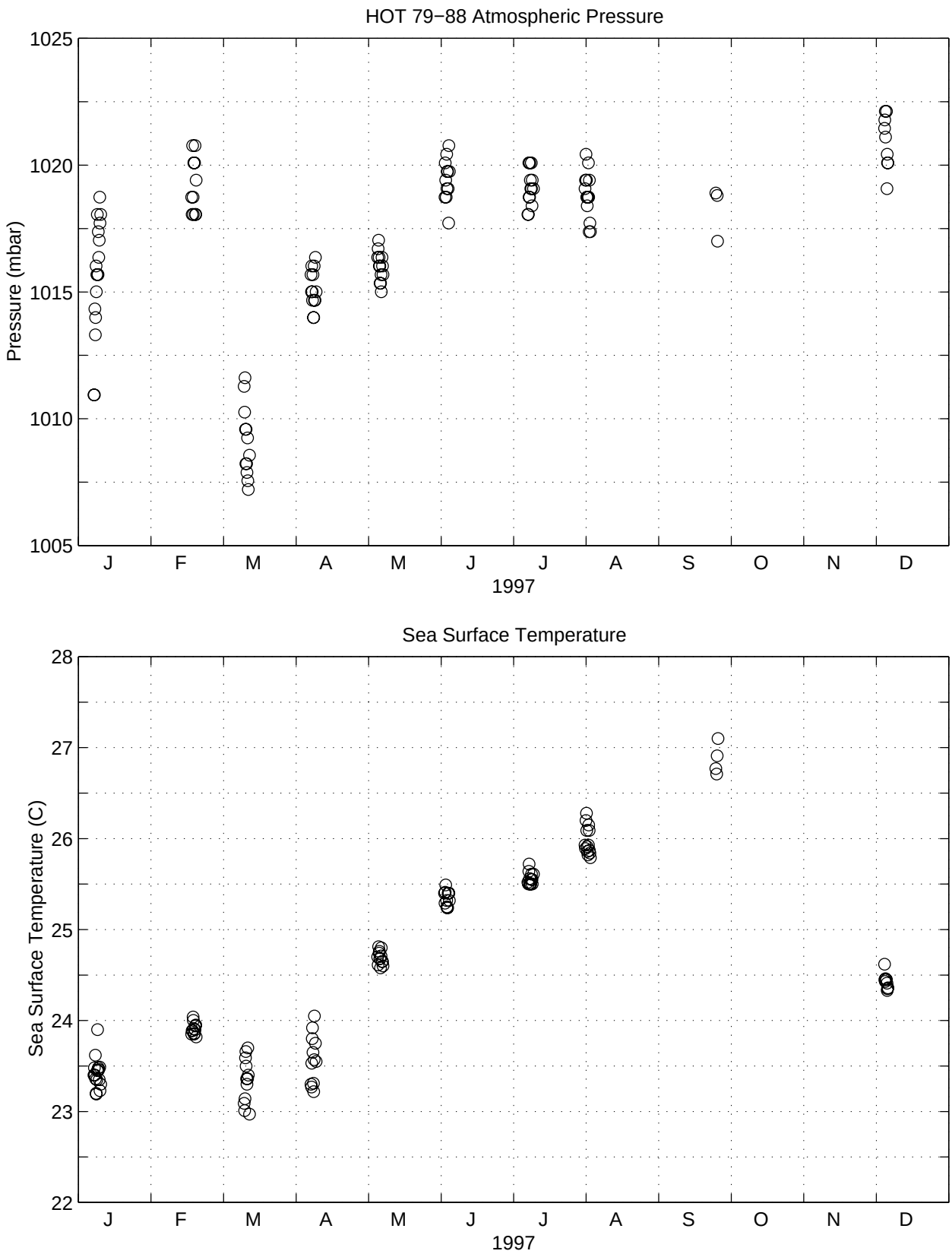
HOT 79−88 Atmospheric Pressure
Pressure (mbar)
1025
1020
1015
1010
1005
J F M A M J J A S O N D
1997
Sea Surface Temperature
Sea Surface Temperature (C)
28
27
26
25
24
23
22
J F M A M J J A S O N D
1997

Figure 6.1.17

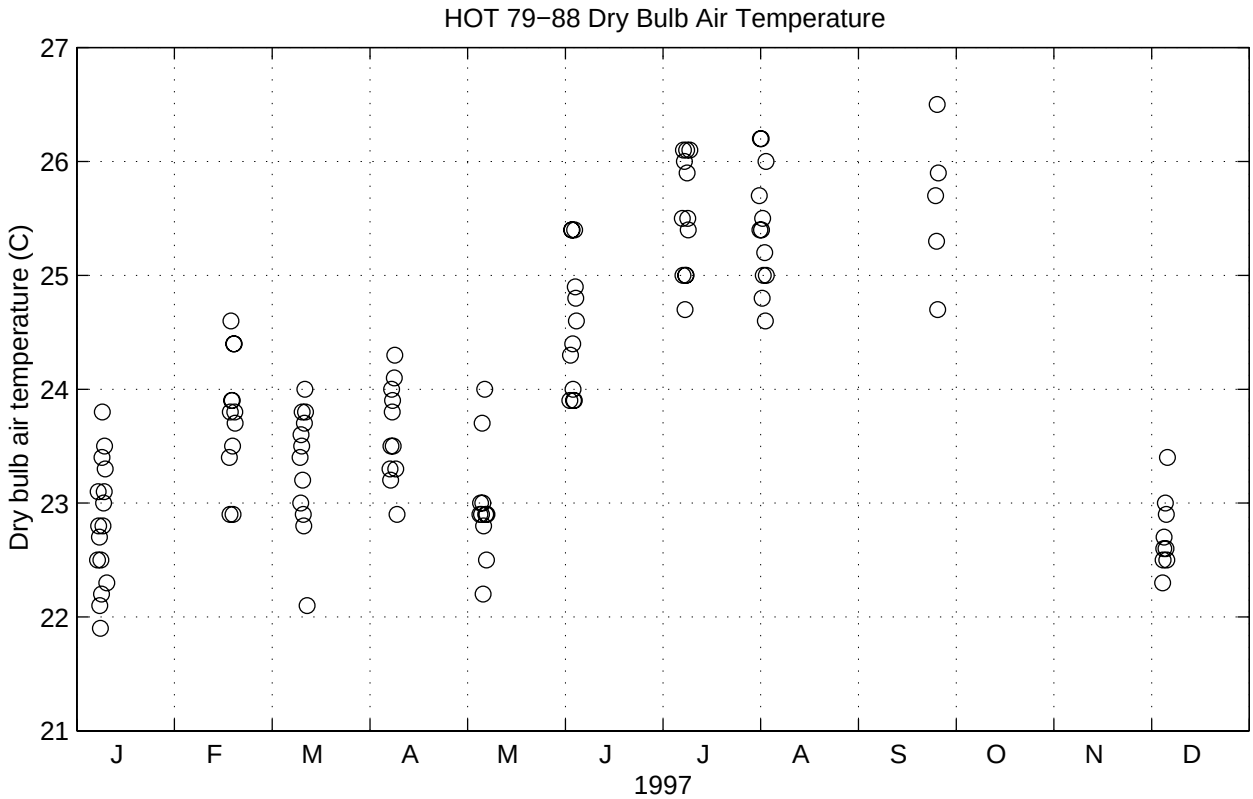
HOT 79−88 Dry Bulb Air Temperature
Dry bulb air temperature (C)
27
26
25
24
23
22
21
J
F
M
A
M
J
J
A
S
O
N
D
1997

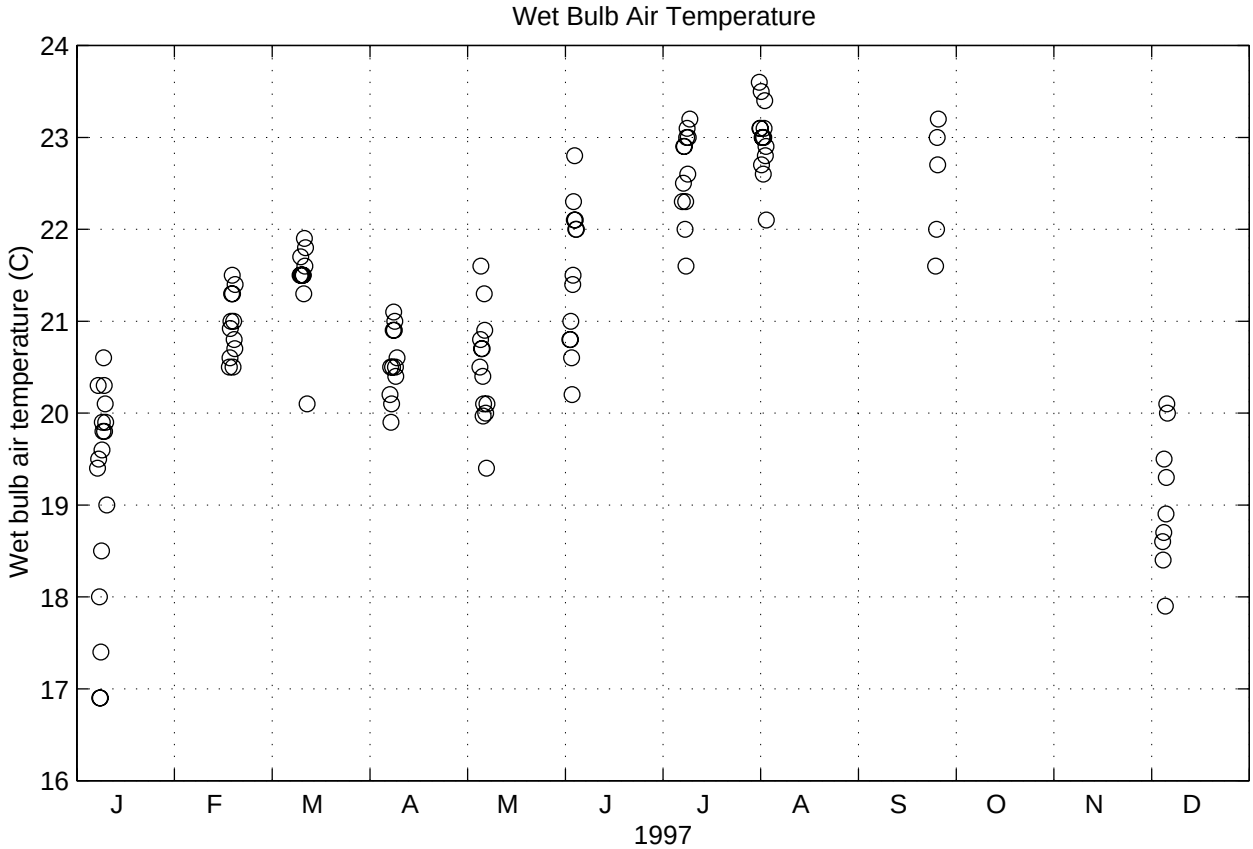
Wet Bulb Air Temperature
Wet bulb air temperature (C)
24
23
22
21
20
19
18
17
16
J
F
M
A
M
J
J
A
S
O
N
D
1997

Figure 6.1.18

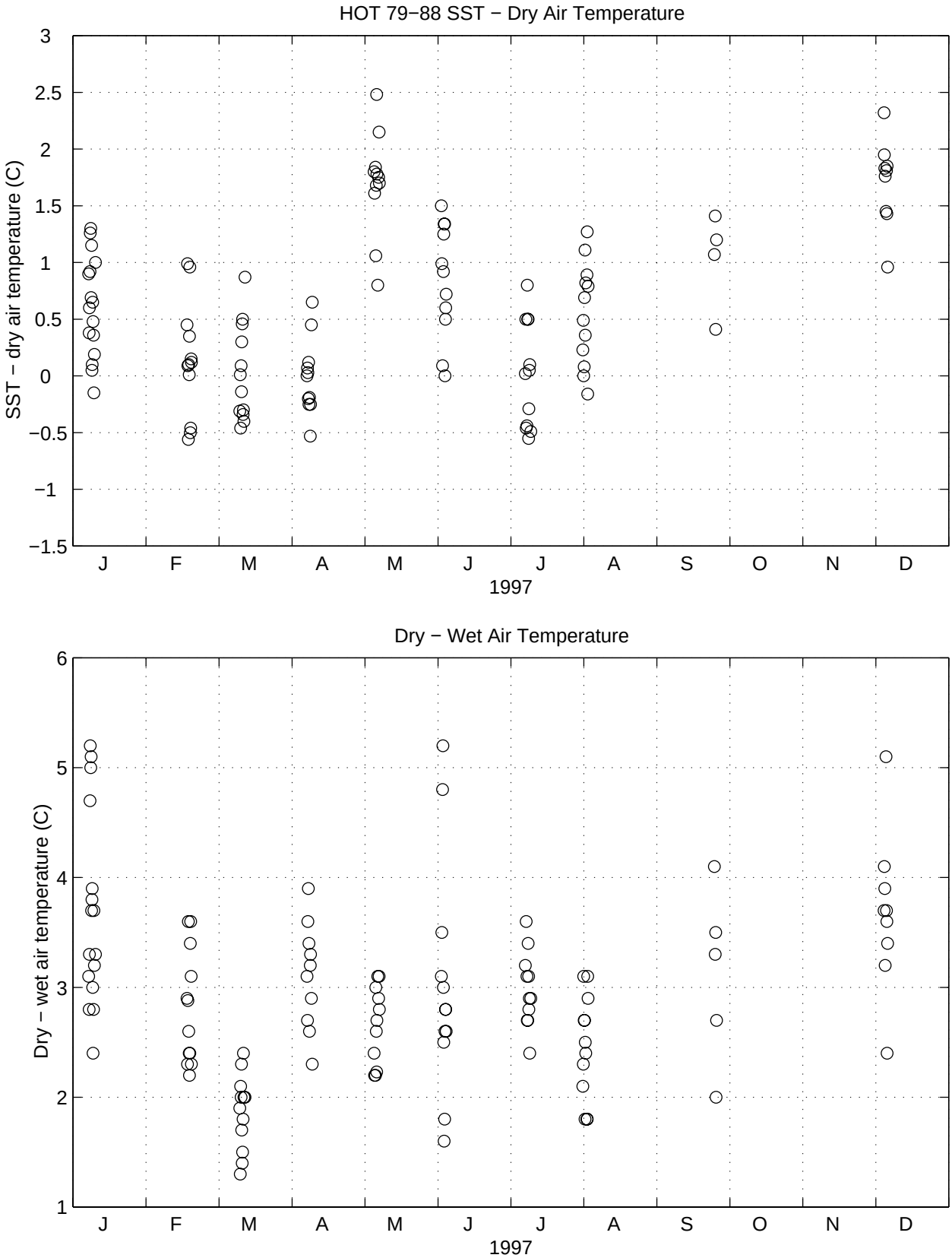
HOT 79−88 SST − Dry Air Temperature
SST − dry air temperature (C)
3
2.5
2
1.5
1
0.5
0
−0.5
−1
−1.5
J F M A M J J A S O N D
1997
Dry − Wet Air Temperature
Dry − wet air temperature (C)
6
5
4
3
2
1
J F M A M J J A S O N D
1997

Figure 6.1.19

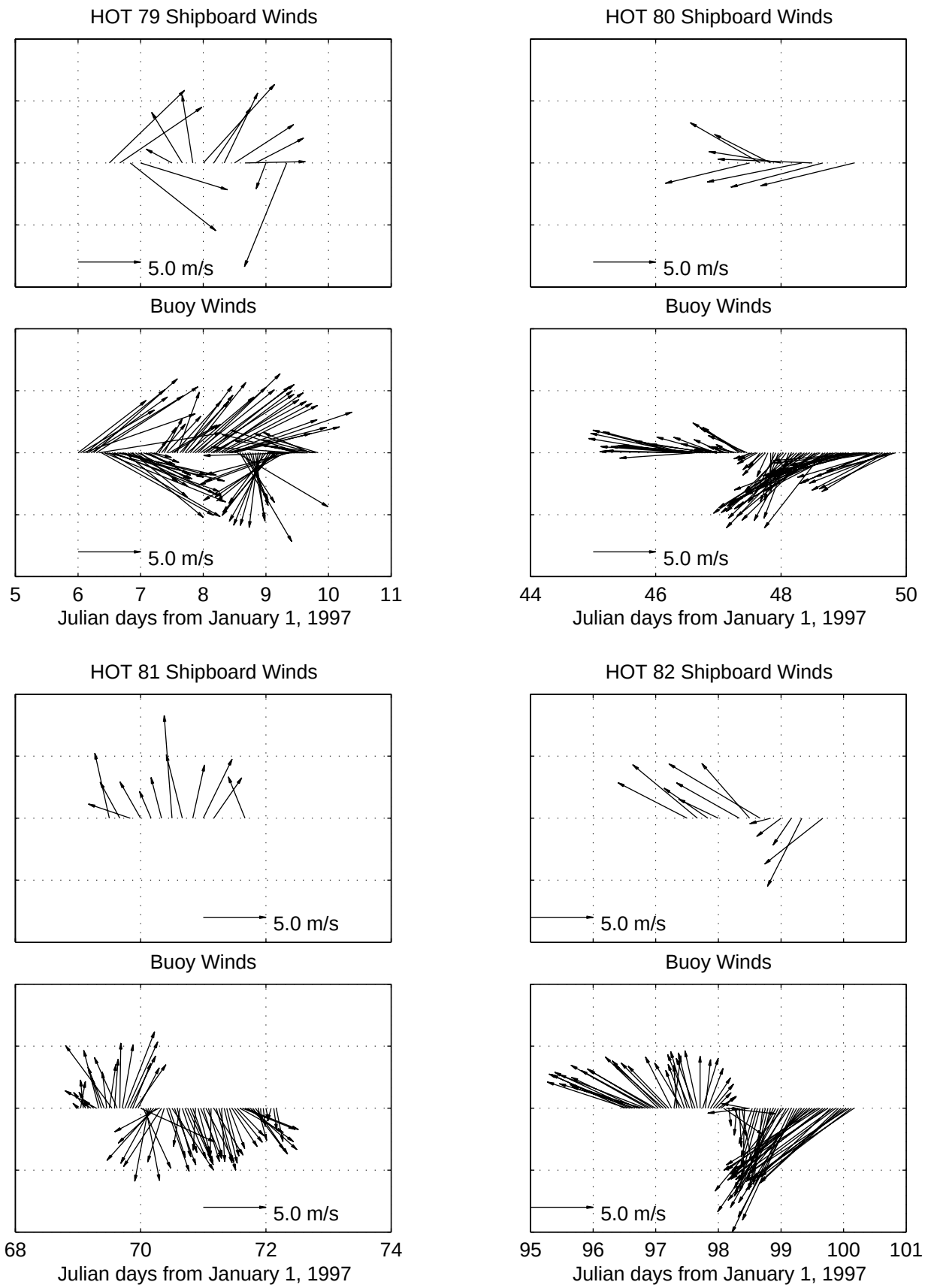

Figure 6.1.20a

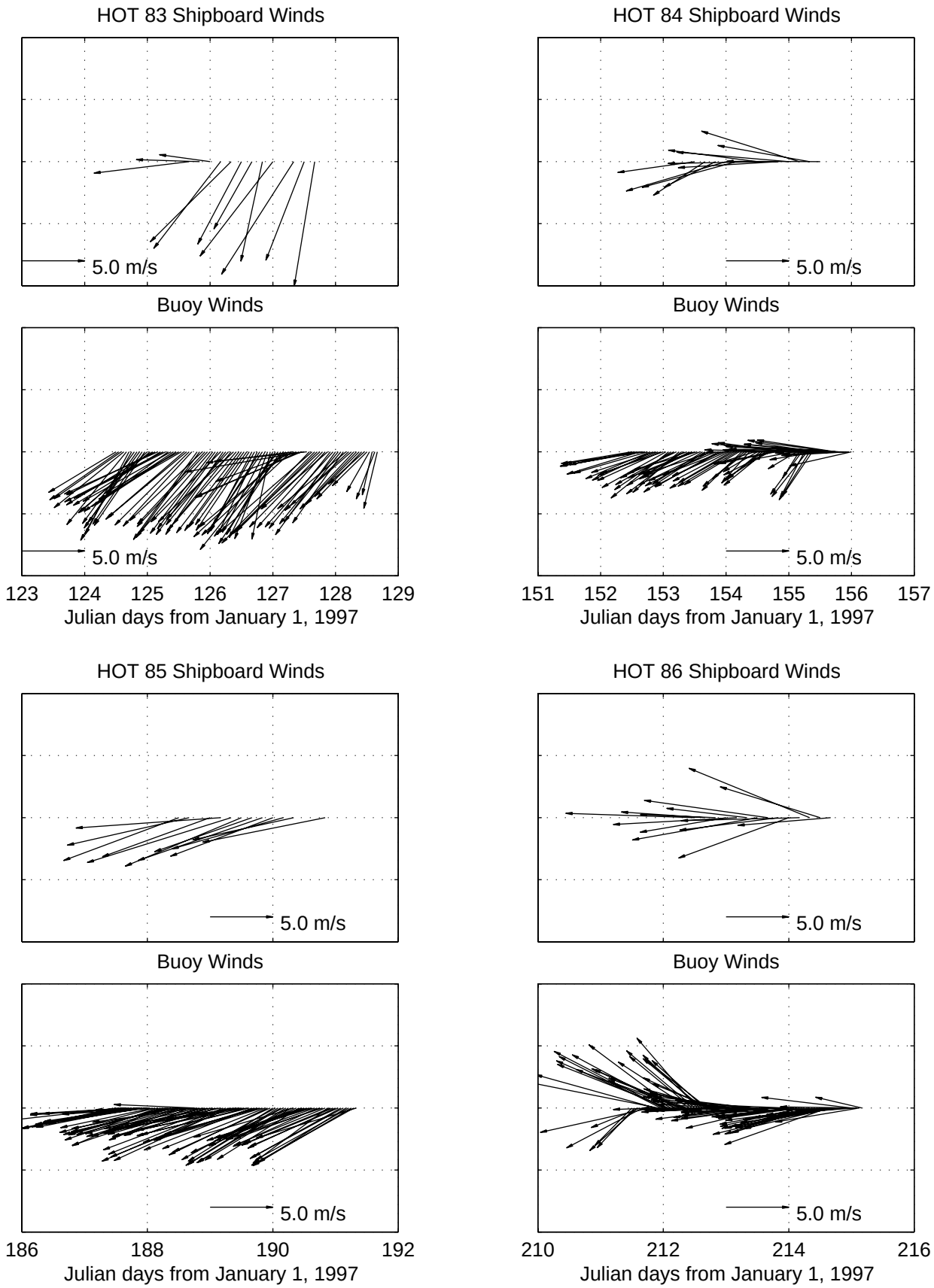

Figure 6.1.20b

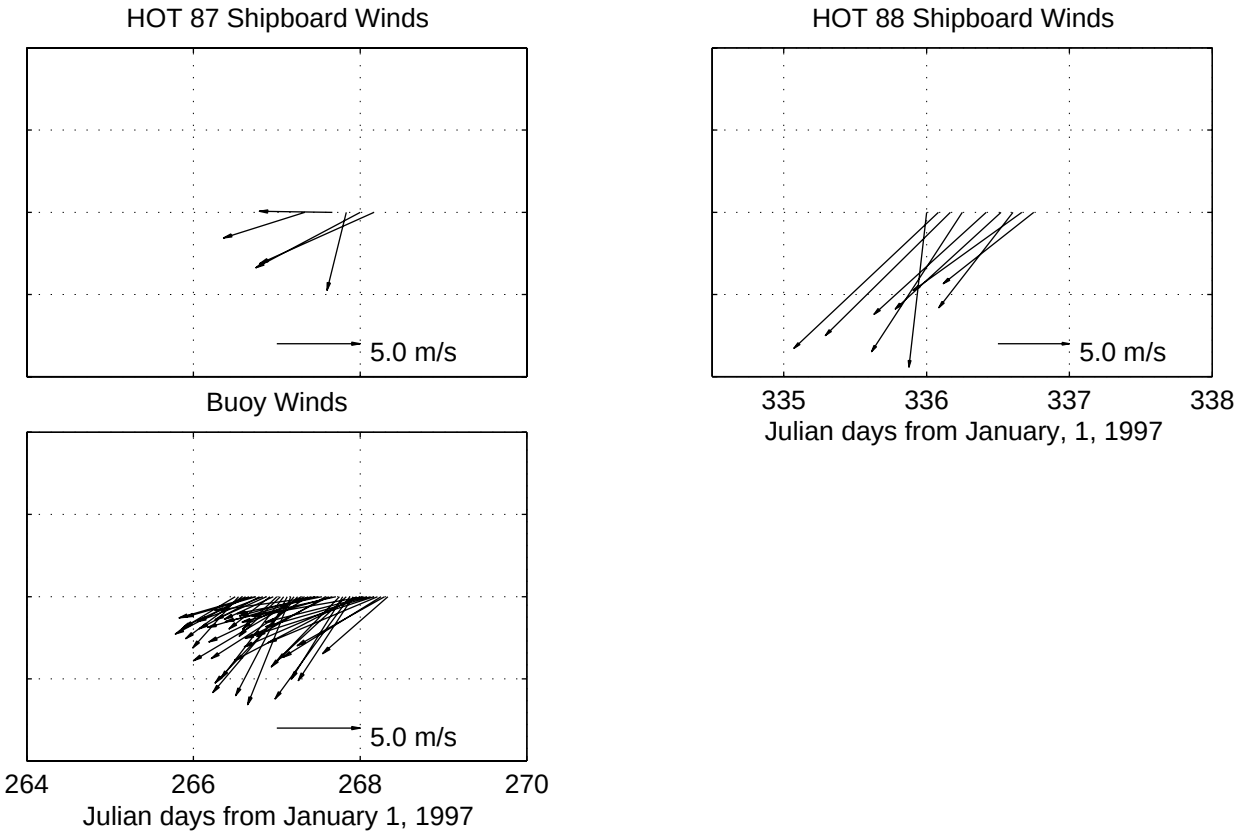

Figure 6.1.20c

6.2. BIOGEOCHEMISTRY

Figure 6.2.1: Contour plot of bottle dissolved oxygen versus pressure for HOT cruises 1-88 from 0-200 m. Location of samples in the water column are indicated by the solid circles.

Figure 6.2.2: [Upper panel] Time series of mean titration alkalinity for HOT cruises 1-88. [Lower panel] Dissolved inorganic carbon for HOT cruises 1-88. Error bars represent standard deviation of pooled samples collected between 0 and 50 dbar.

Figure 6.2.3a: Depth profile from 0-150 m of [nitrate + nitrite] at Station ALOHA for 1997 HOT cruises by the chemiluminescence method.

Figure 6.2.3b: Depth profile from 0-150 m of [nitrate + nitrite] at Station HALE ALOHA for 1997 HOT cruises by the chemiluminescence method.

Figure 6.2.4: Depth profile from 0-250 m of soluble reactive phosphorus at Station ALOHA for 1997 HOT cruises by the magnesium induced coprecipitation (MAGIC) method.

Figure 6.2.5: Contour plot from 0-1000 m of dissolved organic carbon at Station ALOHA for HOT cruises 49-88.

Figure 6.2.6: Contour plot from 0-1000 m of dissolved organic nitrogen at Station ALOHA for HOT cruises 1-88.

Figure 6.2.7: Contour plot from 0-1000 m of dissolved organic phosphorus at Station ALOHA for HOT cruises 1-88.

Figure 6.2.8: [Upper panel] Mean concentrations of particulate carbon at Station ALOHA for HOT cruises 1-88 from 0-50 dbar. [Middle panel] Mean concentrations of particulate nitrogen at Station ALOHA for HOT cruises 1-88 from 0-50. [Lower panel] Mean concentrations of particulate phosphorus at Station ALOHA for HOT cruises 1-88 from 0-50 dbar. Error bars represent standard deviation of pooled samples collected between 0 and 50 dbar.

Figure 6.2.9: Contour plot from 0-200 m of fluorometric chlorophyll a concentrations at Station ALOHA for HOT cruises 1-88.

Figure 6.2.10: Contour plot from 0-500 m of adenosine 5’ triphosphate concentrations at Station ALOHA for HOT cruises 1-88.

Figure 6.2.11: [Upper panel] Integrated (0-200 m) primary production rates from 1988-1997. Solid line represents the average production (477 mg C m^{-2} d^{-1}), dashed line is one standard deviation (122 mg C m^{-2} d^{-1}). [Lower panel] 3-point running mean of integrated primary production rates.

Figure 6.2.12: [Upper panel] Carbon flux at 150 m measured on all HOT cruises from 1988-1997. [Middle panel] Nitrogen flux at 150 m measured on all HOT cruises from 1988-1997.

[Lower panel] Phosphorus flux at 150 m measured on all HOT cruises from 1988-1997. Error bars represent the standard deviation of replicate determinations.

Figure 6.2.13: Depth profile of heterotrophic bacteria and *Prochlorococcus* numbers measured by flow cytometry at Station ALOHA for 1997 .

Figure 6.2.14: Carbon biomass estimates of mesozooplankton divided by size class for samples collected on HOT cruises from 1994-1997.

Figure 6.2.15: Carbon biomass estimates of mesozooplankton from mid-day and mid-night samples collected on HOT cruises from 1994-1997.

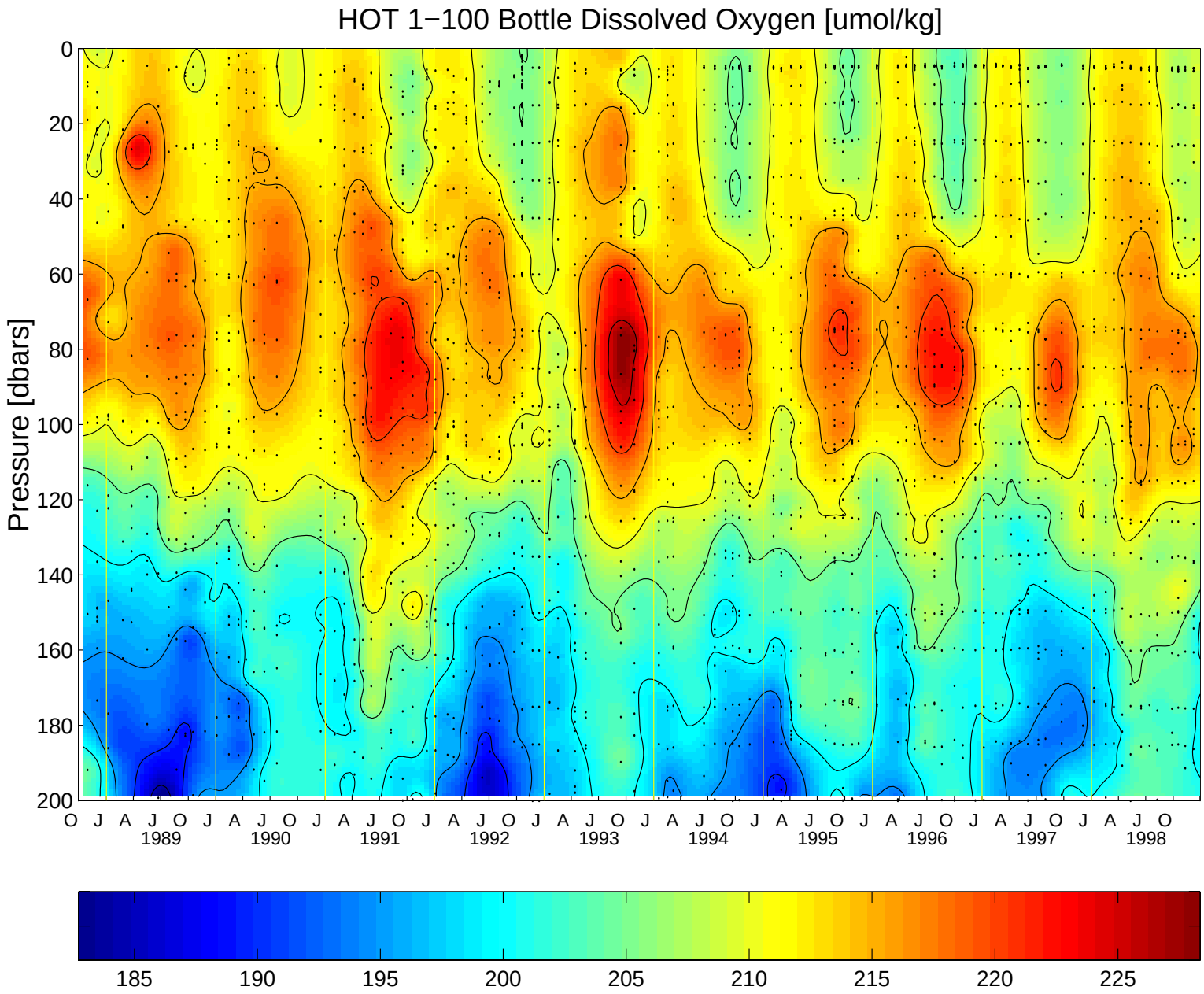
HOT 1−100 Bottle Dissolved Oxygen [umol/kg]
Pressure [dbars]
0
20
40
60
80
100
120
140
160
180
200
O J A J O J A J O J A J O J A J O J A J O J A J O J A J O J A J O J A J O J A J O
1989
1990
1991
1992
1993
1994
1995
1996
1997
1998
185
190
195
200
205
210
215
220
225

Figure 6.2.1

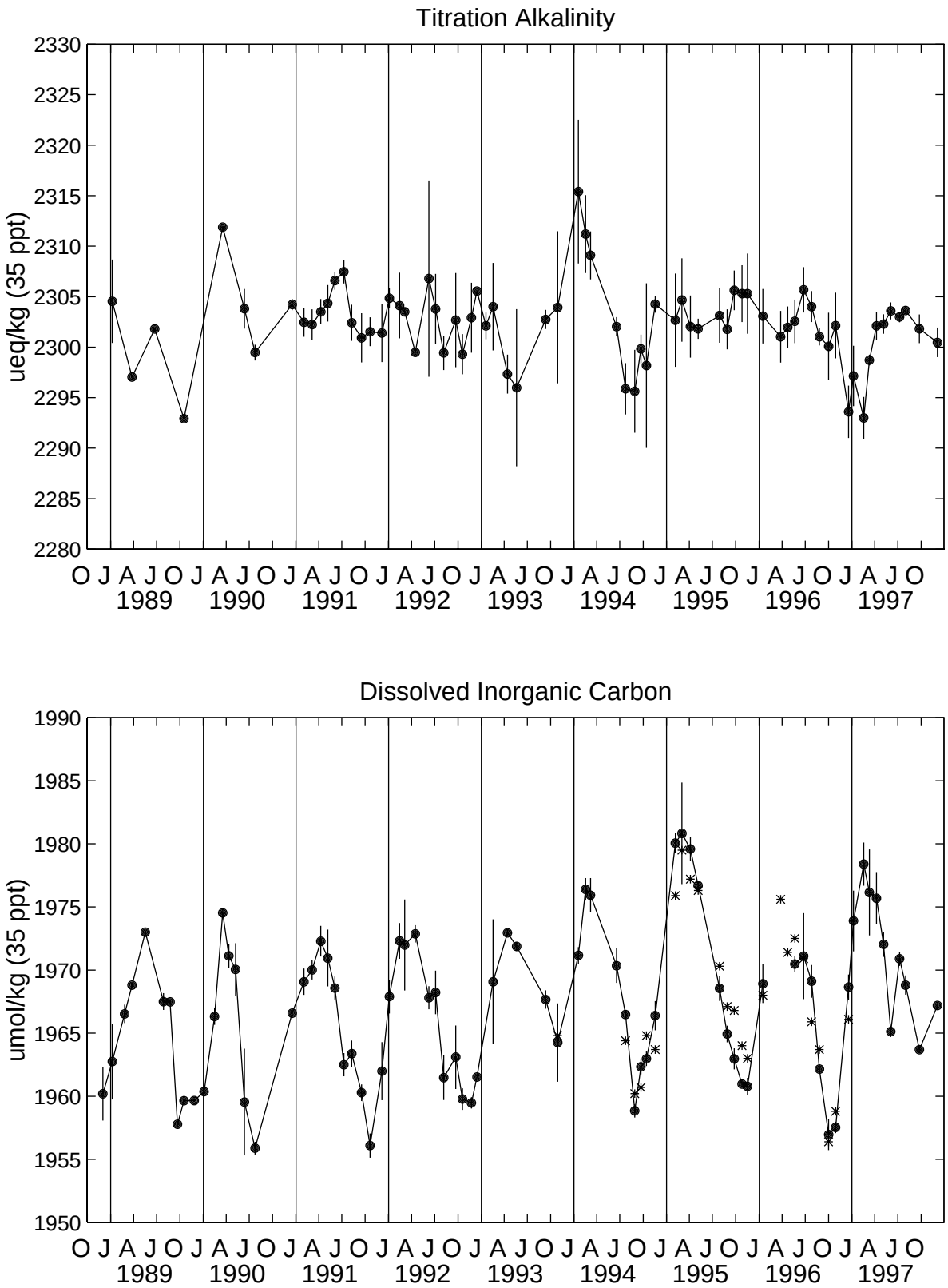
Titration Alkalinity
ueq/kg (35 ppt)
2330
2325
2320
2315
2310
2305
2300
2295
2290
2285
2280
O J A J O J A J O J A J O J A J O J A J O J A J O J A J O J A J O J A J O
1989 1990 1991 1992 1993 1994 1995 1996 1997
Dissolved Inorganic Carbon
umol/kg (35 ppt)
1990
1985
1980
1975
1970
1965
1960
1955
1950
O J A J O J A J O J A J O J A J O J A J O J A J O J A J O J A J O J A J O
1989 1990 1991 1992 1993 1994 1995 1996 1997

Figure 6.2.2

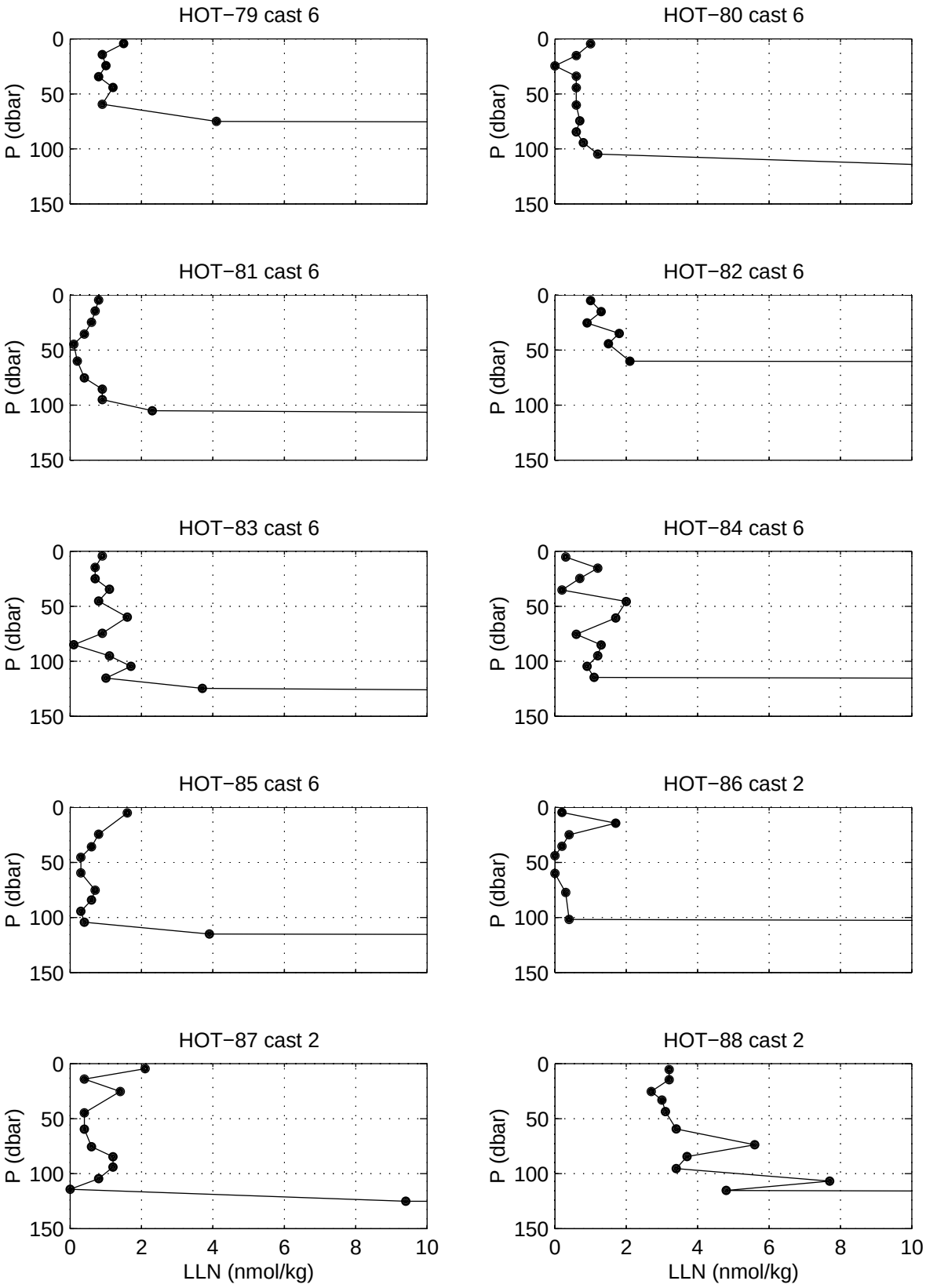
HOT−79 cast 6
HOT−80 cast 6
HOT−81 cast 6
HOT−82 cast 6
HOT−83 cast 6
HOT−84 cast 6
HOT−85 cast 6
HOT−86 cast 2
HOT−87 cast 2
HOT−88 cast 2
P (dbar)
0
50
100
150
LLN (nmol/kg)
0
2
4
6
8
10

Figure 6.2.3

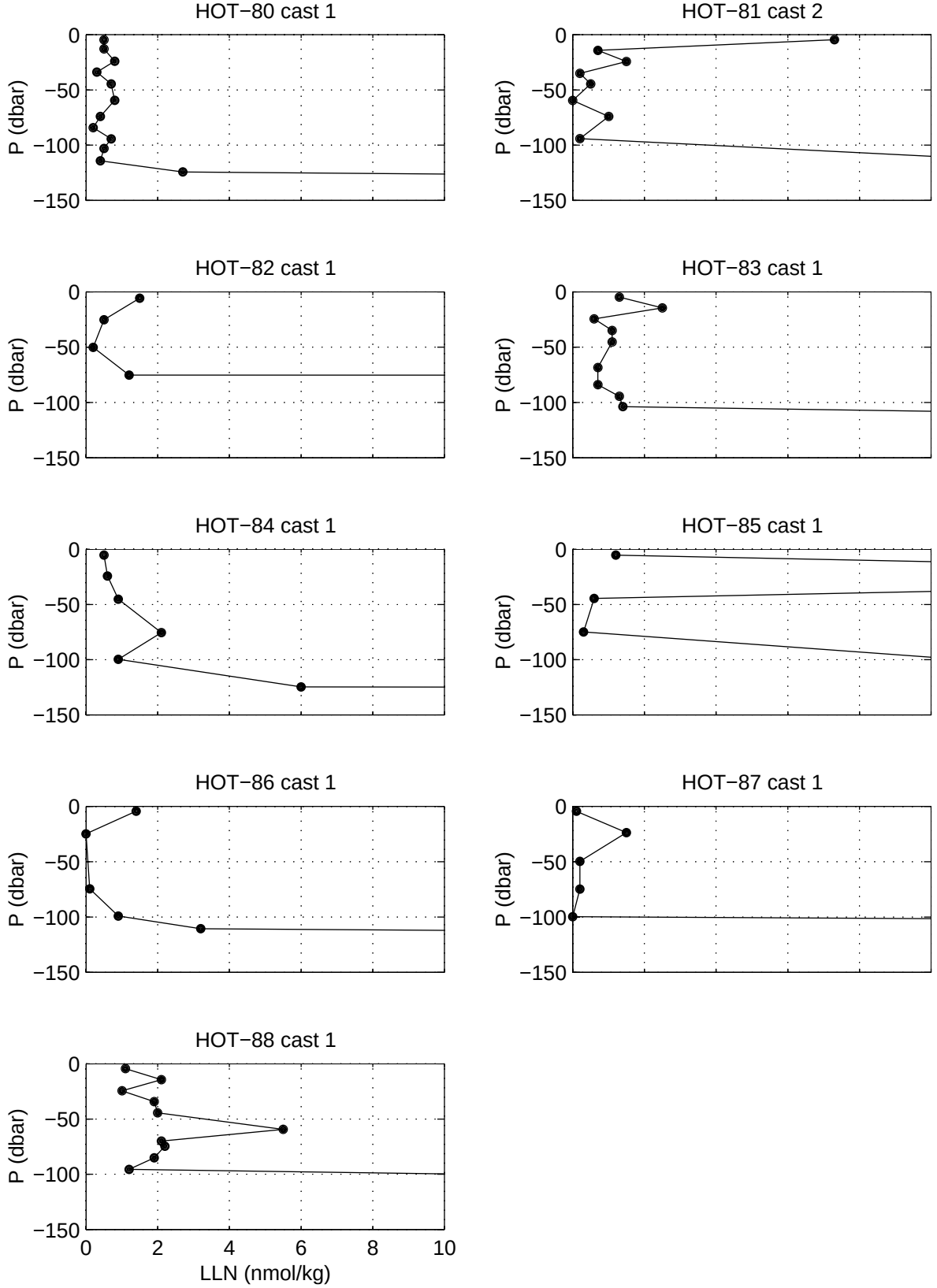

Figure 6.2.3 continued

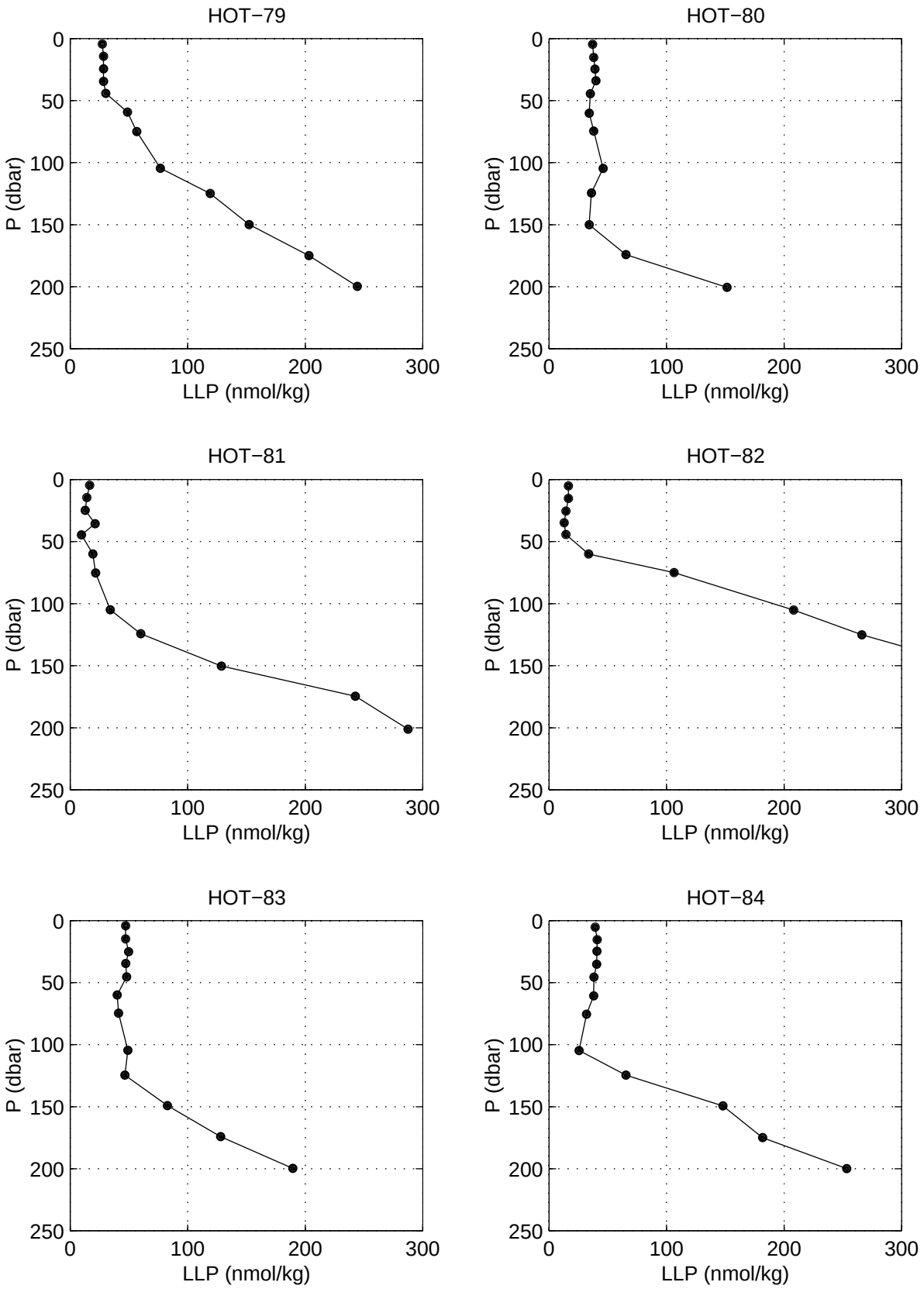
HOT−79
HOT−80
HOT−81
HOT−82
HOT−83
HOT−84
P (dbar)
LLP (nmol/kg)
0
50
100
150
200
250
0
100
200
300

Figure 6.2.4

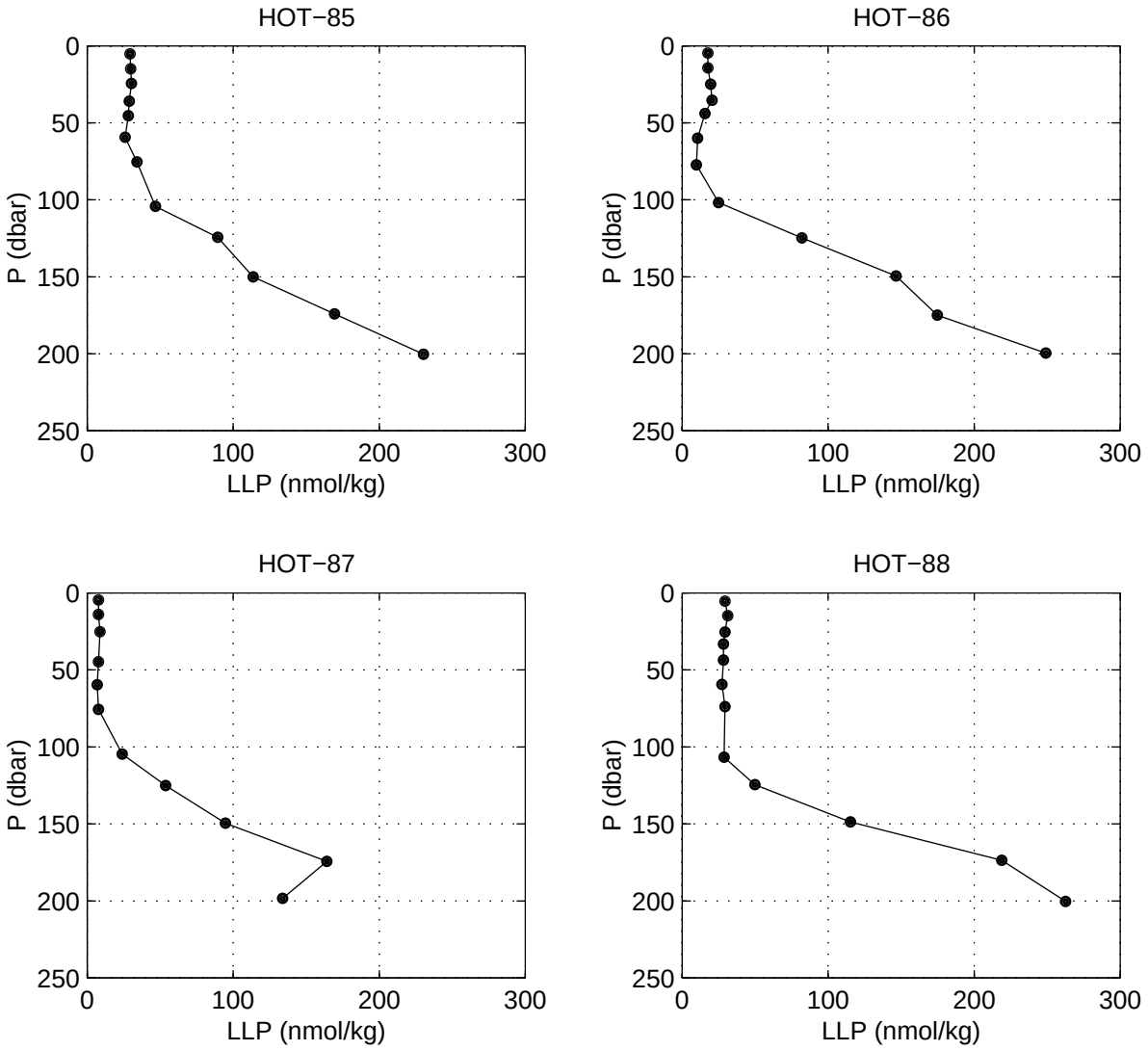

Figure 6.2.4 continued

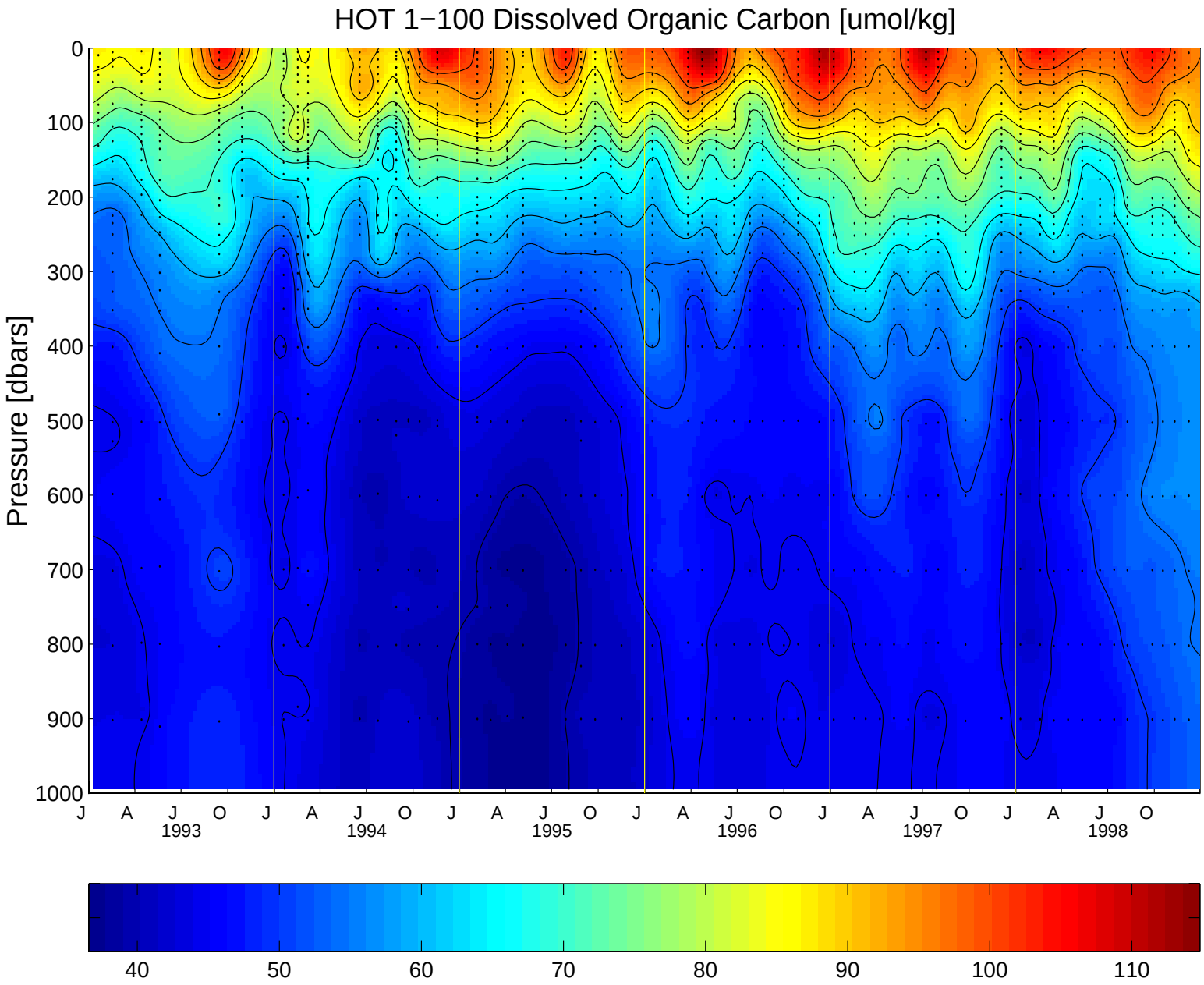
HOT 1−100 Dissolved Organic Carbon [umol/kg]
Pressure [dbars]
0
100
200
300
400
500
600
700
800
900
1000
J A J O J A J O J A J O J A J O J A J O J A J O
1993
1994
1995
1996
1997
1998
40
50
60
70
80
90
100
110

Figure 6.2.5

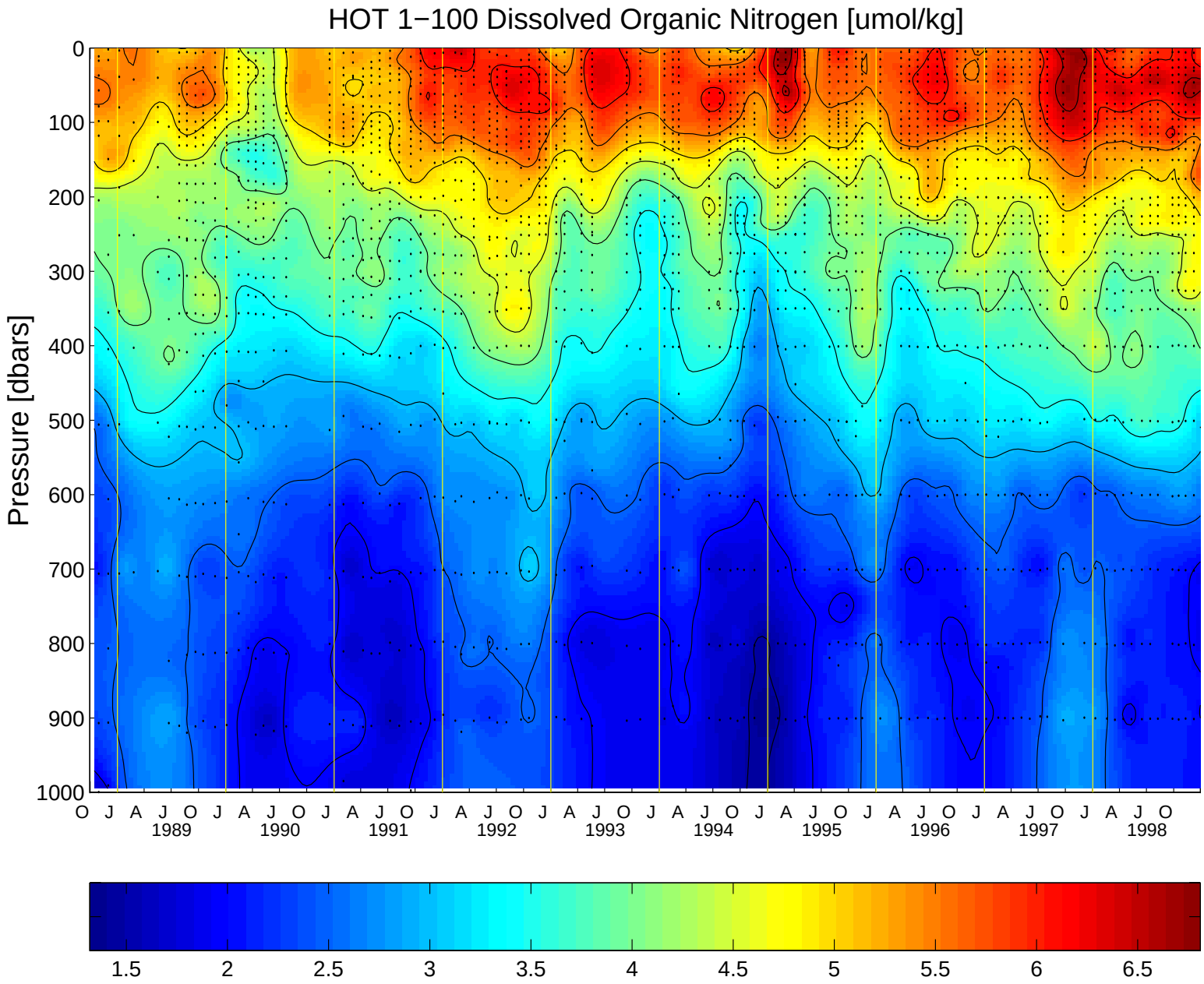
HOT 1−100 Dissolved Organic Nitrogen [umol/kg]
Pressure [dbars]
0
100
200
300
400
500
600
700
800
900
1000
O J A J O J A J O J A J O J A J O J A J O J A J O J A J O J A J O J A J O J A J O
1989
1990
1991
1992
1993
1994
1995
1996
1997
1998
1.5
2
2.5
3
3.5
4
4.5
5
5.5
6
6.5

Figure 6.2.6

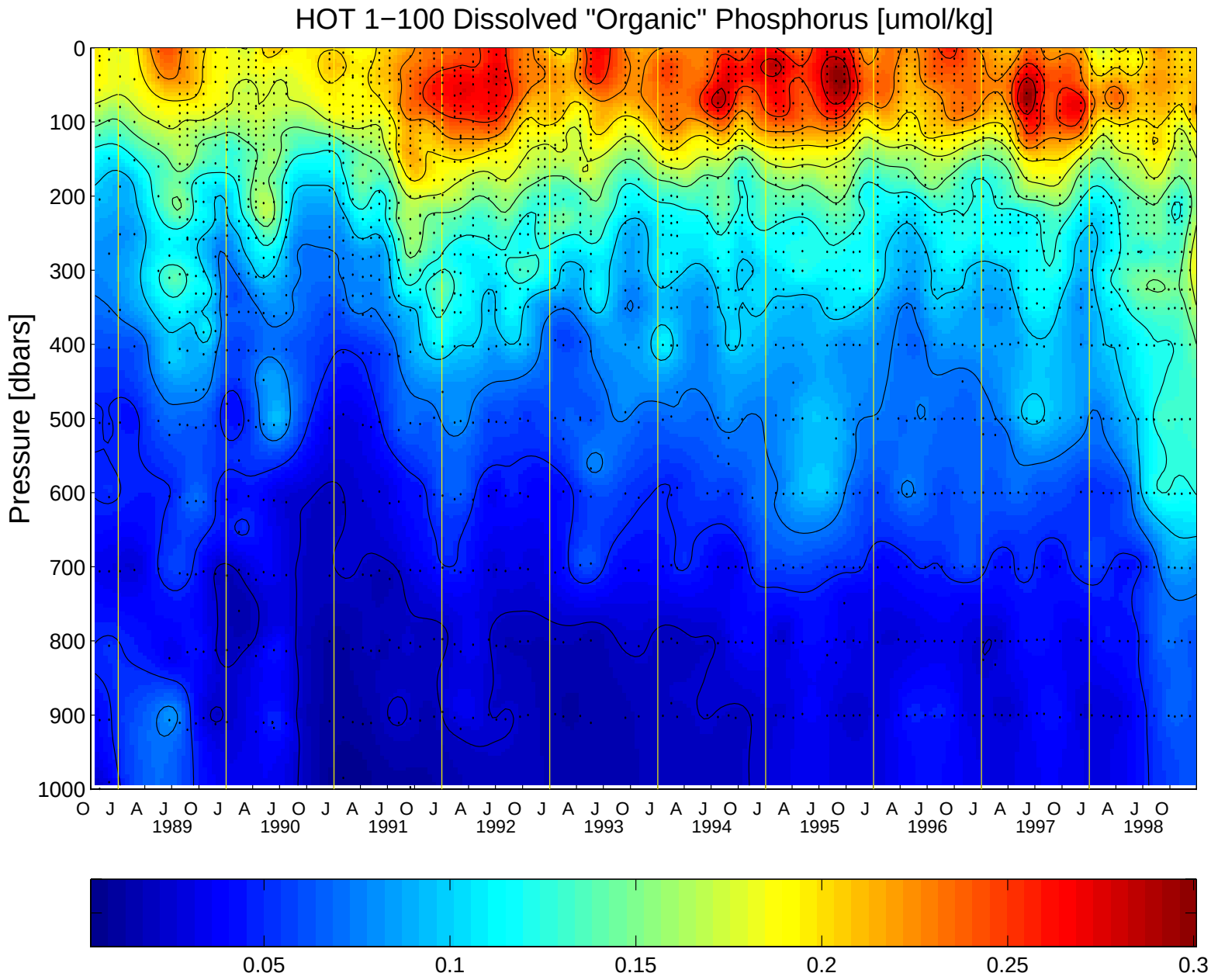
HOT 1−100 Dissolved "Organic" Phosphorus [umol/kg]
Pressure [dbars]
0
100
200
300
400
500
600
700
800
900
1000
O J A J O J A J O J A J O J A J O J A J O J A J O J A J O J A J O J A J O J A J O J A J O
1989
1990
1991
1992
1993
1994
1995
1996
1997
1998
0.05
0.1
0.15
0.2
0.25
0.3

Figure 6.2.7

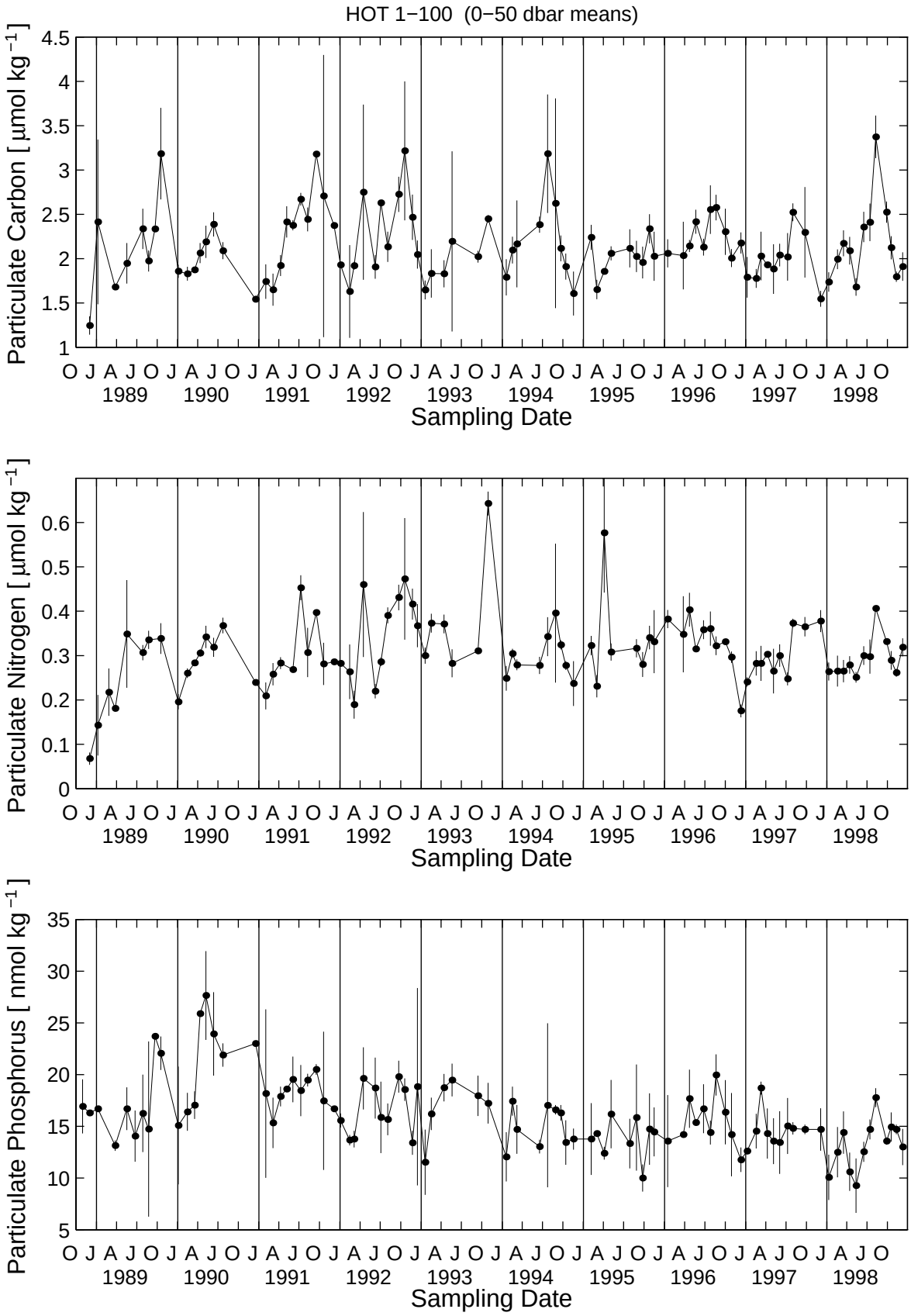
HOT 1−100 (0−50 dbar means)
Particulate Carbon [µmol kg −1]
Sampling Date
Particulate Nitrogen [µmol kg −1]
Sampling Date
Particulate Phosphorus [nmol kg −1]
Sampling Date
O J A J O J A J O J A J O J A J O J A J O J A J O J A J O J A J O J A J O J A J O J A J O J A J O
1989 1990 1991 1992 1993 1994 1995 1996 1997 1998

Figure 6.2.8

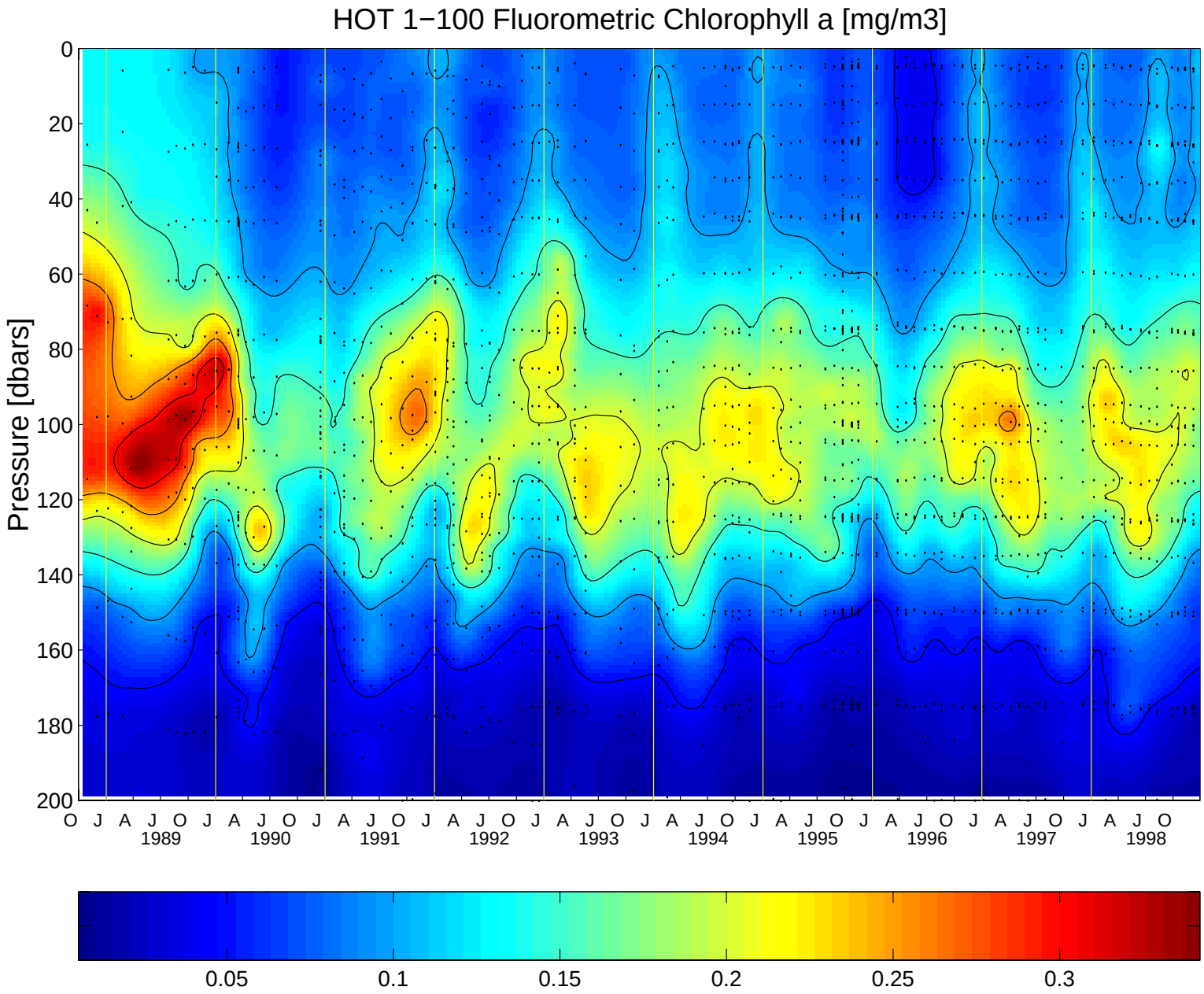
HOT 1−100 Fluorometric Chlorophyll a [mg/m3]
Pressure [dbars]
0
20
40
60
80
100
120
140
160
180
200
O J A J O J A J O J A J O J A J O J A J O J A J O J A J O J A J O J A J O J A J O
1989
1990
1991
1992
1993
1994
1995
1996
1997
1998
0.05
0.1
0.15
0.2
0.25
0.3

Figure 6.2.9

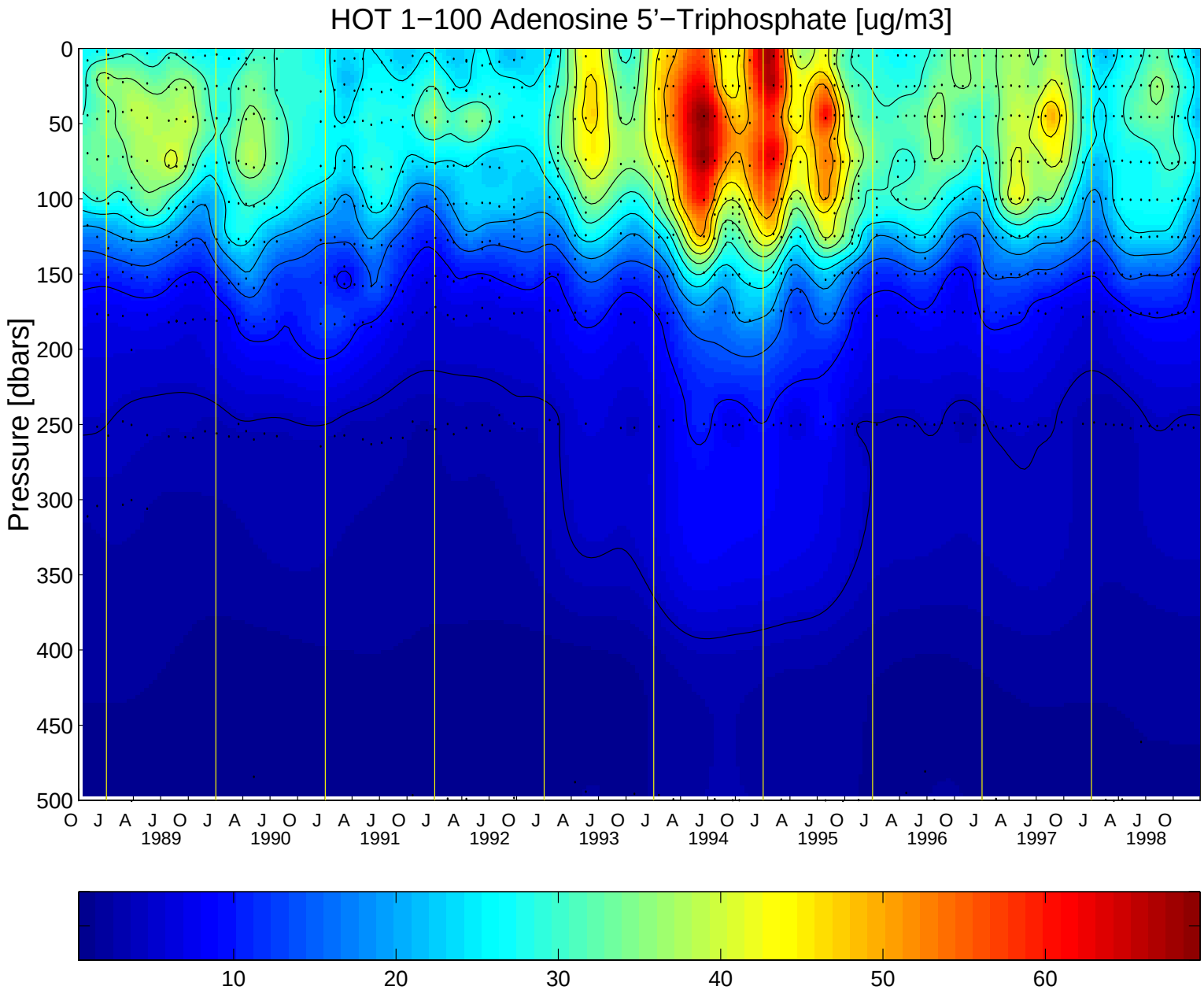
HOT 1−100 Adenosine 5'−Triphosphate [ug/m3]
Pressure [dbars]
0
50
100
150
200
250
300
350
400
450
500
O J A J O J A J O J A J O J A J O J A J O J A J O J A J O J A J O J A J O J A J O
1989
1990
1991
1992
1993
1994
1995
1996
1997
1998
10
20
30
40
50
60

Figure 6.2.10

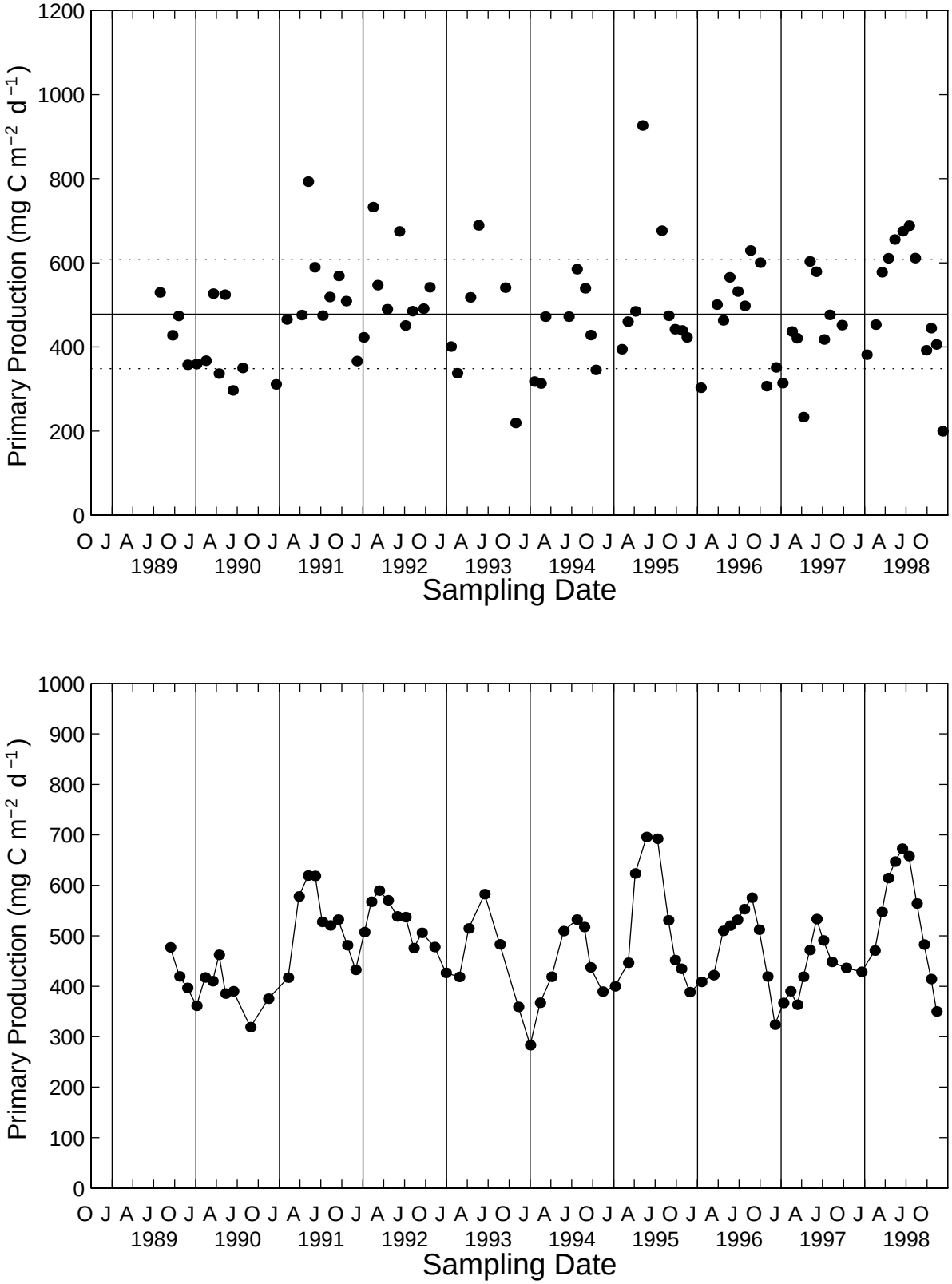
Primary Production (mg C m^{-2} d^{-1})
Sampling Date
O J A J O J A J O J A J O J A J O J A J O J A J O J A J O J A J O J A J O J A J O J A J O
1989
1990
1991
1992
1993
1994
1995
1996
1997
1998

Figure 6.2.11

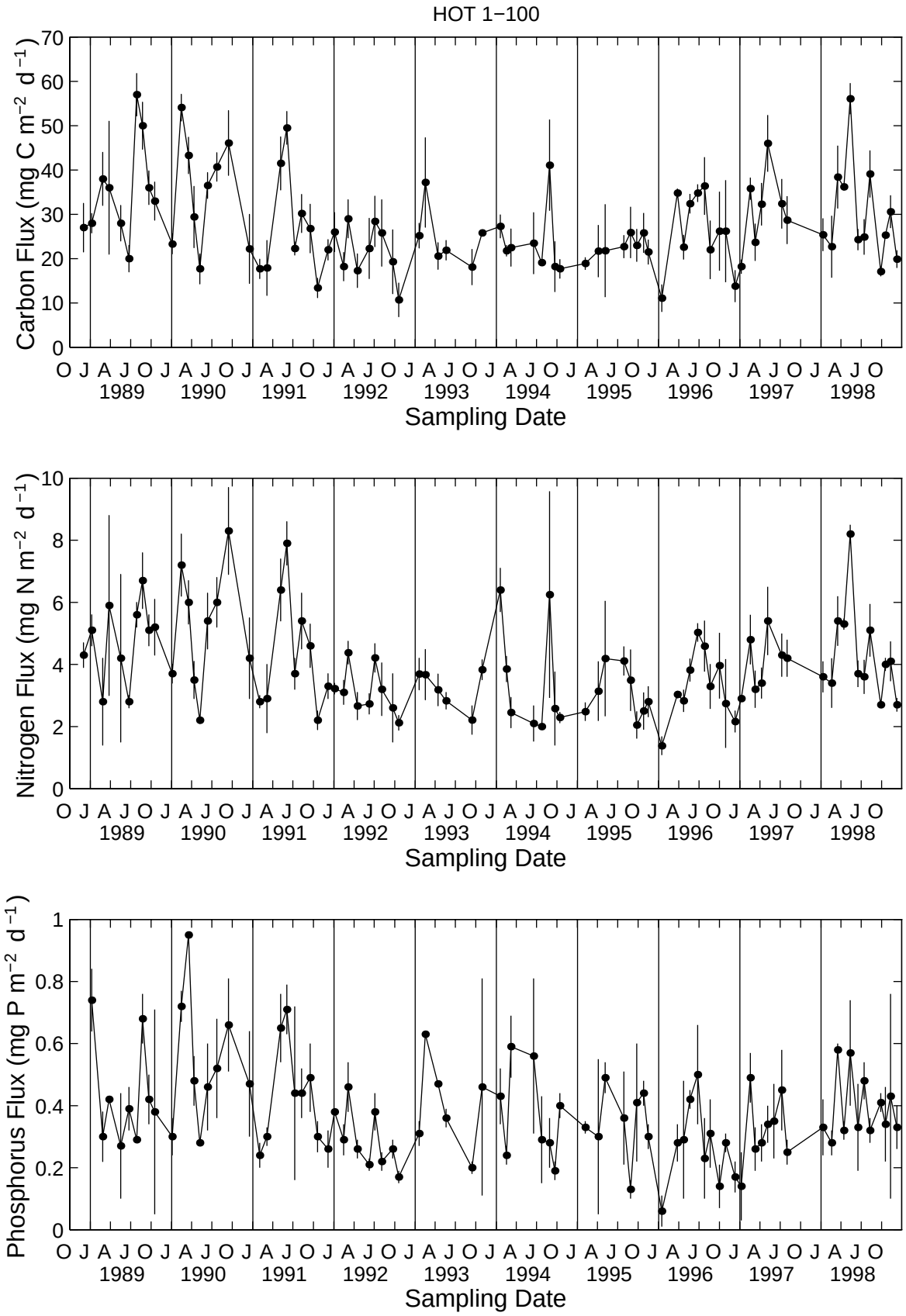
HOT 1−100
Carbon Flux (mg C m−2 d−1)
Nitrogen Flux (mg N m−2 d−1)
Phosphorus Flux (mg P m−2 d−1)
O J A J O J A J O J A J O J A J O J A J O J A J O J A J O J A J O J A J O J A J O J A J O J A J O
1989 1990 1991 1992 1993 1994 1995 1996 1997 1998
Sampling Date

Figure 6.2.12

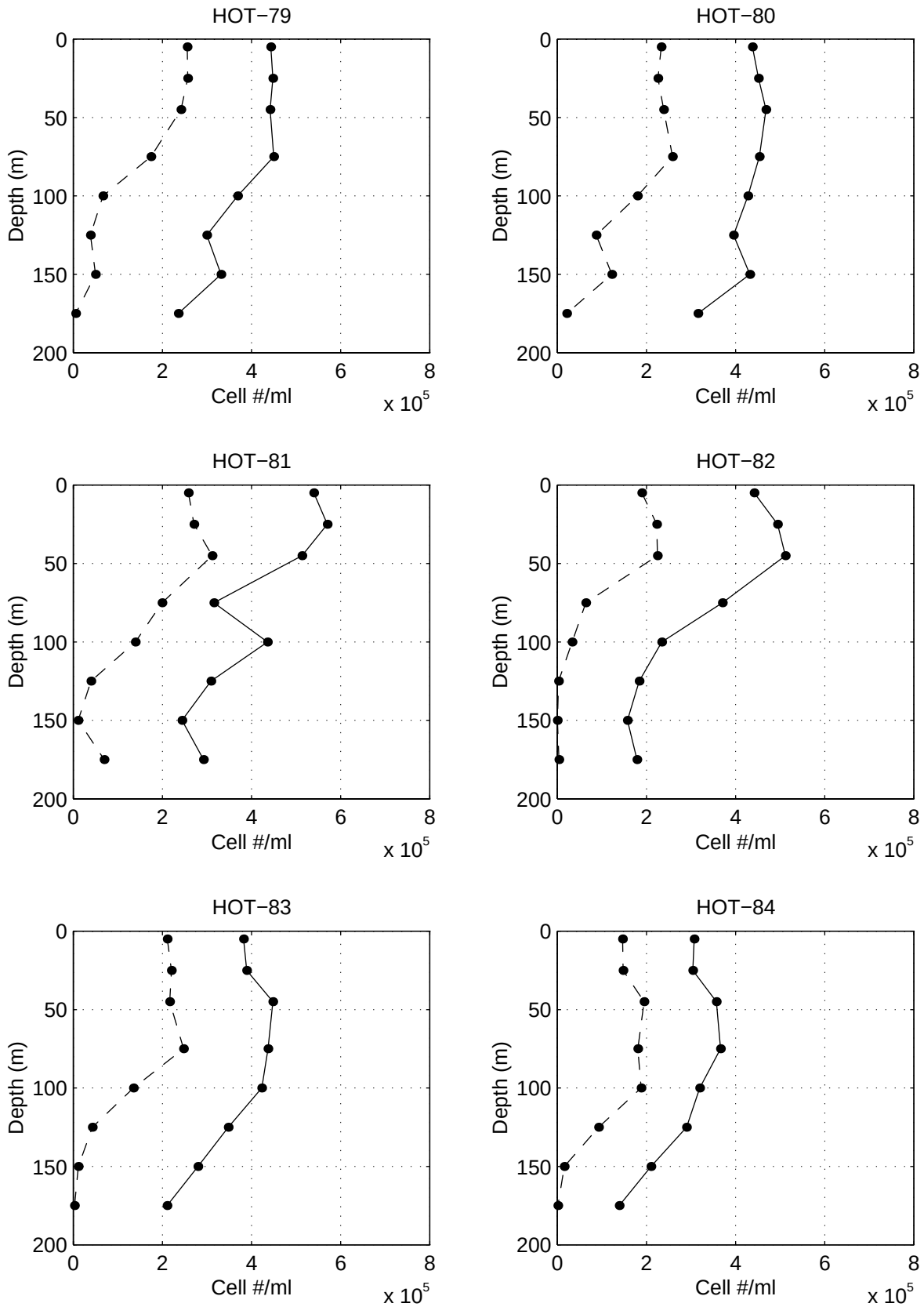
HOT−79
HOT−80
HOT−81
HOT−82
HOT−83
HOT−84
Depth (m)
Cell #/ml
x 10^5
0
50
100
150
200
0
2
4
6
8

Figure 6.2.13

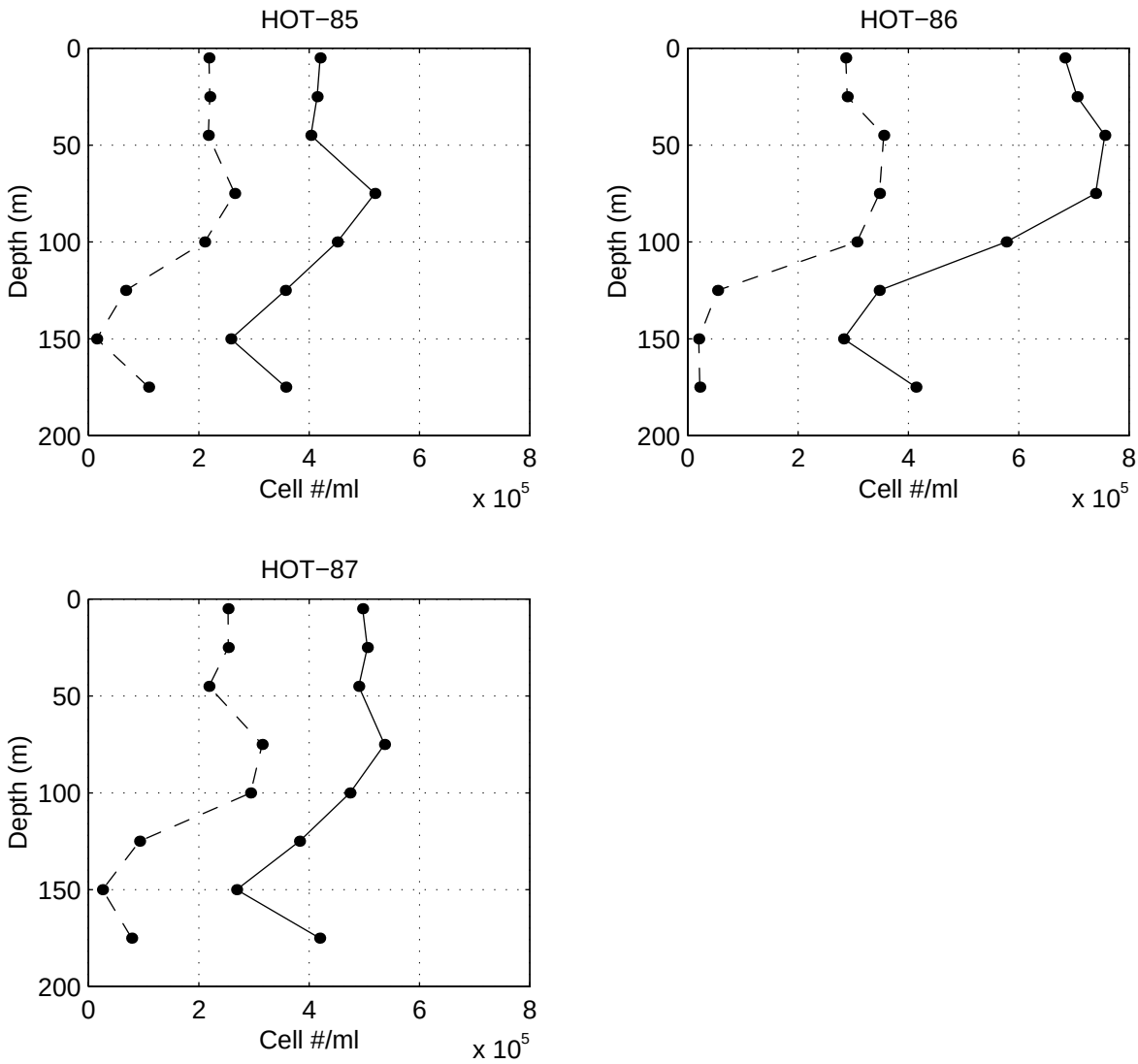

Figure 6.2.13 continued

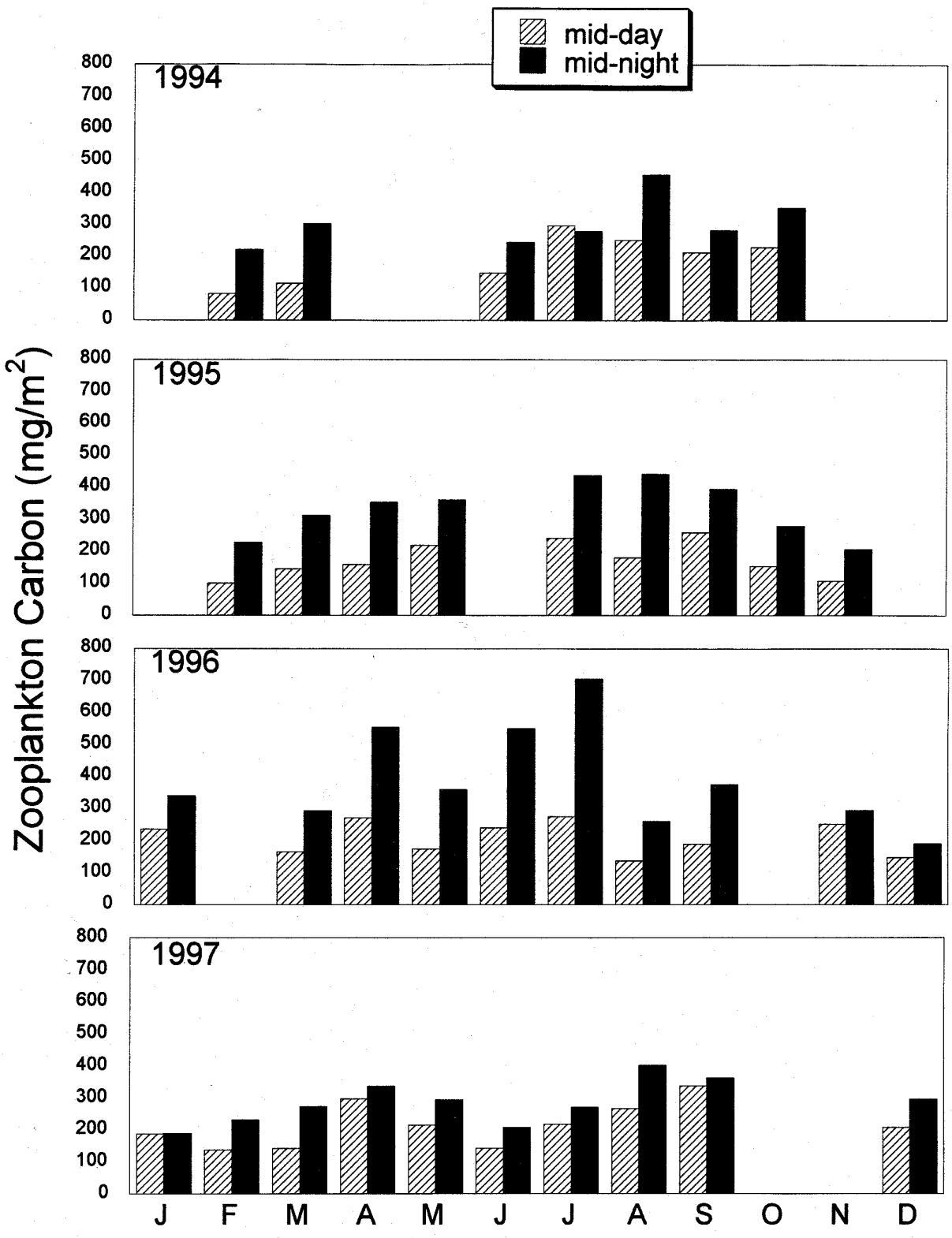
mid-day
mid-night
1994
1995
1996
1997
Zooplankton Carbon (mg/m2)
0
100
200
300
400
500
600
700
800
J
F
M
A
M
J
J
A
S
O
N
D

Figure 6.2.14

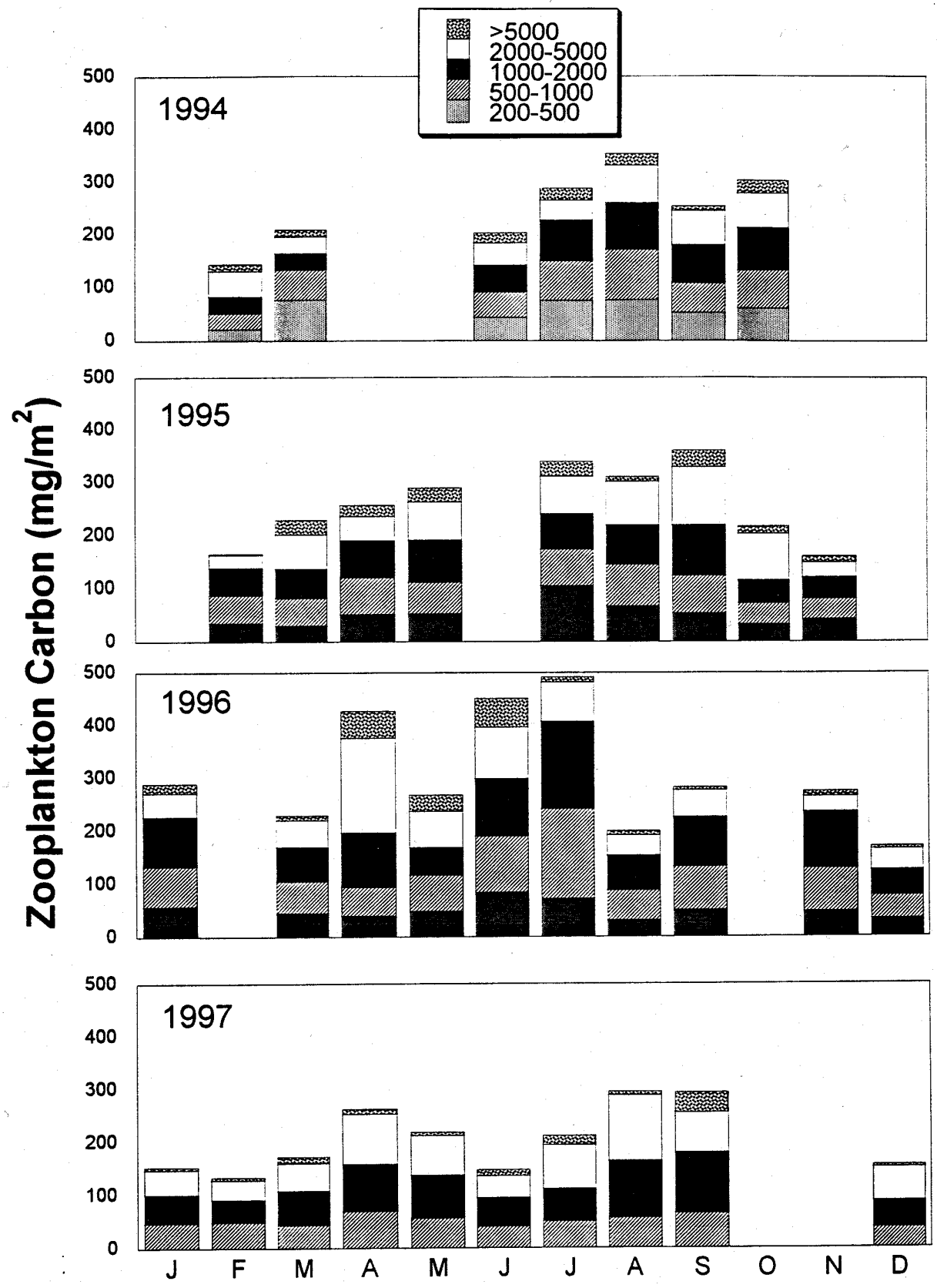
>5000
2000-5000
1000-2000
500-1000
200-500
1994
1995
1996
1997
Zooplankton Carbon (mg/m2)
0
100
200
300
400
500
J
F
M
A
M
J
J
A
S
O
N
D

Figure 6.2.15

6.3. ADCP MEASUREMENTS

Figure 6.3.1a to j. Velocity fields at Station ALOHA. Top panel shows hourly averages at 20-m depth intervals while the ship was on station. The orientation of each stick gives the direction of the current: up is northward and to the right is eastward. The bottom panel shows the results of a least-squares fit of hourly averages to a mean, trend, semi-diurnal and diurnal tides; the on-station time-series were not long enough to fit an inertial cycle. In the first column the arrow shows the mean current and the headless stick shows the sum of the mean plus the trend at the end of the station. For each harmonic the current ellipse is shown in the first column. The orientation of the stick in the second column shows the direction of the harmonic component of the current at the beginning of the station and the arrowhead at the end of the stick shows the direction of rotation of the current vector around the ellipse.

Figure 6.3.2a to j: Velocity fields on the transits to and from Station ALOHA. Velocity is shown as a function of latitude averaged in 10-minute intervals.

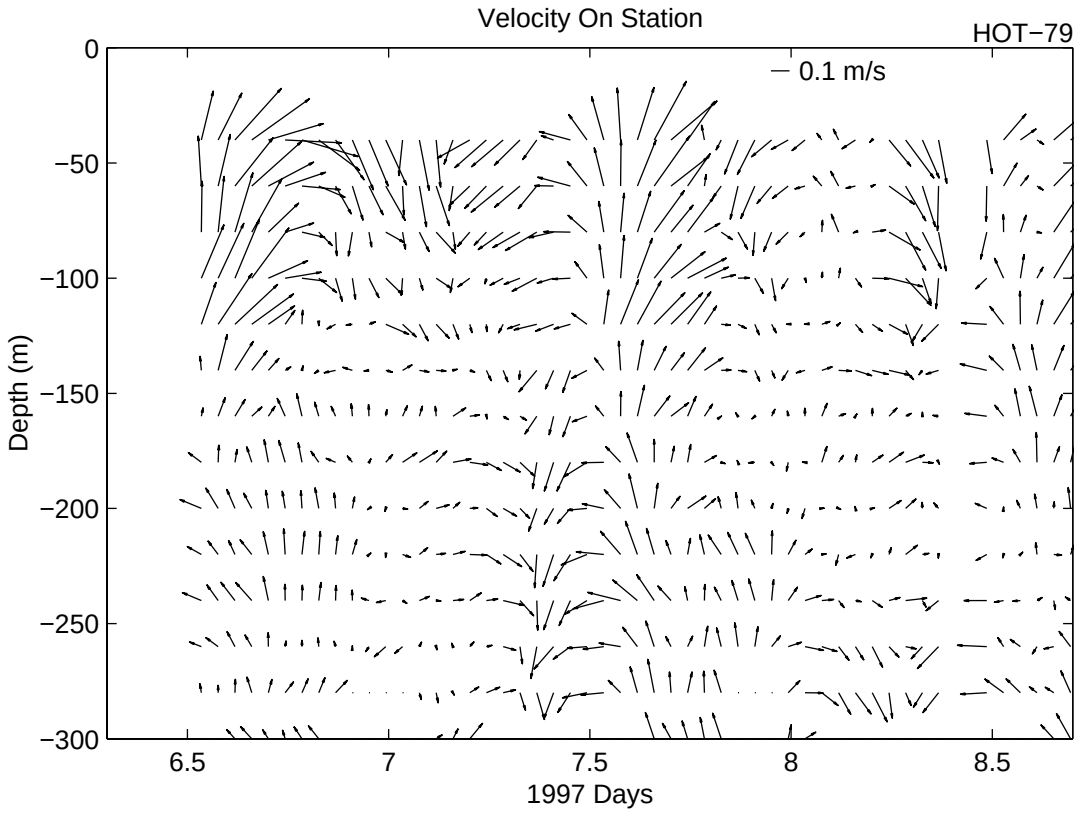
Velocity On Station
HOT−79
0.1 m/s
0
−50
−100
−150
−200
−250
−300
Depth (m)
6.5
7
7.5
8
8.5
1997 Days

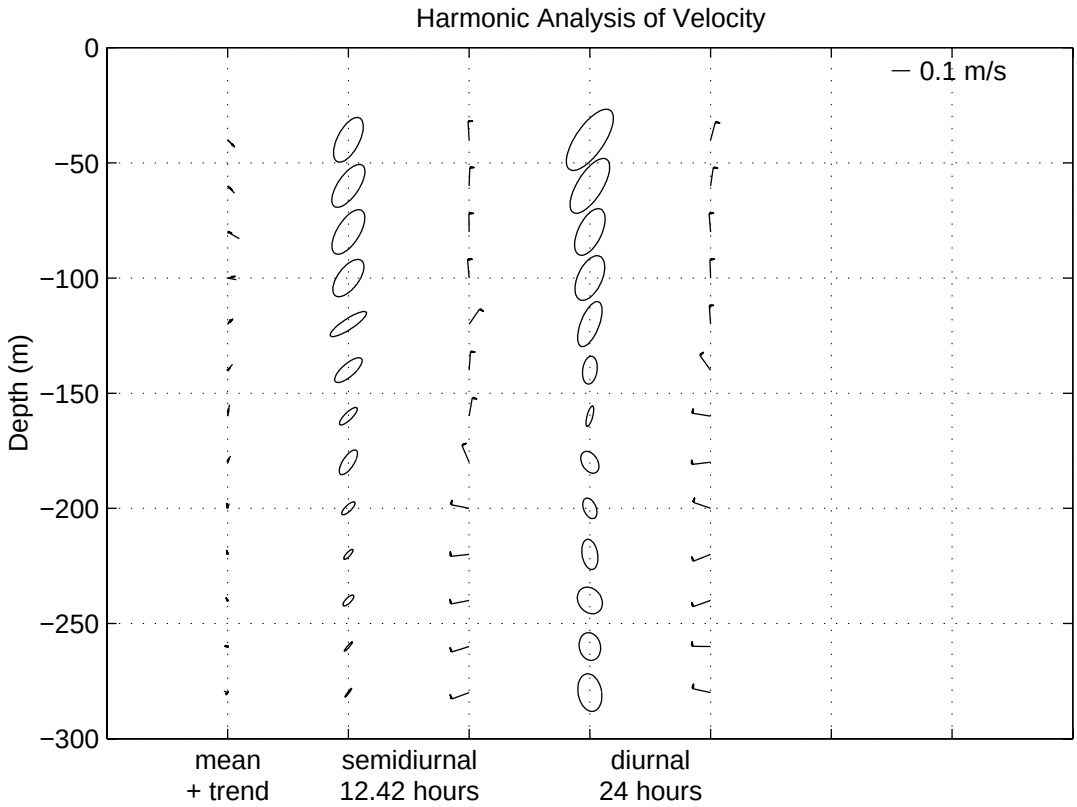
Harmonic Analysis of Velocity
0.1 m/s
0
−50
−100
−150
−200
−250
−300
Depth (m)
mean
+ trend
semidiurnal
12.42 hours
diurnal
24 hours

Figure 6.3.1a

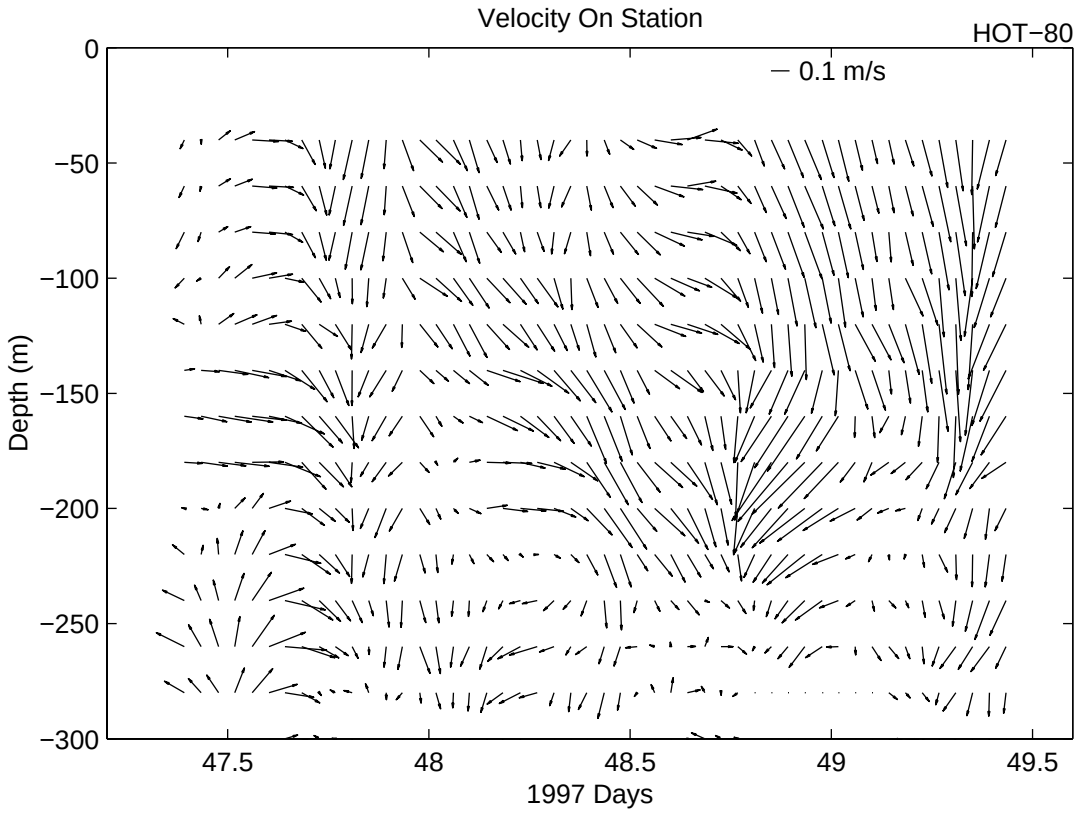
Velocity On Station
HOT−80
0.1 m/s
0
−50
−100
−150
−200
−250
−300
Depth (m)
47.5
48
48.5
49
49.5
1997 Days

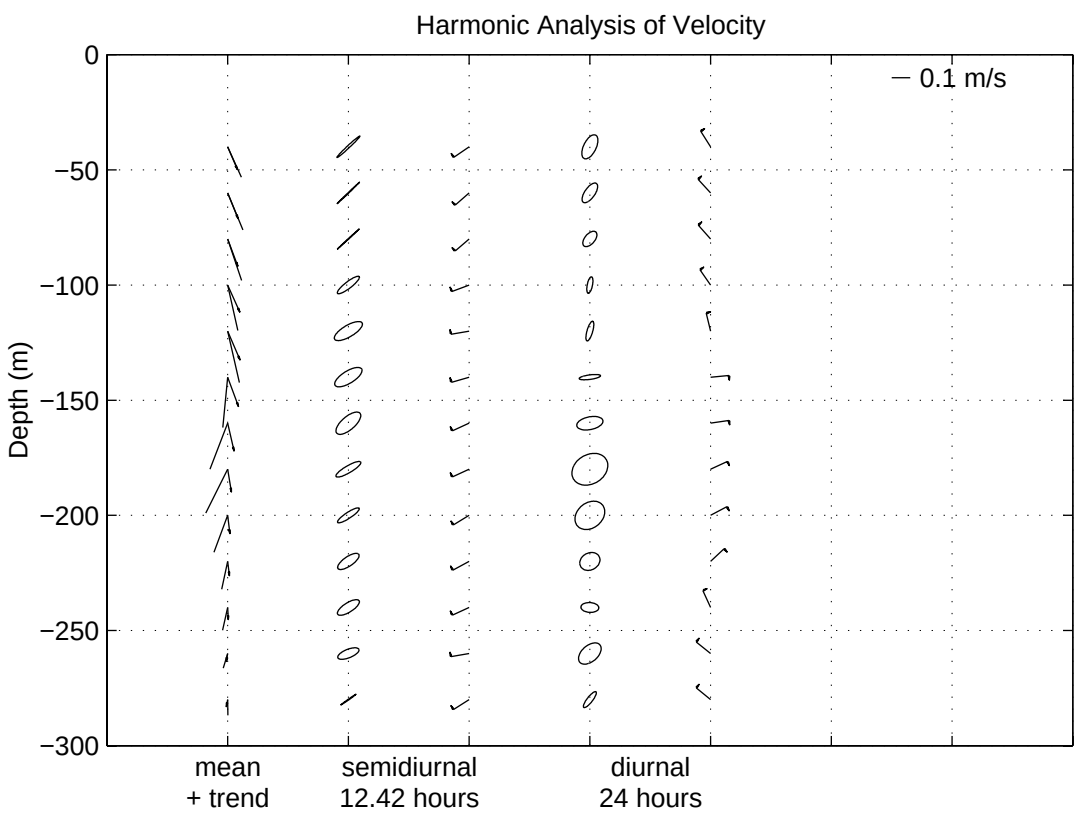
Harmonic Analysis of Velocity
0.1 m/s
0
−50
−100
−150
−200
−250
−300
Depth (m)
mean
+ trend
semidiurnal
12.42 hours
diurnal
24 hours

Figure 6.3.1.b

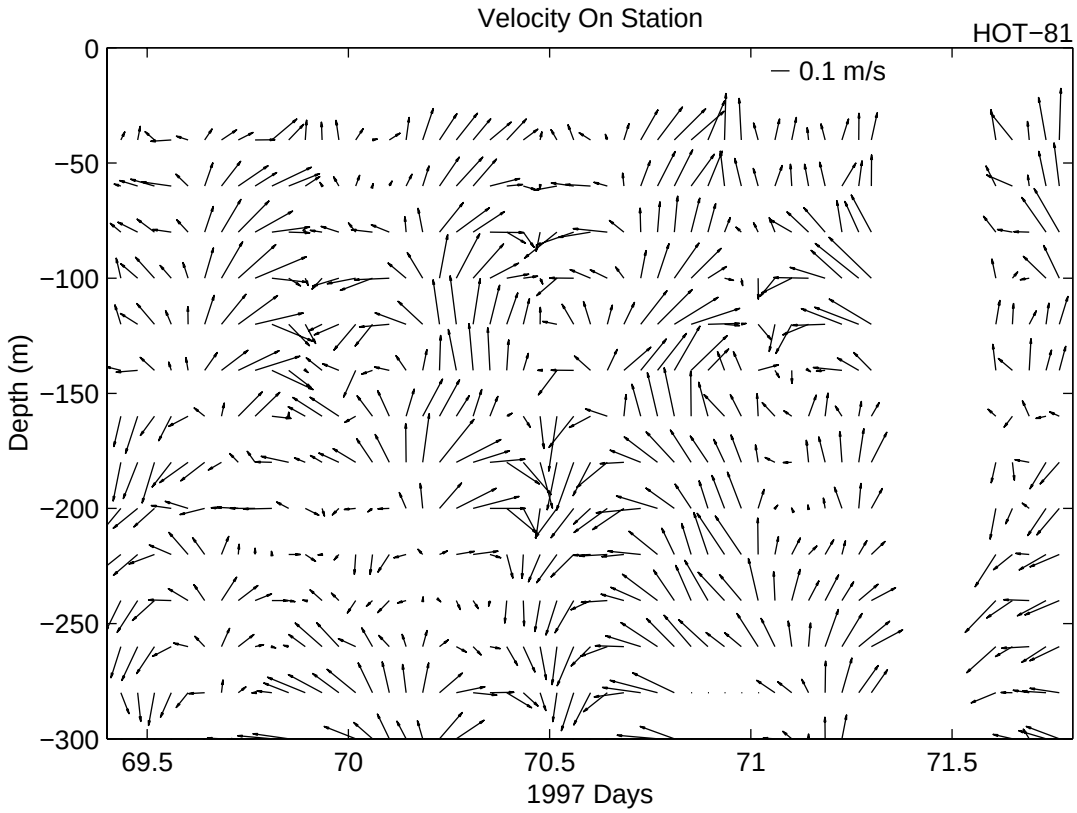
Velocity On Station
HOT−81
0.1 m/s
0
−50
−100
−150
−200
−250
−300
Depth (m)
69.5
70
70.5
71
71.5
1997 Days

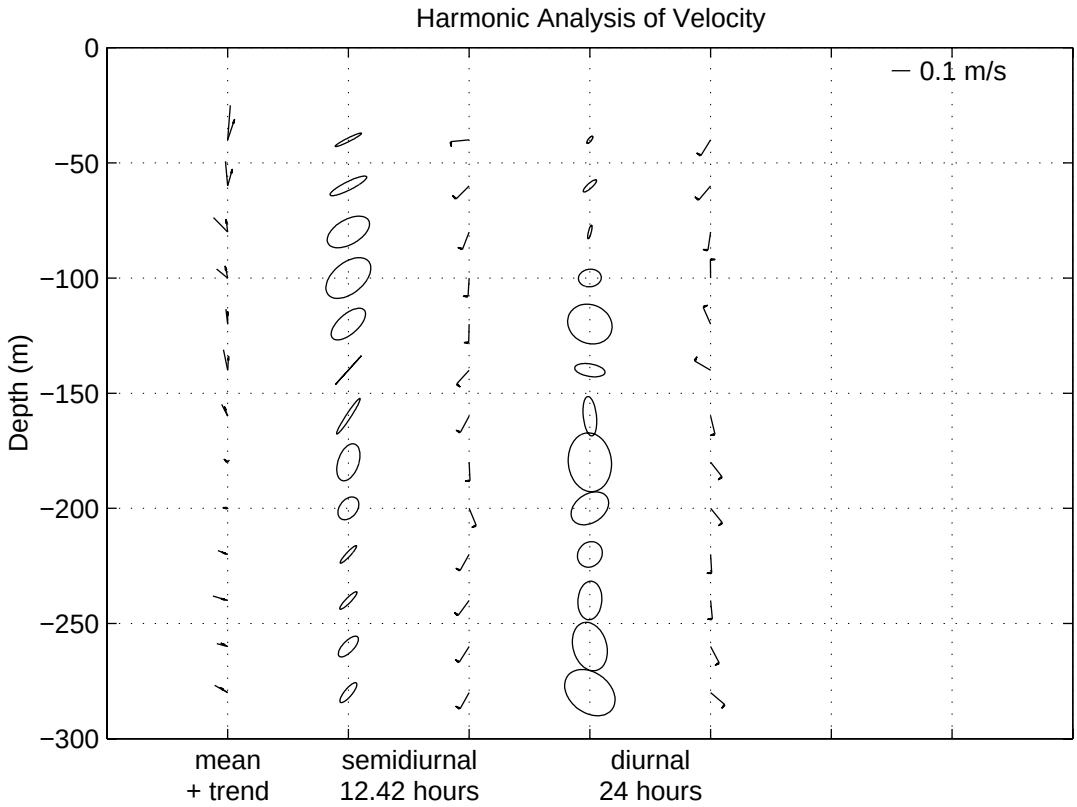
Harmonic Analysis of Velocity
0.1 m/s
0
−50
−100
−150
−200
−250
−300
Depth (m)
mean
+ trend
semidiurnal
12.42 hours
diurnal
24 hours

Figure 6.3.1c

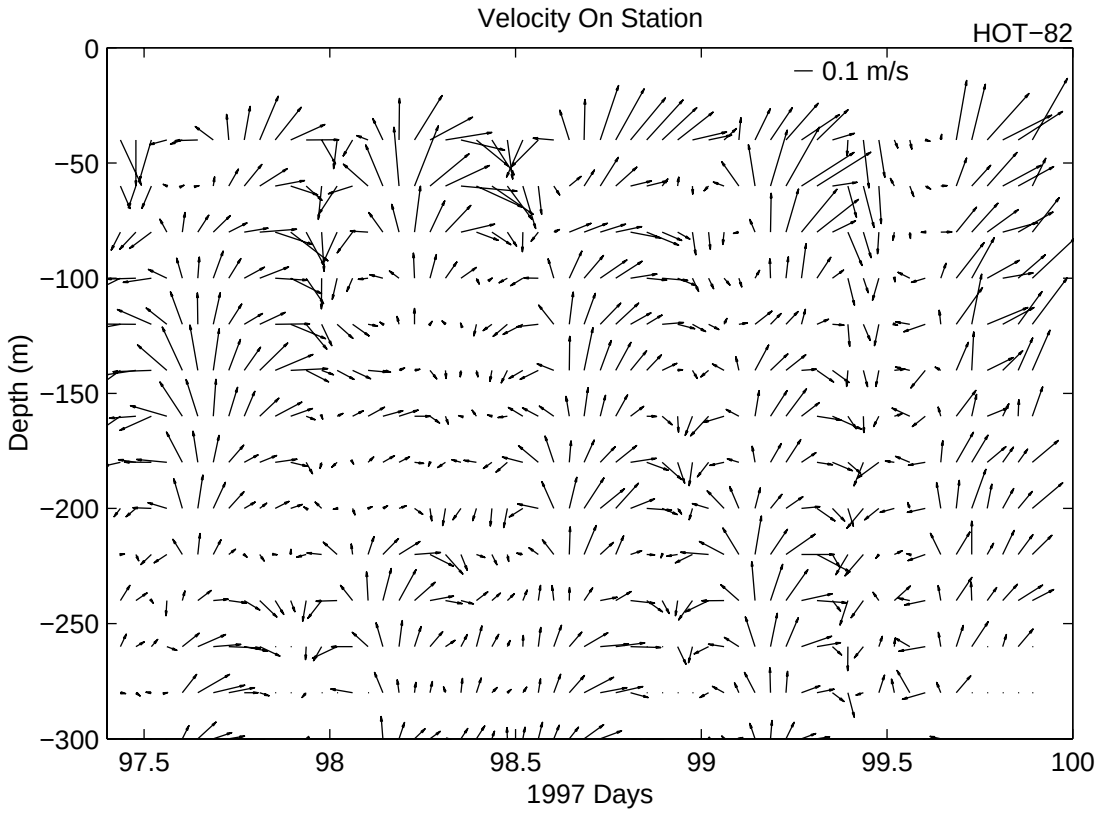
Velocity On Station
HOT−82
− 0.1 m/s
Depth (m)
0
−50
−100
−150
−200
−250
−300
97.5
98
98.5
99
99.5
100
1997 Days

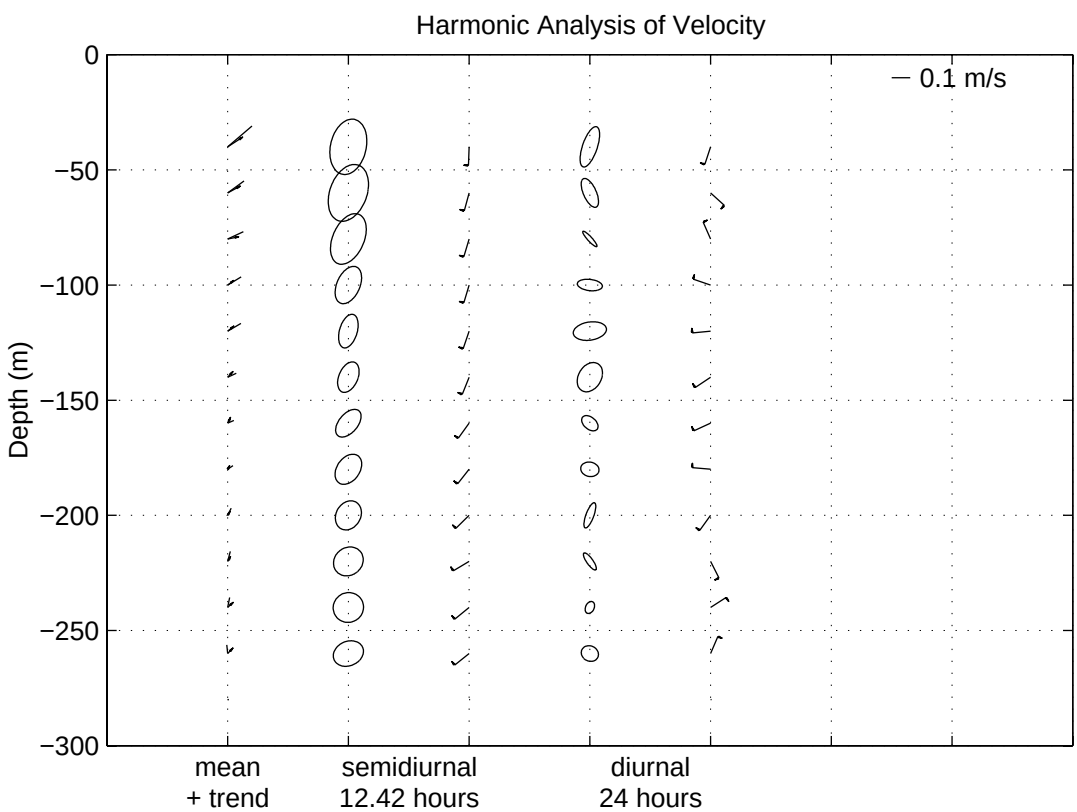
Harmonic Analysis of Velocity
− 0.1 m/s
Depth (m)
0
−50
−100
−150
−200
−250
−300
mean
+ trend
semidiurnal
12.42 hours
diurnal
24 hours

Figure 6.3.1d

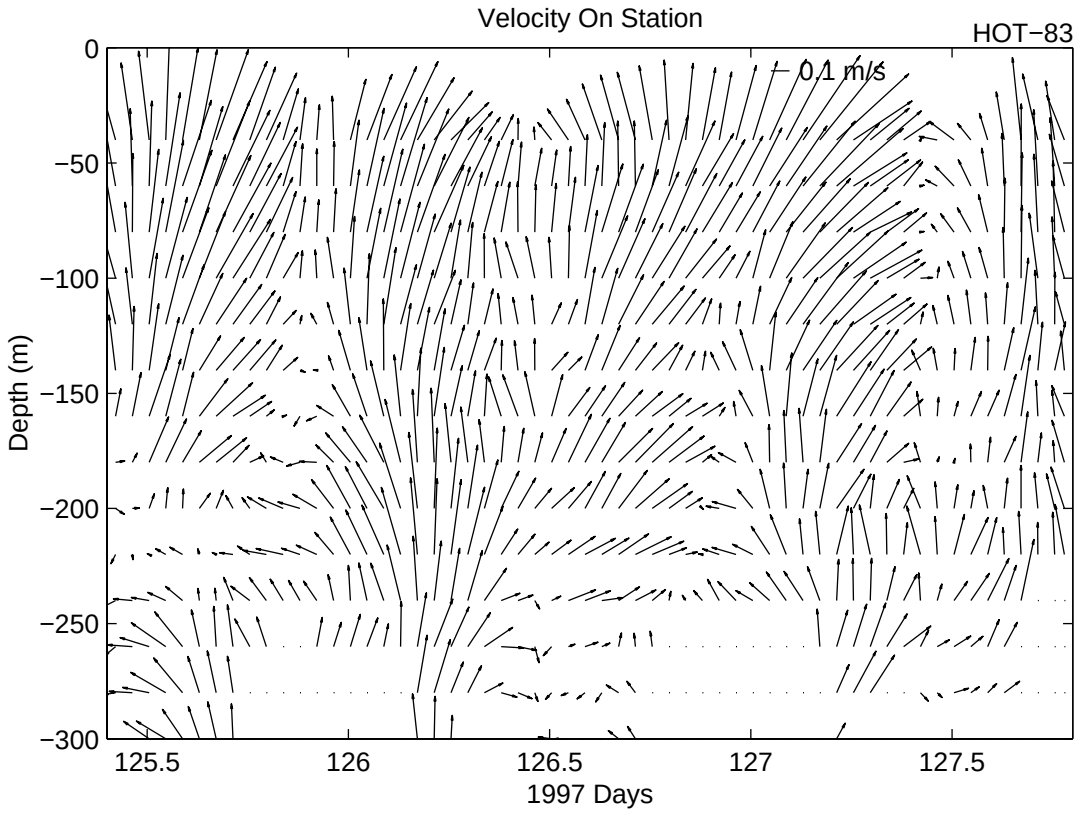
Velocity On Station
HOT−83
0.1 m/s
0
−50
−100
−150
−200
−250
−300
Depth (m)
125.5
126
126.5
127
127.5
1997 Days

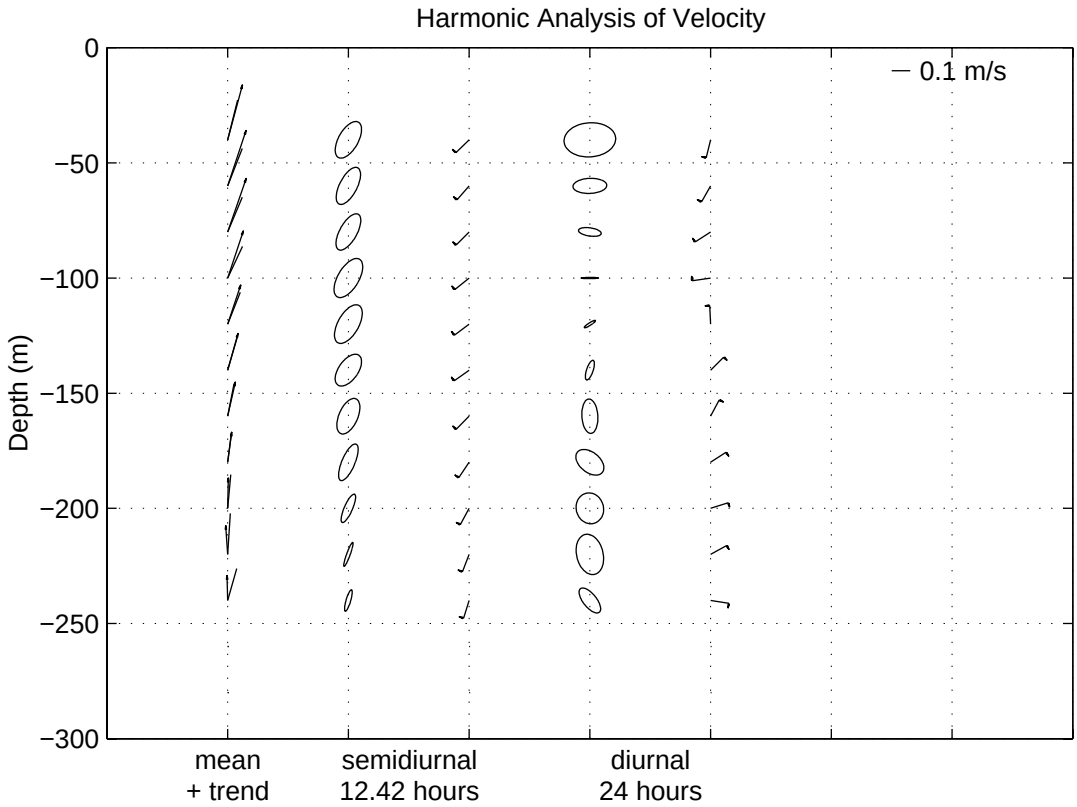
Harmonic Analysis of Velocity
0.1 m/s
0
−50
−100
−150
−200
−250
−300
Depth (m)
mean
+ trend
semidiurnal
12.42 hours
diurnal
24 hours

Figure 6.3.1e

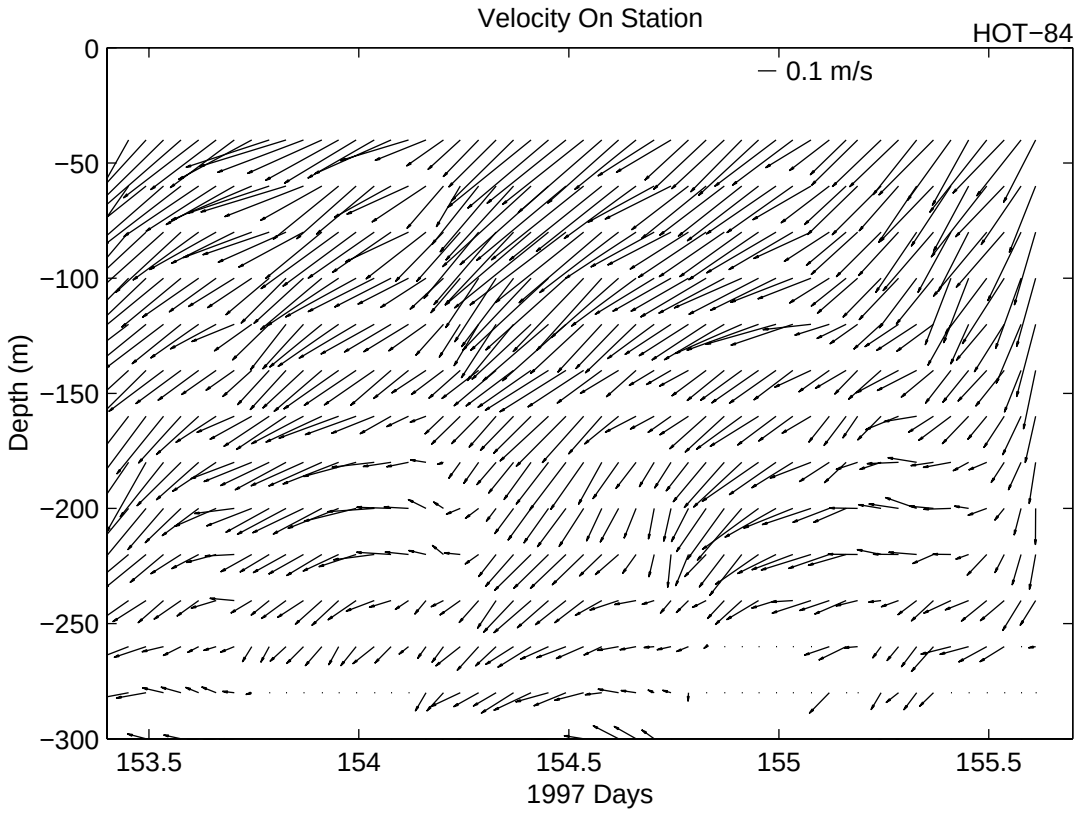
Velocity On Station
HOT−84
0.1 m/s
0
−50
−100
−150
−200
−250
−300
Depth (m)
153.5
154
154.5
155
155.5
1997 Days

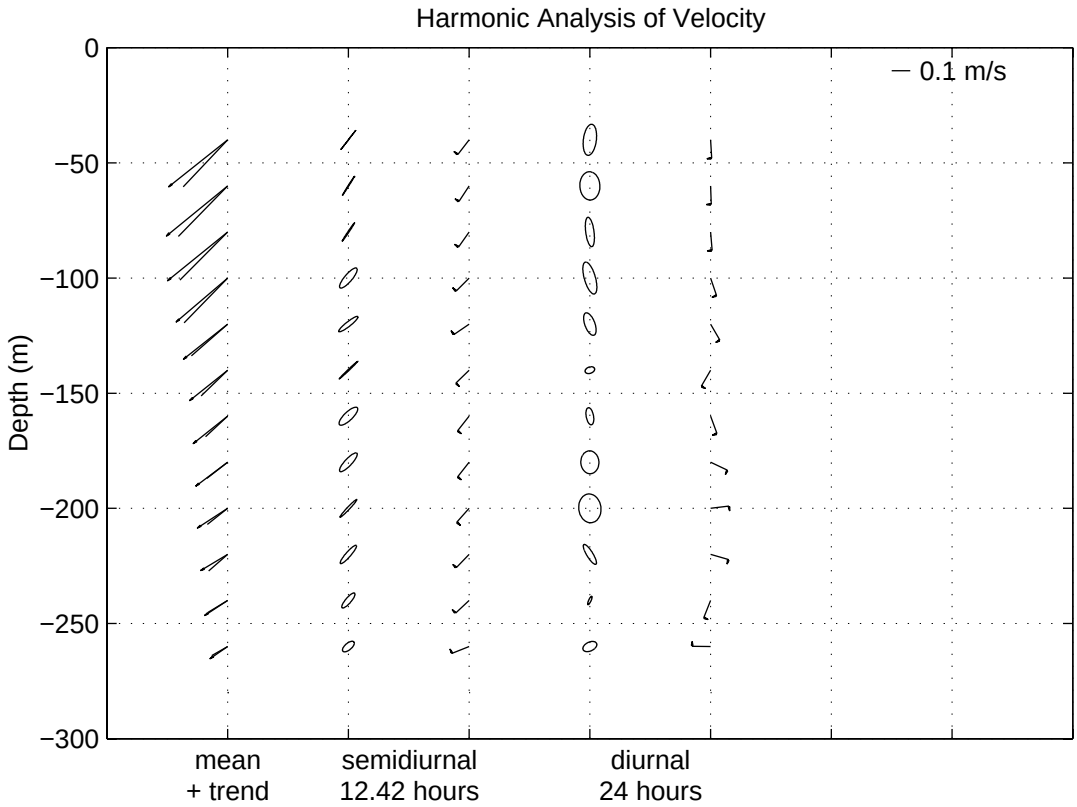
Harmonic Analysis of Velocity
0.1 m/s
0
−50
−100
−150
−200
−250
−300
Depth (m)
mean
+ trend
semidiurnal
12.42 hours
diurnal
24 hours

Figure 6.3.1f

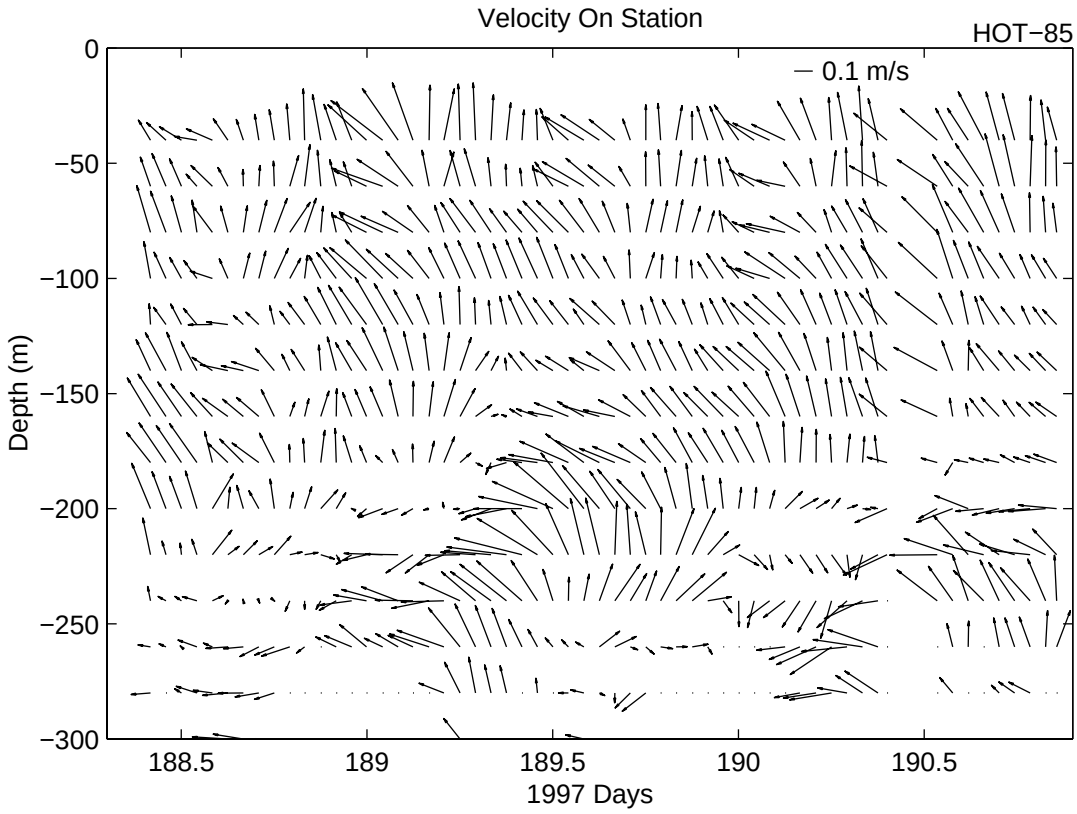
Velocity On Station
HOT−85
— 0.1 m/s
0
−50
−100
−150
−200
−250
−300
Depth (m)
188.5
189
189.5
190
190.5
1997 Days

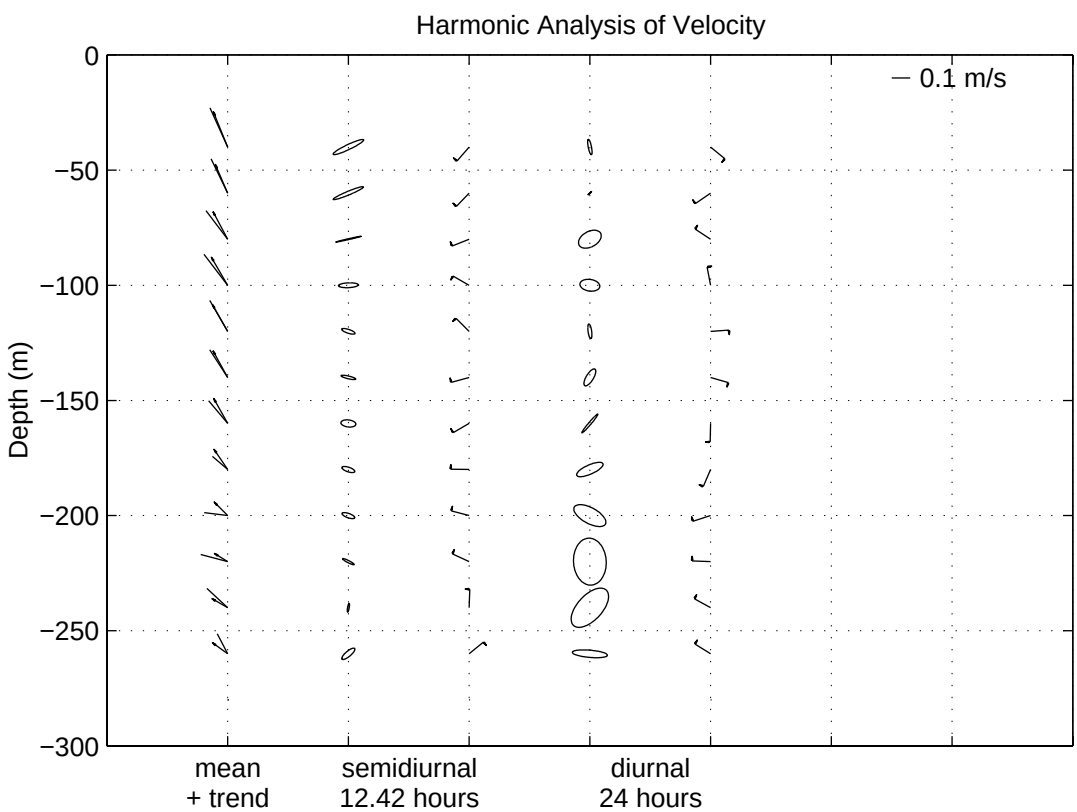
Harmonic Analysis of Velocity
— 0.1 m/s
0
−50
−100
−150
−200
−250
−300
Depth (m)
mean
+ trend
semidiurnal
12.42 hours
diurnal
24 hours

Figure 6.3.1g

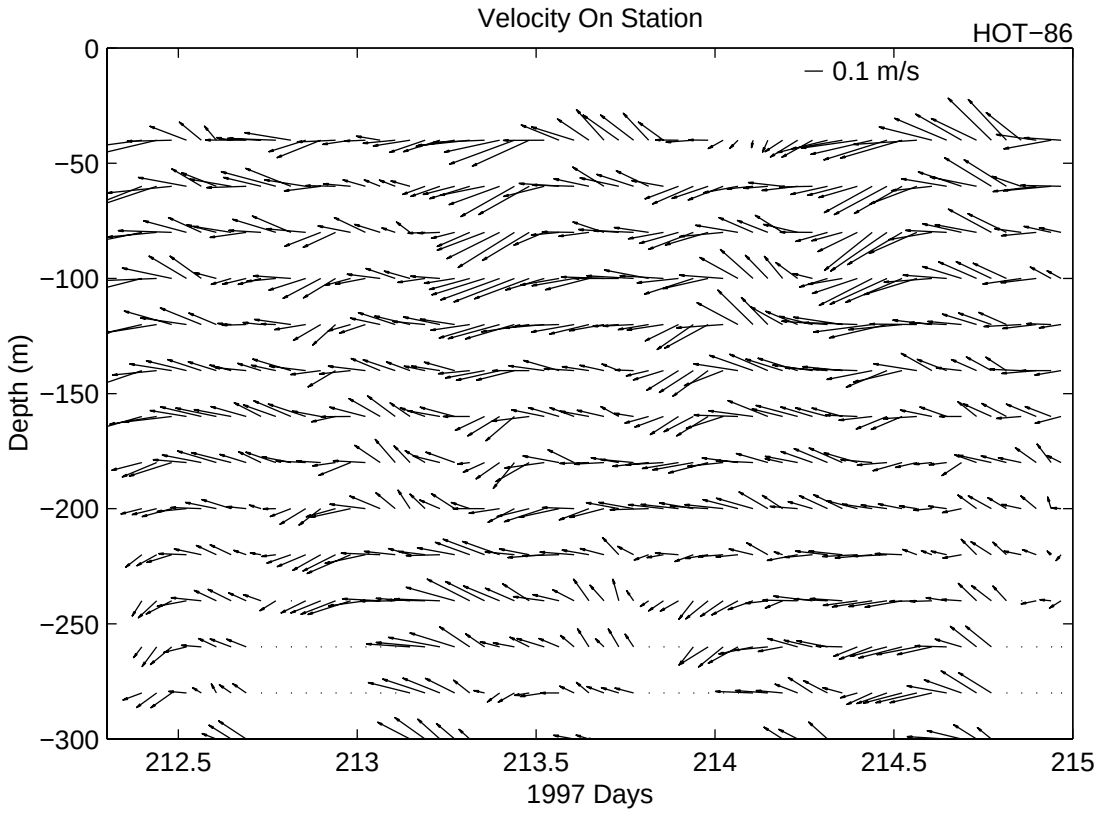
Velocity On Station
HOT−86
0.1 m/s
0
−50
−100
−150
−200
−250
−300
Depth (m)
212.5
213
213.5
214
214.5
215
1997 Days

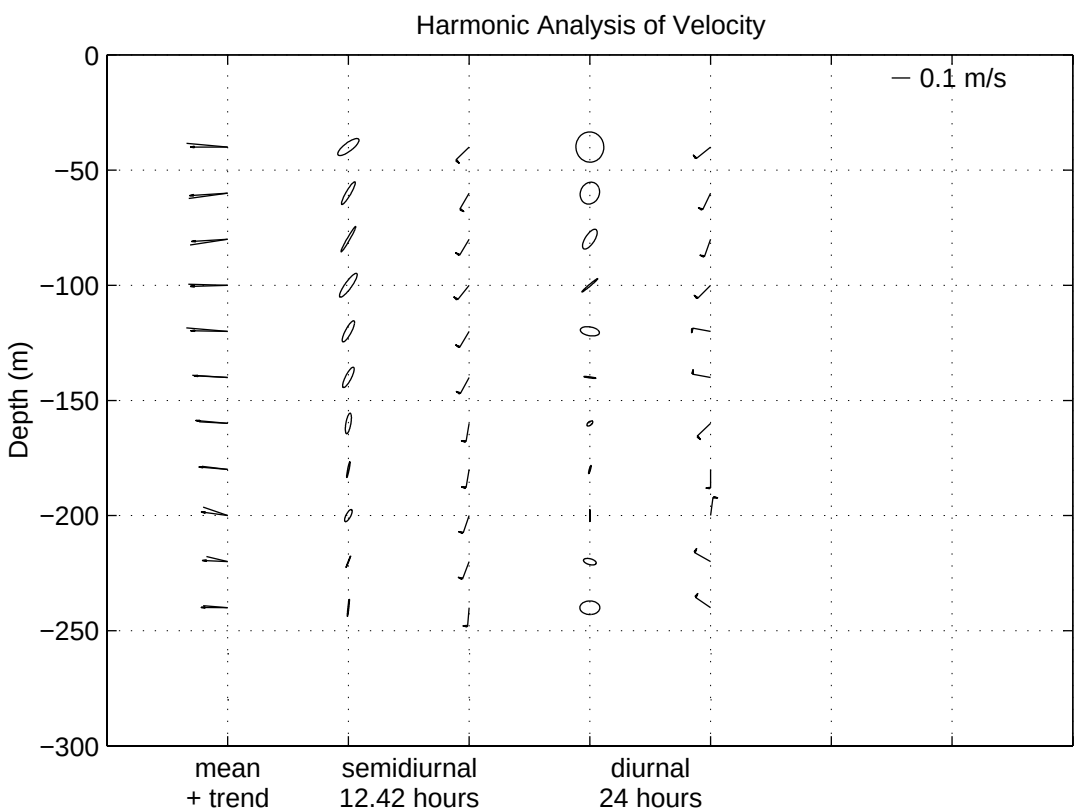
Harmonic Analysis of Velocity
0.1 m/s
0
−50
−100
−150
−200
−250
−300
Depth (m)
mean
+ trend
semidiurnal
12.42 hours
diurnal
24 hours

Figure 6.3.1h

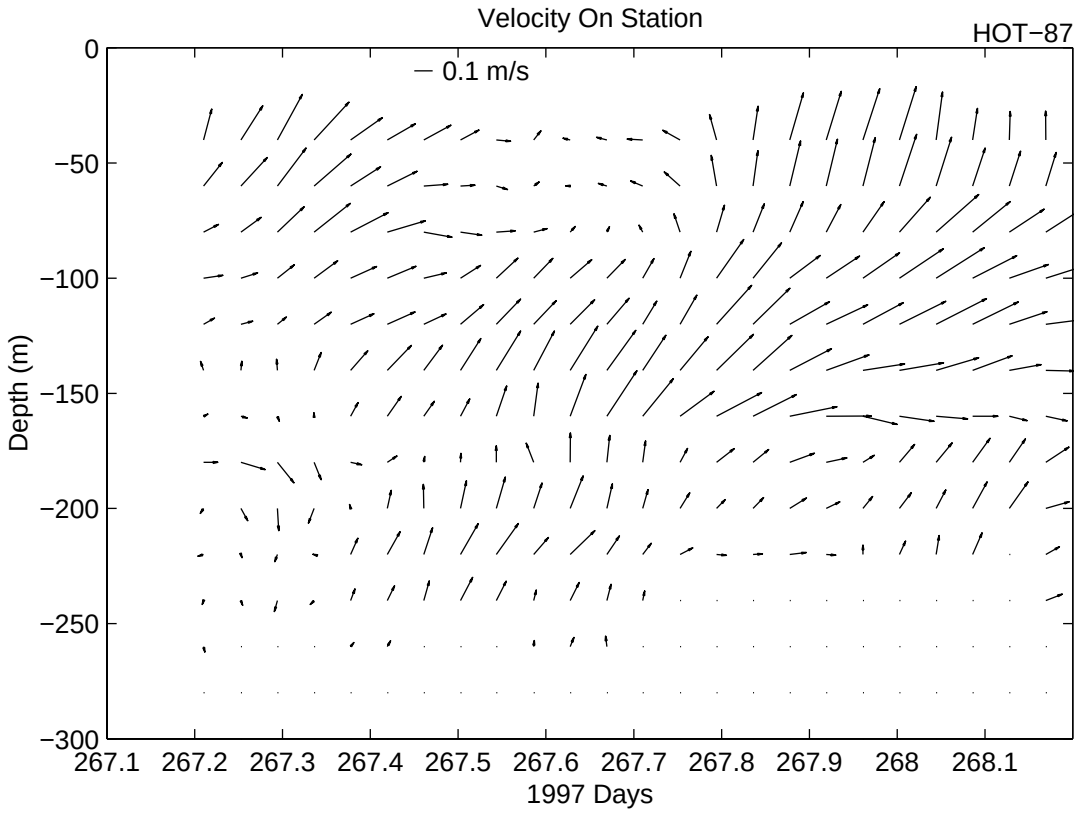
Velocity On Station
HOT−87
− 0.1 m/s
Depth (m)
0
−50
−100
−150
−200
−250
−300
267.1
267.2
267.3
267.4
267.5
267.6
267.7
267.8
267.9
268
268.1
1997 Days

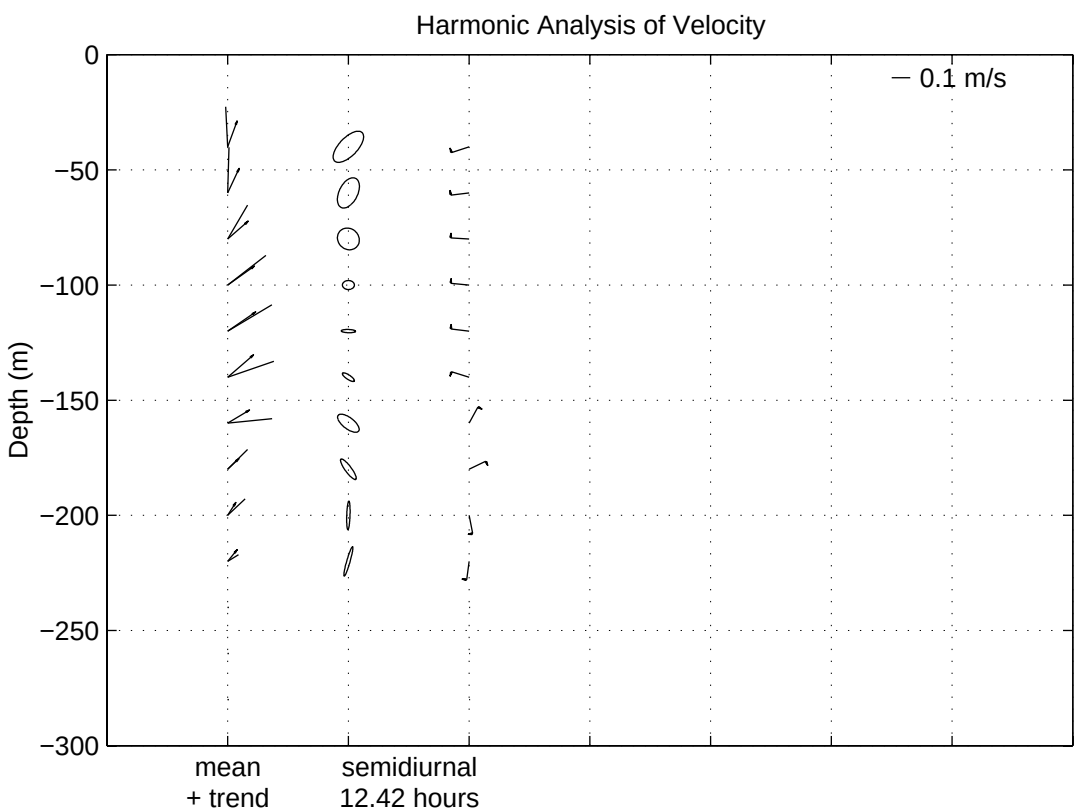
Harmonic Analysis of Velocity
− 0.1 m/s
Depth (m)
0
−50
−100
−150
−200
−250
−300
mean
+ trend
semidiurnal
12.42 hours

Figure 6.3.1i

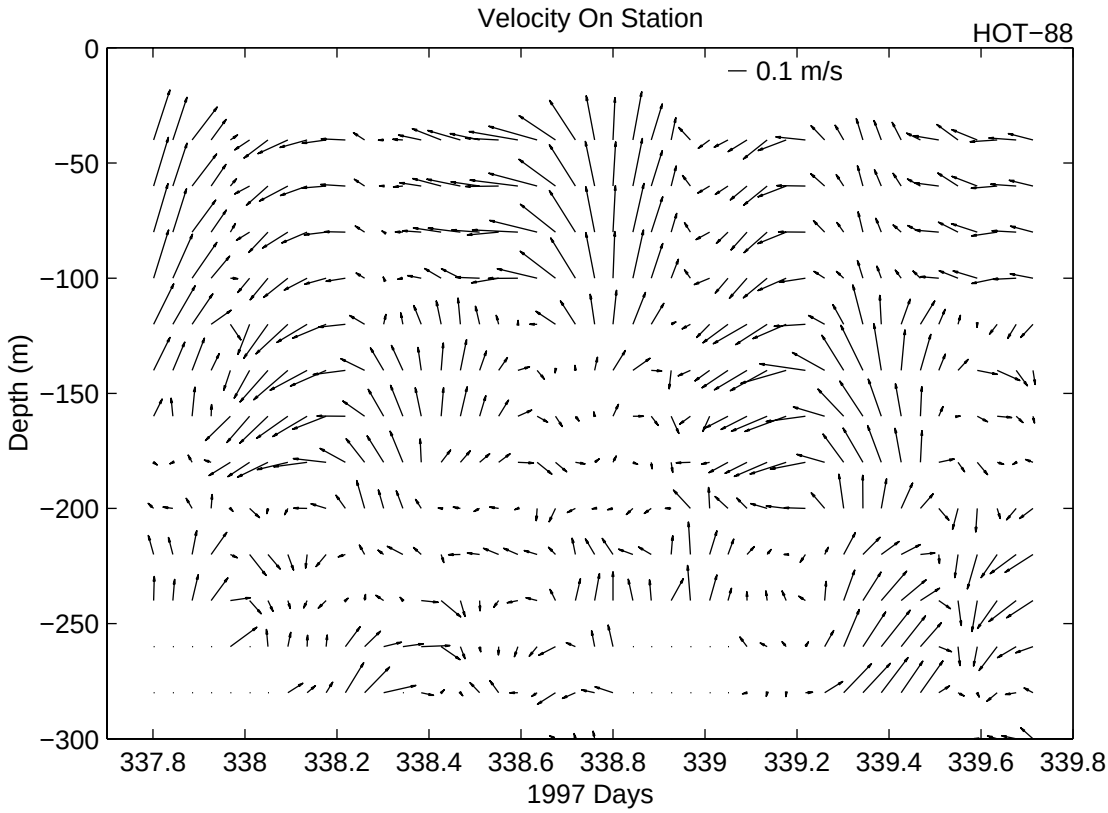
Velocity On Station
HOT−88
− 0.1 m/s
Depth (m)
0
−50
−100
−150
−200
−250
−300
337.8
338
338.2
338.4
338.6
338.8
339
339.2
339.4
339.6
339.8
1997 Days

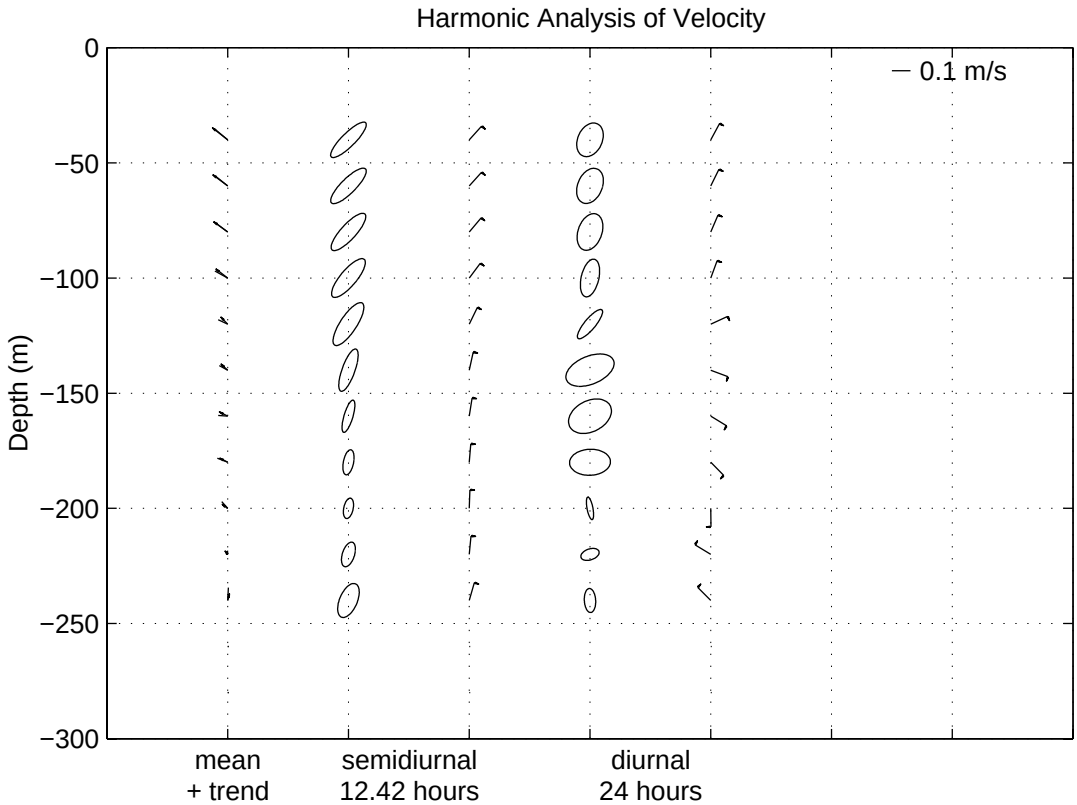
Harmonic Analysis of Velocity
− 0.1 m/s
Depth (m)
0
−50
−100
−150
−200
−250
−300
mean
+ trend
semidiurnal
12.42 hours
diurnal
24 hours

Figure 6.3.1j

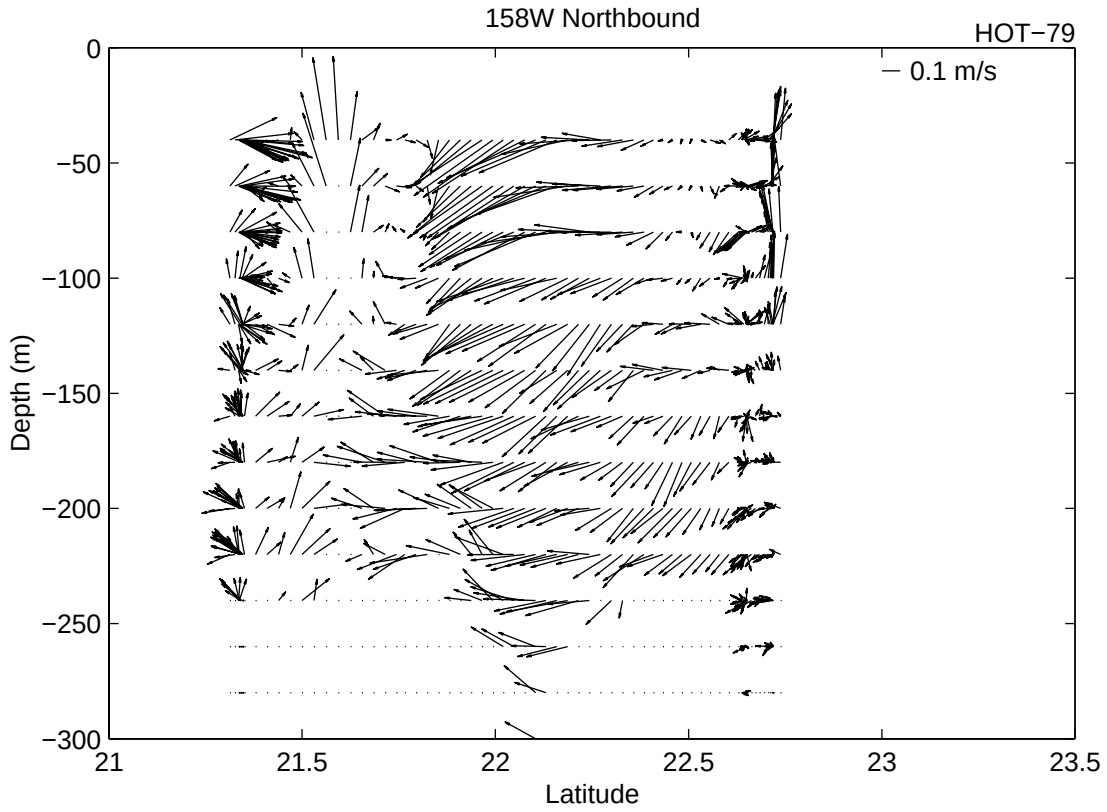
158W Northbound
HOT−79
0.1 m/s
Depth (m)
Latitude
0
−50
−100
−150
−200
−250
−300
21
21.5
22
22.5
23
23.5

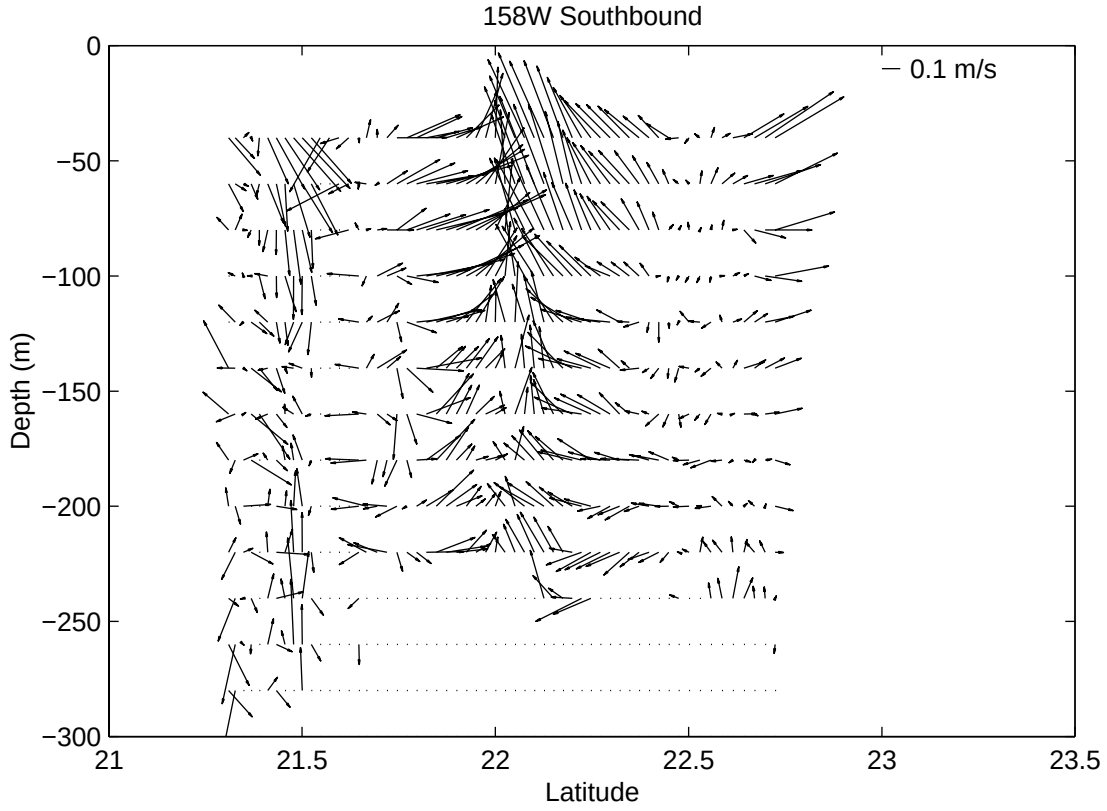
158W Southbound
0.1 m/s
Depth (m)
Latitude
0
−50
−100
−150
−200
−250
−300
21
21.5
22
22.5
23
23.5

Figure 6.3.2a

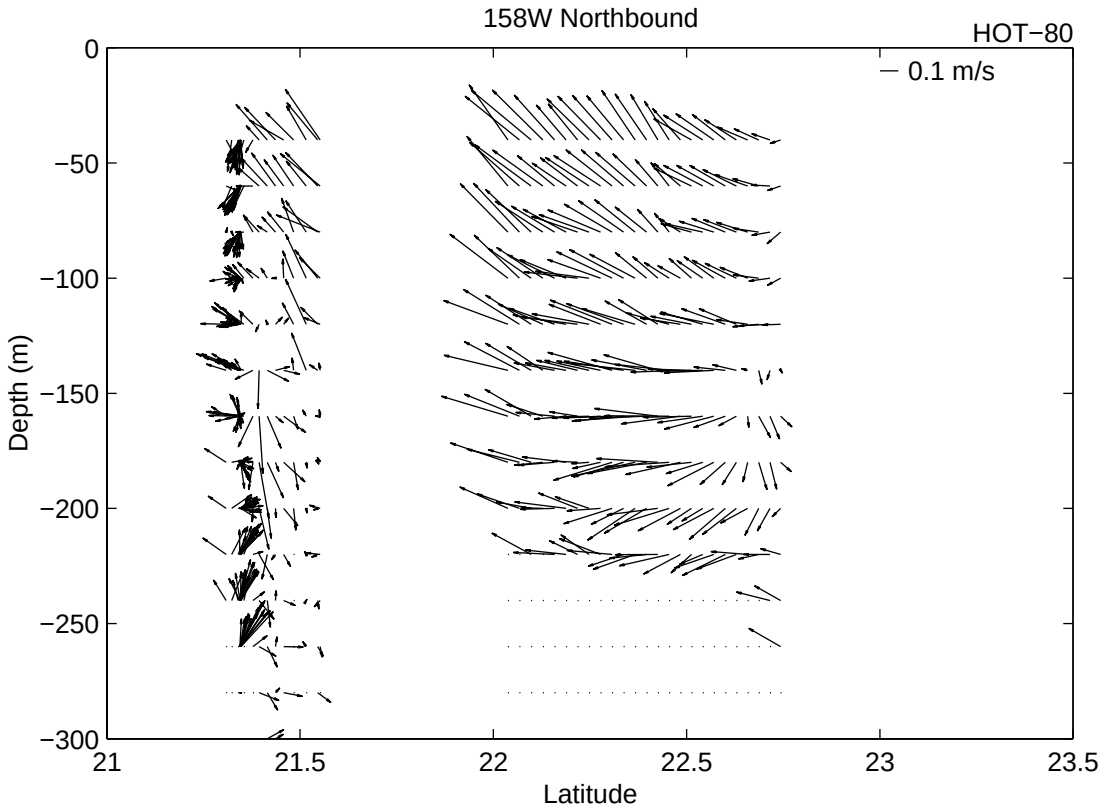
158W Northbound
HOT−80
0.1 m/s
0
−50
−100
−150
−200
−250
−300
Depth (m)
21
21.5
22
22.5
23
23.5
Latitude

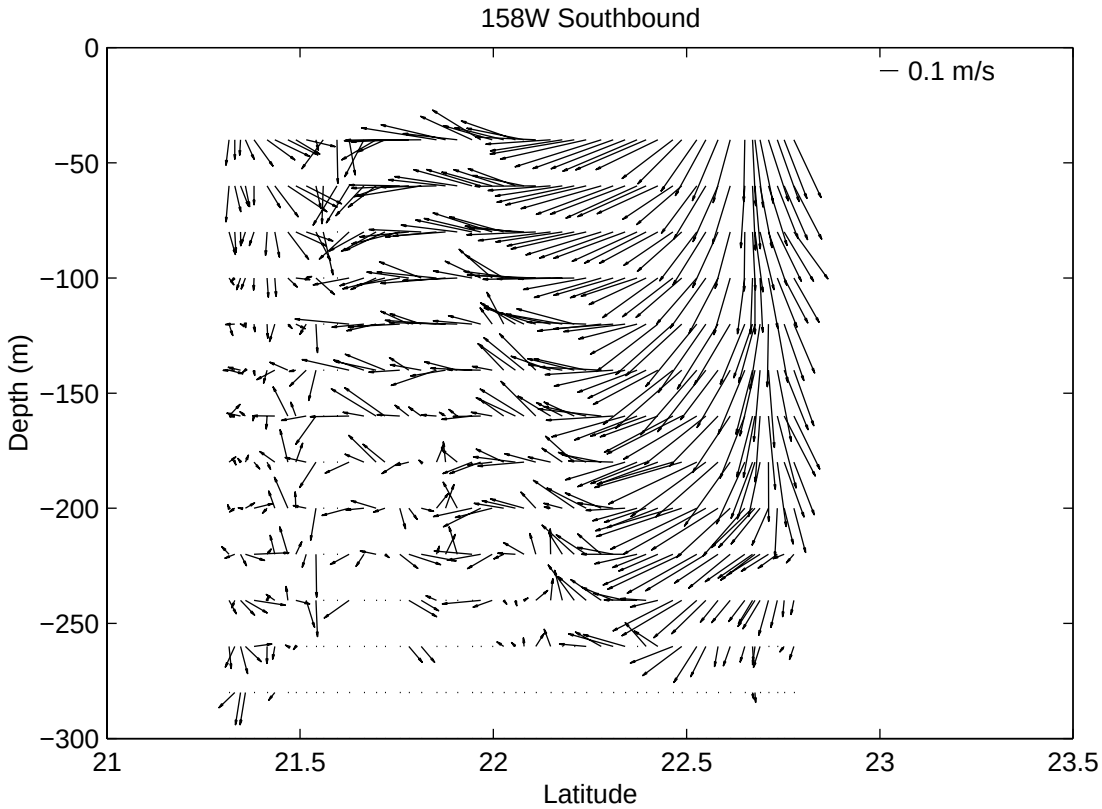
158W Southbound
0.1 m/s
0
−50
−100
−150
−200
−250
−300
Depth (m)
21
21.5
22
22.5
23
23.5
Latitude

Figure 6.3.2b

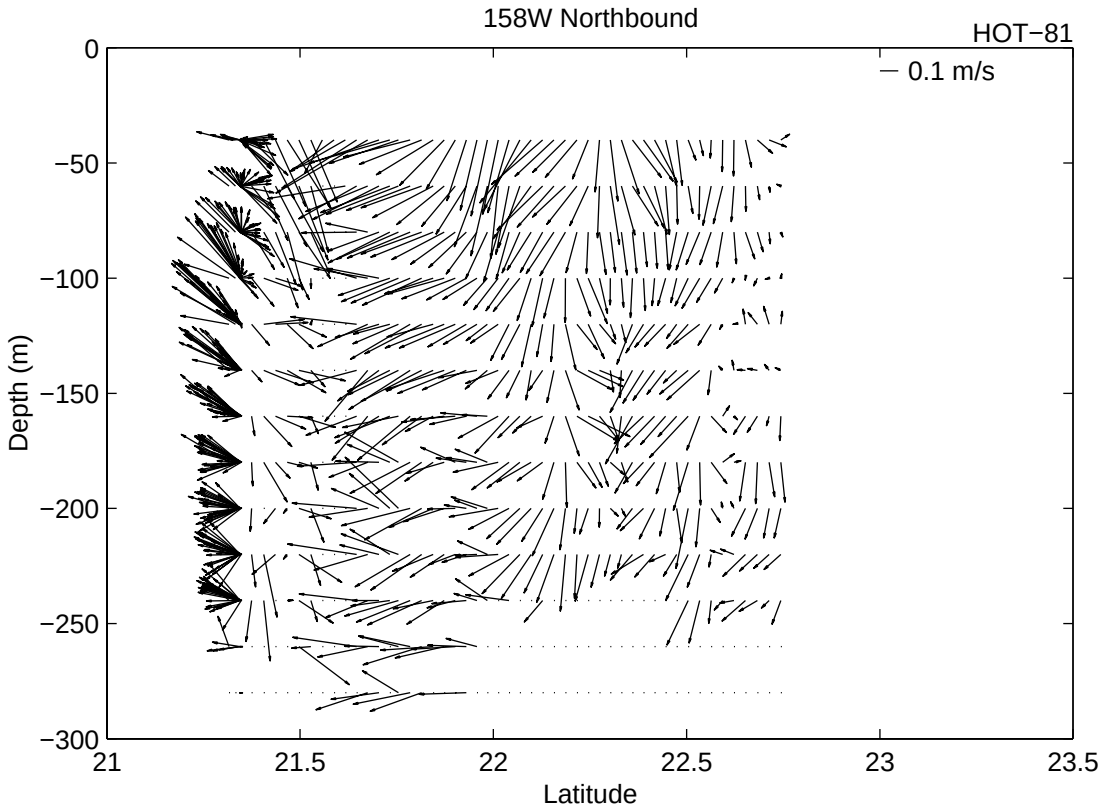
158W Northbound
HOT−81
0.1 m/s
Depth (m)
Latitude
0
−50
−100
−150
−200
−250
−300
21
21.5
22
22.5
23
23.5

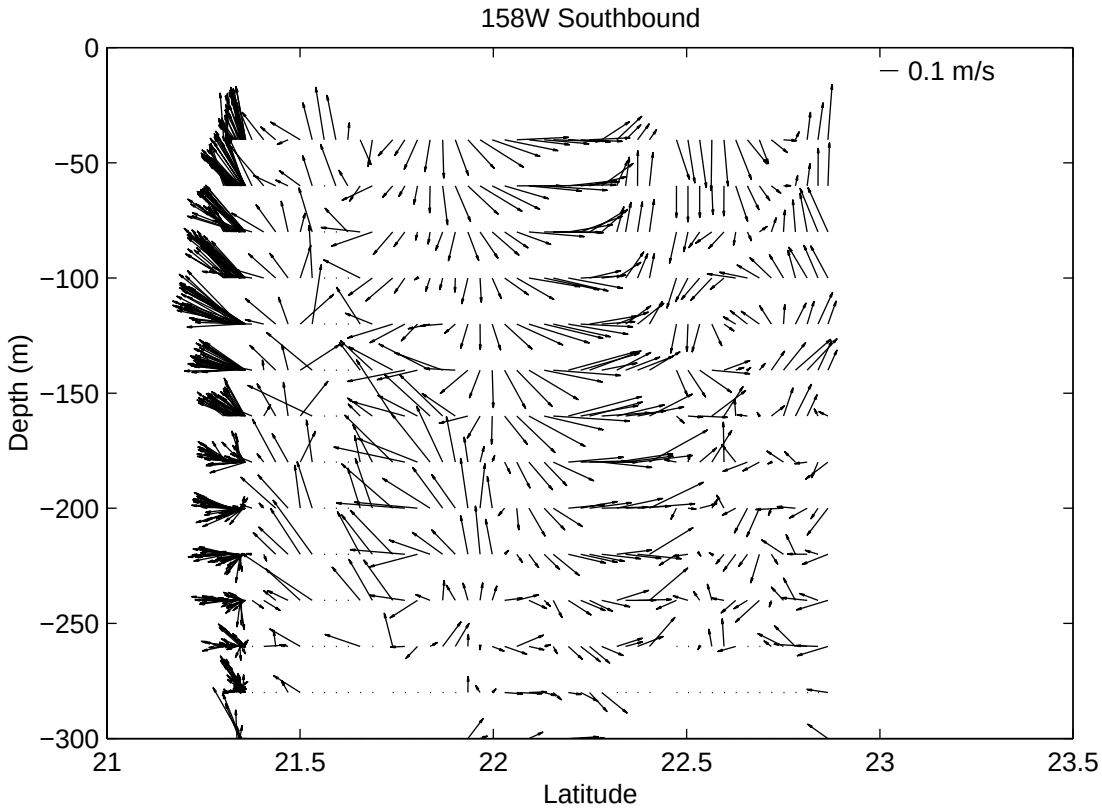
158W Southbound
0.1 m/s
Depth (m)
Latitude
0
−50
−100
−150
−200
−250
−300
21
21.5
22
22.5
23
23.5

Figure 6.3.2c

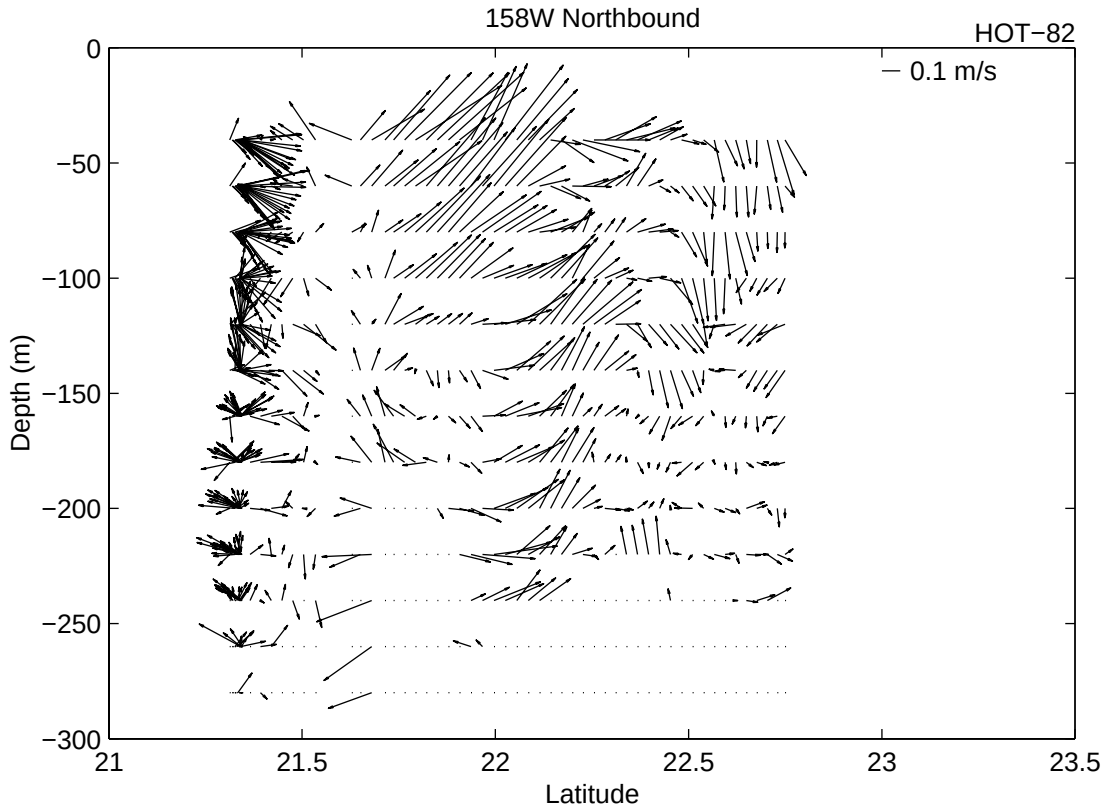
158W Northbound
HOT−82
0.1 m/s
Depth (m)
Latitude
0
−50
−100
−150
−200
−250
−300
21
21.5
22
22.5
23
23.5

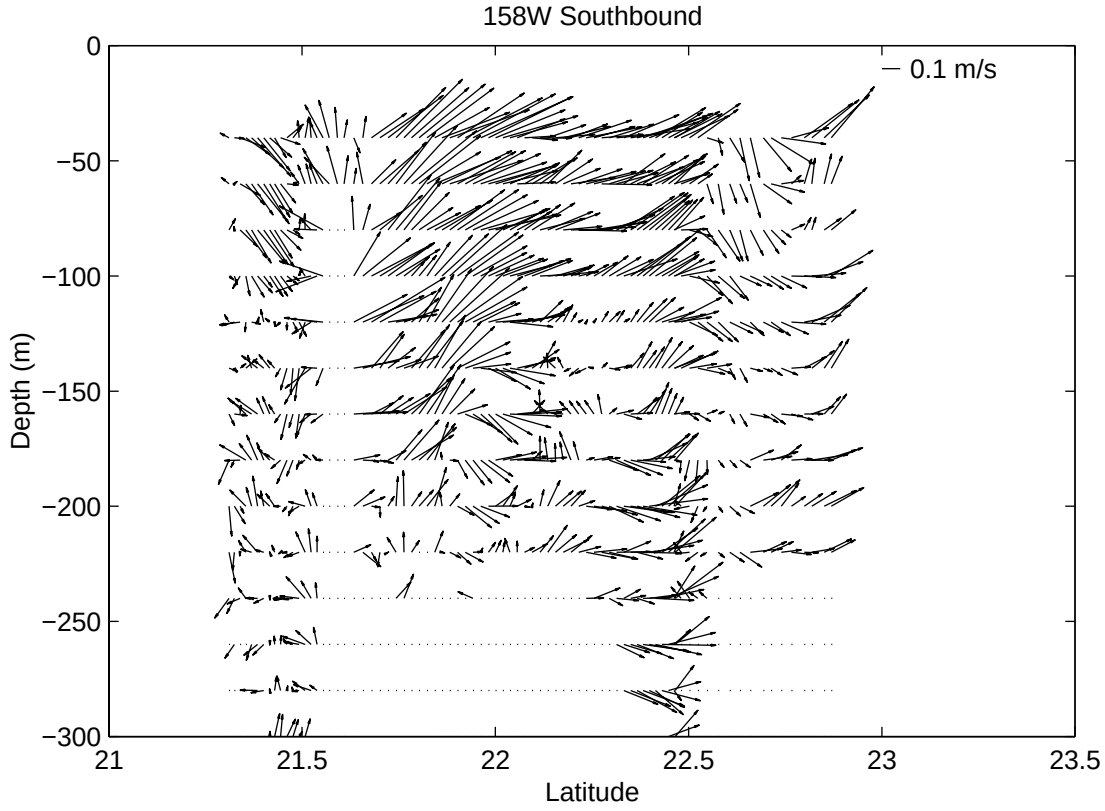
158W Southbound
0.1 m/s
Depth (m)
Latitude
0
−50
−100
−150
−200
−250
−300
21
21.5
22
22.5
23
23.5

Figure 6.3.2d

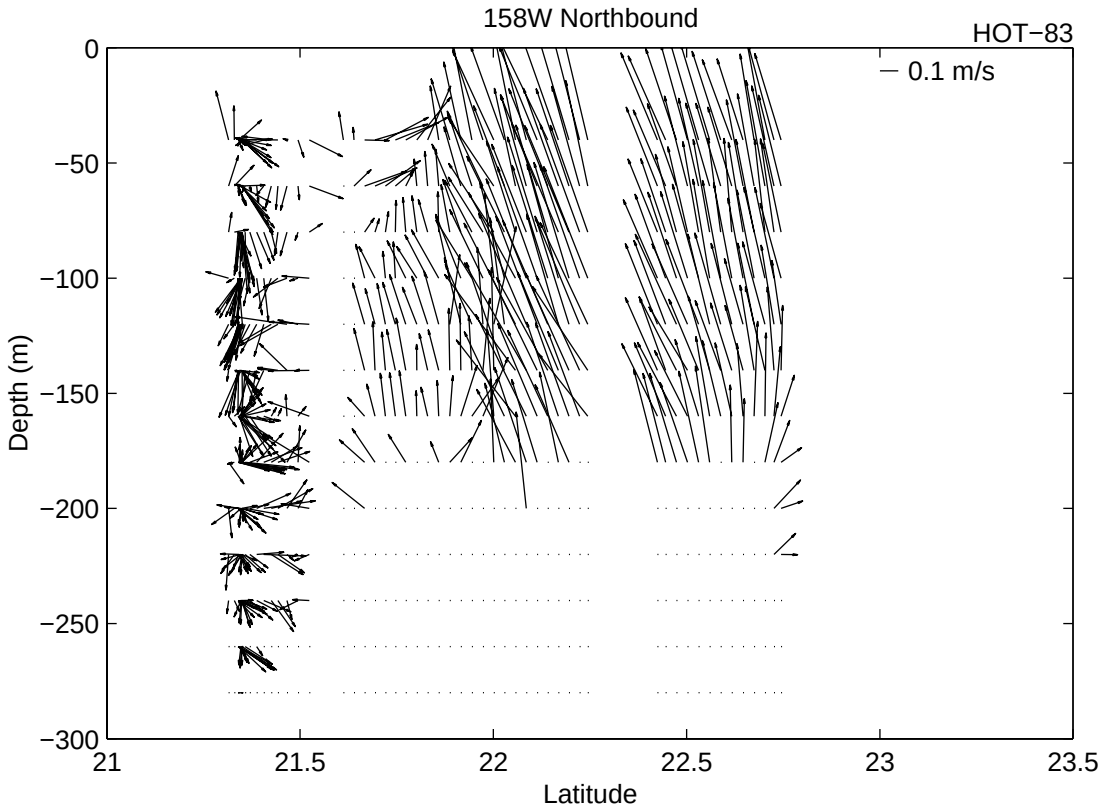
158W Northbound
HOT−83
0.1 m/s
Depth (m)
Latitude
0
−50
−100
−150
−200
−250
−300
21
21.5
22
22.5
23
23.5

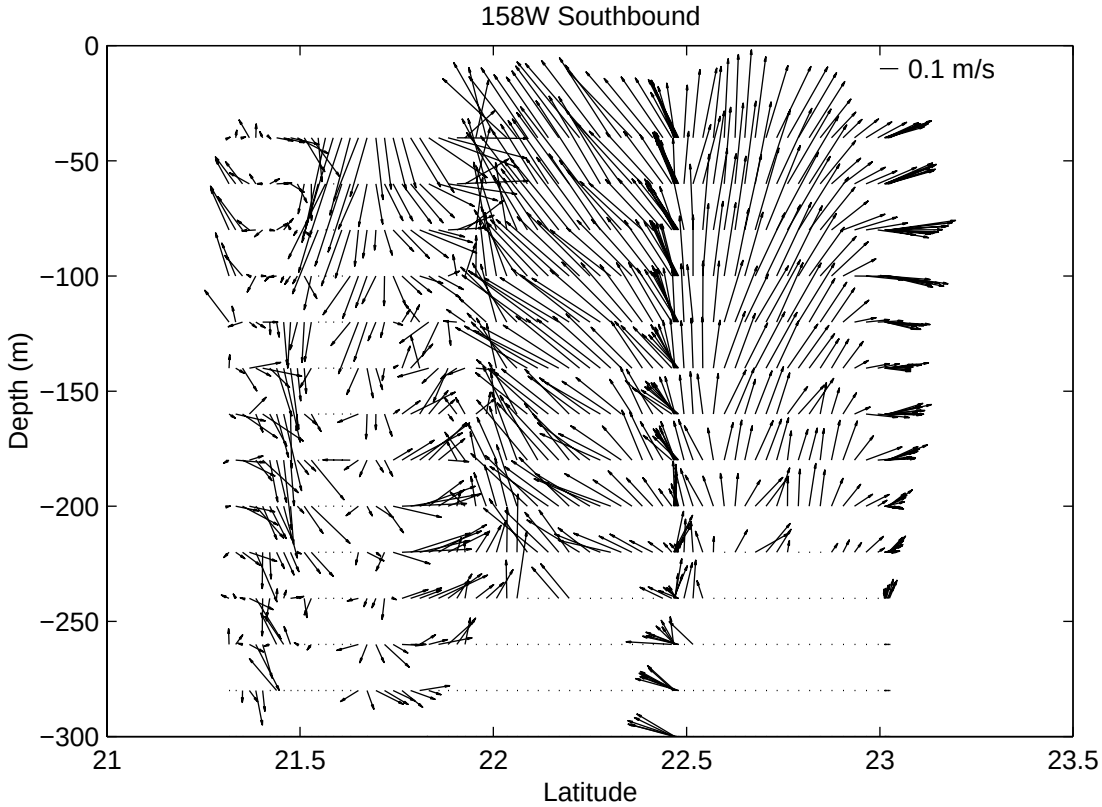
158W Southbound
0.1 m/s
Depth (m)
Latitude
0
−50
−100
−150
−200
−250
−300
21
21.5
22
22.5
23
23.5

Figure 6.3.2e

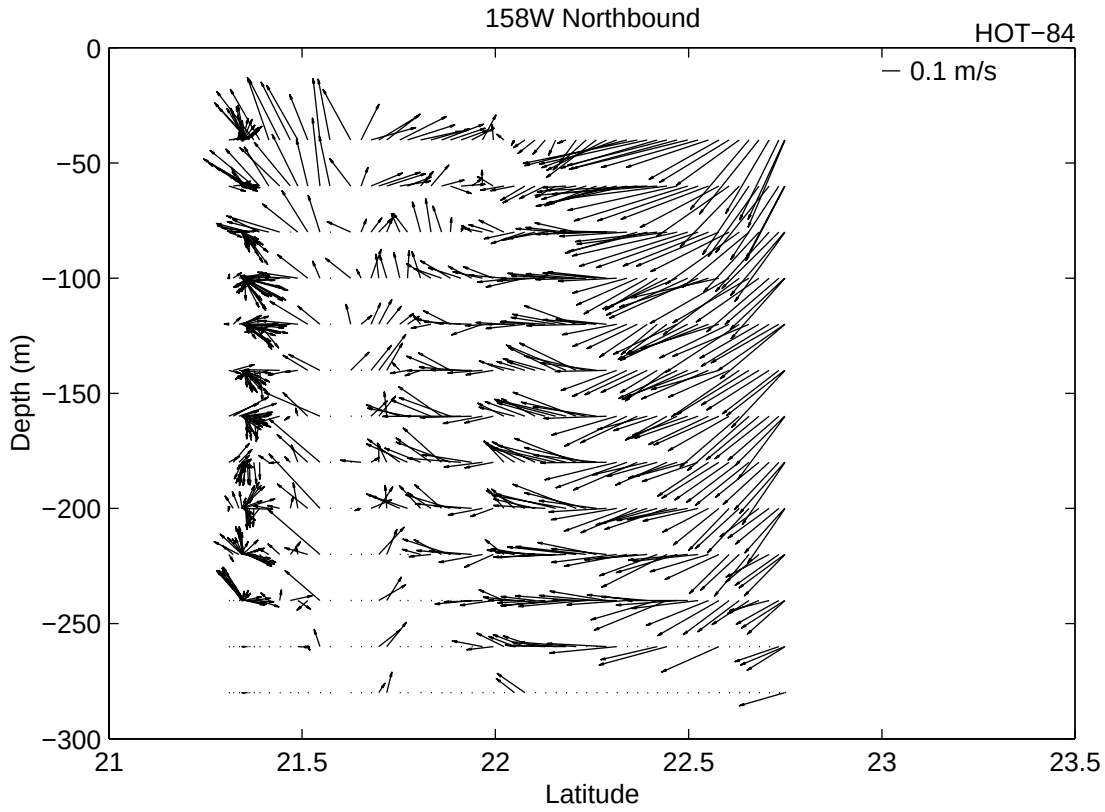
158W Northbound
HOT−84
0.1 m/s
Depth (m)
Latitude
0
−50
−100
−150
−200
−250
−300
21
21.5
22
22.5
23
23.5

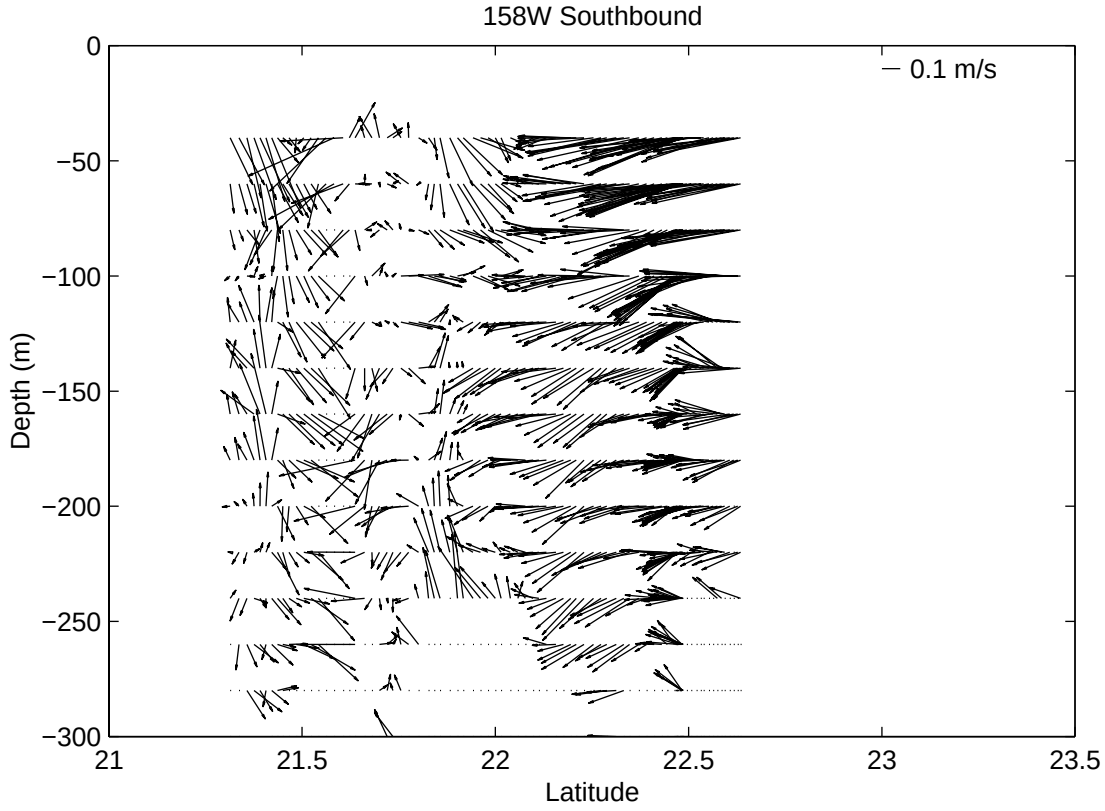
158W Southbound
0.1 m/s
Depth (m)
Latitude
0
−50
−100
−150
−200
−250
−300
21
21.5
22
22.5
23
23.5

Figure 6.3.2f

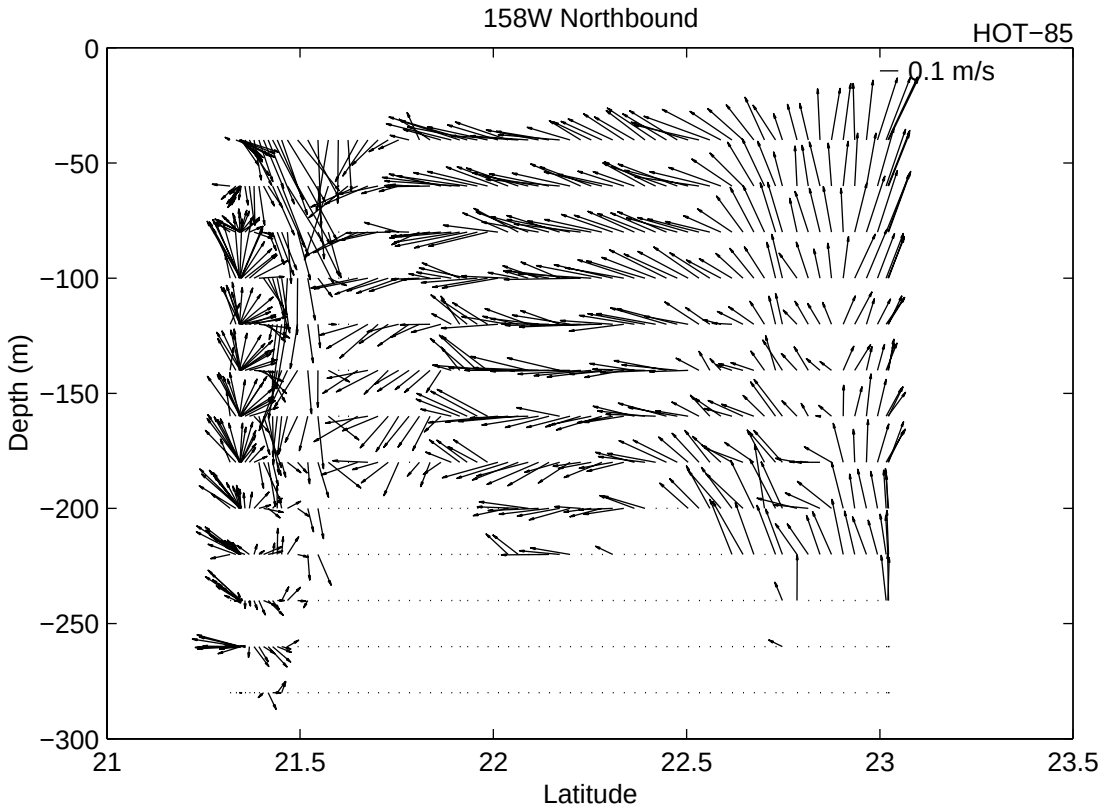
158W Northbound
HOT−85
0.1 m/s
Depth (m)
Latitude
0
−50
−100
−150
−200
−250
−300
21
21.5
22
22.5
23
23.5

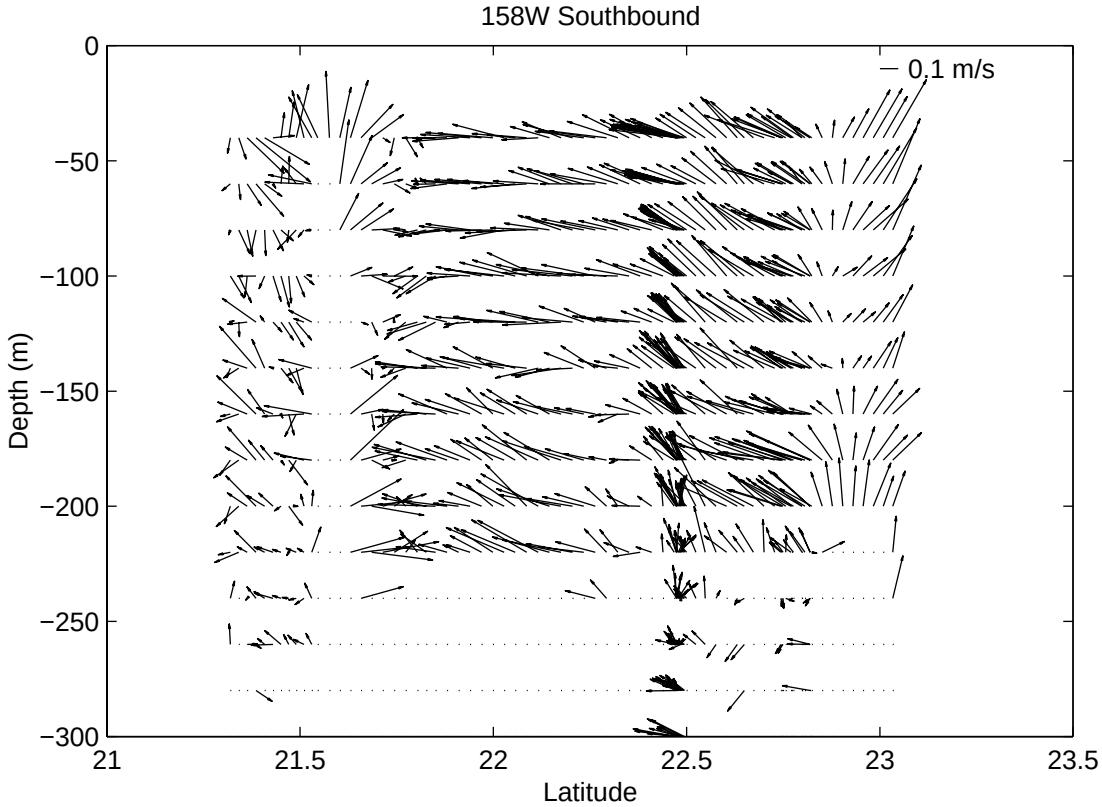
158W Southbound
0.1 m/s
Depth (m)
Latitude
0
−50
−100
−150
−200
−250
−300
21
21.5
22
22.5
23
23.5

Figure 6.3.2g

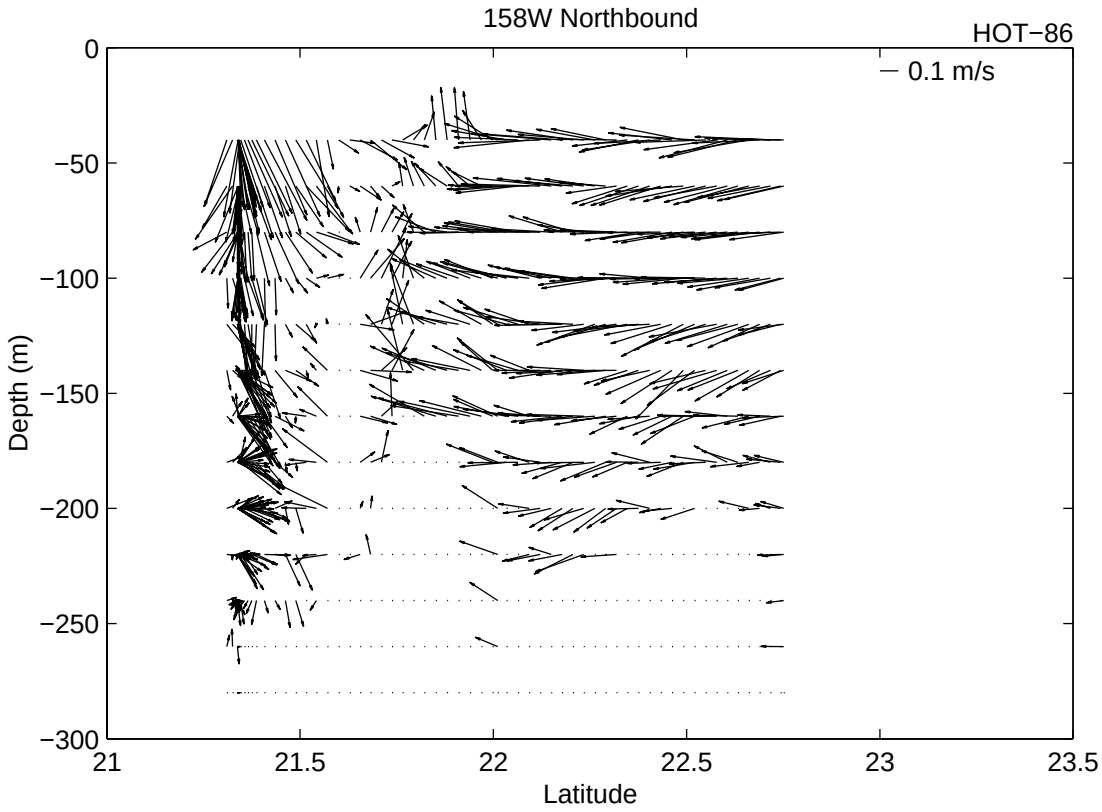
158W Northbound
HOT−86
0.1 m/s
0
−50
−100
−150
−200
−250
−300
Depth (m)
21
21.5
22
22.5
23
23.5
Latitude

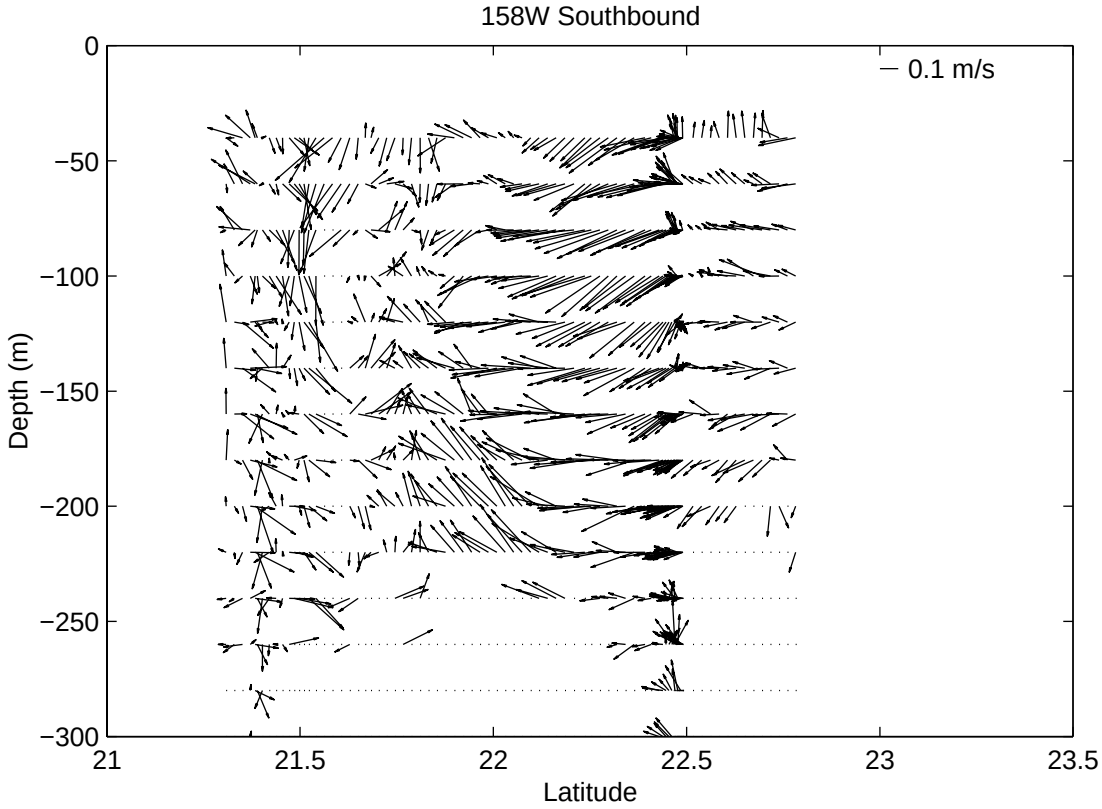
158W Southbound
0.1 m/s
0
−50
−100
−150
−200
−250
−300
Depth (m)
21
21.5
22
22.5
23
23.5
Latitude

Figure 6.3.2h

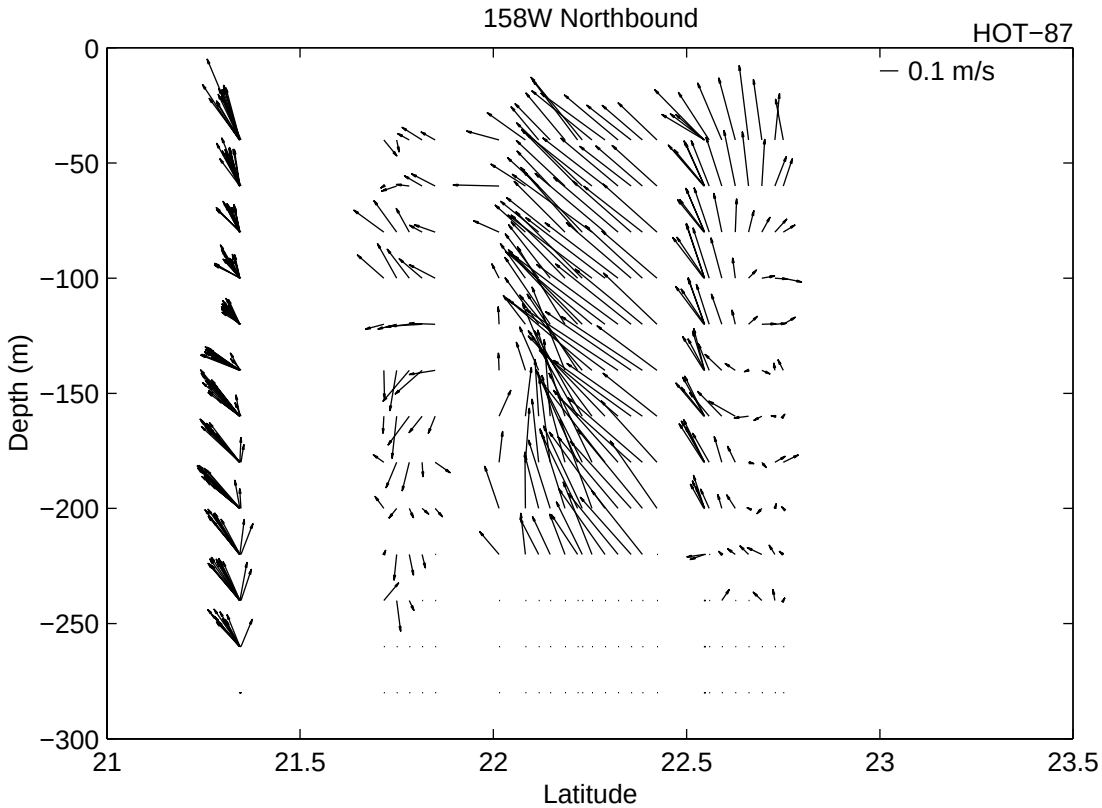
158W Northbound
HOT−87
0.1 m/s
Depth (m)
Latitude
0
−50
−100
−150
−200
−250
−300
21
21.5
22
22.5
23
23.5

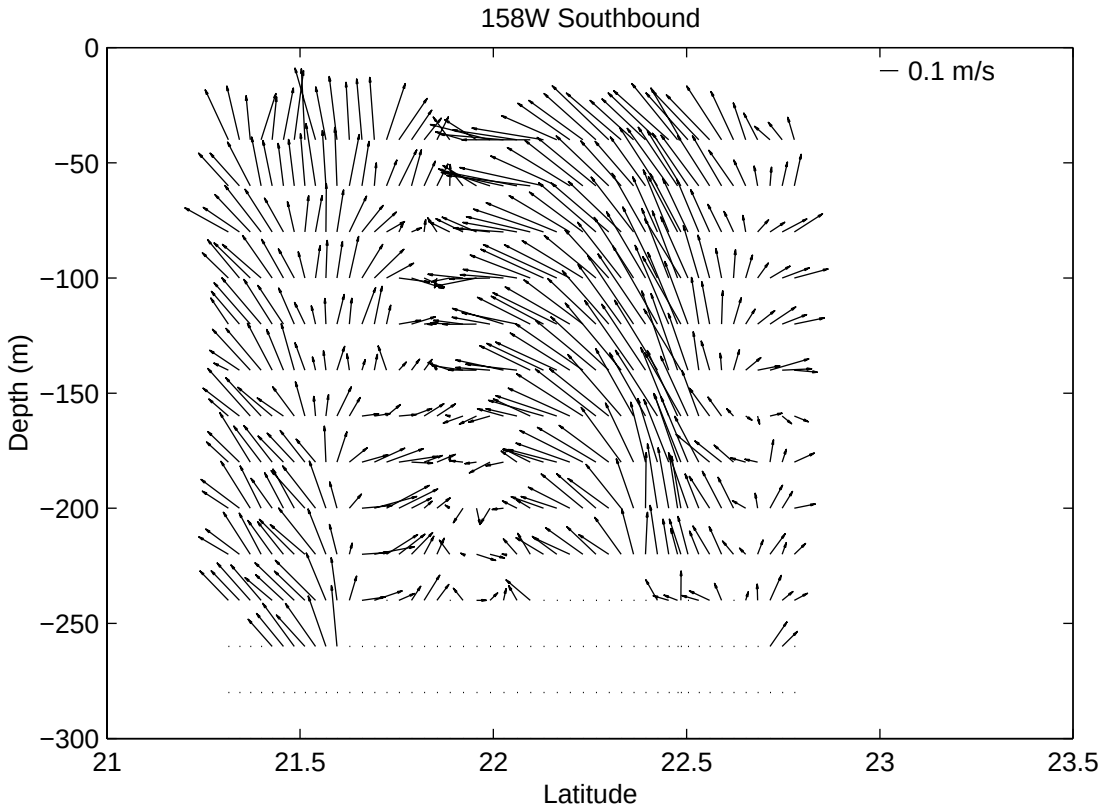
158W Southbound
0.1 m/s
Depth (m)
Latitude
0
−50
−100
−150
−200
−250
−300
21
21.5
22
22.5
23
23.5

Figure 6.3.2i

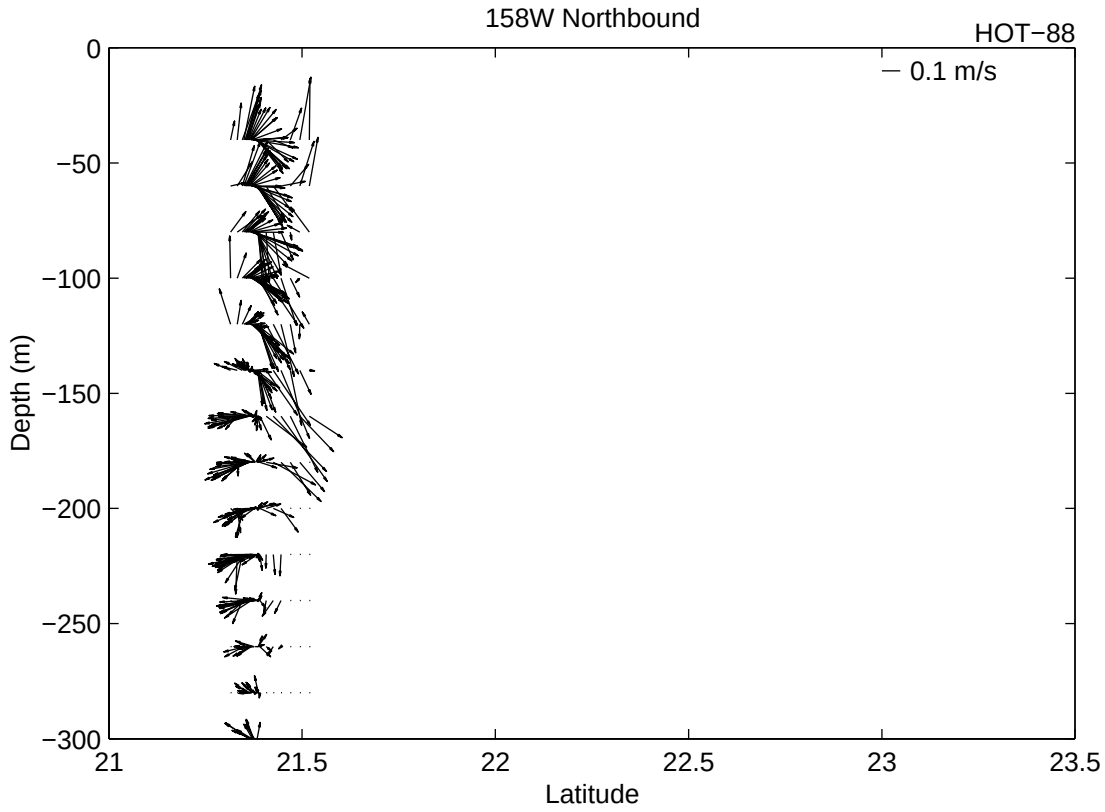
158W Northbound
HOT−88
0.1 m/s
Depth (m)
Latitude
0
−50
−100
−150
−200
−250
−300
21
21.5
22
22.5
23
23.5

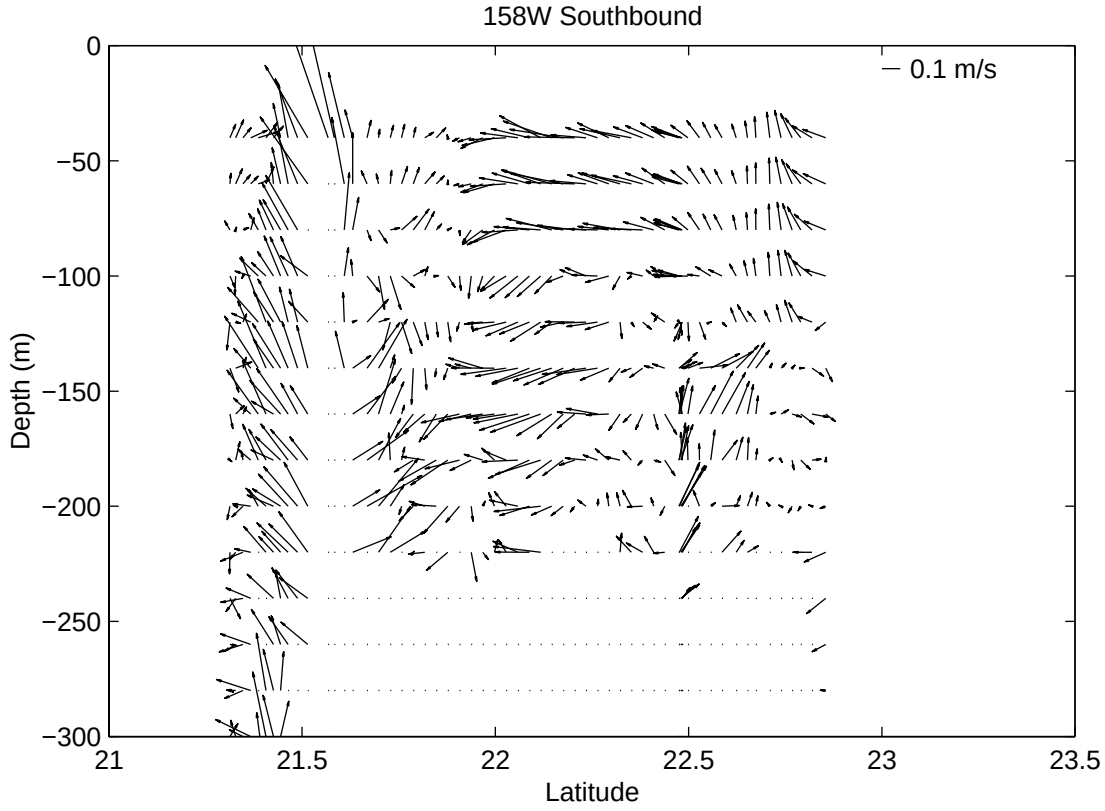
158W Southbound
0.1 m/s
Depth (m)
Latitude
0
−50
−100
−150
−200
−250
−300
21
21.5
22
22.5
23
23.5

Figure 6.3.2j

7. HOT PROGRAM PRESENTATIONS AND PUBLICATIONS

I. Invited Presentations and Published Abstracts

I.1. 1988 Karl, D. NSF-sponsored symposium on Dissertations in Chemical Oceanography, "Research opportunities in Hawaiian waters", Honolulu, Hawaii, November 1988.

I.2. 1988 Karl, D. NSF/GOFS-sponsored workshop on sediment traps, "Determination of total C, N, P flux" and "Screens: A potential solution to the problem of swimmers", Gulf Coast Research Laboratory, Mississippi, November 1988.

I.3. 1989 Winn, C.D., S. Chiswell, D.M. Karl and R. Lukas. Long time-series research in the Central Pacific Ocean. The Oceanography Society 1st Annual Meeting, Monterey, California.

I.4. 1990 Karl, D., R. Letelier, D. Bird, D. Hebel, C. Sabine and C. Winn. An *Oscillatoria* bloom in the oligotrophic North Pacific Ocean near the GOFS station ALOHA. *EOS, Transactions of the American Geophysical Union* 71, 177-178.

I.5. 1990 Winn, C.D., D. Hebel, R. Letelier, D. Bird and D. Karl. Variability in biogeochemical fluxes in the oligotrophic central Pacific: Results of the Hawaii Ocean Time- Series Program. *EOS, Transactions of the American Geophysical Union* 71, 190.

I.6. 1990 Chiswell, S.M. and R. Lukas. The Hawaii Ocean Time-series (HOT). *EOS, Transactions of the American Geophysical Union* 71, 1397.

I.7. 1990 Karl, D. "JGOFS time-series programs," San Francisco, California, December 1990.

I.8. 1991 Winn, C., C. Sabine, D. Hebel, F. Mackenzie and D.M. Karl. Inorganic carbon system dynamics in the central Pacific Ocean: Results of the Hawaii Ocean Time-series program. *EOS, Transactions of the American Geophysical Union* 72, 70.

I.9. 1991 Lukas, R. Water mass variability observed in the Hawaii Ocean Time Series. *EOS, Transactions of the American Geophysical Union* 72, 70.

I.10. 1991 Letelier, R., D. Karl, R. Bidigare, J. Christian, J. Dore, D. Hebel and C. Winn. Temporal variability of phytoplankton pigments at the U.S.-JGOFS station ALOHA (22°45'N, 158°W). *EOS, Transactions of the American Geophysical Union* 72, 74.

I.11. 1991 Karl, D. "The Hawaii Ocean Time-series program: Carbon production and particle flux", The Oceanography Society 2nd Annual Meeting, St. Petersburg, Florida, March 1991.

I.12. 1991 Karl, D. NATO symposium on Biology and Ecology of Diazotrophic Marine Organisms, "*Trichodesmium* blooms and new nitrogen in the North Pacific gyre", Bamberg, Germany, May 1991.

I.13. 1992 Anbar, A. D. Rhenium in seawater: Confirmation of generally conservative behavior. *EOS, Transactions of the American Geophysical Union* 73, 278.

I.14. 1992 Schudlich, R. and S. R. Emerson. Modeling dissolved gases in the subtropical upper ocean: JGOFS/WOCE Hawaiian Ocean Time-series. *EOS, Transactions of the American Geophysical Union* 73, 287.

I.15. 1992 Tupas, L.M., B.N. Popp and D.M. Karl. Dissolved organic carbon in oligotrophic waters: experiments on sample preservation, storage and analysis. *EOS, Transactions of the American Geophysical Union* 73, 287.

I.16. 1992 Karl, D., C. Winn, D. Hebel, R. Letelier, J. Dore and J. Christian. The U.S.-JGOFS Hawaii Ocean Time-Series (HOT) program. American Society for Limnology and Oceanography Aquatic Sciences Meeting, Santa Fe, NM, February 1992.

I.17. 1992 Campbell, L., R. R. Bidigare, R. Letelier, M. Ondrusek, S. Hall, B. Tsai and C. Winn. Phytoplankton population structure at the Hawaii Ocean Time-series station. American Society for Limnology and Oceanography Aquatic Sciences Meeting, Santa Fe, NM, February 1992.

I.18. 1992 Karl, D. NSF-sponsored GLOBEC scientific steering committee meeting, "Hawaii Ocean Time-series (HOT) program: A GLOBEC 'Blue Water' initiative", Honolulu, Hawaii, March 1992.

I.19. 1992 Karl, D. IGBP International Symposium on Global Change, "Oceanic ecosystem variability: Initial results from the JGOFS Hawaii Ocean Time-series (HOT) experiment", Tokyo, Japan, March 1992.

I.20. 1992 Karl, D. Conoco HOT Topics Seminar Series, "The U.S.-JGOFS Hawaii Ocean Time- Series (HOT) Program: Biogeochemical Vignettes from the Oligotrophic North Pacific Ocean" and "Temporal Variability in Bioelement Flux at Station ALOHA (22°45'N, 158°W)", Woods Hole, Massachusetts, May 1992

I.21. 1992 Bidigare, R. R., L. Campbell, M. Ondrusek, R. Letelier and D. Vaulot. Characterization of picophytoplankton at Station ALOHA (22°45'N, 158°W) using HPLC, flow cytometry and immunofluorescence techniques. PACON 1992 Meeting, June 1992.

I.22. 1992 Winn, C.D., D. Hebel, R. Letelier, J. Christian, J. Dore, R. Lukas and D.M. Karl. Long time-series measurements in the central North Pacific: Results of the Hawaii Ocean Time-series program. PACON conference, Kona, Hawaii, June 1992.

I.23. 1993 Atkinson, M. J. A potentiometric solid state sensor for oceanic CTDs, Abstract of The Oceanography Society Annual Meeting, Seattle, Washington, April 1993.

I.24. 1993 Campbell, L., H.A. Nolla and D. Vaulot. Microbial biomass in the subtropical central North Pacific Ocean (Station ALOHA): The importance of *Prochlorococcus*, Abstract of The Oceanography Society Annual Meeting, Seattle, Washington, April 1993.

I.25. 1993 Emerson, S., P. Quay, C. Stump, D. Wilbur and R. Schudlich. Oxygen cycles and productivity in the oligotrophic subtropical Pacific Ocean. Abstract of The Oceanography Society Annual Meeting, Seattle, Washington, April 1993.

I.26. 1993 Sharp, J. H., R. Benner, L. Bennett, C.A. Carlson, S.E. Fitzwater, E.T. Peltzer, and L. Tupas. Dissolved organic carbon: Intercalibration of analyses with equatorial Pacific samples. Abstract of The Oceanography Society Annual Meeting, Seattle, Washington, April 1993.

I.27. 1993 Winn, C.D., C.J. Carrillo, F.T. Mackenzie and D.M. Karl. Variability in the inorganic carbon system parameters in the North Pacific subtropical gyre. Abstract of The Oceanography Society Annual Meeting, Seattle, Washington, April 1993.

I.28. 1993 Yanagi, K. and D.M. Karl. Note on the fractional determination of TDP in seawater by an UV-irradiation method combined with the MAGIC procedure. Abstract of the Oceanography Society of Japan annual meeting, Tokyo, Japan, April 1993.

I.29. 1993 Campbell, L., H. Liu, R. R. Bidigare and D. Vaulot. Immunochemical characterization of *Prochlorococcus*. Abstract of the American Society of Limnology and Oceanography 1993 Annual Meeting, Edmonton, Alberta, Canada, May 1993.

I.30. 1993 Christian, J. R. and D.M. Karl. Bacterial exoenzymes in marine waters: Implications for global biogeochemical cycles. Abstract of the American Society of Limnology and Oceanography 1993 Annual Meeting, Edmonton, Alberta, Canada, May 1993.

I.31. 1993 Moyer, C.L., L. Campbell, D.M. Karl and J. Wilcox. Restriction fragment length polymorphism (RFLP) and DNA sequence analysis of PCR-generated clones to assess diversity of picoeukaryotic algae in the subtropical central North Pacific Ocean (Station ALOHA). Abstract of the American Society of Limnology and Oceanography 1993 Annual Meeting, Edmonton, Alberta, Canada, May 1993.

I.32. 1993 Sharp, J.H., R. Benner, L. Bennett, C.A. Carlson, S.E. Fitzwater and L. Tupas. The equatorial Pacific intercalibration analyses of dissolved organic carbon in seawater. Abstract of the American Society of Limnology and Oceanography 1993 Annual Meeting, Edmonton, Alberta, Canada, May 1993.

I.33. 1994 Yuan, J., C. I. Measures and J. A. Resing. Rapid determination of iron in seawater: In-line preconcentration flow injection analysis with spectrophotometric detection. *EOS, Transactions of the American Geophysical Union* 75, 25.

I.34. 1994 Smith, C.R., S. Garner, D. Hoover and R. Pope. Macrobenthos, mechanisms of bioturbation and carbon flux proxies at the abyssal seafloor along the JGOFS Equatorial Pacific Transect. *EOS, Transactions of the American Geophysical Union* 75, 70.

I.35. 1994 Farrenkopf, A.M., G.W. Luther, III and C.H. Van Der Weijden. Vertical distribution of dissolved iodine species in the northwest Indian Ocean. *EOS, Transactions of the American Geophysical Union* 75, 78.

I.36. 1994 Campbell, L., C.D. Winn, R. Letelier, D. Hebel and D.M. Karl. Temporal variability in phytoplankton fluorescence at Station ALOHA. *EOS, Transactions of the American Geophysical Union* 75, 100.

I.37. 1994 Winn, C., F.T. Mackenzie, C. Carrillo, T. Westby and D.M. Karl. Air-sea carbon dioxide exchange at Station ALOHA. *EOS, Transactions of the American Geophysical Union* 75, 112.

I.38. 1994 Lukas, R., F. Bingham and A. Mantyla. An anomalous cold event in the bottom water observed north of Oahu. *EOS, Transactions of the American Geophysical Union* 75, 205.

I.39. 1994 Tupas, L.M., B.N. Popp and D.M. Karl. Dissolved organic carbon in oligotrophic waters; experiments on sample preservation, storage and analysis. *EOS, Transactions of the American Geophysical Union* 75, 287.

I.40. 1994 Bingham, F.M. Drifter observations of the North Hawaiian Ridge Current. *EOS, Transactions of the American Geophysical Union* 75, 307.

I.41. 1994 HOT Program P.I.s, staff and students. The Hawaii Ocean Time-series (HOT) program: The first five years, p. 59. Abstract of The Oceanography Society Pacific Basin Meeting, Honolulu, Hawaii, July 1994.

I.42. 1994 HOT Program P.I.s, staff and students. HOT: a time-series study of carbon cycling in the oligotrophic North Pacific, p. 24. Abstract of The Oceanography Society Pacific Basin Meeting, Honolulu, Hawaii, July 1994.

I.43. 1994 Bidigare, R.R., L. Campbell, M.E. Ondrusek, R. Letelier, D. Vaulot and D.M. Karl. Phytoplankton community structure at station ALOHA (22°45'N, 158°W) during fall 1991, p. 58. Abstract of The Oceanography Society Pacific Basin Meeting, Honolulu, Hawaii, July 1994.

I.44. 1994 Bingham, F.M. and B. Qiu. Interannual variability of surface and mixed layer properties observed in the Hawaii Ocean Time-series, p. 89. Abstract of The Oceanography Society Pacific Basin Meeting, Honolulu, Hawaii, July 1994.

I.45. 1994 Bingham, F.M. and R. Lukas. Seasonal cycles of temperature, salinity and dissolved oxygen observed in the Hawaii Ocean Time-series, p. 90. Abstract of The Oceanography Society Pacific Basin Meeting, Honolulu, Hawaii, July 1994.

I.46. 1994 Christian, J. Vertical fluxes of carbon and nitrogen at Station ALOHA, p. 61. Abstract of The Oceanography Society Pacific Basin Meeting, Honolulu, Hawaii, July 1994.

I.47. 1994 Dore, J.E. and D.M. Karl. Nitrite distributions and dynamics at Station ALOHA, p. 60. Abstract of The Oceanography Society Pacific Basin Meeting, Honolulu, Hawaii, July 1994.

I.48. 1994 Firing, E. Currents observed north of Oahu during the first five years of HOT, p. 90. Abstract of The Oceanography Society Pacific Basin Meeting, Honolulu, Hawaii, July 1994.

I.49. 1994 Fujieki, L.A., D.V. Hebel, L.M. Tupas and D.M. Karl. Hawaii Ocean Time-series Data Organization and Graphical System (HOT-DOGS), p. 61. Abstract of The Oceanography Society Pacific Basin Meeting, Honolulu, Hawaii, July 1994.

I.50. 1994 Hebel, D.V., F.P. Chavez, K.R. Buck, R.R. Bidigare, D.M. Karl, M. Latasa, M.E. Ondrusek, L. Campbell and J. Newton. Do GF/F filters underestimate particulate chlorophyll *a* and primary production in the oligotrophic ocean?, p. 62. Abstract of The Oceanography Society Pacific Basin Meeting, Honolulu, Hawaii, July 1994.

I.51. 1994 Houlihan, T., J.E. Dore, L. Tupas, D.V. Hebel, G. Tien and D.M. Karl. Freezing as a method of preservation for seawater dissolved nutrient and organic carbon samples, p. 62. Abstract of The Oceanography Society Pacific Basin Meeting, Honolulu, Hawaii, July 1994.

I.52. 1994 Kennan, S.C. and R. Lukas. Saline intrusions in the intermediate waters north of Oahu, p. 91. Abstract of The Oceanography Society Pacific Basin Meeting, Honolulu, Hawaii, July 1994.

I.53. 1994 Letelier, R.M., J. Dore, C.D. Winn and D.M. Karl. Temporal variations in photosynthetic carbon assimilation efficiencies at Station ALOHA (22°45'N; 158°00'W), p. 60. Abstract of The Oceanography Society Pacific Basin Meeting, Honolulu, Hawaii, July 1994.

I.54. 1994 Liu, H. and L. Campbell. Growth and grazing rates of *Prochlorococcus* and *Synechococcus* at Station ALOHA measured by the selective inhibitor technique, p. 59. Abstract of The Oceanography Society Pacific Basin Meeting, Honolulu, Hawaii, July 1994.

I.55. 1994 Lukas, R. Interannual variability of Pacific deep and bottom waters observed in the Hawaii Ocean Time-series, p. 91. Abstract of The Oceanography Society Pacific Basin Meeting, Honolulu, Hawaii, July 1994.

I.56. 1994 Lukas, R., F. Bingham and E. Firing. Seasonal-to-interannual variability observed in the Hawaii Ocean Time-series, p. 28. Abstract of The Oceanography Society Pacific Basin Meeting, Honolulu, Hawaii, July 1994.

I.57. 1994 Tupas, L.M., B.N. Popp, D.V. Hebel, G. Tien and D.M. Karl. Dissolved organic carbon measurements at Station ALOHA measured by high temperature catalytic oxidation: Characteristics and variation in the water column, p. 63. Abstract of The Oceanography Society Pacific Basin Meeting, Honolulu, Hawaii, July 1994.

I.58. 1994 Winn, C.D., F. T. Mackenzie, C. Carrillo and D.M. Karl. Air-sea carbon dioxide exchange at Station ALOHA, p. 58. Abstract of The Oceanography Society Pacific Basin Meeting, Honolulu, Hawaii, July 1994.

I.59. 1994 Liu, H. and L. Campbell. Measurement of growth and mortality rate of *Prochloroccus* and *Synechococcus* at Station ALOHA using a new selective inhibitor technique. Fifth International Phycological Congress, Qingdao, China, July 1994.

I.60. 1994 Winn, C., F. T. Mackenzie, C. Carrillo, T. Westby and D.M. Karl. Air-sea carbon dioxide exchange at Station ALOHA, p. 112. Abstract of the American Society of Limnology and Oceanography 1994 Ocean Sciences Meeting, San Diego, California.

I.61. 1994 Measures, C.I., J. Yuan and J.A. Resing. The rapid determination of iron in seawater at sub-nanomolar concentrations using in-line preconcentration and spectrophotometric detection. Sixth Winter Conference on Flow Injection Analysis, San Diego, CA.

I.62. 1994 Measures, C.I., J. Yuan and J.A. Resing. Determination of iron in seawater using in-line preconcentration and spectrophotometric detection. Workshop on Iron Speciation and its Biological Activity, Bermuda Biological Station for Research, Bermuda.

I.63. 1995 Cortés, M.Y. and H.R. Thierstein. Coccolithophore dynamics during 1994 at the JGOFS time series Station ALOHA, Hawaii. 5th International Conference on Paleoceanography, Halifax, Canada, Abstract, p. 121.

I.64. 1995 Campos, M.L.A.M., T.D. Jickells, A.M. Farrenkopf and G.W. Luther, III. A comparison of dissolved iodine cycling at the Bermuda Atlantic Time Series station and Hawaii Ocean Time-series station. *EOS, Transactions of the American Geophysical Union* 76, S175.

I.65. 1995 Yuan, J. Collecting iron samples from well mounted on CTD rosette. *EOS, Transactions of the American Geophysical Union* 76, S175.

I.66. 1995 Michaels, A.F., D. Karl and A.H. Knap. Insights on ocean variability from the JGOFS time-series stations. Invited plenary lecture, The Oceanography Society Biennial Meeting, April 1995.

I.67. 1995 Emerson, S., P. Quay, L. Tupas and D. Karl. Chemical tracers of productivity and respiration in the upper ocean at US JGOFS station ALOHA, 10th Anniversary JGOFS Science Conference, Villefranche, France, May 1995.

I.68. 1995 Michaels, A.F., D. Karl and A.H. Knap. Insights on ocean variability from the JGOFS time-series stations. Invited lecture, 10th Anniversary JGOFS Science Conference, Villefranche, France, May 1995.

I.69. 1995 Karl, D.M. Oceanic carbon cycle and global environmental change: A microbiological perspective. Invited plenary talk, 7th International Symposium on Microbial Ecology, Santos, Brazil, August 1995.

I.70. 1995 Winn, C., D. Sadler and D.M. Karl. Carbon dioxide dynamics at the Hawaii JGOFS/WOCE time-series station. International Association for the Physical Sciences of the Oceans, Honolulu, Hawaii, August 1995.

I.71. 1996 Campbell, L., H. Liu and H.A. Nolla. Picophytoplankton population dynamics at Station ALOHA, p. OS65. AGU-ASLO Ocean Sciences Meeting, San Diego, CA, February 1996.

I.72. 1996 Christian, J.R., J.E. Dore and D.M. Karl. Mixing and nutrient fluxes at the US-JGOFS Station ALOHA ((22°45'N, 158°00'W), p. OS65. AGU-ASLO Ocean Sciences Meeting, San Diego, CA, February 1996.

I.73. 1996 Dulaney, T.S. and L.R. Sautter. Sedimentation of planktonic foraminifera: Seasonal changes in shell flux north of Oahu, Hawaii, p. OS85. AGU-ASLO Ocean Sciences Meeting, San Diego, CA, February 1996.

I.74. 1996 Emerson, S. Chemical tracers of biological processes: O_2, Ar and N_2 mass balance in the subtropical Pacific at the HOT station, p. OS85. AGU-ASLO Ocean Sciences Meeting, San Diego, CA, February 1996.

I.75. 1996 Hebel, D.V., D.M. Karl, J.R. Christian, J.E. Dore, R.M. Letelier, L.M. Tupas and C.D. Winn. Seasonal and interannual variability in primary production and particle flux at Station ALOHA, p. OS85. AGU-ASLO Ocean Sciences Meeting, San Diego, CA, February 1996.

I.76. 1996 Karl, D.M.. Alternation of N and P control of new and export production in the North Pacific gyre: A hypothesis based on the HOT program data set, p. OS86. AGU-ASLO Ocean Sciences Meeting, San Diego, CA, February 1996.

I.77. 1996 Lawson, L.M. and E.E. Hofmann. Time series sampling and data assimilation in a simple marine ecosystem model, p. OS86. AGU-ASLO Ocean Sciences Meeting, San Diego, CA, February 1996.

I.78. 1996 Lopez, M.D.G., Y. Zhu and M.E. Huntley. Space-time variability of zooplankton-sized particle concentrations at the Hawaii Ocean Time-series station (Station ALOHA), p. OS85. AGU-ASLO Ocean Sciences Meeting, San Diego, CA, February 1996.

I.79. 1996 Quay, P.D. and H. Anderson. Organic carbon export rates in the subtropical N. Pacific, p. OS85. AGU-ASLO Ocean Sciences Meeting, San Diego, CA, February 1996.

I.80. 1996 Richman, J.G., R.M. Letelier, M.R. Abbott and D. Pillsbury. Expandable optical mooring test at Station ALOHA (22°45'N; 158°00'W), p. OS64. AGU-ASLO Ocean Sciences Meeting, San Diego, CA, February 1996.

I.81. 1996 Scharek, R., M. Latasa, D.M. Karl and R.R. Bidigare Diatom abundance and vertical flux at the US-JGOFS/WOCE Station "ALOHA" in the oligotrophic North

Pacific gyre, p. OS85. AGU-ASLO Ocean Sciences Meeting, San Diego, CA, February 1996.

I.82. 1996 Selph, K.E., M.R. Landry, R.J. Miller and H.A. Al-Mutairi. Temporal variability in the mesozooplankton community at ocean Station ALOHA, p. OS85. AGU-ASLO Ocean Sciences Meeting, San Diego, CA, February 1996.

I.83. 1996 Tersol, V., S. Vink, J. Yuan and C.I. Measures. Variations in iron, aluminum and berylium concentrations in surface waters at Station ALOHA, p. OS65. AGU-ASLO Ocean Sciences Meeting, San Diego, CA, February 1996.

I.84. 1996 Tupas, L.M., MP. Sampson and D.M. Karl. Stable nitrogen isotopic analysis of sinking particulate matter at the Hawaii Ocean Time-series site, p. OS86. AGU-ASLO Ocean Sciences Meeting, San Diego, CA, February 1996.

I.85. 1996 Venrick, E.L. A comparison between the phytoplankton species from Station ALOHA and from the Climax region, p. OS65. AGU-ASLO Ocean Sciences Meeting, San Diego, CA, February 1996.

I.86. 1996 Winn, C.D. Carbon dioxide dynamics at the Hawaii JGOFS/WOCE time-series station: Annual and interannual variability, p. OS64. AGU-ASLO Ocean Sciences Meeting, San Diego, CA, February 1996.

I.87. 1996 Lukas, R. Low-frequency climate signals emerge in the Hawaii Ocean Time-series. WOCE Pacific Workshop. Hyatt Newporter, Newport Beach, CA, 19-23 August 1996.

I.88. 1996 Santiago-Mandujano, F. Cold bottom water events observed in the Hawaii Ocean Time-series. WOCE Pacific Workshop. Hyatt Newporter, Newport Beach, CA, 19-23 August 1996.

I.89. 1997 Lukas, R. Physical studies at the Hawaii Ocean Time-series (HOT) Station. Ocean Climate Time-Series Workshop. Johns Hopkins University, Baltimore, MD, 18-20 March 1997.

I.90 1997 Bird, D.F., R. Maranger and D.M. Karl. The importance of bacterial consumption by algae to marine systems. ASLO-Aquatic Sciences Meeting, Santa Fe, NM, February 1997.

I.91 1998 Letelier, R.M., M.R. Abbott, M.H. Freilich, D.M. Karl, P.J. Flament and R. Lukas. Euphotic zone biogeochemical response to a wind-induced upwelling event in the North Pacific subtropical gyre. AGU-Ocean Sciences Meeting, San Diego, CA, February 1998.

I.92 1998 Letelier, R.M. and D.M. Karl. The US-JGOFS Hawaii ocean Time-series (HOT) Program; What we have learned over the first decade. AGU-Ocean Sciences Meeting, San diego, CA, February 1998.

II. Invited/Contributed Book Chapters and Refereed Publications

II.1. 1990 Firing, E. and R.L. Gordon. Deep ocean acoustic Doppler current profiling. In: G. F. Appell and T. B. Curtin (eds.), *Proceedings of the Fourth IEEE Working Conference on Current Measurements*, pp. 192-201. IEEE, New York.

II.2. 1990 Giovannoni, S.J., E.F. DeLong, T.M. Schmidt and N.R. Pace. Tangential flow filtration and preliminary phylogenetic analysis of marine picoplankton. *Applied and Environmental Microbiology* 56, 2572-2575.

II.3. 1991 Chiswell, S. M. Dynamic response of CTD pressure sensors to temperature. *Journal of Atmospheric and Oceanic Technology* 8, 659-668.

II.4 1991 Karl, D.M., J.E. Dore, D.V. Hebel and C. Winn. Procedures for particulate carbon, nitrogen, phosphorus and total mass analyses used in the US-JGOFS Hawaii Ocean Time-Series Program. In: D. Spencer and D. Hurd (eds.), *Marine Particles: Analysis and Characterization*, pp. 71-77. American Geophysical Union, Geophysical Monograph 63.

II.5. 1991 Karl, D.M., W.G. Harrison, J. Dore et al. Chapter 3. Major bioelements workshop report. In: D.C. Hurd and D.W. Spencer (eds.), *Marine Particles: Analysis and Characterization*, pp. 33-42. American Geophysical Union, Geophysical Monograph 63.

II.6. 1991 Karl, D.M. and C.D. Winn. A sea of change: Monitoring the oceans' carbon cycle. *Environmental Science & Technology* 25, 1976-1981.

II.7. 1991 Laws, E.A. Photosynthetic quotients, new production and net community production in the open ocean. *Deep-Sea Research* 38, 143-167.

II.8. 1991 Sabine, C.L. and F.T. Mackenzie. Oceanic sinks for anthropogenic CO_2. *International Journal of Energy, Environment, Economics* 1, 119-127.

II.9. 1991 Schmidt, T.M., E.F. DeLong and N.R. Pace. Analysis of a marine picoplankton community by 16S rRNA gene cloning and sequencing. *Journal of Bacteriology* 173, 4371- 4378.

II.10. 1992 Benner, R., J.D. Pakulski, M. McCarthy, J.I. Hedges and P.G. Hatcher. Bulk chemical characteristics of dissolved organic matter in the ocean. *Science* 255, 1561-1564.

II.11. 1992 Chen, R. F. and J.L. Bada. The fluorescence of dissolved organic matter in seawater. *Marine Chemistry* 37, 191-221.

II.12. 1992 Karl, D.M. The oceanic carbon cycle: Primary production and carbon flux in the oligotrophic North Pacific Ocean. In: Y. Oshima (ed.), *Proceedings of the IGBP Symposium on Global Change*, pp. 203-219. Japan National Committee for the IGBP, Waseda University, Tokyo, Japan.

II.13. 1992 Karl, D.M., R. Letelier, D.V. Hebel, D.F. Bird and C.D. Winn. *Trichodesmium* blooms and new nitrogen in the North Pacific gyre. In: E. J. Carpenter et al. (eds.),

Marine Pelagic Cyanobacteria: Trichodesmium and Other Diazotrophs, pp. 219-237. Kluwer Academic Publishers, Netherlands.

II.14. 1992 Karl, D.M. and G. Tien. MAGIC: A sensitive and precise method for measuring dissolved phosphorus in aquatic environments. *Limnology and Oceanography* 37, 105-116.

II.15. 1992 Quay, P.D., B. Tilbrook and C.S. Wong. Oceanic uptake of fossil fuel CO_2: Carbon- 13 evidence. *Science* 256, 74-78.

II.16. 1993 Anbar, A.D., R.A. Creaser, D.A. Papanastassiou and G.J. Wasserburg. Rhenium in seawater: Confirmation of generally conservative behavior. *Geochimica et Cosmochimica Acta* 56, 4099-4103.

II.17. 1993 Campbell, L. and D. Vaulot. Photosynthetic picoplankton community structure in the subtropical North Pacific Ocean near Hawaii (station ALOHA). *Deep-Sea Research* 40, 2043- 2060.

II.18. 1993 Coble, P.G., C.A. Schultz and K. Mopper. Fluorescence contouring analysis of DOC intercalibration experiment samples: a comparison of techniques. *Marine Chemistry* 41, 173-178.

II.19. 1993 Emerson, S., P. Quay, C. Stump, D. Wilbur and R. Schudlich. Determining primary production from the mesoscale oxygen field. *ICES Marine Science Symposium* 197, 196-206.

II.20. 1993 Hedges, J.I., B.A. Bergamaschi and R. Benner. Comparative analyses of DOC and DON in natural waters. *Marine Chemistry* 41, 121-134.

II.21. 1993 Karl, D.M. Total microbial biomass estimation derived from the measurement of particulate adenosine-5'-triphosphate. In: P. F. Kemp, B. F. Sherr, E. B. Sherr and J. J. Cole (eds.), *Current Methods in Aquatic Microbial Ecology*, pp. 359-368. Lewis Publishers, Boca Raton.

II.22. 1993 Karl, D.M., G. Tien, J. Dore and C.D. Winn. Total dissolved nitrogen and phosphorus concentrations at US-JGOFS Station ALOHA: Redfield reconciliation. *Marine Chemistry* 41, 203-208.

II.23. 1993 Keeling, C.D. Lecture 2: Surface ocean CO_2. *NATO ASI Series* I(15), 413-429.

II.24. 1993 Letelier, R.M., R.R. Bidigare, D.V. Hebel, C.D. Winn and D.M. Karl. Temporal variability study of the phytoplankton community structure at the US-JGOFS Time-series Station ALOHA (22°45'N, 158°00'W) based on pigment analyses. *Limnology and Oceanography* 38, 1420-1437.

II.25. 1993 Mopper, K. and C.A. Schultz. Fluorescence as a possible tool for studying the nature and water column distribution of DOC components. *Marine Chemistry* 41, 229-238.

II.26. 1993 Selph, K.E., D.M. Karl and M.R. Landry. Quantification of chemiluminescent DNA probes using liquid scintillation counting. *Analytical Biochemistry* 210, 394-401.

II.27. 1993 Sharp, J.H., E.T. Peltzer, M.J. Alperin, G. Cauwet, J.W. Farrington, B. Fry, D.M. Karl, J.H. Martin, A. Spitzy, S. Tugrul and C.A. Carlson. Procedures subgroup report. *Marine Chemistry* 41, 37-49.

II.28. 1993 Winn, C.D., R. Lukas, D. Hebel, C. Carrillo, R. Letelier and D.M. Karl. The Hawaii Ocean Time-series program: Resolving variability in the North Pacific. In: N. Saxena (ed.), *Recent Advances in Marine Science and Technology*, pp. 139-150. Proceedings of the Pacific Ocean Congress (PACON).

II.29. 1994 Baines, S.B., M.L. Pace and D.M. Karl. Why does the relationship between sinking flux and planktonic primary production differ between lakes and ocean? *Limnology and Oceanography* 39, 213-226.

II.30. 1994 Björkman, K. and D.M. Karl. Bioavailability of inorganic and organic phosphorus compounds to natural assemblages of microorganisms in Hawaiian coastal waters. *Marine Ecology Progress Series* 111, 265-273.

II.31. 1994 Campbell, L., H.A. Nolla and D. Vaulot. The importance of photosynthetic prokaryote biomass in the subtropical central North Pacific Ocean (Station ALOHA). *Limnology and Oceanography* 39, 954-961.

II.32. 1994 Campbell, L., L.P. Shapiro and E.M. Haugen. Immunochemical characterization of the eukaryotic ultraplankton in the Atlantic and Pacific Oceans. *Journal of Plankton Research* 16, 35-51.

II.33. 1994 Christian, J.R. and D.M. Karl. Microbial community structure at the U.S.-Joint Global Ocean Flux Study Station ALOHA: Inverse methods for estimating biochemical indicator ratios. *Journal of Geophysical Research* 99, 14,269-14,276.

II.34. 1994 Karl, D.M. Accurate estimation of microbial loop processes and rates. *Microbial Ecology* 28, 147-150.

II.35. 1994 Karl, D.M. and B.D. Tilbrook. Production and transport of methane in oceanic particulate organic matter. *Nature* 368, 732-734.

II.36. 1994 Tupas, L.M., B.N. Popp and D.M. Karl. Dissolved organic carbon in oligotrophic waters: experiments on sample preservation, storage and analysis. *Marine Chemistry* 45, 207- 216.

II.37. 1994 Winn, C.D., F.T. Mackenzie, C.J. Carrillo, C. L. Sabine and D.M. Karl. Air-sea carbon dioxide exchange in the North Pacific subtropical gyre: Implications for the global carbon budget. *Global Biogeochemical Cycles* 8, 157-163.

II.38. 1994 Chiswell, S. Using an array of inverted echo sounders to measure dynamic height and geostrophic current in the North Pacific subtropical gyre. *Journal of Atmospheric and Oceanic Technology* 11, 1420-1430.

II.39. 1995 Atkinson, M.A., F.I.M. Thomas, N. Larson, E. Terrill, K. Morita and C. Liu. A micro-hole potentiostatic oxygen sensor for oceanic CTDs. *Deep-Sea Research* 42, 761-771.

II.40. 1995 Chavez, F.P., K.R. Buck, R.R. Bidigare, D.M. Karl, D. Hebel, M. Latasa, M. E. Ondrusek, L. Campbell and J. Newton. On the chlorophyll *a* retention properties of glass-fiber GF/F filters. *Limnology and Oceanography* 40, 428-433.

II.41. 1995 Christian, J.R. and D.M. Karl. Bacterial exocellular enzymes in marine waters: activity ratios and temperature kinetics in three oceanographic provinces. *Limnology and Oceanography* 40, 1042-1049.

II.42. 1995 Christian, J.R. and D.M. Karl. Measuring bacterial ectoenzyme activities in marine waters using mercuric chloride as a preservative and a control. *Marine Ecology Progress Series* 123, 217-224.

II.43. 1995 Emerson, S., P.D. Quay, C. Stump, D. Wilbur and R. Schudlich. Chemical tracers of productivity and respiration in the subtropical Pacific Ocean. *Journal of Geophysical Research* 100, 15,873-15,887.

II.44. 1995 Jones, D. R., D.M. Karl and E.A. Laws. DNA:ATP ratios in marine microalgae and bacteria: Implications for growth rate estimates based on rates of DNA synthesis. *Journal of Phycology* 31, 215-223.

II.45. 1995 Karl, D.M. A reply to a comment by J.A. McGowan "HOT and the North Pacific gyre." *Nature* 378, 21-22.

II.46. 1995 Karl, D.M., R. Letelier, D. Hebel, L. Tupas, J. Dore, J. Christian and C. Winn. Ecosystem changes in the North Pacific subtropical gyre attributed to the 1991-92 El Niño. *Nature* 373, 230-234.

II.47. 1995 Liu, H., L. Campbell and M.R. Landry. Growth and mortality rates of *Prochlorococcus* and *Synechococcus* measured with a selective inhibitor technique. *Marine Ecology Progress Series* 116, 277-287.

II.48. 1995 Maranger, R. and D.F. Bird. Viral abundance in aquatic systems: a comparison between marine and fresh waters. *Marine Ecology Progress Series* 121, 217-226.

II.49. 1995 Sabine, C.L. and F.T. Mackenzie. Bank-derived carbonate sediment transport and dissolution in the Hawaiian Archipelago. *Aquatic Geochemistry* 1, 189-230.

II.50. 1995 Sabine, C.L., F.T. Mackenzie, C. Winn and D.M. Karl. Geochemistry of particulate and dissolved inorganic carbon at the Hawaii Ocean Time-series station, ALOHA. *Journal of Biogeochemical Cycles* 9, 637-651.

II.51. 1995 Sharp, J.H., R. Benner, L. Bennett, C.A. Carlson, S.E. Fitzwater, E.T. Peltzer and L.M. Tupas. Analyses of dissolved organic carbon in seawater: the JGOFS EqPac methods comparison. *Marine Chemistry* 48, 91-108.

II.52. 1995 Thomas, F.I.M. and M.J. Atkinson. Field calibration of a microhole potentiostatic oxygen sensor for oceanic CTDs. *Journal of Atmospheric and Oceanic Technology* 12, 390-394.

II.53. 1995 Thomas, F.I.M., S.A. McCarthy, J. Bower, S. Krothapalli, M.J. Atkinson and P. Flament. Response characteristics of two oxygen sensors for oceanic CTDs. *Journal of Atmospheric and Oceanic Technology* 12, 687-690.

II.54. 1995 Tilbrook, B.D. and D.M. Karl. Methane sources, distributions and sinks from California coastal waters to the oligotrophic North Pacific gyre. *Marine Chemistry* 49, 51-64.

II.55. 1995 Winn, C.D., L. Campbell, R. Letelier, D. Hebel, L. Fujieki and D.M. Karl. Seasonal variability in chlorophyll concentrations in the North Pacific subtropical gyre. *Global Biogeochemical Cycles* 9, 605-620.

II.56. 1996 Andersen, R., R. Bidigare, M. Keller and M. Latasa. A comparison of HPLC pigment signatures and electron microscopic observations for oligotrophic waters of the North Atlantic and Pacific Oceans. *Deep-Sea Research* 43, 517-537.

II.57. 1996 Atkinson, M., F. Thomas and N. Larson. Effects of pressure on oxygen sensors. *Journal of Atmospheric and Oceanic Technology* 13, 1267-1277.

II.58. 1996 Bingham, F. and R. Lukas Seasonal cycles of temperature, salinity and dissolved oxygen observed in the Hawaii Ocean Time-series. *Deep-Sea Research* 43, 199-213.

II.59. 1996 Campos, M. L., A. Farrenkopf, T. Jickells and G. Luther. A comparison of dissolved iodine cycling at the Bermuda Atlantic Time-series Study station and Hawaii Ocean Time-series station. *Deep-Sea Research* 43, 455-466.

II.60. 1996 Chiswell, S. Intraseasonal oscillations at Station ALOHA, north of Oahu, Hawaii. *Deep-Sea Research* 43, 305-319.

II.61. 1996 Dore, J.E., T. Houlihan, D.V. Hebel, G. Tien, L.M. Tupas and D.M. Karl. Freezing as a method of seawater preservation for the analysis of dissolved inorganic nutrients in seawater. *Marine Chemistry* 53, 173-185.

II.62. 1996 Dore, J.E. and D.M. Karl. Nitrification in the euphotic zone as a source for nitrite, nitrate and nitrous oxide at Station ALOHA. *Limnology and Oceanography* 41, 1619-1628.

II.63. 1996 Dore, J.E. and D.M. Karl. Nitrite distributions and dynamics at Station ALOHA. *Deep-Sea Research* 43, 385-402.

II.64. 1996 Feller, R. J. and D.M. Karl. The National Association of Marine Laboratories: A connected web for studying long-term changes in US coastal and marine waters. *Biological Bulletin* 190, 269-277.

II.65. 1996 Firing, E. Currents observed north of Oahu during the first 5 years of HOT. *Deep-Sea Research* 43, 281-303.

II.66. 1996 Jones, D.R., D.M. Karl and E.A. Laws. Growth rates and production of heterotrophic bacteria and phytoplankton in the North Pacific subtropical gyre. *Deep-Sea Research* 43, 1567-1580.

II.67. 1996 Karl, D.M., J.R. Christian, J.E. Dore, D.V. Hebel, R.M Letelier, L.M. Tupas and C.D. Winn. Seasonal and interannual variability in primary production and particle flux at Station ALOHA. *Deep-Sea Research* 43, 539-568.

II.68. 1996 Karl, D.M. and A.F. Michaels. Preface: The Hawaiian Ocean Time-series (HOT) and the Bermuda Atlantic Time-series study (BATS). *Deep-Sea Research* 43, 127-128..

II.69. 1996 Karl, D.M. and R. Lukas. The Hawaii Ocean Time-series (HOT) program: Background, rationale and field implementation. *Deep-Sea Research* 43, 129-156.

II.70. 1996 Karl, D.M. and G. Tien. Temporal variability in dissolved phosphorus concentrations at Station ALOHA (22°45'N, 158°W). *Marine Chemistry* 56, 77-96.

II.71. 1996 Kennan, S.C. and R. Lukas. Saline intrusions in the intermediate waters north of Oahu, Hawaii. *Deep-Sea Research* 43, 215-241.

II.72. 1996 Latasa, M., R.R. Bidigare, M.E. Ondrusek and M.C. Kennicutt II. HPLC analysis of algal pigments: a comparison exercise among laboratories and recommendations for improved analytical performance. *Marine Chemistry* 51, 315-324.

II.73. 1996 Lawson, L., Y. Spitz and E. Hofmann. Time series sampling and data assimilation in a simple marine ecosystem model. *Deep-Sea Research* 43, 625-651.

II.74. 1996 Letelier, R.M., J.E. Dore, C.D. Winn and D.M. Karl. Temporal variations in photosynthetic carbon assimilation efficiencies at Station ALOHA. *Deep-Sea Research* 43, 467-490.

II.75. 1996 Letelier, R.M. and D.M. Karl. The role of *Trichodesmium* spp. in the productivity of the subtropical North Pacific Ocean. *Marine Ecology Progress Series* 133, 263-273.

II.76. 1996 Lukas, R. and F. Santiago-Mandujano. Interannual variability of Pacific deep and bottom waters observed in the Hawaii Ocean Time-series. *Deep-Sea Research* 43, 243-255.

II.77. 1996 Mitchum, G. On using satellite altimetric heights to provide a spatial context for the Hawaii Ocean Time-series measurements. *Deep-Sea Research* 43, 257-280.

II.78. 1996 Moyer, C.L., J.M. Tiedje, F.C. Dobbs and D.M. Karl. A computer-simulated restriction fragment length polymorphism analysis of bacterial small-subunit rRNA genes: Efficacy of selected tetrameric restriction enzymes for studies of microbial diversity in nature. *Applied and Environmental Microbiology* 62, 2501-2507.

II.79 1996 Roy-Barman, M., J.H. Chen and G.J. Wasserburg. ^{230}Th-^{232}Th systematics in the central Pacific Ocean: The sources and the fates of thorium. *Earth and Planetary Science Letters* 139, 351-363.

II.80. 1996 Schudlich, R. and S. Emerson. Gas saturation in the surface ocean: The roles of heat flux, gas exchange and bubbles. *Deep-Sea Research* 43, 569-589.

II.81 1996 Anbar, A.D., G.J. Wasserburg, D.A. Papanastassiou and P.S. Andersson. Iridium in natural waters. *Science* 273, 1524-1528.

II.82 1996 De La Rocha, C.L. and M.A. Brzezinski. Purification, recovery, and laser-driven fluorination of silicon from dissolved and particulate silica for the measurement of natural stable isotope abundances. *Analytical Chemistry* 68, 3746-3750.

II.83. 1997 Campbell, L., H. Liu, H.A. Nolla and D. Vaulot. Annual variability of phytoplankton and bacteria in the subtropical North Pacific Ocean at Station ALOHA during the 1991-1994 ENSO event. *Deep-Sea Research* 44, 167-192.

II.84. 1997 Liu, H., L. Campbell and H.A. Nolla. *Prochlorococcus* growth rate and contribution to primary production in the equatorial and subtropical North Pacific Ocean. *Aquatic Microbial Ecology* 12, 39-42.

II.85. 1997 Sansone, F.J., B.N. Popp and T.M. Rust. Stable carbon isotopic analysis of low-level methane in water and gas. *Analytical Chemistry* 69, 40-44.

II.86. 1997 Troy, P.J., Y.H. Li and F.T. Mackenzie. Changes in surface morphology of calcite exposed to the oceanic water column. *Aquatic Geochemistry* 3, 1-20.

II.87. 1997 Christian, J.R., M. R. Lewis and D.M. Karl. Vertical fluxes of carbon, nitrogen and phosphorus in the North Pacific subtropical gyre. *Journal of Geophysical Research* 102, 15,667-15,677.

II.88. 1997 Karl, D.M., R. Letelier, L. Tupas, J. Dore, J. Christian and D. Hebel. The role of nitrogen fixation in biogeochemical cycling in the subtropical North Pacific Ocean. *Nature* 388, 533-538.

II.89. 1997 Emerson, S., P. Quay, D. Karl, C. Winn, L. Tupas and M. Landry. The marine carbon pump: Flux accuracy and implications for the global carbon cycle. *Nature* 389, 951-954.

II.90. 1997 Winn, C.D., Y.H. Li, F.T. Mackenzie and D.M. Karl. Rising surface ocean total dissolved inorganic carbon at the Hawaii Ocean Time-series site. *Marine Chemistry* 60, 33-47..

II.91. 1997 Karl, D.M. and K. Yanagi. Partial characterization of the dissolved organic phosphorus pool in the oligotrophic North Pacific Ocean. *Limnology and Oceanography* 42, 1398-1405.

II.92. 1997 Karl, D.M. and F. C. Dobbs. Molecular approaches to microbial biomass estimation in the sea. *Molecular Approaches to the Study of the Ocean (K. E. Cooksey, Ed.)*, pp. 29-89.

II.93. 1997 Karl, D.M. Oceanic carbon cycle and global environmental change: A microbiological perspective. In: M. T. Martins (ed.), *Progress in Microbial Ecology*. Proceedings of Seventh International Symposium on Microbial Ecology, Santos, Sao Paulo, Brazil, 1995. Sociedade Brasileira de Microbiologia / International Committee of Microbial Ecology, Brazil, pp. 163-172.

II.94. 1997 Letelier, R.M. and D.M. Karl. *Trichodesmium* spp. physiology and nutrient fluxes in the North Pacific subtropical gyre. *Aquatic Microbial Ecology* 15, 265-276.

II.95. 1997 Karl, D.M. and G. Tien. Temporal variability in dissolved phosphorus concentrations in the subtropical North Pacific Ocean. *Marine Chemistry* 56, 77-96.

II.96. 1997 Benner, R., B. Biddanda, B. Black and M. McCarthy. Abundance, size distribution and stable carbon and nitrogen isotopic composition of marine organic matter isolated by tangential-flow ultrafiltration. *Marine Chemistry* 57, 243-263.

II.97. 1997 Venrick, E.L. Comparison of the phytoplankton species composition and structure in the Climax area (1973-1985) with that of Station ALOHA (1994*). Limnology and Oceanography* 42, 1643-1648.

II.98. 1998 Loisel, H. and A. Morel. Light scattering and chlorophyll concentration in case 1 waters: A reexamination. *Limnology and Oceanography* 43, 847-858.

II.99. 1998 Karl, D.M., D.V. Hebel, K. Bjorkman and R.M. Letelier. The role of dissolved organic matter fluxes in the productivity of the oligotrophic North pacific Ocean. *Limnology and Oceanography* 43, 1270-1286.

II.100. 1998 Zehr, J.P., M.T. Mellon and S. Zani. New nitrogen-fixing microorganisms detected in oligotrophic oceans by amplification of nitrogenase (*nif*H) genes. *Applied and Environmental Microbiology* 64, 3444-3450.

II.101. 1998 Dore, J.E., B.N. Popp, D.M. Karl and F.J. Sansone. Nitrification in the upper ocean is a significant source of isotopically depleted atmospheric N_2O. *Nature* 396, 63-66.

II.102. 1998 Michaels, A.F., D.M. Karl and A.H. Knap. Biogeochemical dynamics in oligotrophic oceans: The U.S. JGOFS time-series stations. In R. Hanson, H. Ducklow

and J. Field (eds.), *The Changing Carbon Cycle in the Sea*, Cambridge Univ. Press, in press.

II.103. 1998 Thomson-Bulldis, A. and D. Karl. Application of a novel method for phosphate and non-phosphate phosphorus determinations in the oligotrophic North Pacific Ocean. *Limnology and Oceanography*, in press.

II.104. 1998 Scharek, R., M. Latasa, D.M. KARL and R.R. Bidigare. Temporal variations in diatom abundance and downward vertical flux in the oligotrophic North Pacific gyre. *Deep-Sea Research*, in press.

II.105. 1998 Scharek, R., D.M. Karl and L. Tupas. Diatom sinking to the deep sea at U.S.-JGOFS/WOCE Station 'ALOHA' in the oligotrophic North Pacific Gyre. *Marine Ecology Progress Series*, in press.

III. Submitted Papers

III.1. Li, Y. H., D. Karl, C. Winn, F. Mackenzie and K. Gans. Remineralization ratios and preformed nutrients in the subtropical North Pacific Gyre. Submitted to *Aquatic Geochemistry*.

III.2. Nosse, C. Cross calibration of standard seawater batches P114, P115, P118, P121, P123, P128 and P130 through the Hawaii Ocean Time-series. Submitted to *Deep Sea Research*.

III.3. Karl, D.M., R.R. Bidigare and R.M. Letelier. Climate-related, long-tern changes in pankton community structure and productivity in the subtropical North Pacific Ocean. Submitted to *Nature*.

III.4. Karl, D.M. A sea of change: Biogeochemical variability in the North Pacific subtropical gyre. Submitted to *Ecosystems*.

III.5. Ondrusek, M.E., R.R. Bidigare, K. Waters and D.M. Karl. Predictive models for estimating rates of primary production in the subtropical North Pacific Ocean. Submitted to *Deep-Sea Research*.

III.6. Lukas, R., F. Santiago-Mandujano , F. Bingham and A. Mantyla. Cold bottom water events observed in the Hawaii Ocean Time-series: Implications for vertical mixing. Submitted to *Deep-Sea Research*.

IV. Theses and Dissertations

IV.1. 1992 Sabine, C. L. Geochemistry of particulate and dissolved inorganic carbon in the central North Pacific. Ph.D. Dissertation, May 1992

IV.2. 1993 Kennan, S. Variability of the intermediate water north of Oahu. M.S. Thesis, December 1993.

IV.3. 1994 Letelier, R. M. Studies on the ecology of *Trichodesmium* spp. (*Cyanophyceae*) in the central North Pacific gyre. Ph.D. Dissertation, April 1994.

IV.4. 1994 Liu, H. B. Growth and mortality rates of *Prochlorococcus* and *Synechococcus* measured by a selective inhibitor technique. M.S. Thesis, May 1994.

IV.5. 1995 Dore, J. E. Microbial nitrification in the marine euphotic zone: Rates and relationships with nitrite distributions, recycled production and nitrous oxide generation. Ph.D. Dissertation, May 1995.

IV.6. 1995 Christian, J. R. Biochemical mechanisms of bacterial utilization of dissolved and particulate organic matter in the upper ocean. Ph.D. Dissertation, December 1995.

V. Data Reports and Manuals

V.1. 1990 Karl, D.M., C.D. Winn, D.V. W. Hebel and R. Letelier. Hawaii Ocean Time-series Program Field and Laboratory Protocols, September 1990. School of Ocean and Earth Science and Technology, Univ. of Hawaii, Honolulu, HI, 72 pp.

V.2. 1990 Collins, D. J., W. J. Rhea and A. Van Tran. Bio-optical profile data report: HOT-3. National Aeronautics and Space Administration JPL Publ. #90-36.

V.3. 1990 Chiswell, S., E. Firing, D. Karl, R. Lukas and C. Winn. Hawaii Ocean Time-series Program Data Report 1: 1988-1989. SOEST Tech. Report 90-1, School of Ocean and Earth Science and Technology, Univ. of Hawaii, Honolulu, HI, 269 pp.

V.4. 1992 Winn, C., S. Chiswell, E. Firing, D. Karl and R. Lukas. Hawaii Ocean Time-series Program Data Report 2: 1990. SOEST Tech. Report 92-1, School of Ocean and Earth Science and Technology, Univ. of Hawaii, Honolulu, HI, 175 pp.

V.5. 1993 Winn, C., R. Lukas, D. Karl and E. Firing. Hawaii Ocean Time-series Program Data Report 3: 1991. SOEST Tech. Report 93-3, School of Ocean and Earth Science and Technology, Univ. of Hawaii, Honolulu, HI, 228 pp.

V.6. 1993 Tupas, L., F. Santiago-Mandujano, D. Hebel, R. Lukas, D. Karl and E. Firing. Hawaii Ocean Time-series Program Data Report 4: 1992. SOEST Tech. Report 93-14, School of Ocean and Earth Science and Technology, Univ. of Hawaii, Honolulu, HI, 248 pp.

V.7. 1994 Tupas, L., F. Santiago-Mandujano, D. Hebel, E. Firing, F. Bingham, R. Lukas and D. Karl. Hawaii Ocean Time-series Program Data Report 5: 1993. SOEST Tech. Report 94-5, School of Ocean and Earth Science and Technology, Univ. of Hawaii, Honolulu, HI, 156 pp.

V.8. 1994 Voss, C. I. and W. W. Wood Synthesis of geochemical, isotopic and groundwater modeling analysis to explain regional flow in a coastal aquifer of Southern Oahu, Hawaii. In: *Mathematical Models and Their Applications to Isotope Studies in Groundwater Hydrology*, pp. 147-178, International Atomic Energy Agency, Vienna, Austria.

V.9. 1995 Tupas, L., F. Santiago-Mandujano, D. Hebel, E. Firing, R. Lukas and D. Karl. Hawaii Ocean Time-series Program Data Report 6: 1994. SOEST Tech. Report 95-6, School of Ocean and Earth Science and Technology, Univ. of Hawaii, Honolulu, HI, 199 pp.

V.10. 1996 Karl, D., L. Tupas, F. Santiago-Mandujano, C. Nosse, D. Hebel, E. Firing and R. Lukas. Hawaii Ocean Time-series Program Data Report 7: 1995. SOEST Tech. Report 96-9, School of Ocean and Earth Science and Technology, Univ. of Hawaii, Honolulu, HI, 228 pp.

V.11. 1997 Tupas, L., F. Santiago-Mandujano, D. Hebel, C. Nosse, L. Fujieki, E. Firing, R. Lukas and D. Karl. Hawaii Ocean Time-series Program Data Report 8: 1996. SOEST Tech. Report 97-3, School of Ocean and Earth Science and Technology, Univ. of Hawaii, Honolulu, HI, 296 pp.

V.12 1998 Tupas, L., F. Santiago-Mandujano, D. Hebel, C. Nosse, L. Fujieki, R. Lukas and D. Karl. Hawaii Ocean Time-series Program Data Report 9: 1997. SOEST Tech. Report 98-3, School of Ocean and Earth Science and Technology, Univ. of Hawaii, Honolulu, HI, 159 pp.

VI. Newsletters

VI.1. 1989 Karl, D.M. Hawaiian Ocean Time-series program: It's HOT. *GOFS Newsletter* 1(2), 1-3.

VI.2. 1990 Karl, D.M. HOT Stuff: An update on the Hawaiian Ocean Time-series program. *US JGOFS Newsletter* 2(1), 6,9.

VI.3. 1990 Karl, David M. HOT Stuff: Rescue at sea. *US JGOFS Newsletter* 2(2), 8.

VI.4. 1991 Karl, D.M. HOT Stuff: Retrospect and prospect. *US JGOFS Newsletter* 2(3), 10.

VI.5. 1991 Karl, D.M. HOT Stuff: Hectic spring schedule keeps HOT team hustling. *US JGOFS Newsletter* 2(4), 9-10.

VI.6. 1991 Lukas, R. and S. Chiswell. Submesoscale water mass variations in the salinity minimum of the North Pacific. *WOCE Notes*, 3(1), 6-8.

VI.7. 1992 Karl, D.M. Hawaii Time-series program: Progress and prospects. *US JGOFS Newsletter* 3(4), 1,15.

VI.8. 1992 Michaels, A. F. Time-series programs compare results, methods and plans for future. *US JGOFS Newsletter* 4(1), 7,9.

VI.9. 1992 Winn, C. W. HOT program builds time-series set of carbon measurements for central Pacific. *US JGOFS Newsletter* 4(2), 7.

VI.10. 1992 Dickey, T. D. Oversight committee reviews time-series programs, issues recommendations. *US JGOFS Newsletter* 4(2), 14-15.

VI.11. 1992 Firing, E. and P. Hacker. ADCP results from WHP P16/P17. *WOCE Notes*, 4(3), 6-12.

VI.12. 1992 Chiswell, S. Inverted echo sounders at the WOCE deep-water station. *WOCE Notes*, 4(4), 1, 3-6.

VI.13. 1993 Karl, D.M. HOT Stuff: The five-year perspective. *US JGOFS Newsletter* 5(1), 6,15.

VI.14. 1994 Karl, D.M. HOT Stuff: Surprises emerging from five years' worth of data. *US JGOFS Newsletter* 5(4), 9-10.

VI.15. 1994 Tupas, L. M. Euphotic zone nitrate variability in the central North Pacific gyre at the Hawaii Ocean Time-series Station ALOHA. *International WOCE Newsletter* 17, 21-23.

VI.16. 1994 Lukas, R. HOT results show interannual variability of Pacific Deep and Bottom waters. *WOCE Notes* 6(2), 1, 3, 14-15.

VI.17. 1995 Karl, D.M. HOT and COLD: A trapper's tale of two oceans. *US JGOFS Newsletter* 6(2): 7, 15.

VI.18. 1995 Karl, D.M. HOT Stuff: New hypotheses and projects evolve from growing data set. *US JGOFS Newsletter* 7(1): 11.

VI.19. 1996 Winn, C.D. and P. G. Driscoll. Hawaii Time-series data reveal rising ocean CO_2 levels. *US JGOFS Newsletter* 7(4): 7-8.

VI.20. 1996 Karl, D.M. The Hawaii Ocean Time-series study: Still HOT at 75. *US JGOFS Newsletter* 7(4): 8-9.

VI.21. 1997 Karl, D.M. HOT scientists deploy mooring at Station ALOHA. *US JGOFS Newsletter* 8(2): 4.

VI.22. 1997 Karl, D.M. Ocean time-series meetings explore new collaboration for future. *US JGOFS Newsletter* 8(3): 15.

VII. HOT symposiums

VII.1. Presentations from the "HOT Program: Progress and Prospectus" symposium, 3-4 June 1992, East-West Center, Honolulu, HI

Campbell, L. Bacterial numbers by flow cytometry: A new approach
Chiswell, S. Results from the inverted echo sounder network
Christian, J. Biomass closure in the epipelagic zone
Christian, J. Exoenzymatic hydrolysis of high molecular weight organic matter

Dore, J. Annual and short-term variability in the distribution of nitrite at the US-JGOFS time-series station ALOHA

Dore, J. and D. Hebel. Low-level nitrate and nitrite above the nutricline at Station ALOHA

Firing, E. Ocean currents near ALOHA

Hebel, D., R. Letelier and J. Dore. Evaluation of the depth dependence and temporal variability of primary production at Station ALOHA

Hebel, D., R. Letelier and J. Dore. Past and present dissolved oxygen trends, methodology, and quality control during the Hawaii Ocean Time series

Hebel, D. and U. Magaard. Structure and temporal variability in biomass estimates at Station ALOHA

Houlihan, T. and D. Hebel. Organic and inorganic nutrients: Water column structure and usefulness in time-series analysis

Karl, D. Carbon utilization in the mesopelagic zone: AOU-DOC relationships

Karl, D. HOT/JGOFS program objectives: A brief overview

Karl, D. P-control of N_2 fixation: An ecosystem model

Karl, D. Primary production and particle flux

Karl, D. et al. Review and re-assessment of core measurements: Suggestions for refinement and improvement

Karl, D. and G. Tien. Low-level SRP above the nutricline at Station ALOHA

Karl, D., L. Tupas, G. Tien and B. Popp. "High-temperature" DOC: Pools and implications

Karl, D., K. Yanagi and K. Bjorkman. Composition and turnover of oceanic DOP

Letelier, R. Temporal variability of algal accessory pigments at Station ALOHA: What does it tell about the phytoplankton community structure at the DCML?

Letelier, R. and D. Hebel. Evaluation of fluorometric and HPLC chlorophyll *a* measurements at Station ALOHA

Letelier, R. and F. Santiago-Mandujano. Wind, sea surface temperature and significant wave height records from NDBC buoy #51001 compared to ship observations at Station ALOHA

Lukas, R. Water mass variability observed in the Hawaii Ocean Time-series

Sadler, D., C. Winn and C. Carrillo. Time-series measurements of pH: A new approach for HOT

Schudlich, R. Upper ocean gas modeling at Station ALOHA

Winn, C. DIC variability

Winn, C. and C. Carrillo. DIC and alkalinity profiles and elemental ratios

VII.2. Presentations from the "HOT Golden Anniversary Science Symposium," 16 November 1993, East-West Center, Honolulu, HI

Bingham, F. M. The oceanographic context of HOT

Campbell, L., H. Nolla, H. Liu and D. Vaulot. Phytoplankton population dynamics at the Hawaii Ocean Time series Station ALOHA

Campbell, L., H. Nolla and D. Vaulot. The importance of *Prochlorococcus* to community structure in the central North Pacific Ocean

Christian, J. Vertical fluxes of carbon and nitrogen at Station ALOHA

Dore, J. Nitrate diffusive flux cannot support new production during quiescent periods at Station ALOHA

Dore, J. Nitrification in lower euphotic zone at Station ALOHA: Patterns and significance

Firing, E. The north Hawaiian ridge current and other flows near ALOHA

Hebel, D. Temporal distribution, abundance and variability of suspended particulate matter (particulate carbon, nitrogen and phosphorus) at Station ALOHA -- Observations of a seasonal cycle

Karl, D., D. Hebel, L. Tupas, J. Dore and C. Winn. Station ALOHA particle fluxes and estimates of export production

Karl, D.M., R. Letelier, L. Tupas, J. Dore, D. Hebel and C. Winn. N_2 fixation as a contributor to new production at Station ALOHA

Karl, D.M., G. Tien and K. Yanagi. Phosphorus dynamics at Station ALOHA

Kennan, S. C. Possibilities for stirring along the Hawaiian ridge

Krothapalli, S., Y. H. Li and F. T. Mackenzie. What controls the temporal variability of carbon flux at Station ALOHA?

Letelier, R. M. Inorganic carbon assimilation at Station ALOHA: Possible evidence of a change in carbon fluxes

Letelier, R. M. Spatial and temporal distribution of *Trichodesmium* sp. at Station ALOHA: How important are they?

Liu, H. and L. Campbell. Measurement of growth and mortality rates of *Prochlorococcus* and *Synechococcus* at Station ALOHA using a new selective inhibitor technique

Lukas, R. and F. Bingham. Annual and interannual variations of hydrographic properties observed in the Hawaii Ocean Time-series (HOT)

Lukas, R., F. M. Bingham and A. Mantyla An anomalous cold event in the bottom water observed at Station ALOHA

Moyer, C. L., L. Campbell, D.M. Karl and J. Wilcox. Restriction fragment length polymorphism (RFLP) and DNA sequence analysis of PCR-generated clones to assess diversity of picoeukaryotic algae in the subtropical central North Pacific Ocean (Station ALOHA)

Polovina, J. J. and D. R. Kobayashi. HOT and Hawaii's fisheries landings: Complementary or independent time-series?

Sadler, D. Time series measurement of pH at Station ALOHA

Smith, C. R., D. J. DeMaster, R. H. Pope, S. P. Garner, D. J. Hoover and S. E. Doan. Seabed radionuclides, bioturbation and benthic community structure at the Hawaii Ocean Time-series Station ALOHA

Tupas, L. M., B. N. Popp and D.M. Karl. Dissolved organic carbon in oligotrophic waters: Experiments on sample preservation, storage and analysis

Winn, C.D. Air-sea carbon dioxide exchange at Station ALOHA

Yuan, J. and C. I. Measures. Sampling and analysis of dissolved iron

VII.3. Presentations from the "HOT-75 Commemorative Science Symposium," 9 September 1996, East-West Center, Honolulu, HI

Atkinson, M. A Potentiostatic, Solid-state Oxygen Sensor for Oceanic CTDs

Bidigare, R., M. Latasa, R. Andersen and M. Keller. A Comparison of HPLC Pigment Signatures and Electron Microscopic Observations for Oligotrophic Waters of the North Atlantic and North Pacific Oceans

Campbell, L., H. Liu, H. Nolla and D. Vaulot. Annual Variability of Phytoplankton and Bacteria in the Subtropical North Pacific Ocean at Station ALOHA during the 1991-1994 ENSO Event

Christian, J., M. Lewis and D. Karl. Vertical Fluxes of Carbon, Nitrogen and Phosphorus at the US-JGOFS Time-Series Station ALOHA

Dore, J. and D. Karl. Nitrification, New Production and Nitrous Oxide at Station ALOHA

Ducklow, H. Joint Global Ocean Flux Study -- Vision and Progress

Emerson, S., C. Stump and D. Wilber. Inert Gases as Tracers of Diapycnal Mixing in the Upper Ocean

Firing, E. Currents in the Vicinity of Station ALOHA: An Update

Fujieki, L. HOTDOGS: A New Tool for HOT Program Data Base Analysis and Presentation

Hebel, D., L. Tupas and D. Karl. The Importance of Organic Exudates in the Measurement of Oligotrophic Ocean Primary Productivity

Karl, D., D. Hebel and L. Tupas. Regionalization of Station ALOHA

Karl, D., G. Tien, K. Björkman, K. Yanagi, R. Letelier, A. Colman and A. Thomson. The "Forgotten" Open Ocean P-Cycle

Karl, D., L. Tupas, D. Hebel, R. Letelier, J. Christian and J. Dore. Station ALOHA N-Cycle: The Case for N2 Fixation

Landry, M., K. Selph and H. Al-Mutairi. Seasonal and Diurnal Variability of the Mesozooplankton Community at Ocean Station ALOHA

Letelier, R. and M. Abbott. Effects of a Subsurface *Trichodesmium* spp. Bloom on the Optical Reflectance Measured in the Upper 150 m of the Water Column in the North Pacific Subtropical Gyre

Liu, H., L. Campbell and H. Nolla. *Prochlorococcus* Growth Rate and Daily Variability at Station ALOHA

Lopez, M. and M. Huntley. Particle Concentrations at the Hawaii Ocean Time-series Station (Station ALOHA) Measured with an Optical Plankton Counter

Michaels, A. and A. Knap. The Bermuda Atlantic Time-Series Study (BATS): A View from the "Other" Ocean

Nolla, H., J. Kirshtein, M. Landry, D. Karl, L. Campbell and D. Pence. Flow Cytometry Correction Factors for Enumeration of Heterotrophic Bacteria and Phytoplankton

Quay, P. and H. Anderson. A Dissolved Inorganic Carbon Budget at Station ALOHA

Santiago-Mandujano, F. and R. Lukas. Cold Bottom Water Events Observed in the Hawaii Ocean Time-Series: Modelling and Implications for Vertical Mixing

Scharek, R., M. Latasa, D. Karl and R. Bidigare. Vertical Flux of Diatoms at the JGOFS/WOCE Station ALOHA

Smith, C., R. Miller, R. Pope and D. DeMaster. Seafloor Inventories of Pb-210, Th-234 and Benthic Biomass as Proxies for Deep POC Flux: Placing Export Production at the HOT Station in a General Oceanic Context

Tien, G., D. Pence and D. Karl. Hydrogen Peroxide Measurements at Station ALOHA

Tupas, L., G. Tien, D. Hebel and D. Karl. Dissolved Organic Carbon Dynamics in the Upper Water Column at Station ALOHA

Vink, S., K. Falkner, V. Tersol, J. Yuan and C. Measures. Variations in Iron, Aluminum, Beryllium and Barium Concentrations in Surface Waters at Station ALOHA

Winn, C. Secular Changes in Inorganic Carbon Parameters at HOT and BATS

8. DATA AVAILABILITY AND DISTRIBUTION

8.1. Hard Copies

Data collected by HOT program scientists are made available to the oceanographic community in various ways as soon after processing as possible. The complete data set, containing data collected since year 1 of the HOT program (1988), as well as 2 dbar averaged CTD data, are available from two sources. The first is through the National Oceanographic Data Center. The second source is from the HOT data base residing in a workstation at the University of Hawaii, and may be accessed using anonymous ftp on the Internet or the World Wide Web (www). Access via ftp or through the web is described in more detail below. Details of each web page are described in the section 8.3.

8.2. File Transfer Protocol

In order to maximize ease of access, the data are in ASCII files. File names are chosen so that they may be copied to DOS machines without ambiguity. (DOS users should be aware that Unix is case-sensitive, and Unix extensions may be longer than 3 characters.)

The data are in a subdirectory called ***/pub/hot***. More information about the data base is given in several files called ***Readme.**** at this level. The file ***Readme.first*** gives general information on the data base; we encourage users to read it first.

The following is an example of how to use ftp to obtain HOT data. The user's command are denoted by bold italicized text. The workstation's Internet address is ***mana.soest.hawaii.edu***, or ***128.171.154.9*** (either address should work). All information, except optical data, reside at this address. Optical data are stored at ***hahana.soest.hawaii.edu***, or ***128. 171. 154. 13***.

1. At the Prompt >, type ***ftp 128.171.154.9*** or ***ftp mana.soest.hawaii.edu.***

2. When asked for your login name, type ***anonymous***.

3. When asked for a password, type ***your email address***.

4. To change to the HOT database, type ***cd /pub/hot***. To view files type **ls**. A directory of files and subdirectories will appear.

5a. To obtain information about the database type ***get Readme.first***. This will transfer an ASCII file to your system. Use any text editor to view it.

5b. To obtain a list of publications, type ***cd publication-list*** then ***get hotpub.lis***.

5c. To obtain the HOT Field and Laboratory Protocols manual, type ***cd protocols*** then ***get 1142.asc***.

5d. To obtain CTD data, type ***cd ctd/hot-#***, where # is the HOT cruise of interest, then type ***mget *.ctd*** to transfer all the cruise CTD files to your system.

5e. To obtain water column data, type ***cd water***, then ***get <filename>*** where the filename is hot#.gof (JGOFS data) or hot#.sea (WOCE data) and # is the HOT cruise of interest.

6. To exit type ***bye***.

7. Data on optical parameters are located on another server. To obtain light data, at the prompt type ***ftp 128.171.154.13*** or ***ftp hahana.soest.hawaii.edu*** then follow steps 2 to 4.

8.3. World Wide Web

The Hawaii Ocean Time-series Program maintains a site on the World Wide Web where data and information about the program and its activities can easily be accessed over the Internet. The address is http://hahana.soest.hawaii.edu/hot/hot.html. This web page is the springboard from which the homepages of the WOCE and JGOFS components are accessible. Regardless of which site is accessed, there is only one common data base which is referred to by both components. The first half of the most recent year's data is usually available by July and the second half by January the following year with certain quality control caveats. All data are quality controlled by around April of the following year. Down loading of data is through ftp but the web pages provide a more detailed means of access.

8.3.1. HOT-WOCE Homepage

The World Ocean Circulation Experiment component of the HOT program maintains a web page at http://www.soest.hawaii.edu/HOT_WOCE. This web page includes (underlined items provide access to the specified section):

- Introduction:
  - HOT objectives
  - Site location
  - Observations description
  - HOT-WOCE Hydrographic sampling Procedures Manual
- Cruise Dates and Summaries:
  - Summaries of cruise's CTD station and cast
  - Chief Scientist's Reports
- Data description and Transfer:
  - Current status of HOT database
  - Data format information
  - Data transfer (FTP)
- WOCE Highlights:
  - Color contour of HOT time-series
  - Abstracts and figures of published papers from current research
  - Poster: Ocean Climate Variations in HOT
- Personnel:
  - The people that make the WOCE component of HOT possible

Accessing data files from the HOT-WOCE site can be accomplished by going to the Data description and transfer section. This section includes 1) data format and transfer information and 2) ftp data guides to (underlined items provide access to the specified section or operation):

- Current data status
- CTD data
- Bottle data
- Cruise summary
- ADCP data
- XBT data
- Meteorological observations
- Inverted Echo Sounder

8.3.2. HOT-JGOFS Homepage

The Joint Global Ocean Flux Study component of the HOT program maintains a web page at http://hahana.soest.hawaii.edu/hot/hot_jgofs.html. This web page includes (underlined items provide access to the specified section):

What's new (and updated)

Overview

- Introduction
  - Ancillary Projects Supported by HOT
  - Location of the HOT Water Column and Bottom Stations
  - Parameters Measured
- Cruise Schedules and Reports
- Principal Investigators and Staff
  - Past Cruise Participants
- HALE ALOHA - physical/biogeochemical mooring
  - Pictures of the Deployment
  - Mooring Positions
  - Bottom Topography
  - Results
- Special Topics and Events
  - Deep-Sea Research Special Volume
  - HOT-75 Commemorative Science Symposium

Data Links

- Interactive Access to HOT Data (HOT-DOGS)
- Request sample acquisition &/or Cruise Participation
- Analytical Methods and Results
- Current Data Trends
- References
  - Field and Laboratory Protocols
  - Publications

8.3.2.1. Data Access

Accessing of data through the HOT-JGOFS can be accomplished by going to the Analytical Methods and Results section. This section includes:

- Status & Summaries
  - Current Status of the HOT data base
  - Corrections
  - Cruise summaries

- Methods and Results
  - Hydrography
    (includes pressue, temperature, conductivity, oxygen, fluorescence and beam transmission)
  - Biogeochemistry
    (includes salinity, oxygen, dissolved inorganic carbon, titration alkalinity, pH, dissolved inorganic nutrients, dissolved organic nutrients, low-level nutrients, particulate matter, pigments, ATP)
  - Primary Production
  - Particle Flux
  - ADCP Measurements
  - Meteorology
  - Light Measurements
  - XBT
  - Buoy and shipboard Observations
  - Inverted Echo Sounder Observations
  - Bottom Moored Sediment Traps
  - Macrozooplankton
  - Thermosalinograph

- Endeco Towfish

8.3.2.2. HOT-DOGS©

HOT-DOGS© is the acronym for HOT Data Organizational and Graphical System. HOT-DOGS is a Matlab© based program that displays HOT data in a graphical format, as depth profiles or contour plots, or the numerical data for each parameter measured. All figures can be printed as hard copies or files. In addition to its graphical capabilities, HOT-DOGS provides a means of downloading data of selected parameters during specific years of the program. The program allows the user to perform the following:

- Data Extraction
  - Bottle
  - Particle Flux
  - Primary Production

- Display (vertical water column)
  - Bottle
  - CTD
  - HPLC Pigments
  - Particle Flux
  - Primary Production

- Standard depths (vertical water column)
  - Bottle
  - HPLC Pigments
  - Primary Production

- Time-series
  - Bottle
  - HPLC
  - Particle Flux
  - Primary Production

An advanced version of HOT-DOGS is available but at present only operable in the HOT-JGOFS workstation. This version can do more sophisticated graphical presentations such as contour plots. This software can also do graphical presentations of other JGOFS data bases such as the Bermuda Atlantic Time-series and the JGOFS process studies data bases. Development is underway to make the advanced version available through the world-wide web.